

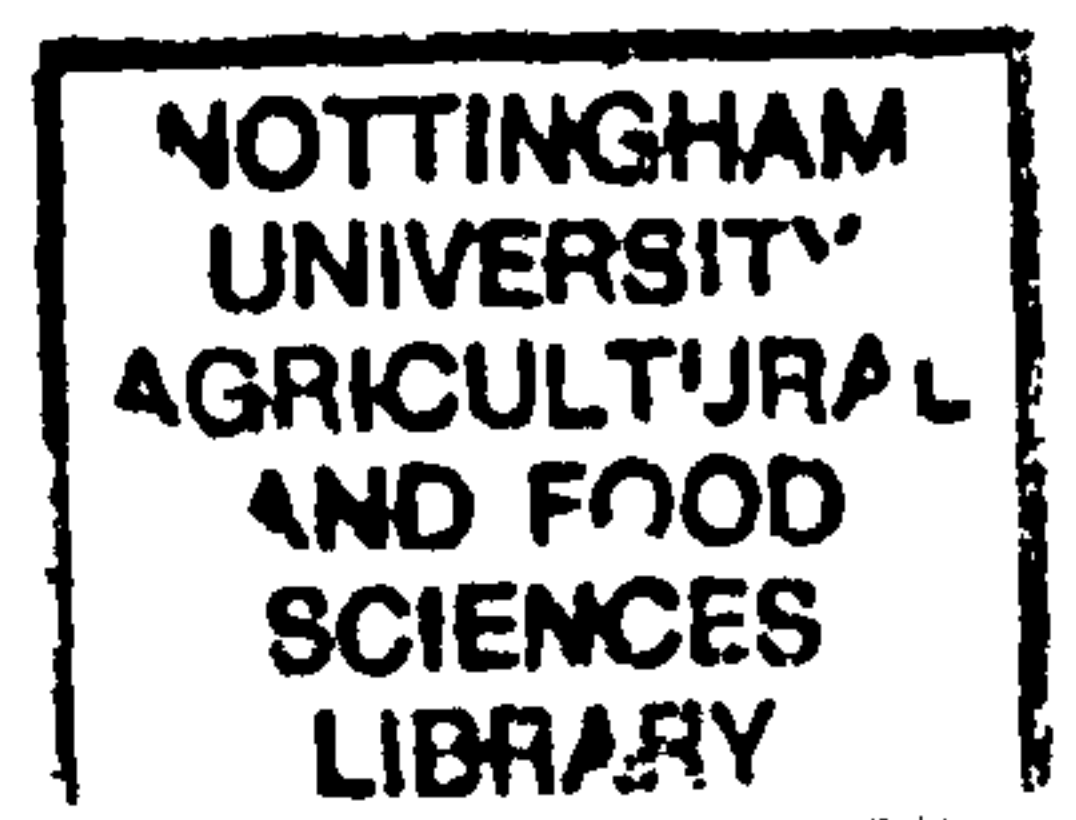
POTENTIAL IMPACTS OF CLIMATE CHANGE ON THE ENERGY BALANCE OF UK LIVESTOCK

by

John R. Turnpenny, Bsc (Hons)

Thesis submitted to the University of Nottingham for the degree of
Doctor of Philosophy, November 1997.

University of Nottingham



ABSTRACT

The wide-ranging potential impacts of climate change on both ecology and human infrastructure have led to a large amount of research; however, studies of the projected impacts on agricultural systems have so far focussed mainly on crops. Given the proven adverse effects of extreme weather conditions on the productivity and welfare of livestock, this thesis assesses the potential impact of such a change on the thermal balance of livestock in the UK.

A series of mathematical models was designed to predict the metabolic rate and occurrence of thermal stress in sheep and cattle outdoors, and pigs and broiler chickens indoors by solution of the energy balance equations. The models run on commonly-available hourly weather data, and as far as possible were based on the physics of heat and mass transfer rather than empirical relationships. The animals were modelled as systems of geometrical shapes, incorporating the underlying tissue, a coat and the external environment. Physiological responses to hot and cold conditions, including panting, sweating, vasomotor action and shivering were parameterised. Validation of the model output showed good agreement with measured data. The climate predictions for the year 2050 were reduced to synthetic hourly weather data using a stochastic weather generator and several simple downscaling techniques. The climate change impact assessment was made for an upland and a dry lowland site in the UK.

There are two main conclusions to the work. First, climate change is predicted to have little effect on ruminants outdoors, or on the suitability of a site for grazing livestock. Second, animals indoors will experience significantly more heat stress under climate change, probably since indoor animals are at greater risk of heat stress in the current climate than those outdoors. In the next fifty years, pig and broiler chicken farms will have to introduce methods for alleviation of heat stress to avoid economic and welfare problems. Future work will need to focus more on collection of accurate heat balance data rather than on more mathematical modelling.

CONTENTS

CHAPTER 1: INTRODUCTION

1.1	CLIMATE CHANGE	1-1
1.1.1	Evidence and causes of climate change	1-1
1.1.2	Assessing results of climate change	1-3
1.1.3	Potential impacts of climate change	1-8
1.1.3.1	Existing impact studies	1-8
1.2	ENERGY BALANCE OF HOMEOTHERMS	1-12
1.2.1	Introduction to energy balance	1-12
1.2.1.1	Metabolic heat production	1-14
1.2.1.2	Conduction, radiation, convection and evaporation	1-17
1.2.1.3	External work and heat storage	1-18
1.2.2	Energy balance of buildings	1-19
1.2.3	The metabolic diagram	1-20
1.3	EFFECTS OF THERMAL STRESS ON LIVESTOCK	1-22
1.3.1	Introduction	1-22
1.3.2	Impact of thermal stress on animals	1-23
1.3.2.1	Heat and cold stress	1-23
1.3.2.2	Productivity	1-24
1.4	STRATEGIES AND AIMS	1-27
1.4.1	Impact of climate change on UK agriculture	1-28
1.4.2	Mathematical modelling of agricultural systems	1-29
1.4.3	Aims and objectives	1-31

CHAPTER 2: THE ENERGY BALANCE OF A UNICORN

2.1	INTRODUCTION	2-1
2.2	THE UNICORN MODEL	2-2
2.3	HEAT FLOW THROUGH THE TISSUE	2-6
2.4	HEAT FLOW THROUGH THE COAT	2-7
2.4.1	Sensible heat transfer	2-8
2.4.1.1	Forced convection	2-9
2.4.1.2	Free convection	2-10
2.4.1.3	Conduction through trapped air	2-12
2.4.1.4	Longwave radiation transfer	2-13

2.4.1.5	Resistance to sensible heat transfer	2-14
2.4.2	Latent heat transfer	2-15
2.4.3	Total heat flow through the coat	2-18
2.5	HEAT FLOW TO THE ENVIRONMENT	2-19
2.5.1	Convection	2-20
2.5.2	Longwave radiation	2-22
2.5.3	Evaporation	2-24
2.5.4	Solar radiation	2-25
2.5.5	Total heat flow to the environment	2-27
2.6	ENERGY BALANCE FOR THE SYSTEM	2-27
2.7	RUNNING THE ENERGY BALANCE MODEL	2-29
2.7.1	TEST 1: Bare cylinder	2-29
2.7.2	TEST 2: Free and forced convection: the effect of wind speed	2-30
2.7.3	TEST 3: Effect of solar radiation	2-31
2.8	RAINFALL	2-32
2.9	APPENDAGES	2-33
2.10	PHYSIOLOGICAL RESPONSE TO ENVIRONMENT - THERMOREGULATORY RESPONSE OF HOMEOTHERMS	2-34
2.10.1	Vasomotor control	2-34
2.10.2	Sweating	2-35
2.10.3	Panting	2-35
2.10.4	Response to cold conditions	2-36
2.10.4.1	TEST 4: Cold wet conditions	2-37
2.11	DISCUSSION AND CONCLUSIONS	2-38
APPENDIX 2.1	SUMMARY OF INPUTS TO AND OUTPUTS FROM LIVESTOCK ENERGY BALANCE MODEL	2-39
APPENDIX 2.2	PROCEDURE FOR CONVECTION ASSESSMENT	2-41
APPENDIX 2.3	SHAPE FACTOR EXPRESSION	2-43

CHAPTER 3: MODELLING THE HEAT BALANCE OF ANIMALS OUTDOORS

3.1	INTRODUCTION	3-1
3.2	GENERAL CONSIDERATIONS FOR ANIMALS	

	OUTDOORS	3-1
	3.2.1 Winter housing	3-2
	3.2.2 Shelters	3-3
3a	SHEEP	3-5
3a.1	DIMENSIONS	3-5
3a.2	HEAT FLOW THROUGH TISSUE	3-7
3a.3	HEAT FLOW THROUGH COAT	3-8
	3a.3.1 Sensible heat transfer	3-8
	3a.3.2 Latent heat transfer	3-9
3a.4	HEAT FLOW TO THE ENVIRONMENT	3-10
	3a.4.1 Convection	3-10
	3a.4.2 Evaporation	3-10
	3a.4.3 Solar radiation	3-11
3a.5	PHYSIOLOGICAL RESPONSE TO ENVIRONMENT	3-12
	3a.5.1 Vasomotor control	3-12
	3a.5.2 Panting	3-12
3a.6	COMPARISON OF MODEL RESULTS WITH MEASUREMENTS ON REAL SHEEP	3-15
	3a.6.1 TEST 1: Heat loss from a shorn sheep	3-16
	3a.6.2 TEST 2: Effects of fleece length and wind speed on heat loss	3-17
	3a.6.3 TEST 3: Physiological response to thermal stress	3-19
	3a.6.4 TEST 4: The effect of solar radiation	3-21
3b	CATTLE	3-22
3b.1	DIMENSIONS	3-23
3b.2	HEAT FLOW THROUGH TISSUE	3-24
3b.3	HEAT FLOW THROUGH COAT	3-26
	3b.3.1 Sensible heat transfer	3-26
	3b.3.2 Latent heat transfer	3-27
3b.4	HEAT FLOW TO THE ENVIRONMENT	3-27
	3b.4.1 Convection	3-27
	3b.4.2 Solar radiation	3-30
3b.5	PHYSIOLOGICAL RESPONSE TO ENVIRONMENT	3-31
	3b.5.1 Vasomotor control	3-32
	3b.5.2 Sweating	3-32

3b.5.3	Response to cold conditions	3-33
3b.6	CATTLE MODEL VALIDATION	3-34
3b.6.1	TEST 1: Effect of coat length and wind speed on heat loss	3-34
3b.6.2	TEST 2: Heat loss from Friesian calves	3-37
3b.6.3	TEST 3: Penetration of the coat by solar radiation	3-39
3.3	BEHAVIOURAL RESPONSES OF OUTDOOR ANIMALS	3-40
3.3.1	Animal choice	3-40
3.3.2	Shelter from wind	3-41
3.3.3	Shade	3-43
3.4	DISCUSSION AND CONCLUSIONS	3-44
	APPENDIX: WOOL GROWTH RATES	3-46

CHAPTER 4: MODELLING ANIMALS IN OUTDOOR ENVIRONMENTS

4.1	INTRODUCTION	4-1
4.2	GENERAL CONSIDERATIONS FOR ANIMALS INDOORS	4-1
4a	PIGS	4-3
4a.1	DIMENSIONS	4-4
4a.2	TISSUE INSULATION	4-5
4a.3	HEAT LOSS TO THE ENVIRONMENT	4-6
4a.3.1	Convection	4-6
4a.3.2	Evaporation	4-7
4a.3.3	Conduction to the floor and other animals	4-7
4a.4	RESPONSES TO THE ENVIRONMENT	4-9
4a.4.1	Body temperature changes	4-9
4a.4.2	Shivering	4-10
4a.5	COMPARISON OF MODEL WITH MEASURED DATA	4-10
4a.5.1	TEST 1: Effects of environmental temperature on heat loss	4-10
4a.5.2	TEST 2: Effects of air speed on heat loss	4-13
4a.5.3	TEST 3: Thermoregulatory responses to the environment	4-14
4a.5.4	TEST 4: Conduction from piglets to the floor	4-16
4b	BROILER CHICKENS	4-17
4b.1	DIMENSIONS	4-18

4b.2	HEAT FLOW THROUGH THE BODY	4-19
4b.3	HEAT FLOW TO THE ENVIRONMENT	4-21
4b.4	PHYSIOLOGICAL RESPONSES TO THERMAL ENVIRONMENT	4-22
4b.4.1	Vasomotor control	4-22
4b.4.2	Panting and body temperature rise	4-22
4b.4.3	Feather fluffing	4-23
4b.5	COMPARISON OF CHICKEN MODEL WITH MEASURED DATA	4-24
4b.5.1	TEST 1: Effects of air temperature and humidity on heat loss	4-24
4b.5.2	TEST 2: Effects of air temperature on components of heat loss, skin and body temperature	4-36
4b.5.3	TEST 3: Effects of extremely hot conditions on components of heat loss	4-28
4.3	BEHAVIOURAL RESPONSES TO OUTDOOR ENVIRONMENT	4-29
4.4	DISCUSSION AND CONCLUSIONS	4-30
APPENDIX 4.1	CALCULATION OF THERMAL RESISTANCE OF FLOOR	4-31

CHAPTER 5: MODELLING THE IMPACT OF CLIMATE CHANGE ON LIVESTOCK ENERGY BALANCE

5.1	CLIMATE CHANGE AND THE NEED FOR DOWNSCALING	5-1
5.2	GENERATION OF HOURLY WEATHER DATA FROM CLIMATE CHANGE SCENARIOS	5-3
5.2.1	Rainfall	5-5
5.2.2	Cloud cover, diffuse and direct solar radiation	5-5
5.2.3	Ground, sky and air temperatures	5-9
5.2.3.1	Air temperature	5-9
5.2.3.2	Radiant temperature of the sky	5-10
5.2.3.3	Ground surface temperature	5-11
5.2.4	Vapour pressure and wind speed	5-12
5.3	VALIDATION OF THE HOURLY WEATHER DATA GENERATOR	5-14
5.3.1	Solar radiation	5-15

5.3.2	Air temperature	5-16
5.3.3	Ground and sky temperatures	5-17
5.3.4	Other variables	5-18
5.4	MODELLING THE IMPACT OF CLIMATE CHANGE ON THE THERMAL BALANCE OF LIVESTOCK	5-19
5.4.1	Inputs to the thermal balance model	5-19
5.4.2	Principles of impact assessment	5-20
5.5	CONCLUSIONS	5-22
APPENDIX 5.1:	CALCULATION OF SOLAR ELEVATION	5-24
APPENDIX 5.2:	CALCULATION OF T_g	5-25

CHAPTER 6: RESULTS AND ANALYSIS

6.1	INTRODUCTION	6-1
6.2	INDICATORS OF THERMAL STRESS	6-1
6.3	RESULTS: INTEGRATED MODEL	6-2
6.3.1	Sheep	6-3
6.3.2	Beef calves	6-4
6.3.3	Dairy cattle	6-5
6.3.4	Pig	6-6
6.3.5	Broiler chicken	6-7
6.3.6	Summer heat stress	6-8
6.3.7	Economic impacts	6-10
6.4	RESULTS: THERMAL BALANCE MODEL EXPERIMENTS	6-11
6.5	SENSITIVITY ANALYSIS	6-13
6.6	CONCLUSIONS	6-19
APPENDIX 6.1		6-20

CHAPTER 7: DISCUSSION AND CONCLUSIONS

7.1	INTRODUCTION	7-1
7.2	NOVEL FEATURES	7-2

7.3	MAIN ASSUMPTIONS	7-2
7.3.1	Thermal balance models	7-2
7.3.2	Hourly weather data generator	7-8
7.4	IMPLICATIONS OF RESULTS	7-10
7.4.1	Effects of climate change on thermal balance	7-10
7.4.2	Economic considerations	7-11
7.5	ALLEVIATING THERMAL STRESS	7-12
7.6	FUTURE WORK	7-16
7.6.1	Using the current model	7-16
7.6.2	Modifying the current model	7-17
7.7	FINAL COMMENTS	7-18

<u>REFERENCES</u>	R-1
--------------------------	------------

<u>APPENDIX A: SUMMARY OF DEFAULT INPUTS TO THE THERMAL BALANCE MODELS</u>	A-1
---	------------

<u>APPENDIX B: CLIMATE CHANGE SCENARIO</u>	B-1
---	------------

SYMBOLS

Unless otherwise stated all areas refer to skin surface area.

ROMAN SYMBOLS

A,B	Constants of proportionality in Nusselt number relationships
A_c	coat surface area (m^2)
A_f	Area of animal in contact with floor (m^2)
A_h	area of shadow cast by animal (m^2)
A_{he}	skin surface area of head (m^2)
A_L	total skin surface area of legs on one animal (m^2)
A_o	Area of animal in contact with other animals (m^2)
A_s	skin surface area (m^2)
A_t	skin surface area of trunk (m^2)
a,b	constants in regression of k_a with temperature
C	Heat flux density due to convection ($W m^{-2}$)
C_g	Convective heat flux density at the ground ($W m^{-2}$)
c	fractional cloud cover (0 = clear, 1 = totally cloudy)
c'	parameter describing wind penetration in coats (m)
c_p	Specific heat of air ($J kg^{-1} K^{-1}$)
D(T)	Diffusion coefficient of water vapour at temperature T ($m^2 s^{-1}$)
D_o	Dimensionless term accounting for variation in earth's distance from sun (range: 0.97 - 1.03)
$d_{t,h,L}$	diameter of body part (trunk, head, leg) (m)
DAY	Julian day
E	Heat flux density due to latent heat loss ($W m^{-2}$)
E'	Total latent heat flux density per unit coat area ($E_r' + E_c'$)
E_c	Latent heat flux density from skin ($W m^{-2}$)
E_c'	Latent heat flux density from skin per unit coat surface area ($W m^{-2}$)
E_g	Evaporative heat flux density at the ground ($W m^{-2}$)
E_{max}	Maximum latent heat flux density ($W m^{-2}$)
E_r	Latent heat flux density from respiratory tract ($W m^{-2}$)
E_r'	Latent heat flux density from respiratory tract ($W m^{-2}$ coat surface area)
e	Vapour pressure (Pa)
e_a	vapour pressure of ambient air (Pa)
$e_s(T)$	saturation vapour pressure at T
F	respiration rate (breaths min^{-1})
F_i	fuel heat input to building ($W m^{-2}$)
F_r	respiration rate below thermoneutral zone
G	A general heat flux density ($W m^{-2}$)

G_c	Heat flux density through coat layer (W m^{-2})
G_e	Heat flux density from animal to environment (W m^{-2})
G_e'	Heat flux density from animal to environment per unit coat surface area (W m^{-2})
G_f	Heat flux density of conduction to the floor
G_H	sensible heat flux
G_{mod}	modelled heat flux density (W m^{-2})
G_{meas}	measured heat flux density (W m^{-2})
G_s	Total heat flux density through tissue layer (W m^{-2})
G_w	Heat flux density due to external work (W m^{-2})
g_v	Conductance of water vapour in air (m s^{-1})
Gr	Grashof number
H_f	Total heat loss to the floor (W)
h	hour angle
h_s	Hour angle of sunrise (radians)
I_{max}	maximum rainfall intensity in a day (mm hr^{-1})
J	Quantity of heat stored (W m^{-2})
k	Thermal conductivity of a general material ($\text{W m}^{-1} \text{K}^{-1}$)
k_a	thermal conductivity of air ($\text{W m}^{-1} \text{K}^{-1}$)
k_b	thermal conductivity due to free convection in the coat ($\text{W m}^{-1} \text{K}^{-1}$)
k_e	Efficiency of conversion of food to energy
K_M	Mass transfer coefficient ($\text{m}^2 \text{s}^{-1}$)
K_T	Thermal conductance ($\text{W m}^{-2} \text{K}^{-1}$)
L	Net longwave radiative heat flux density (W m^{-2})
L_g	Radiant heat flux density at the ground (W m^{-2})
l	coat depth (m)
l_t	coat depth on trunk (m)
l_w	depth of wind penetration into coat (m)
LCT	lower critical temperature ($^{\circ}\text{C}$ or K)
M	Thermoneutral metabolic rate (W m^{-2})
M_f	Metabolizable energy (W m^{-2})
M_m	Zero energy retention metabolic rate (W m^{-2})
m_b	Mass of the animal (liveweight) (kg)
N	Number of animals in the group
Nu	Nusselt number
n,m	Exponents in Nusselt number relationships
O	overall error
P	Total atmospheric pressure (Pa)
P_d	total precipitation in the day (mm)

P_h	precipitation in previous hour (mm)
p	parameter describing longwave radiation transfer in the coat (m^{-1})
Q	Heat flux density due to conduction ($W m^{-2}$)
Q_g	Ground heat flux density ($W m^{-2}$)
Q_w	heat conducted through building walls and floor ($W m^{-2}$)
R_n	Heat flux density due to net radiation ($W m^{-2}$)
r	resistance to heat transfer ($s m^{-1}$)
r_a	External resistance to heat transfer ($s m^{-1}$)
r_b	resistance to heat transfer by free convection in the coat ($s m^{-1}$)
r_{CH}	Total resistance to heat transfer through the coat ($s m^{-1}$)
$r_{CH(0)}$	Total resistance to heat transfer through the coat in still air ($s m^{-1}$)
r_d	resistance to heat transfer by conduction through air trapped in the coat ($s m^{-1}$)
r_f	Resistance of floor material (approx. $100 s m^{-1}$ for concrete)
r_{f45}	Resistance of floor for a 45 kg pig with 20% of its surface in contact with the floor
r_H	Resistance to convective transfer through atmospheric boundary layer ($s m^{-1}$)
r_{pt}	Thermal resistance of chicken feathers ($s m^{-1}$)
r_R	Resistance to longwave radiation transfer through atmospheric boundary layer ($s m^{-1}$)
r_R'	resistance to longwave radiative heat transfer through the coat ($s m^{-1}$)
r_s	Resistance to heat transfer through tissue ($s m^{-1}$)
$r_{st,h,L}$	tissue resistance of trunk, head legs ($s m^{-1}$)
r_{stmax}	Maximum tissue resistance of animal trunk (Constricted blood vessels) ($s m^{-1}$)
r_{stmin}	Minimum tissue resistance of animal trunk ($s m^{-1}$)
r_{tt}	Thermal resistance of chicken tissue ($s m^{-1}$)
r_v	Resistance to water vapour transfer from skin surface ($s m^{-1}$)
Re	Reynolds number
S_a	total solar radiation absorbed by ground ($W m^{-2}$)
S_{abs}	Solar radiation absorbed by the animal ($W m^{-2}$ coat surface area)
S_b	Solar radiation on a horizontal surface - direct beam ($W m^{-2}$)
S_d	Solar radiation on a horizontal surface - diffuse ($W m^{-2}$)
S_g	hourly global radiation at earth's surface ($W m^{-2}$)
S_{gt}	Daily total of global solar radiation (MJ)
S_i	Solar radiation intercepted by animal ($W m^{-2}$ of coat surface area)
S_o	Solar constant ($1370 W m^{-2}$)
S_{TOA}	Daily total solar radiation above the atmosphere (MJ)
T	temperature ($^{\circ}C$ or K)
T_1	temperature of summit metabolism ($^{\circ}C$ or K)

T_2	temperature when evaporative heat loss starts to rise (°C or K)
T_a	Air (dry bulb) temperature (°C or K)
T_b	body temperature (°C or K)
T_c	coat surface temperature (°C or K)
T_{deep}	Soil temperature at 1m (Kelvin)
T_g	ground surface temperature (K)
T_{max}	Daily maximum air temperature (°C)
T_{min}	Daily minimum air temperature (°C)
T_{mid}	mean of coat top and skin surface temperatures (°C or K)
T_r	radiant temperature of environment (°C or K)
T_s	skin temperature (°C or K)
T_{sky}	radiant temperature of the sky (K)
$T_{st, h, L}$	skin temperature on trunk, head, legs (K or °C)
T_v	Virtual temperature (K)
T_{vs}, T_{va}	virtual temperatures of skin and air (K)
\bar{T}	mean of skin surface and air temperatures (°C or K)
\bar{T}_{cr}	mean of coat surface temperature and radiant temperature of environment (°C or K)
TCI	Thermal circulation index
t	hour of day (noon = 0)
t_n	time from solar noon
t_w	degree of coat wetness
u	wind speed ($m\ s^{-1}$)
UCT	upper critical temperature (°C or K)
V	Sensible and latent heat flux density transferred by ventilation of building ($W\ m^{-2}$)
V_r	respiration volume ($m^3\ s^{-1}$)
$Y_{t,h,L}$	length of body part (trunk, head, leg) (m)
Z	shade factor (= 1 if in shade, 0 if in open)

GREEK SYMBOLS

α	solar elevation (radians in model)
β	Dimensionless parameter modifying r_{CH} for skin surface area
γ	Psychrometer constant ($66\ Pa\ K^{-1}$ at $0^\circ C$)
Δz	soil depth at which T_{deep} is measured (1 metre)
δ	Solar declination (convert to radians for the model)
ϵ	emissivity
ϵ_c	emissivity of animal coat surface
ϵ_r	mean emissivity of environment

θ	animal orientation to solar beam (0° = head on)
λ	latent heat of vaporisation of water ($\cong 2.5 \times 10^6 \text{ J kg}^{-1}$ at 20°C)
ρ	Density of air (1.0 kg m^{-3})
ρ_c	reflectivity of the animal coat
ρc_p	Volumetric specific heat of air ($1220 \text{ J m}^{-3} \text{ K}^{-1}$ at 20°C)
ρ_g	reflectivity of the ground
σ	Stefan-Boltzmann constant ($5.67 \times 10^{-8} \text{ W m}^{-2} \text{ K}^{-1}$)
τ	Daily Clearness Index, DCI (atmospheric transmittance)
τ_{\max}	DCI when cloud cover is zero
τ_{\min}	DCI when cloud cover is total
ϕ	Latitude of site (convert to radians for the model)
χ	concentration of mass (density) (kg m^{-3})

CHAPTER 1: INTRODUCTION

This chapter provides an introduction to the three major areas of interest in the thesis: climatic change, the energy balance of homeotherms and the effects of thermal stress on livestock. The fourth section draws these diverse areas together, and outlines the aims and methods of work to assess the impact of climate change on the energy balance of livestock in the UK.

1.1 CLIMATE CHANGE

The state of the global climate has received unprecedented attention in the past ten years. Since about 1989, awareness of the possible impact of human activity on the environment has increased significantly, and 'green' issues are now very much in the public consciousness. Perhaps the most wide-ranging concern (in terms of the number of people and activities likely to be affected) is that of climatic change. The idea that human activity in a world reliant on heavy industry can cause a significant impact on the climate of the whole world was not a serious suggestion until about a decade ago. However, the magnitude of the possible impacts of such climate change have propelled climate change research to one of the major world priorities in just a few years. In this section, the causes of, and evidence for, climate change, and the likely impacts of climate change are reviewed.

1.1.1 Evidence and causes of climate change

The global climate is extremely variable on all timescales ranging from seconds to millions of years. The climate is ultimately forced by changes in the balance between the amount of energy received from solar radiation and the thermal radiation emitted by the Earth as a consequence of its temperature (Houghton et al, 1990; IPCC,

1994a). Such energy balance changes are known as *radiative forcing*. Many variations in climate are caused by superpositions of various effects such as the eccentricity of the Earth's orbit, and the angle of inclination of the Earth to the ecliptic, or the plane of the orbit. In the current work, most attention will be given to the impact on climate of changes in the composition of the Earth's atmosphere. All gases in the atmosphere are relatively poor absorbers of short-wave solar radiation, and changing the concentrations of gases has little effect on the solar radiation absorbed. However, some gases are good absorbers of thermal radiation emitted by the Earth, most notably carbon dioxide, methane and water vapour. Increasing the concentrations of these gases results in a decrease in the thermal radiation emitted into space, and therefore a net increase in the global mean temperature. This is the '*greenhouse effect*'. The natural concentrations of gases which enhance the greenhouse effect are such that the global temperature is more than 30°C higher than it would be were these gases absent. Since about 1750, however, largely as a consequence of the Industrial Revolution, human activity such as burning of fossil fuels and intensive farming had, by 1990, raised the concentration of carbon dioxide by 26% and methane by 115% over the pre-industrial levels. This is the cause of the *enhanced greenhouse effect*, and the extent to which such increases affect the global climate, and the possible scenarios of future emissions, are currently of major international concern.

The theory that raised carbon dioxide levels due to human activity are likely to cause a global warming has been in place for more than twenty years. Broecker (1975) suggested that the cooling trend observed from 1940 - 1975 was a natural climatic fluctuation which more than compensated for the increased temperature due to carbon dioxide emissions. Broecker predicted a sharp rise in global mean temperature of about 1°C above the 1900 value by the year 2000. Houghton et al (1990), in the first of a series of major reports on the scientific assessment of climate change by the Intergovernmental Panel on Climate Change (IPCC), stated

"We are certain that emissions resulting from human activities are substantially increasing the atmospheric concentrations of the greenhouse gases.....these increases will enhance the greenhouse effect, resulting on average in an additional warming of the Earth's surface."

This was the first major admission that human activity can have a significant effect on climate.

In addition to increases in greenhouse gas concentrations, there have been increases in sulphur and nitrogen oxide gases, and of atmospheric aerosol (microscopic particulate matter), principally from road transport and biomass burning. Such substances induce a negative radiative forcing by scattering a fraction of the incoming solar radiation, ie. increases in aerosol partially compensate for the increase in global temperature due to raised greenhouse gas levels (Houghton et al 1995). The largest effects of atmospheric aerosol are found over the most industrial parts of the world (ie. Western Europe and North America), as indicated by recent models which include the effect of sulphate aerosol (eg. IPCC 1994a). Volcanic activity, which releases large quantities of sulphur dioxide and ash, also has an effect on global climate. The Mount Pinatubo eruption of 1991 resulted in a temporary reduction in global mean temperature of about 0.5°C for about a year after the eruption (IPCC 1994a). However, the relatively short atmospheric residence time of aerosol means the offset effect is short-lived, and cannot be relied upon to reverse the effects of increased carbon dioxide, methane and other anthropogenic gases, which have residence times of decades.

1.1.2 Assessing results of climate change

Modelling the global climate pattern is an extremely difficult task. The amount of computer power needed to run such models (known as *general circulation models*, or *GCMs*) is a limiting factor on the resolution of the results. The UK Meteorological

Office has run two GCMs with a horizontal resolution of 3.75° longitude by 2.5° latitude. The Transient Experiment (UKTR) examined the consequences of an increase in global carbon dioxide concentration by 1% per year for 75 years, and the Equilibrium Experiment (UKHI) compared the global climate at current carbon dioxide levels with that for a fixed raised carbon dioxide concentration (Viner & Hulme, 1994). The UKHI experiment can be used for a wide range of emissions scenarios, which depend on decisions made by the emitters of greenhouse gases. Several 'standard' emissions scenarios were proposed by Houghton et al (1990), and modified by Houghton et al (1992), to represent possible options for future global emissions activity. The IPCC Scenario SA90 (Houghton et al, 1990) is the so-called 'Business As Usual' scenario, and assumes continued reliance on coal-based energy, leading to an increase in global carbon dioxide emissions from the current value of 7 Gt of carbon per year to 20 Gt per year by 2100. Scenarios B90, C90 and D90 all assume varying degrees of abandonment of fossil fuels; the scenarios are summarised in Table 1.1, in Appendix 1.1. The business as usual SA90 was modified in 1992 to allow for changes in population and economic growth as well as changes in energy use. The main assumptions made in producing these scenarios are outlined in Table 1.1. All the 1990 scenarios assume a constant population and economic growth. IPCC 92a and b gives similar emissions to SA90, as the effects of population increase in the 1992 scenarios almost cancels those due to the decrease in CFC (chlorofluorocarbon) emissions arising from the banning of CFC production.

The initial predictions of the effect of increasing emissions on global climate were made in 1990. Using SA90, the global mean temperature was predicted to increase by about 0.3°C per decade, resulting in a temperature about 1°C above the present value by 2025, and about 3°C above the present by 2100. Sea levels were predicted to rise to about 65 cm above the present level by 2100, due mainly to thermal expansion of sea water (Houghton et al, 1990). The SA90 predictions were confirmed by later models (Houghton et al, 1992), although at that stage the effects of sulphate aerosols were not modelled. By 1995, the balance of experimental evidence suggested a

Table 1.1: Descriptions of emissions scenarios (Houghton et al, 1990, 1992)

SCENARIO	DESCRIPTION
1990 A (SA90): Business-As-Usual	Continue with mainly coal-intensive energy sources - global CO ₂ production rises to 20 Gt carbon per year by 2100
1990 B	Shift from coal to gas as main energy source. Large increase in efficiency of energy generation
1990 C	Shift from coal to renewables and nuclear power between 2050 and 2100
1990 D	Shift to renewables/nuclear 2000 to 2050
1992 A and B (IPCC 92a,b)	Very similar to SA90, but population rises to 11.3 billion by 2100. Fewer CFC emissions.
1992 C (IPCC 92c)	Lowest emissions scenario: lower population growth, transfer away from fossil fuels. Global CO ₂ emission = 5 Gt carbon per year by 2100
1992 D (IPCC 92d)	As IPCC 92c, but restrictions on fossil fuels less strict. Global CO ₂ emission = 9 Gt carbon per year by 2100
1992 E (IPCC 92e)	Highest emissions scenario. Moderate population and economic growth and increase in fossil fuel use. Global CO ₂ production = 36 Gt carbon per year by 2100

Notes:

- 1 Gt = 1 million million tonnes
- Current global CO₂ production = 6 Gt carbon per year

'discernible human influence on global climate' (Houghton et al, 1995). Increased awareness of possible implications of climate change produced many observations which confirmed the existence of climate change. A sixty-kilometre long crack was found in the Antarctic ice shelf (Yorkshire Post, 24 March 1995), and the break-up of the sea ice near the Antarctic Peninsula has continued since. Houghton et al (1995) asserted that climate has changed over the past century, with a global mean temperature increase of between 0.3 and 0.6°C since the late 1800s, and a corresponding sea level increase of between 10 and 25 cm. The warmth of the past hundred years has been confirmed by observations made by the Climatic Research Unit at the University of East Anglia, which show that the last hundred years were the warmest for 1000 years (reported in The Times, 13 July 1995 and 6 January 1996).

Recent GCMs have included the negative radiative forcing effects of sulphate aerosols, and improved the representation of ice melt and the interaction between ocean and atmosphere. The best current estimate is for a 2°C global mean temperature rise, and a rise in sea level of about 50 cm by the year 2100 (Houghton et al, 1995). However, there are still many uncertainties in the predictions. The sensitivity of the climate is one of the main unknowns. Sensitivity is defined as 'the equilibrium change in surface air temperature following a unit change in radiative forcing' (Houghton et al, 1992). Estimates of sensitivity range from 1.5 - 4.5°C, and consequently the predictions of global mean temperature given a certain increase in greenhouse gas concentration are subject to uncertainty. Houghton et al's (1995) predictions can be reduced to a 1°C global mean temperature rise by 2100 if a low emissions scenario (IS92c) and the lowest climate sensitivity are used. There are approximately 100% uncertainties as to the magnitude of radiative forcing caused by sulphate aerosols. Changes in vegetation cover caused by increased carbon dioxide levels may also offset global warming: vegetation is a major sink of carbon dioxide (The Times, 25 October 1996).

A major area of continuing research is the effects of clouds on global energy balance. Changes in cloudiness under a changed climate are extremely difficult to forecast, and

different types of cloud affect the energy balance to different extents. High cirrus clouds are relatively transparent to incoming solar radiation, but absorb thermal radiation well, thus accentuating the greenhouse effect. Thick low clouds reflect more sunlight, and have a temperature similar to the Earth's surface, so resulting in a net cooling. Research at the UK Meteorological Office has shown that increased cloudiness will have an overall cooling effect: only 1% more incoming sunlight must be reflected than at present to offset a temperature rise caused by a doubling of carbon dioxide concentration (reported in *The Times*, 10 July 1995). Predictions of increased rainfall in a warmer world may therefore introduce a negative feedback effect to reduce the global mean temperature. Lack of knowledge of the current state and behaviour of the ocean, and a poor understanding of the atmosphere-ocean coupling, is a source of much uncertainty. One possible consequence of global warming on ocean dynamics is the weakening, migration or reversal of the warm North Atlantic Drift due to increased fresh water input from melting ice (Rahmstorf, 1997). Western Europe would then experience a climate similar to present-day Canada due to local cooling, in contrast to many model predictions which do not include complex ocean dynamics.

The use of global mean temperature to describe future climate masks the wide spatial and seasonal variations in climate predicted by the GCMs. Nearly all models, whether transient (Meteorological Office, 1994) or equilibrium (Viner & Hulme, 1994), predict the greatest warming over the continental Arctic in the northern hemisphere winter. The mean winter temperature in Spitzbergen, for example, is reported to have risen by 9°C in the past 90 years, increasing the occurrence of grasses and flowering plants on once barren land (*The Times*, 23 March 1995). In contrast, summer temperatures in northern high latitudes are not predicted to change significantly. Summers in the UK have not changed significantly over the past 300 years - nearly all the warming has occurred in the winter half of the year (W.J.Burroughs, pers. comm.). The southern hemisphere will experience less pronounced warming due to the thermal inertia of the oceans. Rainfall is predicted to

increase in high latitudes in the winter, and decrease in the summer; in the UK, the already wet north-west will see an increase of 10 - 20% in winter rainfall total, while the south-east is predicted to suffer a fall in summer precipitation of up to 10% (Viner & Hulme, 1994). The implications for water supply are serious.

Changes in the mean value of variables could be accompanied by changes in frequency of extreme values (Wigley, 1988; Easterling, 1989). Due to the nature of the frequency distribution of variables such as temperature and precipitation, changes in the mean values and the corresponding probabilities of extreme events occurring are highly non-linear (Mearns et al, 1984; Wigley, 1985). Mearns et al. analysed air temperature measurements made at Des Moines, Iowa, where the mean daily July maximum is 30°C. They found that the probability of five days in a row with maximum temperatures greater than 35°C increased threefold by increasing the mean by 1.7°C and leaving the variance of the distribution constant at the current value of about 4°C. Wigley (1985) showed that if the mean annual precipitation in England and Wales (920 mm) was to fall by 0.9 standard deviations (100 mm, or 11%), which is feasible from current predictions, a drought with a current return period of 100 years would be expected 7.5 times more frequently. Changing the variance was found to have an even greater effect. The probability of the occurrence of the five hot days in Des Moines rose from 5% at a variance of 2.8°C to 70% at a variance of 5.6°C, assuming the mean remained constant at 30°C. The variance of variables such as rainfall with non-normal distributions changes markedly with the mean. Rainfall distributions are limited at zero, so as the mean decreases, the variance goes down and the skewness rises. Waggoner (1989) used 660 cases of monthly rainfall totals at a wide variety of sites to show that the variance increases with the 1.3 power of the mean. The observed response to changes in variance was confirmed in a theoretical treatment by Katz & Brown (1992). Evidently, under climate change, a combination of changes in the mean and variance will occur which are extremely difficult to predict.

1.1.3 Potential impacts of climate change

Climatic change will have a wide range of impacts in addition to direct effects on weather and sea level described in the previous section. The Second Working Group of the Intergovernmental Panel on Climate Change (IPCC) was responsible for reviewing the possible impacts of climate change on the environment, health and socio-economic systems including agriculture (Watson et al, 1995). Climate change presents a new stress to the global environment, in addition to overpopulation, pollution and resource depletion. Assessing the possible impacts of climate change is a complicated process. The various steps involved are outlined in Section 5.4.2, though the assessment procedure presented relates only to the current work. Other methods of assessment analysis are reviewed in Section 1.4.2.

1.1.3.1 Existing impact studies

The main areas of likely impact of climate change were summarised by Mannion (1995) and Watson et al (1995). The areas of interest can be divided into two main groups: human infrastructure, which includes agriculture, industry, transport, the economy and health considerations, and ecological impacts, which include forestry, hydrology and ecology.

Human infrastructures such as industry and transport are not especially sensitive to changes in mean temperatures or rainfall, but are vulnerable indirectly through change in other areas such as agriculture. Human activities are also vulnerable to increased frequency of extreme events, for example increases in the frequency of violent storms or heatwaves affect quality of life and property (Watson et al, 1995). Water availability, especially in zones which are currently marginal or sub-marginal, such as

the Sahel and the south-western US, is expected to decrease with increased desertification. Changes may occur in the spread of airborne and water-borne diseases, and the frequency of respiratory diseases caused by air pollution. The impact of such climate-forced events is inevitably linked with economic and social considerations. Changes in prices of crops, for example, may cause widespread economic problems in poorer areas, and crop and livestock failures in the developing world will serve to increase the economic imbalance between the 'North' and 'South'.

Conflicts of interest are already arising from the issue of climate change. At the Conference of the Parties (COP1) which signed the UN First Framework Convention on Climate Change (UNFCCC) at the 'Earth Summit' in Rio in 1992, differences emerged as to how far greenhouse gas emissions should be reduced. Small island states in danger of inundation from rising sea levels argued for the tightest controls, while large oil producers were opposed to any further measures. Developing countries such as India and China are opposed to emission reduction measures which are seen as being directed by the West and targeting the poor (Akumu, 1994). As the impacts of climate change become more evident, such disputes can only intensify.

The climate zones suitable for forests, especially the cold forests of Asia and North America, are predicted to move poleward in a warmer climate (Futang, 1993; Watson et al 1995). The impact on the total forested area is not certain. Watson et al and Futang state that the likely movement of the favourable habitat will be faster than most species can migrate, and therefore many species will become extinct. However, Hill et al (1994) modelled the likely movement of British species such as oak and suggested that dispersal would be sufficient to avoid extinction. The movement of insects and other pests will be increased by climate change. A warmer climate in a given area increases the reproductive ability of insects which rely on a certain number of degree-days, allowing more insects to survive over winter than at present, and aiding migration (Kingsolver, 1989; Shuhua, 1993). Harrington (1996) stated that weather is the dominant factor in determining insect populations in the UK. The aphid population in any summer is *exponentially* related to the mean temperature of the

preceding winter, and every degree Celsius rise in mean winter temperature brings forward the first appearance of aphids in spring by about two weeks. The implications for crop cultivation of a climatic change where nearly all the warming occurs in the winter are obvious.

A modification of the hydrological regime in large areas is predicted with changes in rainfall duration and intensity, and with changing temperature. Melting glaciers and changes in runoff and evaporation, which are non-linear with respect to changes in precipitation and temperature, will alter the flow rate and ecology of rivers and lakes (Watson et al, 1995). Hydrological impacts on a regional scale are very sensitive to catchment topography, and to the climate scenario (Reynard & Arnell, 1994). Thus, at present, it is difficult to make accurate predictions of runoff characteristics under a changed climate.

The ecological impacts are linked to the impacts on the human infrastructure. There have been many studies of the impact of climate change on crop production (eg. Seino, 1993; Mavi et al, 1993; Armstrong, 1996). A comprehensive review of various studies of the effects of climatic variability on crops can be found in Harrison et al (1995). Armstrong (1996) concluded that climate change predictions for the UK brought forward the start of grass growth but decreased production later in the year as a greater soil moisture deficit than in the current climate inhibited growth. The effects of water stress are likely to be especially important in southern Europe. Elsewhere in Europe, overall crop growth is predicted to benefit from elevated carbon dioxide and temperature; however, the development of some species (eg broccoli) is stunted by very high temperatures (Harrison et al, 1995). Outside Europe, rising temperatures may not be so beneficial. Extensive research of the impact of climate on rice yields has shown that the rice crop is sensitive to temperature and rainfall. In Japan, the modelled rice yield decreased by 10 - 20% when temperature was increased by 2 - 4°C (Seino, 1993), and a study in the Punjab showed a 2°C cooling from present levels was most beneficial for rice growth (Mavi et al, 1993). Most crop models do

not include the effects of changes in weed populations, or insect or fungal crop pests, so some of the expected benefits of climate change may not be realised. There is therefore a need for integrated models, which simulate the responses of whole systems, to climate change, rather than the responses of single components.

There have been few studies on the possible impact of climate change on livestock. Most have been conducted in the USA, and focus on the effects on livestock of changing rangeland and feed availability under a changed climate. Baker et al (1993) used weather and GCM predictions for the US to drive a grass growth model, which was then incorporated into a livestock production model. The impacts varied between the north and south of the USA. In the northern states, increased forage availability early in the season, plus higher digestibility caused by the slightly higher temperatures, resulted in a 20% increase in calf weaning weight under climate change. However, it was noted that the rangeland ecosystem may not be able to support such a large mass increase. Cattle in the south suffered from poorer feed quality and reduced intake due to hotter conditions, and a consequent reduction of weaning weight of 6% below current values. The economic impact of Baker et al's findings was assessed by Eckert et al (1995); the impact depends both on the climate impact and the numbers of cattle produced in a region. Northern states are predicted to benefit from climate change, but southern states are expected to suffer an 11% drop in market value of rangeland products due to the lower weaning weights. Klinedinst et al (1993) used long-term monthly mean temperatures and humidity and empirical linear relationships between milk production and temperature-humidity index to deduce that milk production would decrease by between 10 and 20% in the south-western US under climate change. Declines in production were predicted to be much less in the north (only 1% in the northern Rockies). Outside North America, nearly all other research on the impact of climate change on livestock originates in countries such as mainland China and Mongolia, where rangeland production plays a large role in the economy. Again, the direct impact of changed climate is not usually modelled explicitly, and impacts are assessed in terms of changed pasture production.

Bolortsetseg & Tuvaansuren (1996) concluded that climate change in Mongolia would adversely affect livestock production as grass growth is predicted to fall with increased desertification of central Asia. Yinsuo et al (1993) also predicted a change to a more arid climate in northern China, with a corresponding decrease in the sustainability of livestock. One solution suggested was to change to different breeds of animal, or to change the dominant species from sheep or cattle to animals such as goats or camels, which are more capable of living in an arid climate. Studies on the impact of climate change on fisheries have suggested associated increases in water temperature will be generally beneficial. For example, freshwater fish in Chinese lakes, subject to a water temperature increase of 2 - 4°C associated with a doubling of atmospheric CO₂ concentration, are expected to extend their period of optimal growth by 1 to 2 months to nearly nine months per year in some cases (Naizhuang & Zhifeng, 1993). In summary, climatic change will have contrasting effects on livestock on regional scales, thus making accurate prediction of impacts using large-scale GCMs difficult.

1.2 ENERGY BALANCE OF HOMEOTHERMS

1.2.1 Introduction to energy balance

Animals which maintain a relatively constant deep body temperature over a wide range of environmental conditions are termed *homeothermic*. Much has been written on the energetics of homeotherms, including several books and conference proceedings (eg. Mount, 1968 on pigs; Monteith & Mount, 1974 and Mount, 1979 on Man and livestock generally; Parsons, 1993 on Man) and there are many books in which energy balance of homeotherms is discussed to some extent (eg. Morris & Freeman, 1974; Gates, 1980; Monteith & Unsworth, 1990, Wathes & Charles, 1994).

Homeotherms, which include Man and most breeds of livestock can only survive over a very narrow range of deep body temperature. In Man, for example, with a normal deep body temperature of about 37.5°C, if the body temperature falls below 35°C, there is the risk of hypothermia, and below 33°C hypothermia is severe (Parsons, 1993). Conversely, body temperatures of 38 - 40°C may indicate fever, and 40°C marks the beginning of hyperthermia, or heat stroke. There are significant temperature variations within the body core. Bianca (1965) found that in cows the temperature in the rumen was about 2°C higher than the rectal temperature due to micro-organism activity in the gut. This anomaly is presumably present in other ruminants. Studies on goats (Jessen & Kuhnen, 1996) compared brain temperature with the temperature of the arterial blood, which is approximately equal to the rectal temperature. They found that the brain temperature was about 0.25°C greater than the blood temperature when the blood temperature was low. However, the brain temperature was about 0.25°C lower than that of the blood when blood temperature was high. The implication is that least variability occurs in the brain, ie. measuring the rectal temperature is likely to overestimate the variability of the core temperature.

In this discussion, 'deep-body temperature' refers to the rectal temperature, which is the most often measured. There are other methods of measuring core temperature such as radiotelemetry from a transmitter implanted within the body core (Lefcourt & Adams, 1996) but such methods are rarely used due to their complexity. In the current research, rectal temperature was assumed to be a good approximation to the temperature in the core of the body.

Homeotherms are generally far more adaptable to their thermal environment than poikilotherms, which do not regulate physiologically their body temperature and thus their ability to function depends on the external environment. However, homeothermy, especially in large mammals such as livestock, may also have detrimental effects. Gordon (1996), from analysis of body temperatures of rodents responding to cellular injury such as toxic ingestion or physical injury, found that

temporary reduction of body temperature aided recovery. In livestock and Man, however, which control body temperature far more tightly, such a response does not occur, resulting in a slower recovery from injury. One implication of Gordon's work is the problem in extrapolating to humans the results of experiments measuring the response of laboratory rodents to drugs and toxins.

In order to maintain the deep body temperature within such narrow limits, a homeotherm must balance heat produced by the metabolism of food with the inevitable exchange of energy with the environment driven by temperature and moisture gradients. The starting point of an analysis of the thermal behaviour of homeotherms is therefore an energy balance: heat production balances heat loss from the animal. The full heat balance equation was given by Alexander (1974) as:

$$M - G_w + R_n = E + C + Q + J \quad [1.1]$$

Terms on the right hand side of Eq 1.1 are the heat loss terms, and the left hand side represents heat production. Each term is defined and discussed below. All terms have units of energy flux, ie. watts, or MJ day⁻¹, and may be expressed as watts per unit area of heat transfer (W m⁻²) provided the area in question is the same for all terms.

1.2.1.1 Metabolic heat production, M

The thermoneutral heat production of a homeotherm is the heat liberated from the metabolism of the feed intake. The thermoneutral metabolic rate is dependent on level of feed intake and species and physiological state of an animal (eg pregnant, lactating etc.). The total metabolic heat production is equal to the thermoneutral

metabolic rate only under a limited range of environmental conditions. In the cold, metabolic rate must increase to match the increasing thermal demand by the environment. In hot conditions, where the environmental demand is less than the thermoneutral heat production, physiological and behavioural responses can be employed to increase heat loss and maintain a constant body temperature, or alternatively heat production can be reduced (eg. by lowering of feed intake). A more detailed discussion of the dependence of metabolic rate on environmental conditions is given in Section 1.2.3. In the following discussion, and the rest of the current work, M is used to represent the thermoneutral heat production, independent of environmental conditions.

For an animal on a maintenance (ie. zero energy retention) diet, metabolic rate M_m is given in watts by:

$$M_m = 3.403 (m_b^{0.75}) \quad [1.2]$$

where m_b = mass (commonly called *live weight*) of the animal (kg) (Gates 1980). For a 100 kg ewe, for example, M_m is about 108 W. For animals with greater intake than maintenance, M is greater than M_m by a factor depending on the efficiency of metabolization. The amount of energy metabolized is given by:

$$M = M_m + (1 - k_e) (M_f - M_m) \quad [1.3]$$

where M_f is the total metabolizable energy and k_e indicates the proportion of the extra intake that is retained by the animal, mainly in the form of fat and protein build-up (Mount, 1979). Mount gave k_e as about 0.7 for most breeds of livestock; hence the proportion of intake above maintenance lost as heat is about 0.3. Lactation and

pregnancy may double the thermoneutral heat production from the values given in Equations 1.2 and 1.3 (Parsons et al. 1995). High intake, mechanical work and fast growth rates also increase heat production.

Thermoneutral metabolic rate is not constant throughout the day, but varies along with deep body temperature and heat loss. The variations are known as circadian rhythms, and have been observed in many mammals (Aschoff et al, 1974). Heat production is related to feed intake, and as a consequence is highest in the daytime. Temperature is also usually highest in the daytime, so the heat production is sometimes greater than heat loss. The body temperature rises slightly, and the excess energy is stored to be dissipated under cooler conditions (see Section 1.2.1.3). At night, with lower temperatures and heat production, heat loss is generally greater than production, and body temperature falls. The circadian rhythms are therefore feed-driven rather than sleep-driven (Aschoff et al, 1974; Mohr & Krzywanek, 1995). The rise in body temperature so caused is not as large as the rises seen under heat stress; the diurnal variations of heat production and loss are usually small enough to avoid the need for any other physiological responses. For example, Jessen & Kuhnen (1996) found that the body temperature of goats varied about the daily mean by only about $\pm 0.5^{\circ}\text{C}$ in summer, and less in winter. The seasonal variation (also observed in pigs, Mount, 1968) implies the diurnal amplitude of air temperature affects body temperature. In man, the largest amplitude of diurnal variation of body temperature occurred at 24°C - above and below this temperature the amplitude is less (Aschoff et al, 1974). The variation in heat production through the day, and the time of maxima and minima depends on the species. Holmes & Mount (1967) found the variation in thermoneutral heat production of pigs varied by about 15% above and below the daily mean in the summer. As for body temperature, the amplitude was less in winter (about $\pm 10\%$). The maximum heat production in pigs occurred at about 3 pm, and the minimum at about 3 am. Bianca (1965) found the maximum heat production in cattle occurred at about 6 pm, due to the greater thermal inertia of the larger animals.

There are three methods generally used to measure M. The first is *direct calorimetry*.

This involves direct measurement of heat loss from the animals, which must be placed in a whole-body calorimeter chamber (Parsons, 1993). Such a procedure is expensive, and exposure to the environment must be sufficiently long to remove the effects of diurnal variations of body temperature. For these reasons, only a few studies measuring heat production by animals have used this method (eg. McLean & Calvert, 1972 on dairy cattle; Timmons & Hillman, 1993 on chickens). The second method is *indirect calorimetry*. The heat production of an animal is widely known to be related to its oxygen consumption (eg. Giles & Gooden, 1993). Oxygen consumption is measured by comparing the fraction of O₂ in the inspired air with the fraction in the expired air. Several methods for the measurement are outlined by Parsons (1993). Indirect calorimetry is relatively simple to perform, and as such is the most common method used for measuring metabolic rates of animals. A third method is the *doubly labelled water* method. This has been introduced relatively recently, and involves injecting known amounts of deuterium and oxygen-18 into the animal and monitoring the passage of the labelled isotopes through the body (Schoeller, 1988). From data on the transport of the injected elements, rates of carbon dioxide and water exchange can be calculated. The relationships between carbon dioxide production and heat production established for indirect calorimetry are then used. The main advantage of this method is its ease - it dispenses with the need for face masks and breathing apparatus used in measurements of gas exchange in standard indirect calorimetry. Schoeller & Hnilicka (1996) showed that the doubly labelled water method produces heat production values accurate to between 3 and 6%.

1.2.1.2 Conduction Q, radiation R_n, convection C and evaporation E

These four terms account for the heat loss from the animal to the environment. The magnitude of all the terms depends on the presence of a gradient: of temperature for G, C and R_n and of vapour pressure for E. Q is usually small except for indoor

animals such as pigs when kept on uninsulated floors (eg. Mount, 1967). The net radiative flux R_n is calculated as the difference between absorbed short wave radiation from the sun and sky, and net longwave radiation loss from the animal. Since incoming short wave radiation can exceed 900 W m^{-2} on a sunny summer day, and the net longwave loss is usually less than about 100 W m^{-2} (Monteith & Unsworth, 1990), R_n is usually positive during the day, ie. the radiative term is a gain, and hence on the left hand side of equation 1.1. Heat flux densities are influenced by the amount of insulation, and the geometry of the animal, as well as by environmental conditions. A full description of all the heat loss terms can be found in Chapter 2.

1.2.1.3 External work G_w , and heat storage J

The metabolic rate measured by indirect calorimetry is actually the metabolic heat production M , plus a term G_w which accounts for external work performed by the animal. The true level of metabolic heat production, M , is therefore the measured value minus G_w . G_w is hard to determine, although measurements have been made on animals performing standard tasks. For example, Close & Poornan (1993) found that a pig increased its heat production above the basal level by 20% by walking 1 km on level ground. Most measurements of rate of external work have been made on humans: tables in Parsons (1993) show the metabolic rate more than doubles under even moderate exercise. Animals in the field obviously do not perform standard tasks, and assessing the magnitude of G_w is difficult for real animal behaviour. G_w is often assumed to be zero owing to inaccuracies in the measurement of M and G_w (Parsons, 1993).

Heat storage, J , is non-zero when the body is not in thermal equilibrium (ie. heat loss \neq heat production). In hot conditions, when heat production is greater than heat loss (eg. in the middle of the day), the energy difference is stored by the body by allowing the body temperature to rise. When the environment cools (eg. in the evening), the

stored energy is dissipated and the body temperature falls to its thermoneutral value. Zhou et al (1996) found that between 17 and 35% of the additional heat produced by walking birds was stored by increasing body temperature. After walking stopped, the birds took 1 - 2 h to lose the excess heat. The timescales are longer for larger animals such as cattle. Very large animals can have extremely long time constants: dead whales, for example, were found to have core temperatures of 28°C (usual value 35°C) eight days after death (Innes, 1986). An animal's body temperature rise associated with heat storage (ΔT_b) can be calculated from:

$$\Delta T_b = \frac{J}{3480 m_b} \quad [1.3]$$

where m_b is the mass of the animal, J is the total energy stored (Joules per unit time) and $3480 \text{ J kg}^{-1} \text{ K}^{-1}$ is the specific heat of body tissue (Tzschentke et al 1996). For example, if body temperature of a 95 kg ewe rises by 0.7°C in one hour, the associated rate of heat storage J is about 65 W, which is a significant fraction of thermoneutral metabolism.

1.2.2 Energy balance of buildings

The energy balance equation 1.1 for animals can also be applied to buildings. Clark & McArthur (1994) gave the energy balance of a building as:

$$M + F_i + R_n = V + Q_w + J \quad [1.5]$$

where M is the heat input from the animals, F_i is the heat energy input from fuel, R_n is the net radiation on the building, V is the sensible and latent heat loss transferred by ventilation, Q_w is the heat conducted through walls and floor, and J is the heat stored due to temperature changes in the animals and building materials. Q_w and J are usually small compared to V over timescales of more than a few hours, in well-insulated buildings. The main heat loss route is by ventilation, driven by mass transfer from the building. F_i and V can be altered to control the interior temperature. The development of the building energy balance for the current work, which was separate from the animal thermal balance, is described in Section 1.4. The target temperature inside the house is the solution to the energy balance equation, and in practice is usually determined by trial.

1.2.3 The metabolic diagram

The effect of environmental temperature on heat production and loss from homeotherms is well-documented. Alexander (1974), Mount (1979) and Gates (1980) all give a schematic representation of the relationship between heat production, heat loss and ambient temperature. A version of the schematic is given in Fig 1.1. In all cases, for thermal balance, the heat production is equal to the sum of evaporative and non-evaporative (ie. convection, long wave radiation, conduction) heat losses. Heat loss and heat production are both represented as positive on the graph. The thermoneutral metabolic rate is governed by feed intake, as explained in Section 1.2.1.1. The *lower critical temperature*, LCT, is the temperature at which heat production balances the heat loss with a maximal value of resistance to heat transfer through the animal's body tissue (ie. blood vessels fully constricted). At the LCT, the evaporative heat flux is minimal. Below the LCT, metabolic rate increases to balance environmental demand. The value of the LCT depends on other environmental

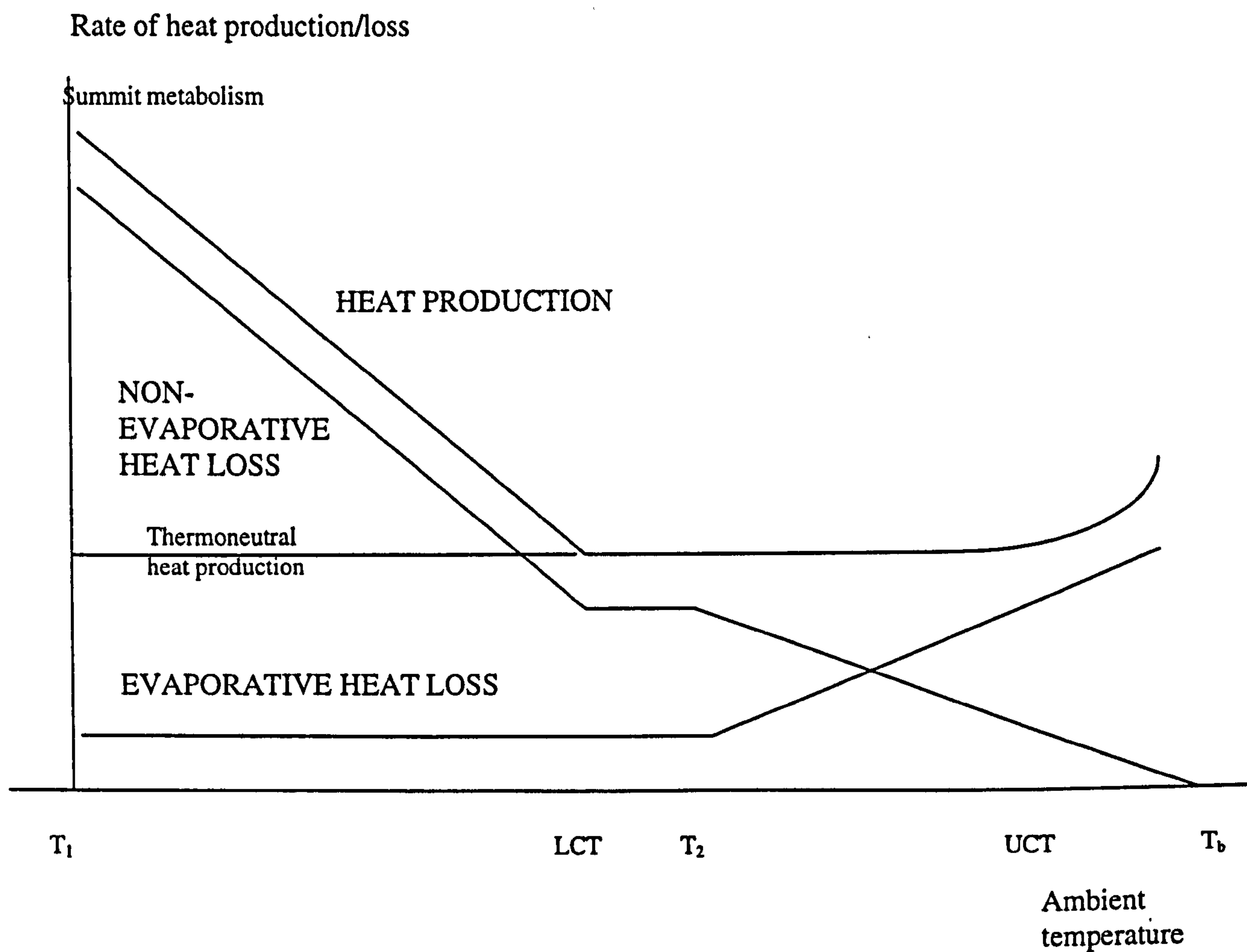


Fig 1.1: Schematic representation of routes of heat loss and production from a homeotherm as a function of ambient temperature

conditions such as wind speed and humidity, and on the thermoneutral metabolic rate, as governed by the feed level. At all other temperatures, the animal has to respond physiologically or behaviourally to maintain energy balance. Such responses are discussed in more detail in Section 2.10, but the general concepts are outlined in this section.

Below the LCT, non-evaporative, or *sensible* heat loss rises as environmental temperature falls. Heat production must increase correspondingly, for example by shivering or by increasing external work, to maintain homeothermy. The heat production reaches a peak at the *summit metabolism*, which is defined as "the maximal rate of heat production that is achieved in response to cold and can be sustained for some time without hypothermia" (Poczopko, 1981). The temperature at which this metabolic rate is reached, T_1 , marks the boundary between the cold zone and the cold lethal zone, where the animal is in imminent danger of hypothermia. The magnitude of the summit metabolism varies between species. Whitmore & Young (1986) found that the summit metabolism of sheep is about 5.5 times the basal level. Some human athletes have summit metabolisms about 7 times the basal value. Bennett (1972) found that the summit metabolism was almost directly proportional to body mass.

Above the LCT, blood flow in the tissue is increased, hence reducing tissue resistance and aiding heat loss (See Section 2.10.1). When the blood vessels reach maximum dilation, the evaporative heat loss must rise to compensate for the falling sensible heat loss (at temperature T_2). The sensible heat loss, driven by temperature gradient, continues to fall above T_2 , and approaches zero when the air temperature equals deep body temperature, T_b . The upper critical temperature (UCT) is defined by some authors as the temperature where deep-body temperature starts to rise, and others define the UCT as the point where metabolic rate starts to rise due to the effort in increasing evaporative heat loss (Mount, 1974). In the current work, the UCT is defined as the point at which T_b starts to rise, principally because this quantity is easier to measure than metabolic rate. Fig 1.1 shows a rise in metabolic heat

production above T_2 when T_b starts to rise, and heat storage becomes non-zero. Between the LCT and UCT, the metabolic rate is minimal, and this temperature range is known as the *thermoneutral zone*.

Fig 1.1 presents an idealisation of the thermoregulatory behaviour observed in animals. Later sections on model validation (eg. Section 3a.6) discuss the differences between real data and the idealised metabolic diagram. However, Fig 1.1 is useful to illustrate the principles of thermal energy balance, and to provide definitions of the various zones of response for homeotherms.

1.3 EFFECTS OF THERMAL STRESS ON LIVESTOCK

1.3.1 Introduction

Knowledge of the thermal status of livestock, and the interaction between animal and environment, is essential in determining an animal's productivity, growth rate, feed intake and ability to bear young. The impact of weather conditions on the thermal balance of animals is well documented. Low temperatures, high winds or wetting of the animal reduces the growth rate (Close, 1987) and the feed intake required for maintenance increases (Thompson, 1973). Combinations of cold wet conditions can cause death from hypothermia (eg. Glass & Jacob, 1991). Hot weather also has adverse effects. Hot conditions reduce feed intake and the digestibility of the food (Bianca, 1965), depress milk production, affect the ovulation cycle and increase embryo mortality (Close, 1987; Bianca, 1965). The water requirement also increases.

In addition to adversely affecting economic productivity, the animal's welfare suffers under thermal stress. In this section, the main effects of thermal stress, both heat and cold, on animals are discussed in order to show the importance of climatic considerations to the productivity and welfare of livestock.

1.3.2 Impact of thermal stress on animals

1.3.2.1 Heat and cold stress

The effects of extreme weather events on the welfare of livestock are well-documented. Animals such as dairy cattle, which have high metabolic rates, can be uncomfortably hot at air temperatures as low as 15°C (Garnsworthy et al, 1993; Macmillan, 1996). The problem of heat stress in livestock has been addressed by the UK Ministry of Agriculture, Fisheries and Food (MAFF, 1995a,b, 1996). The literature contains recommendations for building and ventilation design for indoor animals, and advice on shearing, shade and transportation for sheep and cattle outdoors. The effects on animal well-being can be severe if such recommendations are not heeded. Animals outdoors are vulnerable to cold stress, especially when low temperatures combine with high wind and rain. There are many accounts of sheep dying from hypothermia following cold wet spells. In many cases, a sudden moderately cold event just after shearing or lambing can cause more severe cold stress than a severe cold but dry spell when the animal still has its fleece. For example, Glass & Jacob (1991) reported that more than 11 000 out of 44 000 newly shorn sheep in South Australia died at temperatures above 10°C, due to a combination of high winds and heavy rain. The mortality of calves is inversely proportional to air temperature, and directly proportional to rainfall on the day of birth (Azzam et al, 1993). Above 20°C, however, precipitation had little effect on mortality rates. In hot conditions, heart rates increase due to rise in body temperatures (Whittow, 1971), which puts a strain on the heart and agitates the animal. Engineering failures in animal houses cause much suffering. Poultry World (1996) reported that 70 000 out of 121 000 chickens died of heat stress when the ventilation system in their house broke down, and in another incident 15 000 out of 23 000 died when the humidity rose in the building. Weather also affects animals indirectly through illness. Lameness in cattle is significantly positively correlated ($P < 0.05$) with rainfall in the

previous two weeks, and also negatively correlated with soil moisture deficit - ie. the drier the soil, the less lameness occurs (Williams et al, 1986). Reports in the Veterinary Record show that humid weather following a cold spell resulted in an increase in the population and survival ability of airborne viruses, and cases of respiratory diseases such as pneumonia in cattle; conditions for high disease incidence were most favourable in the indoor environment (VIS, 1988; 1991). In summary, climatic conditions play an important role in the health and general well-being of livestock. In the next section, some of the consequences of lack of well-being are examined.

1.3.2.2 Productivity

The problems associated with extreme environments presented in the previous section have implications beyond welfare. Thermal stress leads to decreased animal productivity, and since profit depends on productivity, an understanding of the thermal balance of animals is important. Thermal stress affects several aspects of an animal's productivity: growth rate, meat, milk and egg production, feed intake and reproduction and pregnancy. Chronic heat exposure modifies the partition between muscle and fat (noted by Close, 1987 in pigs and Ain Baziz et al, 1996 in chickens). High temperatures (greater than 25°C) reduced fat deposition slightly in pigs (Close, 1987; Nienaber et al, 1996). Pigs produce pale soft muscle when exposed to high temperatures for long periods, and the breast to total body weight ratio of chickens is reduced; both affect the market price of meat. The growth rate of chickens in tropical climates decreases when the ambient temperature deviates from the approximate range 15 - 20°C. Egg production is also affected by thermal stress. Payne (1966) noted that increasing temperatures above about 15°C resulted in a steady decrease in egg numbers and size. A high nutrient diet, however, produced optimum production at 30°C, even though the eggs were small. However, no mention was made of the thermal stress suffered by the birds. Birds exposed to a large diurnal temperature

variation were able to maintain egg production even when the daily maximum exceeds 30°C (Smith, 1981). The properties of the eggs themselves are also dependent on environmental conditions. Thompson & Hamilton (1993) found that the outside weather conditions were the principal factor affecting egg weight and shell strength, and found a linear negative correlation ($P < 0.01$ in most cases) between outside air temperature and the breaking strength of eggs. In other words, high temperatures result in significantly weaker eggs. Samara et al (1996) confirmed Thompson & Hamilton's results, further showing reductions of about 7% in egg weight and shell thickness when the daily temperature cycle was increased from 10 - 25°C to 21 - 39°C.

The feed intake of livestock is affected directly by the climate. As air temperature increases, so feed intake falls (Thompson, 1973), a consequence of an increase in digestibility (Silanikove, 1992). Bianca (1965) noted that temperatures of 32°C depressed feed intake in cattle by 20%, and at 40°C intake was depressed by 100%. Silanikove & Gutman (1992), found that beef cattle consumed more concentrate when in heat stress since concentrates liberate less heat when digested than grass, which is ruminated. Similar effects of heat stress are found in non-ruminants: chickens more than halve their metabolizable energy intake when the temperature is raised from -3 - 37°C (Emmans, 1974). The feed intake of pigs was found to fall by between 1 and 1.5 g of food per day per kg body weight per °C temperature rise (Close, 1987). The decline in feed intake with temperature is less marked for heavier animals. Nienaber et al (1996) compared the feeding patterns of swine under non heat-stress conditions with animals in hot conditions which were adjusted to reduce feed intake by 13 and 26%. The heat stressed pigs ate at the same rate and took the same number of meals as the controls, but ate for far less time.

Thermal stress in pregnancy affects different species in different ways. Hot conditions in late pregnancy have no noticeable effect on piglet weight, although the sow may

experience discomfort due to the high metabolic rates associated with pregnancy (Close, 1987). In contrast, the rectal temperature in the ewe must be maintained at thermoneutral levels in late pregnancy to avoid significantly smaller lambs (McCrabb et al, 1993a,b). Similar observations were made in cattle (Moore et al, 1992). In pigs, hot conditions in the *first* three weeks of pregnancy are more serious than the last three weeks, and can increase embryo mortality and decrease ovulation rate. Also, the boar's libido and sperm mobility are reduced at very high temperatures, but the consequences are delayed by up to 4 weeks after exposure to heat. The responses of cattle raised in a tropical environment are somewhat different to those born in higher latitudes. Kabuga (1990) compared responses of tropical-born Friesians and imported Friesians to hot humid conditions in Ghana. The imported animals had the lowest conception rates in the hottest conditions: the diurnal temperature range must be large enough for these animals to dissipate excess stored heat in the cooler periods. In contrast, the tropical-born animals had the highest conception rate in the most thermally-stressful part of the year and there were no significant climatic effects on reproductive ability. The Ghana-born animals had much lower milk yields than the imported cattle, which, along with acclimatisation, was probably the reason for their better heat-tolerance. Lactation declines at high temperatures, but Bianca (1965) concluded that milk yield depression is driven by the fall in feed intake rather than directly by the heat. In the cold, milk yield is also depressed, mainly due to the increased energy requirement on the rest of the body, but also due to local cooling of the udders.

Animals can recover well from thermal stress. Non-livestock species such as rats under hyperthermia have been observed to depress the cold-response, allowing rapid recovery from heat stress; their thermal balance was back to normal within 2 or 3 days (Szelenyi et al, 1996). After a week exposed to temperatures either 5 or 9°C above the optimum, with an associated decrease in growth rate, pigs significantly increased their growth rate above that of animals kept at optimum conditions (Morrison & Heitman, 1982). The rate of gain increased with the severity of the stress episode.

In summary, the effects of thermal stress on animals are many, and an adequate understanding of the interaction between animal and thermal environment is necessary to avoid depression of productivity and poor animal welfare. The importance of accurate forecasts of seasonal weather in planning stocking densities and selling policies, for example, was highlighted by Bowman et al (1995) in a study on wool production in Victoria, Australia. Accurate forecasts leading to adjusting of management strategies led to a 5% increase in returns, but poor forecasts increased costs severely. Analysis of agricultural systems cannot be made from one point of view alone (eg. climatic or economic) - an integrated approach must be used. Part of the next section outlines the nature of modelling of agricultural systems and the necessity for a holistic approach to modelling.

1.4 STRATEGIES AND AIMS

The preceding three sections indicate that

- There is increasing scientific evidence of climate change.
- Climatic change has the potential for wide-ranging impacts.
- To date, most studies of the potential impact of climate change on agriculture have focussed on crops.
- Most species of livestock are homeotherms, which means that they suffer thermal stress when exposed to environmental conditions outside their thermoneutral range.

- The consequences of thermal stress are lower productivity, poor welfare, increased mortality, and an economic cost
- There is a possibility that climate change will affect the productivity of livestock, and the impact on agriculture will indirectly affect many other areas (eg. large population movement through food shortages).
- The likely impact of climate change on livestock systems has not been fully assessed.

The need is apparent for an integrated climate change impact study which includes detailed analysis of the impact of environmental change on the thermal balance of livestock.

1.4.1 Impact of climate change on UK agriculture

This research project, which examines the impact of climate change on livestock energy balance, was commissioned by the UK Ministry of Agriculture, Fisheries and Food (MAFF) as part of a much larger project aimed at assessing the impact of a possible future change in climate on the whole UK agricultural system (Parsons et al, 1995). The results are intended to be used to advise policy-makers of the effects that such climate change would have. As well as the livestock energy balance, the project included models of grass growth, livestock feeding, foraging and livestock housing. There are many complex relationships between these sub-models, and a summary of these is given in Chapter 5. The work described in this thesis relates almost entirely to the thermal balance of livestock. Outputs from other models were used as inputs for the thermal models and the linkages are acknowledged in the thesis without description of the other models. The grass growth model was produced by the

Agricultural Development and Advisory Service (ADAS) (Armstrong, 1996). The models of livestock nutrition and housing energy balance were developed by Silsoe Research Institute, Bedford. Details of all the models can be found in Parsons et al (1997b), Turnpenny et al (1997) and Matthews et al (1997).

1.4.2 Mathematical modelling of agricultural systems

Mathematical modelling is a powerful tool which can be used to quantify and understand the behaviour of biological systems. Among the many benefits, it allows predictions to be made without lengthy field experiments which in some cases cannot be done, for example examining the impacts of climate change. Models can also be used as an aid to decision-making, and allow experimentation with hypothetical scenarios to find answers to 'what if?' questions (France et al, 1984). However, models of biological systems are necessarily complicated, involving links between climatic considerations, physiology and nutrition which are not always well-understood (Bruce, 1993).

There are many different types of models, and a comprehensive review of the types and techniques involved in agricultural modelling is given by France & Thornley (1984). The simplest is generally the *empirical* model, which describes observed behaviour by fitting mathematical relationships to measured data. The simplicity is its biggest advantage, but empirical models are only strictly valid for the set of conditions they were derived from. Extrapolation of results from empirical models can give very wayward predictions. The opposite of an empirical model is a *mechanistic* model, which is based on an understanding of the processes occurring within the system. In modelling all but the simplest systems, the mechanistic model has to work with some simplifying assumptions; the usefulness of the model is dependent on making assumptions which simplify the model without having too much effect on the predictive power. Validation of the model output by comparison with measured data

over as wide a range of conditions as possible is vital in proving the worth of a mechanistic model (Black et al, 1993). Models can either be *static* or *dynamic*. Static models do not contain time as a variable, and can be a good approximation in some systems (eg. in an equilibrium). Dynamic models contain time explicitly, and the resulting differential equations are often complex and must be solved numerically. Every model is also either *deterministic* or *stochastic*. Deterministic models make predictions without an assessment of the likely probability distribution of the results; stochastic models give a predicted value and an associated variance. Stochastic models are more desirable in terms of usefulness of output, but the complexity can be prohibitive, especially when dealing with complex biological systems. Generally, mechanistic models make more effective predictions than empirical models, and the results can be applied more confidently to a wider range of conditions.

There are several possible approaches to describing how a system (eg. the climate itself, agriculture etc.) will change over a given time. The simplest assessment is to use spatial or temporal analogues, by describing the future scenario at a certain location in terms of the current situation at another location, or by comparing future conditions with an event from the past. Cannell & Pitcairn (1993) reviewed a series of studies which assessed the impact of the mild winters and hot summers in the UK from 1988-1990. Extrapolating the findings to a future climate might allow assessment of climate change impact. The method's advantage is that the results are easy to understand, but the response of a system to what is now an extreme weather event (eg. the extremely hot spell at the start of August 1990 [Brugge, 1991]) may be very different to the response if such conditions were more frequent under a changed climate. In other words, adaptation is not included in the analysis. Other factors also change, including economic components such as the price of feed, and changes in breed of animal or strain of crop. An integrated approach is needed which takes account of the interacting components in a system, and interactions outside the system such as profitability, and ease of use of the model in terms of computer time etc. (France et al, 1984; Black et al, 1993). However, a model made up of a system of

sub-models is made less effective by weaker sub-models: great attention to detail in one particular area can produce less accurate results overall when an interacting component is poorly understood and makes low confidence predictions.

1.4.3 Aims and objectives

The main aim of this study was to develop a computer model to assess the impact of climate change on livestock energy balance. The model should represent the heat balance of farm animals (sheep, pigs, dairy cows, beef calves and chickens) in relation to the climatological variables. This model must be mechanistic, based on the physics of heat and moisture transfer and physiology rather than empirical relationships between metabolic rate and weather. The model must output the net thermal energy transfer from the animal (either as hourly or daily values), given the metabolic heat production, which is an output from a livestock feeding model (developed elsewhere). The general form of the model should be common to all breeds of livestock, with facility to change the parameters as required. The model should also include special considerations for particular animals when it is run for the different species.

The model should:

- predict the overall maintenance energy requirements of an animal under specified meteorological conditions over a given period, and
- assess the duration and severity of heat or cold stress likely to be imposed by a changed climate or, alternatively, specify the change in climate likely to produce a risk of thermal stress

Ideally the model should be highly stochastic, since there are many uncertainties associated with climate change scenarios and biological modelling, and some assessment of the accuracy of the predictions would be useful. However, because the whole system is so complicated, a deterministic approach is the only one practicable. The study will aim to provide validation of the model predictions with measured data, and, if necessary, include some empirical tuning. Validation will allow some element of confidence in the predictions without a full stochastic analysis.

The thesis contains seven Chapters. Chapter 2 describes the general concepts involved in the physics of heat transfer, and applies these to the design of a model for a general homeotherm (a unicorn). Chapter 3 contains the adaptation of the unicorn model for sheep and cattle outdoors, along with discussion of considerations unique to outdoor animals such as shelter-seeking. Chapter 4 applies the unicorn model to indoor animals (pigs and poultry). Chapter 5 discusses how the models were set up to run and the steps taken to assess the impact of climate change, including methods for obtaining the data in the correct spatial and temporal resolution. The results of the impact assessment are presented in Chapter 6, along with the sensitivity analysis. Chapter 7 draws the major strands of the project together, and discusses the usefulness and implications of the model predictions, some methods for alleviating thermal stress and adapting to the effects of climate change, and recommendations for future work.

CHAPTER 2: THE ENERGY BALANCE OF A UNICORN

2.1 Introduction

There are several models in existence dealing with animal energy balance (eg. Bakken, 1976; McArthur, 1987 model general concepts applicable to all animals; McArthur and Monteith, 1980a,b; McArthur, 1980; Mount & Brown, 1982; Stafford Smith et al, 1985 modelled sheep; Higgins & Dodd, 1989; Ehrlemark & Sällvik, 1996 cattle; Bruce & Clark, 1979; Bruce, 1981; Hoff et al, 1993 pigs; Bouchillon et al, 1970; Wathes & Clark, 1981a; Gates & Timmons, 1988; Kettlewell & Moran, 1992 poultry). Most of these are either simple empirical models with meteorological data as inputs, or more detailed mechanistic models but with idealised inputs. The aim of the current work was to combine these two approaches and produce a physical model, based on established principles of heat and moisture transfer, to output energy requirements for hourly periods, given the meteorological conditions. In the current work, parameterisations of physical and physiological processes available in existing literature have been used along with new schemes.

The animal heat balance model was developed first for the general case of a unified homeothermic animal (the 'unicorn'), which simulates thermoregulatory responses normally found in farm animals. The aim was to produce a model which could be used to model any farm animal by inputting species or breed-specific parameters. The model was then extended to sheep (whose poor sweating ability simplifies the energy balance analysis), cattle, chickens (indoors) and pigs (indoors and outside). This chapter is concerned with the formulation of the model, rather than detailed discussions of each species; later chapters consider in-depth the particular responses of each animal.

The model was developed to predict the heat loss from a single 'unicorn' in steady state under specified meteorological conditions. The programming language adopted for the model was FORTRAN 77, chosen for compatibility with the other models in the Grassland-Livestock Integrated Model. Thermal balance was assumed for each hour, and each hour was modelled independently of previous hours, following the example of many thermal balance models to date. A summary of the model outputs and input data requirements is given in Fig 2.1, and a more detailed summary is given in Appendix 2.1. Energy inputs are the feed energy, intercepted solar and thermal radiation; outputs are in the form of heat and moisture exchange with the environment (heat transfer is usually from animal to environment), and mechanical work (eg. foraging, shade-seeking etc.). The rates of heat and moisture exchange with the environment are affected by many factors, including coat thickness and fibre density, solar radiation load (itself affected by time of day/year, cloud amount and animal orientation), wind speed, humidity, air temperature and rainfall; these must all be included as model input.

The model requires meteorological data at hourly intervals, as in most cases thermal stress is likely to occur over only a few hours of the day, and would not be predicted by daily mean values of the meteorological variables. One of the problems in the realistic modelling of animal heat balance is the lack of weather stations with long sets of hourly data for the necessary variables, especially solar radiation. Daily solar radiation totals can be estimated empirically from hours of bright sunshine, but a realistic model of the animal heat balance requires mean hourly values of the solar radiation load on the animal. Animal physiology is another major factor to be considered; for example the body insulation, coat insulation, and the sweating abilities of different types of livestock must be modelled, as must human modification of the animal's responses to its environment (eg. shearing of sheep, fattening of animals for slaughter).

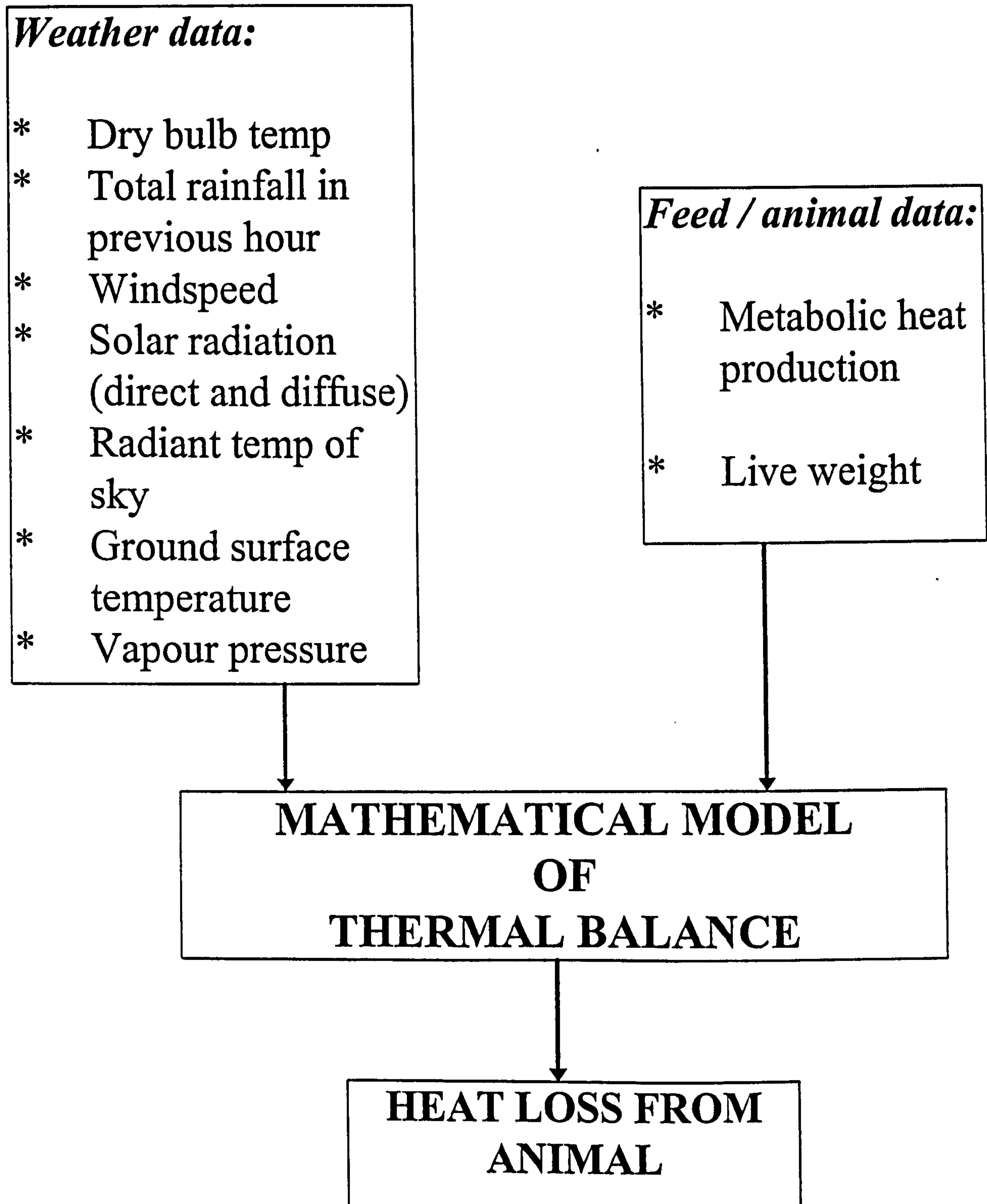


Fig 2.1: Block diagram of inputs and outputs of the thermal balance model

The unicorn model was based on a cylinder with a layer of outer insulation analogous to a hair coat. The model therefore consisted of three layers: the underlying tissue, the coat and the outside environment.

The general flux-difference relationship for rate of heat transfer per unit area per unit time (or heat flux density) through a medium is:

$$HEAT FLUX DENSITY = K_T [TEMPERATURE DIFFERENCE] \quad [2.1a]$$

Heat flux density has units of $W m^{-2}$ and temperature difference has units of Kelvin, so the constant of proportionality, K_T , has units of $W m^{-2} K^{-1}$. The quantity K_T is known as the *thermal conductance* of the medium, or the *heat transfer coefficient*. This is not a physical property of the material, as it varies with thickness of insulation and with the geometry of the surfaces. There are several other units which express the ability of a material to transfer heat. *Thermal conductivity*, k , in $W m^{-1} K^{-1}$, is most widely used in engineering and building design, as it is an intrinsic property of a material and does not vary with thickness (Ede, 1967; McKetta, 1992; Hewitt et al, 1994). It does, however, change with geometry of the surface. Values of k for heat flow through a flat slab range from below $0.02 W m^{-1} K^{-1}$ for air or eiderdown to several hundred $W m^{-1} K^{-1}$ for highly conductive metals (eg. copper or silver). Thermal conductivity is obtained by multiplying thermal conductance by the thickness of material.

Transport of mass (for example water vapour) can also be represented in a similar way to Eq 2.1a, as a function of concentration difference:

$$MASS FLUX = K_M [CONCENTRATION DIFFERENCE] \quad [2.1b]$$

The mass flux has units of $\text{kg m}^{-2} \text{s}^{-1}$, and concentration has units of kg m^{-3} , so the constant of proportionality K_M (the *mass transfer coefficient*), has units of m s^{-1} . The value of K_M depends on the substance being transferred and the distance over which mass transfer occurs. A more common unit is the *diffusion coefficient*, D , which is K_M multiplied by the distance. The quantity D is a function of temperature (see Section 2.4.2) and the substance being transferred. At 20°C , the diffusion coefficient of water vapour in air is about $2.5 \times 10^{-5} \text{ m}^2 \text{s}^{-1}$. Transport of water vapour is the primary example of mass transfer considered in the current work.

Lewis (quoted in Ede, 1967) showed that the mass transfer coefficient is given by the heat transfer coefficient divided by the volumetric specific heat of the fluid. This simple relationship between mass and heat transfer is due to the similarity of the molecular processes for transport of heat and mass (Monteith & Unsworth, 1990). The relationship is extremely useful as it allows conclusions to be easily drawn about heat transfer properties from mass transfer experiments (and vice versa). In summary, the Lewis relation is:

$$K_M = \frac{K_T}{\rho c_p} \quad [2.2]$$

Volumetric specific heat, ρc_p , is obtained by multiplying the density of air, ρ , by the specific heat of air, c_p , which gives a value for ρc_p of about $1220 \text{ J m}^{-3} \text{K}^{-1}$ at 20°C (Gates 1980; Monteith & Unsworth 1990). The inverse of K_M is termed the *resistance* to transport of heat or mass, r , and has units of s m^{-1} . Resistance is used by most animal modellers (eg. Cena & Monteith 1975a,b,c; McArthur & Monteith 1980) as it can be used to describe both heat and mass transfer, and is also useful in describing transfer processes in terms of an electrical analogue. For these reasons, resistances in s m^{-1} were chosen for use in the unicorn model.

Combining Eq 2.1a and 2.2, heat transfer through any medium can then be expressed in a form similar to Ohm's Law:

$$HEAT\ FLUX\ DENSITY \propto \frac{TEMPERATURE\ DIFFERENCE}{RESISTANCE} \quad [2.3a]$$

and Eq 2.1b can be written as:

$$MASS\ FLUX\ DENSITY = \frac{CONCENTRATION\ DIFFERENCE}{RESISTANCE} \quad [2.3b]$$

The constant of proportionality of Eq 2.3a is the volumetric specific heat. The general equation for heat transfer, G ($W\ m^{-2}$) is then:

$$G = \frac{\rho\ c_p\ \Delta T}{r} \quad [2.4]$$

where r is the resistance and ΔT is the temperature difference. The conversion of the mass flux equation 2.3b to a heat flux equation is described in Section 2.4.2.

Fig 2.2 is a diagram of the heat exchange and resistances in the model. The symbols used are defined below:

C = convective heat transfer ($W\ m^{-2}$)

L = net longwave radiative heat transfer ($W\ m^{-2}$)

E = evaporative heat transfer ($W\ m^{-2}$)

T_b = body core temperature (K)

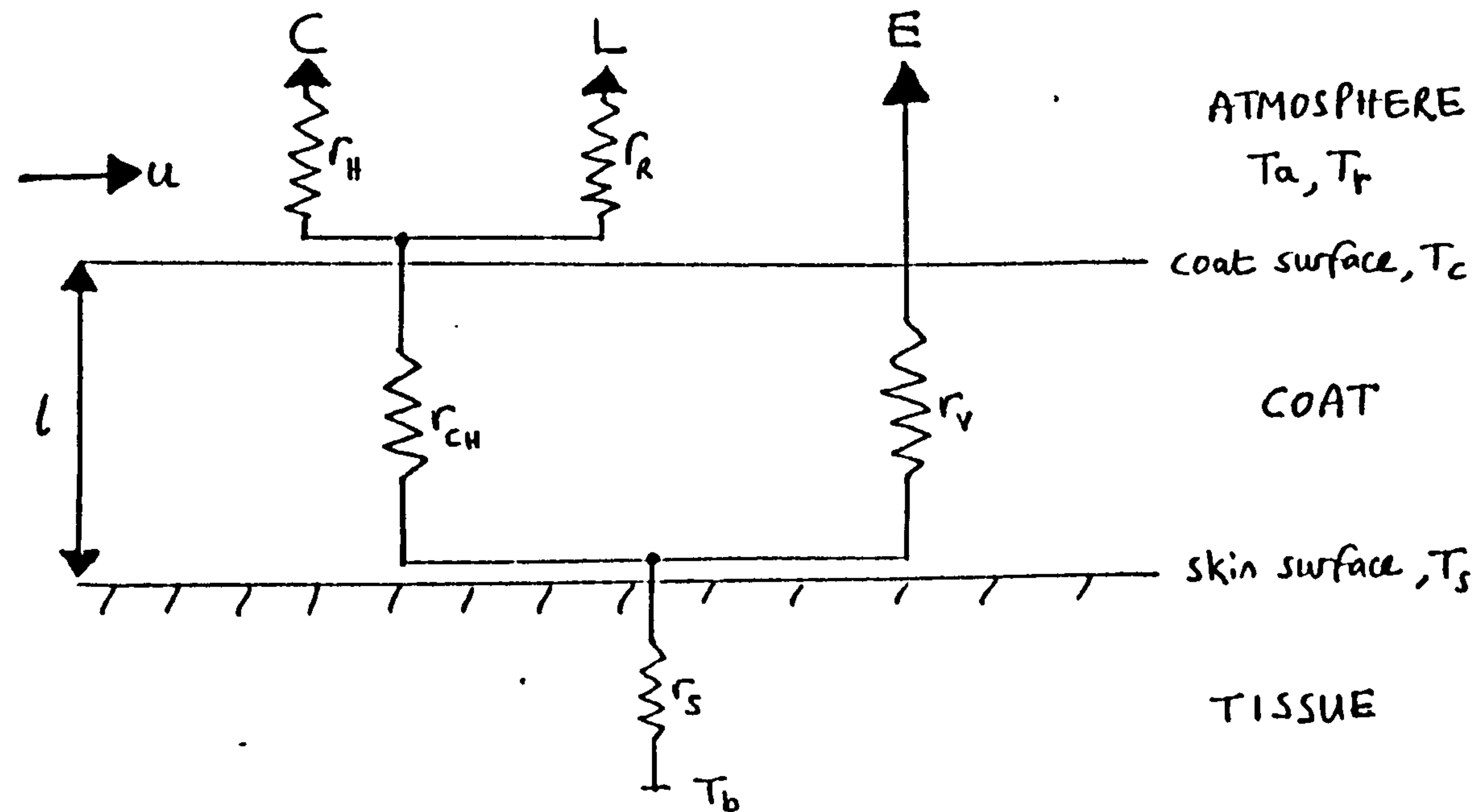


Fig 2.2: Heat exchange and resistances in the three-layer unicorn model

T_s = skin temperature (K)

T_c = coat top temperature (K)

T_a = dry bulb air temperature (K)

T_r = radiant temperature of environment (K)

r_s = resistance to heat transfer through tissue ($s\ m^{-1}$)

r_{H} = resistance to heat transfer through atmospheric boundary layer ($s\ m^{-1}$)

r_R = resistance to longwave radiation transfer through boundary layer ($s\ m^{-1}$)

r_v = resistance to water vapour transfer from skin surface ($s\ m^{-1}$)

r_{CH} = resistance to heat transfer through the coat ($s\ m^{-1}$)

u = wind speed ($m\ s^{-1}$)

l = coat depth (m)

(See symbols list for a full list of symbols and units).

Separate equations were written in the form of Eq 2.4 to describe the heat flows through each of the three layers. The derivation of the transport equations is given in the following three sections.

2.3 Heat flow through the tissue

The total heat loss from an animal, less respiratory losses, must be transferred by conduction from the body core through the tissue to the skin surface. The animal's body core temperature T_b remains constant except in conditions above the upper critical temperature. Values of normal T_b for different homeotherms are quoted widely (eg. Precht et al, 1973; Mount 1979), and range from around 36°C for elephants and camels to 43°C for some birds (eg. hummingbird). For farm animals

the range is smaller, from about 38°C for cattle and sheep to 41°C for poultry. The concept of body core is rather an abstract one; if it is defined as the region of highest and least variable temperature, its diameter varies over different parts of the body. The extent of the body core also varies with environmental conditions. In the cold, the core diameter reduces as blood is brought from the peripheral tissue to protect the homeothermy of the vital organs. In hot conditions, blood transport to the peripheries increases to allow maximum heat loss, and the core region expands. These changes in blood transport affect the resistance to heat transfer through the tissue, r_s . The value of r_s also changes with animal size. Bruce & Clark (1979) proposed that the quantity $r_s/(m_b^{0.33})$ be constant, where m_b is the liveweight (mass) of the animal. The value of the constant varies with species. Blaxter (1967) gave typical values for r_s for different species with blood vessels dilated and constricted. Values for pigs, sheep and cows range from about 50 s m⁻¹ when vasodilated to about 100 to 170 s m⁻¹ when vasoconstricted. The relationship of r_s to mass means that large animals (eg. dairy cows) have larger resistances than small animals (eg. chickens).

The heat flux density per unit skin surface area through the tissue layer, G_s , is given by

$$G_s = \frac{\rho c_p}{r_s}(T_b - T_s) \quad [2.5]$$

2.4 Heat flow through the coat

For most animals, the coat provides the major component of the external insulation, with coat thickness as the main determinant of heat loss. Analysis of energy transfer through animal coats is complicated, due mainly to the inhomogeneity of the medium,

and there have been many studies of the thermal properties of coats and clothing (eg. a review by Kerslake (1972); Cena & Clark (1973, 1978); Cena & Monteith (1975 a,b,c)). Much of the early work on clothing insulation was done during or just after WWII, due to the importance of the applications to military clothing, and the advent of permanent polar scientific bases. In the current model, the heat transfer through this layer has been divided into sensible and latent components.

2.4.1 Sensible heat transfer

Sensible heat transfer processes through the coat are:

- i) Conduction along the fibres
- ii) Forced convection
- iii) Free convection
- iv) Conduction through the trapped air
- v) Longwave radiation transfer between the fibres

The relative importance of each transfer process was discussed by Cena & Clark (1978) and McArthur & Monteith (1980b). Conduction along the fibres is small enough to ignore (Finck 1930, cited in Tregear 1966). The contribution of each of the other processes to total heat flow is about the same, and these have been considered separately in this model.

Heat transfer is driven by the temperature difference across the coat ($T_s - T_c$). While skin surface temperature is relatively easy to measure, the location of the coat surface, and hence the value of T_c and, more importantly, coat depth, is a matter of debate (McArthur & Monteith, 1980a). The various definitions of coat surface location were discussed by Arkin et al (1991). The 'experimental' coat surface and the 'physical' coat surface refer to the closest location to the skin where no hair can be found. This

differs from the 'radiant' coat surface which is the point where temperature equals that measured by an infrared thermometer, and is usually just below the hair tips. The 'convective' coat surface is the location where the velocity profile changes, indicating a change from free air to air trapped between coat fibres. In this model, T_c is assumed to be the temperature measured by an infrared thermometer. Different studies use different definitions of coat surface (eg. Richards, 1977; Joyce & Blaxter, 1964; Stafford Smith et al, 1985 use physical coat surface; Cena & Clark, 1973; McArthur & Monteith, 1980a use radiant surface). Such differences may cause discrepancies when comparing model output with data measured at a different coat surface.

2.4.1.1 Forced convection

Convection is the heat transfer from one part of a fluid to another, or from a solid to a surrounding fluid. The transfer is due to density gradients (caused by temperature or water vapour gradients) in the fluid, movement of the fluid, or both. Free convection occurs when heat transfer due to density gradients dominates over heat transfer due to flow velocity; forced convection occurs when inertial forces due to high fluid velocity dominate. The transition between the two types is termed mixed convection, and is difficult to analyse.

In the model coat, forced convection is parameterised by the relation developed by McArthur and Monteith (1980b) from work by Campbell et al (1980). This proposes that the thermal conductance, K_T , divided by the volumetric specific heat of the fluid (ie. the inverse of thermal resistance, Eq 2-2) increases in direct proportion to wind speed, according to:

$$\frac{\ell}{r_{CH}} = \frac{\ell}{r_{CH}(0)} + c'u \quad [2.6]$$

where l = coat depth (m), $r_{CH}(0)$ ($s\ m^{-1}$) is the coat resistance in still air, c' is a constant (with dimensions of length) and u is wind speed ($m\ s^{-1}$). The parameter c' differs both between species and between different breeds of the same species (Campbell et al 1980). Equation 2-6 was obtained from measurement of heat flow through sheep's fleece. Campbell et al showed that an equation of this form provides a good statistical fit to data for other animal coats. This representation differs from the conclusions of several workers (eg. Joyce et al, 1966), who reported that resistance decreases in proportion to the square-root of wind speed.

2.4.1.2 Free convection

Wind does not penetrate the whole depth of an animal's coat. McArthur and Monteith (1980b) concluded that penetration depth l_w appears to be proportional to wind speed:

$$l_w = \frac{c' u}{\left[\frac{c' u}{l} + \frac{1}{r_{CH}(0)} \right]} \quad [2.7]$$

The simplest development of this proposition is that the convection regime in the coat is split into two distinct layers; in the outer, mixed, layer, (down to depth l_w) temperature gradients are negligible (so T_c is depressed to a distance $(l - l_w)$ above the skin). In this layer, therefore, convection is purely forced. In the lower layer, it is assumed the wind does not penetrate at all, so convection is purely free. The assumption is that the insulation of the outer layer is lost, while that of the remaining

layer depends only on temperature difference. In the current model, l_w is assumed to be constant over the whole animal trunk - this is obviously a simplification as there will be differences in coat penetration between the windward and leeward sides of the animal. There has been very little work on quantifying the magnitude of coat resistance due to free convection, r_b , and most of that available is empirical. From experiments with a model sheep, McArthur (1980) deduced that k_b , the thermal conductivity due to free convection in the fleece is given in $W m^{-1} K^{-1}$ by:

$$k_b = 8.9 \times 10^{-3} (T_s - T_c)^{0.53} \quad [2.8]$$

Buoyancy effects, and hence the magnitude of free convection, vary according to the position on the animal. Equation 2-8 therefore predicts a mean value of thermal conductivity over the whole surface of the animal. The unicorn model requires insulation in resistance units ($s m^{-1}$), and the value of r_b was calculated from k_b (given by Eq 2.8) according to:

$$r_b = \frac{\rho c_p}{k_b} (\ell - \ell_w) \quad [2.9]$$

Combining Equations 2-8 and 2-9, r_b is given by:

$$r_b = \frac{\rho c_p (\ell - \ell_w)}{8.9 \times 10^{-3} (T_s - T_c)^{0.53}} \quad [2.10]$$

2.4.1.3 Conduction through trapped air

The thermal conductivity of air, k_a , is a well-known quantity which can be obtained from standard data tables (eg. in Monteith & Unsworth 1990). The quantity k_a is a function of temperature, and varies by about 15% over the range of temperatures likely to be encountered by an animal in the UK. This variation was parameterised by a linear regression of data in Monteith & Unsworth:

$$k_a = a T_{mid} + b \quad [2.11]$$

where $a = 6.84 \times 10^{-5} \text{ W m}^{-1} \text{ K}^{-2}$, $b = 5.65 \times 10^{-3} \text{ W m}^{-1} \text{ K}^{-1}$ and $T_{mid} = (T_s + T_c)/2$ is the mean temperature of the coat in Kelvin. This analysis assumes a linear temperature gradient through the coat (Cena & Monteith 1975b). This is a reasonable assumption throughout the coat for windless conditions (Gatenby et al 1983a). In windy conditions, T_{mid} represents the mean temperature in the free convection layer - in this case T_{mid} will be half way between the skin surface and the depth t below the outer surface. The standard errors on the regression coefficients were 2-3%.

Converting the thermal conductivity to resistance (as in Section 2.4.1.2) gives the resistance to heat transfer by conduction r_d as:

$$r_d = \frac{\rho c_p \ell}{k_a} \quad [2.12]$$

2.4.1.4 Longwave radiation transfer

Stefan's Law states that the flux density of longwave radiation from a surface, L , is directly proportional to the fourth power of the absolute temperature of the surface:

$$L = \varepsilon \sigma T^4 \quad [2.13]$$

where σ is the Stefan-Boltzmann constant ($5.67 \times 10^{-8} \text{ W m}^{-2} \text{ K}^{-1}$) and ε is the emissivity of the surface. The fourth power relationship is difficult to solve for temperature analytically, so a resistance analogue similar to that for convective heat transfer is used. The resistance to radiative heat transfer in the coat, r_R' , is found from a linearised approximation of Stefan's Law (Cena & Clark 1978), assuming the emissivity is unity (ie. a black body):

$$r_R' = \frac{3 p \ell (\rho c_p)}{16 \sigma T_{mid}^3} \quad [2.14]$$

Cena & Clark (1973) defined a coat penetration parameter, p , which indicates the ease of penetration of radiation through the animal coat. p is the 'projected area of hair on the plane of the skin per unit skin area, for unit depth of coat' (Cena & Clark 1978). p has units of m^{-1} and is proportional to the number of hairs per unit area and the mean diameter of a hair, and also depends on the ratio of coat depth to actual hair length. A

large value of p indicates a low radiative component of thermal conductivity (ie. poor radiation penetration). Typical values are about 500 m^{-1} for sheep, and 1800 m^{-1} for cattle. The high values for cattle are mainly due to the stretched hair length being much larger than the coat depth. Values of p for different animals and breeds are tabulated by Cena & Clark (1973). In order to test the unicorn over a wide range of conditions it was assumed the animal had the properties of a sheep's fleece. This representation of p is valid when considering the mean longwave flux over the whole animal; however local longwave flux varies significantly with angle of emission. Cena & Clark (1973) used a directional radiometer to measure the variation of effective temperature of the coat surface of a sheep with angle to the coat surface. The longwave flux (proportional to the fourth power of effective temperature) normal to the coat was always greater than the flux tangential to the coat. The measured temperature difference (normal minus tangential) ranged from 4 to 23 K, the higher values being obtained under conditions of high net radiation and coat depth.

2.4.1.5 Resistance to sensible heat transfer

The coat resistance in still air, $r_{CH}(0)$, is the result of a parallel arrangement of the resistances due to the due to convection, conduction and radiation (r_b , r_d and r_R') respectively:

$$\frac{\ell}{r_{CH}(0)} = \frac{\ell}{r_d} + \frac{\ell}{r_b} + \frac{\ell}{r_R'} \quad [2.15]$$

The effect of wind (forced convection) is included by combining Eq. 2-15 with Eq. 2-6. Hence, knowing l , r_{CH} can be calculated. Note l is assumed to be constant over the whole trunk.

2.4.2 Latent heat transfer

The analysis of heat flow through the coat also includes a term for cutaneous evaporation, E_c . Evaporative heat loss from the skin may decrease the skin surface temperature, so reducing the heat losses by convection and thermal radiation. At low temperatures (below the animal's lower critical temperature) the evaporative heat loss is small and approximately constant, and is due to vapour diffusion through the skin (Alexander & Williams, 1962; Ingram, 1974; Richards 1974, 1976). At higher temperatures, animals such as cattle increase heat loss by increasing cutaneous evaporation in sweating. The process of transfer of latent heat through coats and clothing has been extensively discussed in the literature (eg. Kerslake, 1972; Cena & Monteith, 1975b; McArthur, 1987; Bruce, 1993). Latent heat transfer occurs in two ways:

- 1) Molecular diffusion of the water vapour, and
- 2) Transfer of the water vapour by convection.

The first process is purely physical, and depends on the gradient of vapour pressure across the coat and the diffusion coefficient of water vapour molecules. The second process depends on the density differences in the coat, caused by temperature and vapour pressure differences, and the air speed. The effects of vapour pressure differences can be included in addition to the effects of temperature differences by substituting *virtual temperatures* in place of the dry bulb temperatures. The virtual temperature of moist air is defined as the temperature at which the air, when

completely dry, would still have the same density. Mathematically, Monteith & Unsworth (1990) give virtual temperature T_v (°C) as:

$$T_v = T \left(1 + \frac{0.38e}{P} \right) \quad [2.16]$$

where T is the dry bulb temperature, e is the vapour pressure (Pascal) and P is total atmospheric pressure (Pascal).

The transfer of latent heat can be expressed by developing the equation for mass transfer given earlier (Eq 2.3b). The concentration difference $\Delta\chi$ (kg m^{-3}) can be written from manipulation of the Ideal Gas Equation as:

$$\Delta\chi = \frac{2.17 \times 10^{-3}}{\bar{T}} \Delta e \quad [2.17]$$

where Δe is the gradient of vapour pressure (Pascals), and \bar{T} is the mean of T_a and T_s .

The latent heat flux density (W m^{-2}) is simply the mass flux density ($\text{kg m}^{-2} \text{s}^{-1}$) multiplied by the specific latent heat of vaporisation of water λ (approximately $2.42 \times 10^6 \text{ J kg}^{-1}$ at skin temperature). The maximum latent heat loss E_{\max} from the skin of an animal occurs when the skin is totally saturated. In the present model, evaporation was assumed to occur at the outer surface of the skin, so latent heat flux depends only on conditions at the skin surface and in the external environment. The maximum latent heat loss therefore occurs when the skin-air difference in vapour pressure is maximal, ie. when the skin is completely wet. Under these conditions, the vapour pressure at the skin surface is the saturated vapour pressure at skin surface temperature, $e_s(T_s)$, and the vapour pressure of the air is denoted by e_a . Combining

Eq 2.3b with 2.17 and letting r_v ($s\ m^{-1}$) be the combined resistance to vapour transfer through coat and external boundary layer, the maximum latent heat flux is given by:

$$E_{\max} = \frac{2.17 \times 10^{-3} \lambda}{\bar{T}} \frac{(e_s(T_s) - e_a)}{r_v} \quad [2.17a]$$

The value of r_v was calculated from a combination of empirical and theoretical work (Cena & Monteith, 1975c), and is given by:

$$r_v = \frac{\ell}{D [1 + 1.54(\frac{\ell}{d_t})(T_{vs} - T_{va})^{0.7}]} \quad [2.17b]$$

where d_t is trunk diameter (m) and T_{vs} and T_{va} are the virtual temperatures of skin and air respectively. D is the diffusion coefficient of water vapour at temperature \bar{T} ($m^2\ s^{-1}$). A linear regression on the data relating D and T in Monteith & Unsworth (1990) yielded the relationship $D = 1.5 \times 10^{-7} \bar{T} - 2.5 \times 10^{-5}$. The temperature T_{vs} was calculated using $e_s(T_s)$ as the vapour pressure in Eq 2.16, with total air pressure assumed standard (101.3×10^3 Pa). The value of $e_s(T_s)$ was found using Tetens' Equation (cited in Monteith & Unsworth, 1990):

$$e_s(T_s) = 611 \exp\left[\frac{17.27(T_s - 273)}{T_s - 36}\right] \quad [2.18]$$

with temperatures in Kelvin. The value of r_v is reduced in windy conditions, enhancing the evaporative heat loss. In the current model, l in Eq 2.17b was replaced by $(l - l_w)$ which limited the resistance to water vapour transfer to the free convection layer within the coat.

An alternative way of writing Eq 2.17a is:

$$E_{\max} = \frac{\rho c_p}{\gamma} \frac{(e_s(T_s) - e_a)}{r_v} \quad [2.19]$$

where γ is the psychrometer constant (Pa K^{-1}). The psychrometer constant is the conversion factor between heat and mass transfer, and is directly proportional to the ratio of molecular weight of air to molecular weight of water vapour. The quantity γ varies with temperature and pressure, and Eq 2.17a is a more complete description of latent heat transfer which was used in the current model.

In the current model, the latent heat loss was initially set to its minimum value, and any increase was due to physiological response to hot conditions (Section 2.10.2).

2.4.3 Total heat flow through the coat

To summarise, total heat flux density per unit skin surface area through the coat, G_c , is given by

$$G_c = \frac{\beta \rho c_p}{r_{CH}} (T_s - T_c) + E_c \quad [2.20]$$

G_e is equal to G_s (Eq 2.5) when the skin surface is in energy balance. The parameter β was defined by McArthur & Monteith (1980b) to modify the resistance r_{ch} to take account of body curvature which makes the coat (outer) surface area greater than the skin area. β depends on coat depth and the diameter and length of the unicorn trunk, and is derived from geometrical considerations of heat flow through concentric cylinders. β is defined with the area of skin surface as the base reference. The skin area is used rather than the area of the coat as metabolic rate is always given in terms of skin surface area; also using coat surface area requires superposition of two functions which change as animal and coat grow. Trunk dimensions, which are incorporated in the model as input parameters in order to make the model as general as possible, can be changed with different livestock and time of year.

2.5 Heat flow to the environment

The total heat transfer from the coat surface to the environment, G_e , is made up of four components as illustrated in Fig 2-2: convection (C), longwave radiation loss (L) and evaporation (E), and a net solar radiation gain (S_{abs}) when an animal is outdoors in sunlight :

$$G_e = C + L + E - S_{abs} \quad [2.21]$$

In this equation G_e is expressed per unit area of coat surface. For animals with short coats (eg. pigs), the difference between the animal's skin surface area and coat surface area is small enough to be ignored, and $G_e \approx G_s$. In contrast, an animal such as the sheep can have a coat surface area twice that of the skin area. For the unicorn model to be applicable to all livestock, the energy balance for the animal must be expressed

in terms of the skin surface area, which is the area used to express metabolic rates. The expression of Eq 2.21 in terms of skin surface area can be found in Section 2.6. Each term in Eq 2-21 is discussed in the following four sections.

Conduction of heat to the ground can also be a factor in the energy exchange with the environment (Gatenby 1977). However, in most outdoor animals ground conduction is incidental and not used actively as a means of regulating heat loss, so this component is ignored in the unicorn. Ground conduction is important in the pig (Mount 1967), and a detailed consideration is given in Chapter 4.

2.5.1 Convection

The equation for the rate of convective heat flow, C (W m^{-2}), is:

$$C = \frac{\rho c_p}{r_H}(T_c - T_a) \quad [2.22]$$

It has been seen that wind speed affects the degree of wind penetration in the coat (Sections 2.4.1.1 and 2.4.1.2), and the resistance of the boundary layer to convective heat transfer, r_H , is also affected by wind speed. An assessment of the type of convection occurring is necessary to quantify this effect. The procedure for the assessment, along with definitions of Reynolds number, Re , and Grashof number, Gr , is given in Appendix 2.2. The value of r_H is directly proportional to the boundary layer thickness, which is determined by wind speed and temperature gradient. However, boundary layer thickness is difficult to measure. Another dimensionless group, the Nusselt number (Nu), is determined empirically from Re and Gr ; Nu is

inversely proportional to boundary layer thickness, and inversely proportional to r_H , so can be used to calculate r_H without needing boundary layer thickness.

For pure forced convection,
$$Nu = A Re^n \quad [2.23]$$

For pure free convection,
$$Nu = B Gr^m \quad [2.24]$$

The values A,B,n and m have to be determined empirically, and vary according to the geometry of the system, and the turbulence of the flow. McArthur (1980) deduced:

$$A = 0.0112$$

$$n = 0.875$$

for the boundary layer around a fleeced model sheep (round-ended cylinder).

For free convection, tables in Monteith & Unsworth (1990) give:

$$B = 0.48, m = 0.25 \text{ for } Gr < 10^9 \text{ (laminar flow)}$$

and
$$B = 0.09, m = 0.33 \text{ for } Gr > 10^9 \text{ (turbulent flow)}$$

for a horizontal bare cylinder (reliable data do not exist for fleeced cylinders). For vertical bare cylinders (eg. the legs) Monteith and Unsworth give

$$B = 0.58 \text{ for laminar flow}$$

and
$$B = 0.11 \text{ for turbulent flow}$$

The mixed convection Nu was calculated by taking a simple average of the Nusselt numbers for free and forced cases under given conditions, assuming that half the time convection is free and the other half forced.

Having calculated Nu, r_H was then calculated as:

$$r_H = \frac{\rho c_p d_t}{k_a Nu} \quad [2.25]$$

where d_t is a characteristic length scale for the system; in this case the diameter of the cylinder.

The convection routine assumed that wind speed was constant; gustiness was not included, as it was assumed that the time constant for the animal to respond was much greater than the time of a gust. Animal orientation was not considered; orientation does not seem to matter very much for heat loss from the animal as a whole, although there are marked variations between leeward and windward sides of the animal (McArthur & Monteith 1980b, Gebremedhin 1987).

2.5.2 Longwave radiation

The longwave radiation transfer between the coat top and the environment consists of two components: outgoing flux at the temperature of the coat surface and incoming flux at the temperature of the surroundings, T_r . Using the representation of Stefan's Law in Section 2.4.1.4, the net longwave flux from the coat surface can be written as

$$L = \sigma [\epsilon_c T_c^4 - \epsilon_r T_r^4] \quad [2.26]$$

where ϵ_c and ϵ_r are the emissivities of the coat surface and the surroundings respectively. The temperature T_r was assumed to depend on two components: the longwave radiation from the sky, emitted at a temperature T_{sky} , and the longwave emitted by the ground, at temperature T_g . In reality, an animal outdoors will be exposed to many different surfaces at different radiant temperatures, each with different areas (eg trees, buildings, other animals etc.). Integral calculus is needed to calculate T_r in such conditions, and it was considered too complicated to introduce variations in view factors for different surfaces, which will change constantly.

The temperature T_{sky} depends mainly on the cloud cover fraction and the air temperature. When the sky is completely covered with low cloud, T_{sky} is almost the same as T_a ; however, under clear skies T_{sky} can be 20 K below T_a (Stafford Smith et al, 1985). An empirical formula to calculate T_{sky} is presented in Chapter 5. The temperature T_g was assumed initially to be equal to T_a , but to cater for conditions of high solar radiation input, or clear night sky, a ground energy balance subroutine was used to solve for T_g (Chapter 5). The value of T_r was then calculated from the arithmetic mean of the upward and downward longwave components impinging on the animal, assuming a horizontal cylinder receives half its longwave radiation input from the ground and half from the sky:

$$T_r = \{(T_g^4 + T_{sky}^4)/2\}^{0.25} \quad [2.27]$$

To simplify computation complexity caused by the fourth power relationship [Eq 2-26], the thermal radiation term was approximated to a linear form, as for the radiative transfer through the coat. The emissivities of both coat surface and environment were assumed to be unity (Gates, 1980; Monteith & Unsworth, 1990). This assumption gives maximum errors in long wave radiation flux of about 3%. The net thermal radiation from coat to environment is given by

$$L = \frac{\rho c_p}{r_R} (T_c - T_r) \quad [2.28]$$

where radiative resistance of the boundary layer is given by:

$$r_R = \frac{\rho c_p}{4\sigma \overline{T_{cr}}^3} \quad [2.29]$$

from the linearisation of the Stefan's Law. The temperature $\overline{T_{cr}}$ is the mean of the coat surface temperature and the radiant temperature of the environment. The dependence of resistance to radiative exchange on the coat surface to environment temperature difference was estimated by iteration to reduce the errors due to the linear approximation of thermal radiation exchange.

2.5.3 Evaporation

Evaporation from the body usually occurs at the skin surface (except when the animal is wet by rain etc.), so the evaporative heat flux density per unit skin area, (E_e , $W m^{-2}$), is the same at the coat surface as at the skin surface. However, in Eq 2.21 the evaporative heat flux density must be expressed per unit coat surface area. The evaporative heat flux density at the coat surface, E_e' , is simply E_e multiplied by the ratio of skin to coat surface area. For a non-sweating animal, E_e' is a small constant (Section 2.4.2).

Evaporative heat loss also takes place from the respiratory tract. Air is expired, almost saturated at deep body temperature (McLean, 1974), and the resulting difference in vapour pressure between inspired and expired air (Δe , Pascals) creates a flux of latent heat (E_r) proportional to the vapour pressure difference:

$$E_r = \frac{\rho c_p g_v}{\gamma} \Delta e \quad [2.30]$$

where g_v is the conductance to vapour transfer (m s^{-1}). In Eq 2.30, E_r is expressed as a flux per unit skin area; for inclusion in Eq 2.21, E_r must be multiplied by the ratio of skin to coat surface area to give E_r' , the respiratory evaporative heat flux density per unit coat area.. The quantity g_v is directly proportional to respiration rate (Knapp & Robinson, 1954; Hales & Webster, 1967; McArthur, 1987). Values of E_r for an animal below its thermoneutral zone vary from about 5 - 10 W m^{-2} for sheep and lambs (Alexander, 1974), to 10 - 15 W m^{-2} for cattle (McLean, 1963) and about 20 W m^{-2} for pigs (Morrison et al, 1967). These figures are approximate due to the dependence of E_r on the vapour pressure of the inspired air. The apparent difference in E_r between species may not be real, due to the wide variation in measurements of resting respiration rate between animals of the same species.

The total evaporative heat flux density per unit coat surface area from the animal is $E' = E_r' + E_c'$.

2.5.4 Solar radiation

The solar radiation is an important term in the energy balance equation. The total solar load incident on the animal, S_i , was calculated from the diffuse and direct solar radiation on a horizontal surface, S_d and S_b , and the reflectivity of the ground, ρ_g :

$$S_i = \frac{\rho_g (S_b + S_d)}{2} + \frac{S_d}{2} + \frac{A_h}{A_c} S_b \quad [2.31]$$

The load S_i consists of three components: the diffuse sky radiation, the radiation reflected from the ground and the direct radiation. The factor of $1/2$ accounts for the assumption that, over the whole animal, the diffuse and reflected components each strike half the animal surface area. Radiation reflected from the ground impacts mainly on the lower half of the cylinder, and diffuse from the sky impacts mainly on the top half. The direct component S_b is multiplied by a dimensionless shapefactor A_h/A_c , the ratio of the area of shadow cast by the animal at a given solar altitude and animal orientation (A_h) to the total surface area (A_c). The shadow area depends on the geometry chosen for the model. In this case a cylinder with round ends produces the smallest errors when compared with data for live animals (Suarez 1988, Gannon 1996). The full expression for A_h/A_c is given in Appendix 2-3.

The radiation load absorbed by the animal, S_{abs} , is then:

$$S_{abs} = (1 - \rho_c) S_i \quad [2.32]$$

where ρ_c is the reflectivity of the coat. The absorption of solar radiation was assumed to take place at the coat surface; this is a reasonable approximation adopted by many modellers (eg. Mount & Brown, 1982; Stafford Smith et al, 1985), and avoids the additional complexity required to model coat penetration and progressive absorption within the coat (eg. McArthur, 1987). A comparison between the current model and a model which includes solar radiation penetration into the coat is made in Chapter 3.

2.5.5 Total heat flow to the environment

Each term in Eq 2.21 (other than absorbed solar radiation), can now be written in terms of temperatures and resistances. Using the prime notation to distinguish between flux per unit skin and coat surface area, and substituting the results from the previous four sections in Eq 2.21, the rate of heat flow from coat surface to environment per unit coat area, G_e' is given by:

$$G_e' = \frac{\rho c_p}{r_H}(T_c - T_a) + \frac{\rho c_p}{r_R}(T_c - T_r) + \frac{A_s}{A_c}(E_r + E_c) - S_{abs} \quad [2.33]$$

2.6 Energy balance for the system

The heat flux densities in $W m^{-2}$ through each of the three layers are given by Eq 2-5, 2-20 and 2-33. The heat balance of the animal was solved by using the law of conservation of energy, assuming that no heat was stored in any of the three layers. The rate of energy flow (in Watts) through each layer was assumed equal, ie. the system was in a steady state. The equations for the heat flux densities through each layer can be equated provided they all refer to the same area. Eq 2.33 was multiplied by the ratio of coat to skin area to express heat flux density from coat top to environment in terms of skin area, G_e :

$$G_e = \frac{A_c}{A_s} \left\{ \frac{\rho c_p}{r_H} (T_c - T_a) + \frac{\rho c_p}{r_R} (T_c - T_r) + \frac{A_s}{A_c} (E_r + E_c) - S_{abs} \right\}$$

[2.34]

Equations 2-20 and 2-34 were then combined as follows. Eq 2.34 can be written:

$$G_e = \frac{A_c}{A_s} \left\{ \frac{\rho c_p}{r_H} (T_s - T_a) - \frac{\rho c_p}{r_H} (T_s - T_c) + \frac{\rho c_p}{r_R} (T_s - T_r) - \frac{\rho c_p}{r_R} (T_s - T_c) - S_{abs} \right\} + E$$

[2.34a]

but from Eq 2.20,

$$(T_s - T_c) = \frac{(G_c - E_c) r_{CH}}{\beta \rho c_p} \quad [2.34b]$$

and $G_c = G_e$ for thermal balance. Substituting Eq 2.34b into Eq 2.34a and gathering terms in G_e gives:

$$G_e + \frac{A_c}{A_s} \frac{(G_e - E) r_{CH}}{\beta} + \frac{A_c}{A_s} \frac{(G_e - E) r_{CH}}{\beta} = \frac{A_c}{A_s} \left[\frac{\rho c_p}{r_H} (T_s - T_a) + \frac{\rho c_p}{r_R} (T_s - T_r) - S_{abs} \right] + E$$

[2.34c]

Multiplying out both sides and making the left hand side in terms of G_e only gives the total heat flux density per square metre of skin area as:

$$G_e = \frac{\frac{A_c}{A_s} \left\{ \rho c_p \left[T_s \left(\frac{1}{r_H} + \frac{1}{r_R} \right) - \frac{T_a}{r_H} - \frac{T_r}{r_R} \right] - S_{abs} \right\} + E \left[1 + \frac{A_c}{A_s} \frac{r_{CH}}{\beta} \left(\frac{1}{r_H} + \frac{1}{r_R} \right) \right]}{1 + \frac{A_c}{A_s} \frac{r_{CH}}{\beta} \left(\frac{1}{r_H} + \frac{1}{r_R} \right)}$$

[2.35]

The energy balance equation 2-35 cannot be solved directly, as the resistances to heat and moisture transfer through the various components (coat, air etc.) depend on the environmental conditions. For example, section 2.4.1.2 shows that r_{CH} is a function of T_s and T_c , which means that an analytical solution cannot be found. A complicated iteration procedure was necessary to solve the equations. The most efficient (ie. computationally cheap) method of solution is to use iteration techniques. The analysis started from assumed input values, and the iteration continued until stable values of skin and coat surface temperature were obtained, with the corresponding heat flux density. The result obtained for G_e was automatically checked with the final values for G_s and G_c . These should be equal if the model had closed properly.

2.7 Running the energy balance model

The unicorn model was run initially using parameters appropriate to the sheep as test data (see Chapter 3 for details). The aim of these runs was to test the relative sensitivity of the model to different inputs (eg. wind speed, coat length, solar radiation etc.). Black et al (1993) stressed the importance of testing a model over as wide a range of conditions as possible, and also made the distinction between model testing and model validation. Testing involves checking that output is mathematically correct; evaluation involves comparing output with real data and assessing the accuracy of prediction. For obvious reasons, the general unicorn model can only be

tested. Representative results of these runs are presented below, and show the relative importance of different parts of the model.

2.7.1 TEST 1: Bare cylinder

Fig 2-3 was obtained by running the model without a coat for values of T_a between -20°C and $+35^{\circ}\text{C}$, with fractional cloud cover of 0.5, and a wind speed of 0.1 m s^{-1} , corresponding to pure free convection. Evaporative heat loss was taken as a constant of 10 W m^{-2} , and solar radiation was set to zero. The core temperature used was that for sheep (39°C). The other inputs to the model can be found in a table of standard inputs for the unicorn and the other livestock in Appendix A at the end of the thesis. Fig 2.3 reveals a non-linearity in the convective heat loss component which is not observed in conditions of pure forced convection; the non-linearity is the result of changes in resistance to convective heat transfer r_H with temperature difference ($T_s - T_a$). Radiative resistance also depends on the radiant temperature difference (Eq 2.29), so the radiative component is also non-linear, but the curvature is in the opposite direction to the convective heat transfer tendency. Combining radiative and convective transfer, these two opposing effects almost cancel, producing a near-linear relationship between sensible heat loss against T_a .

2.7.2 TEST 2: Free and forced convection: the effect of wind speed

The model was run under still air and under windy conditions to demonstrate the effect of wind speed on heat loss from the cylinder. The range of air temperatures was from $-10 - 35^{\circ}\text{C}$, T_b was a constant 39°C and fractional cloud cover was 0.5, with solar load again zero and evaporative heat flux 10 W m^{-2} . The results are shown in the figures 2-4 and 2-5. The model run producing figure 2-4 assumed a wind speed of 7 m s^{-1} and a coat length of 70 mm. The lower end of the temperature range,

Fig 2.3: Components of heat loss against ambient temperature from a bare cylinder

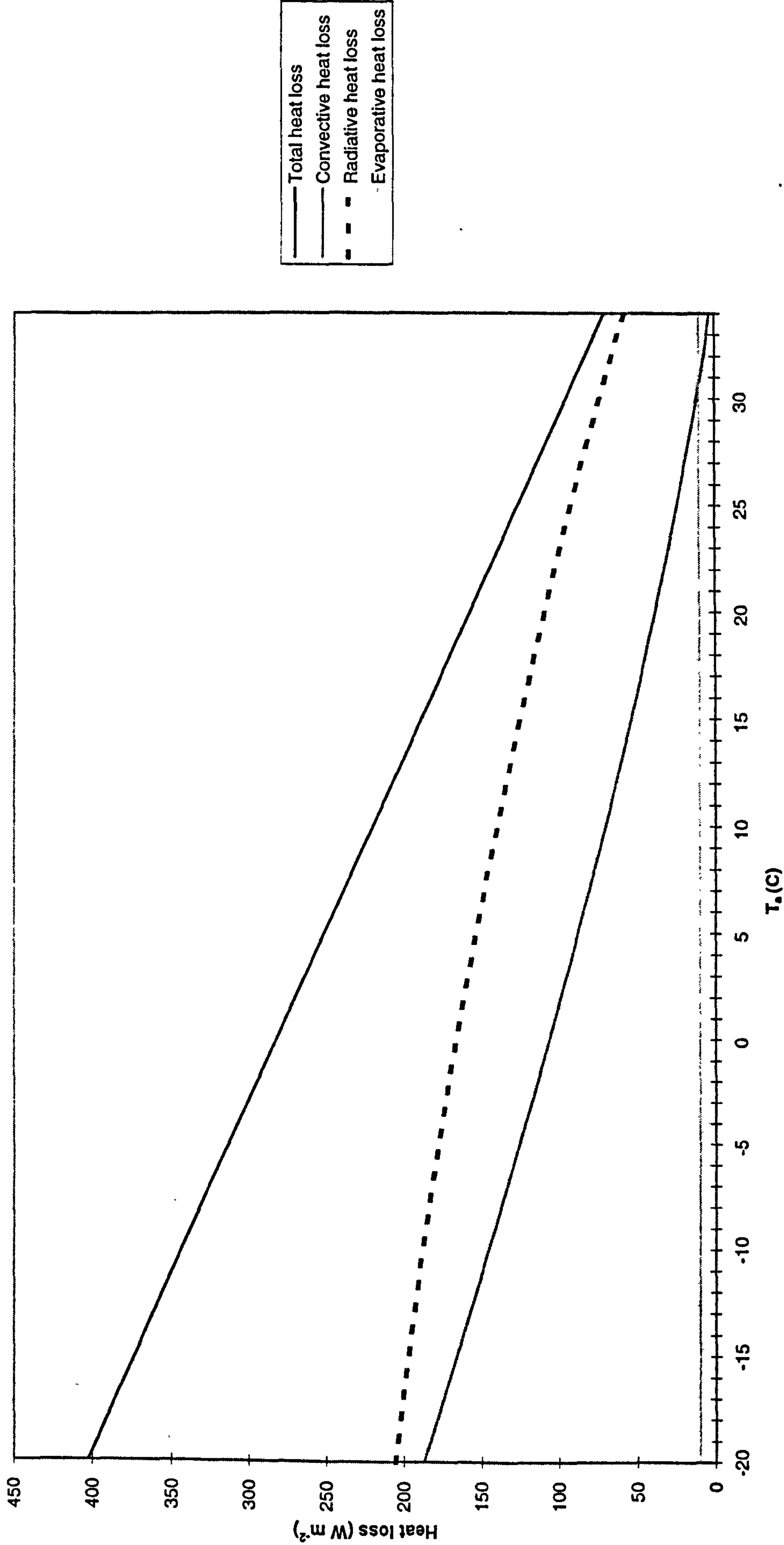
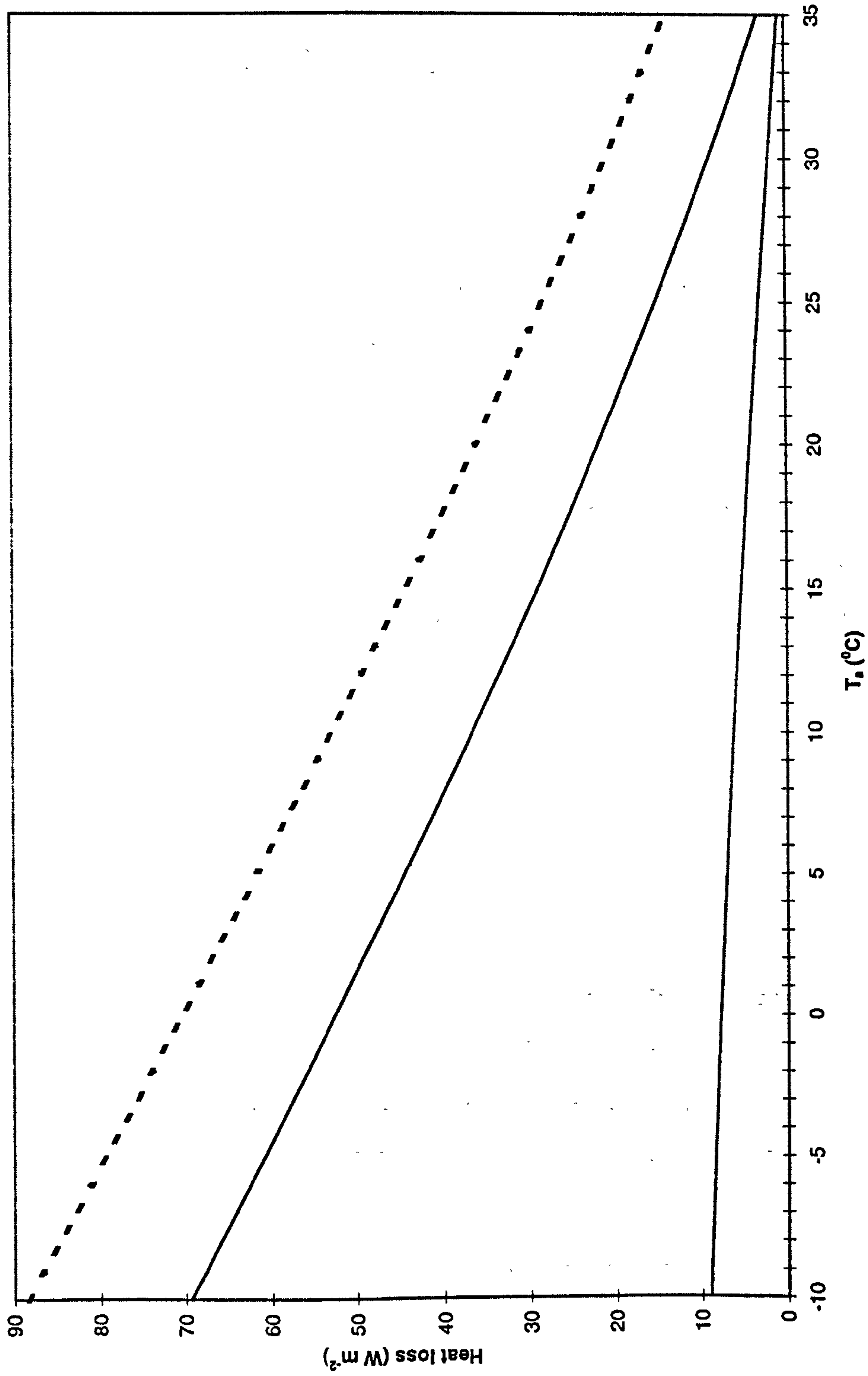


Fig 2.4: Components of heat loss from a coat-covered cylinder under forced convection



— Convective heat loss
— Radiative heat loss
- - - Total heat loss

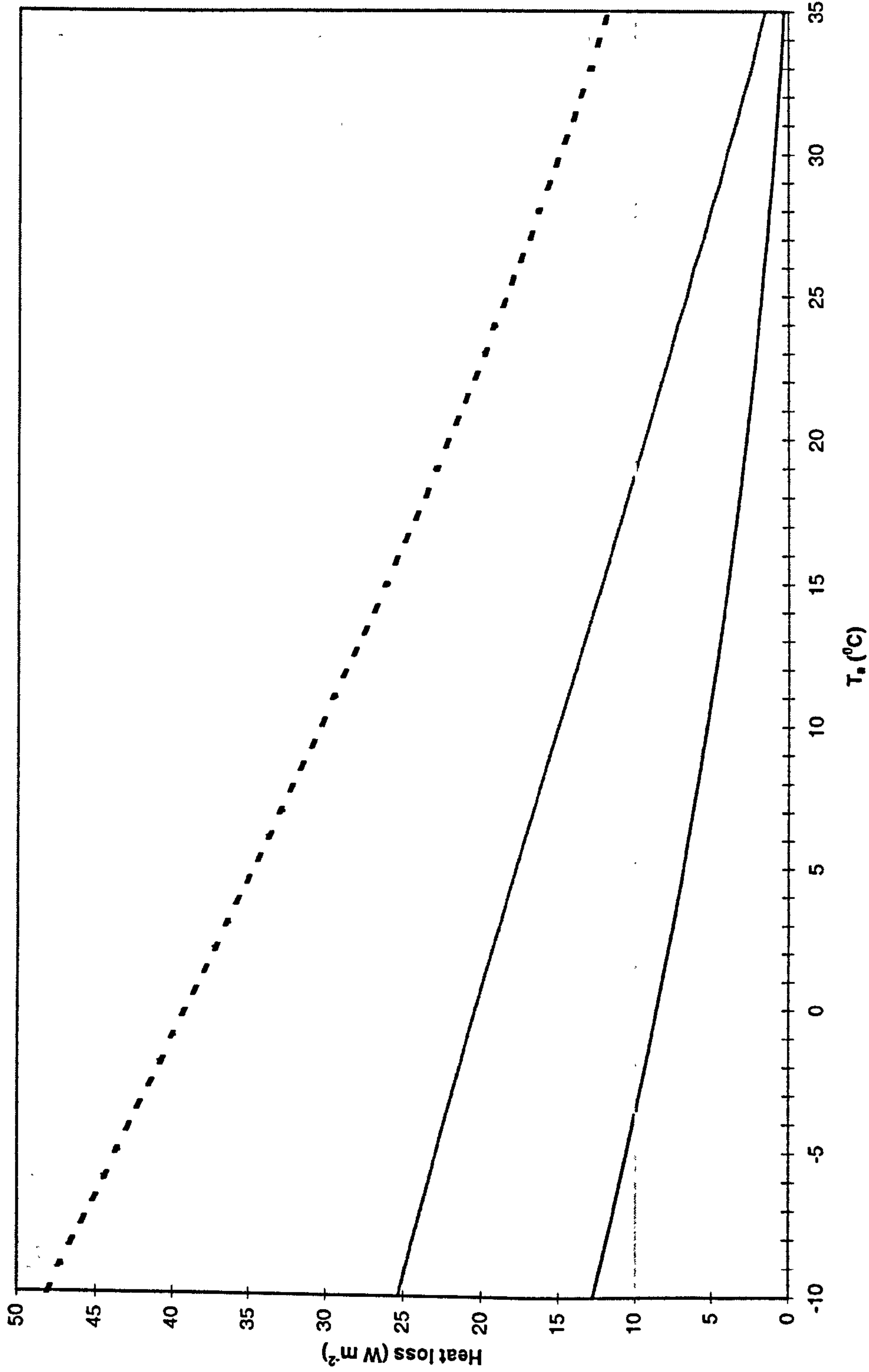
combined with forced convection and a thick coat, simulate a sheep in winter. A thick coat is an effective insulator: the rate of heat loss of 70 to 80 W m⁻² between 0 and -5°C is about a quarter of the loss which occurs at the same temperatures without the coat (Fig 2-3). In forced convection r_H is not a function of temperature, but the temperature difference ($T_c - T_a$) falls with increasing air temperature due to the 'animal' maintaining a core temperature of 39°C. Convective heat loss therefore decreases with increasing air temperature. The slight departure from linearity (ie. a slight dependence of convective heat loss on temperature) was caused by the presence of free convection in the coat. Even at $u = 7 \text{ m s}^{-1}$ the wind only penetrates about 30 mm into the coat, hence the zone of free convection is about 40 mm deep.

Figure 2-5 shows the heat loss, again with a coat length of 70 mm, but with wind speed low ($u = 0.2 \text{ m s}^{-1}$). Such conditions of free convection with a thick coat give rise to the possibility of heat stress at high T_a . Above about -3°C, convective heat loss is less than the evaporative heat loss, even with E taken as a constant 10 W m⁻². This effective removal of one of the heat transfer processes means that the total rate of heat loss is small (less than 25 W m⁻², of which 10 W m⁻² is evaporation) at T_a above about 20°C. In such conditions an animal would have to dissipate significant amounts of heat by evaporation either from the respiratory system by panting, or by sweating, to maintain homeothermy.

2.7.3 TEST 3: Effect of solar radiation

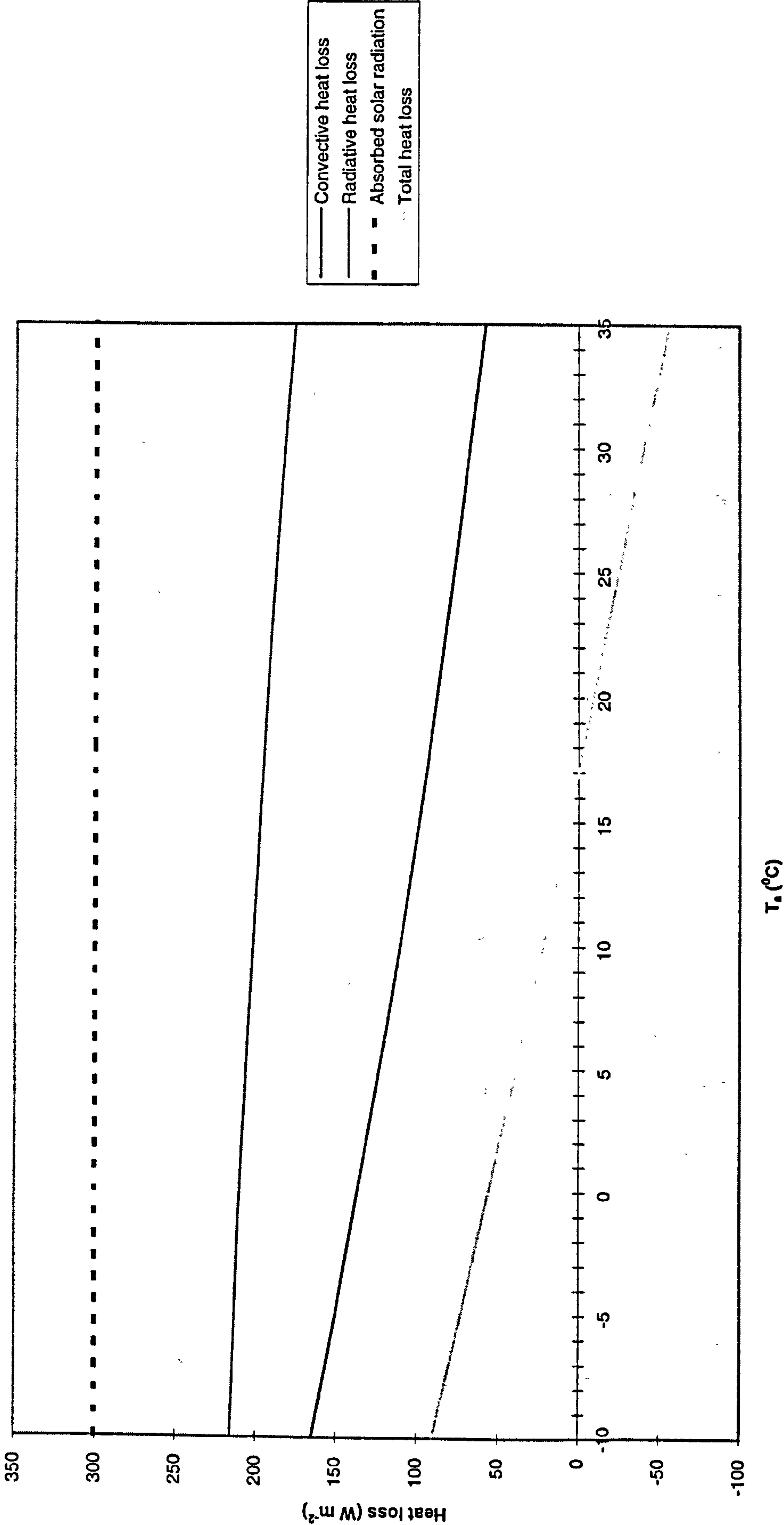
The first part of this test investigated the effect of a constant solar radiation load on heat loss over a range of air temperatures (-10 - 35°C). The only inputs needed to calculate S_{abs} were the day of year (29 June), time of day (noon) and the cloud cover (zero) and albedo of the unicorn's coat (0.26 - assuming a unicorn is white but dirty). Other inputs were: coat length = 5 mm, wind speed = 0.2 m s⁻¹ and evaporative heat flux = 10 W m⁻². Fig 2-6 shows the results of this test. It can be seen that amount of

Fig 2.5: Components of heat loss from a coat-covered cylinder under free convection



— Convective heat loss
— Radiative heat loss
- - - Total heat loss
... Evaporative heat loss

Fig 2.6: Components of heat transfer from a coat-covered cylinder under a high solar load



solar radiation absorbed (S_{abs}) is an extremely important component of animal energy balance outdoors in sunny conditions, even at high latitudes (eg. Clapperton et al 1965; Suarez 1988). The absorbed solar load of about 300 W m^{-2} is about four times maintenance heat production for a sheep and three times maintenance for a dairy cow, and above about 15°C the total heat loss becomes negative, ie. heat flow is from environment towards core.

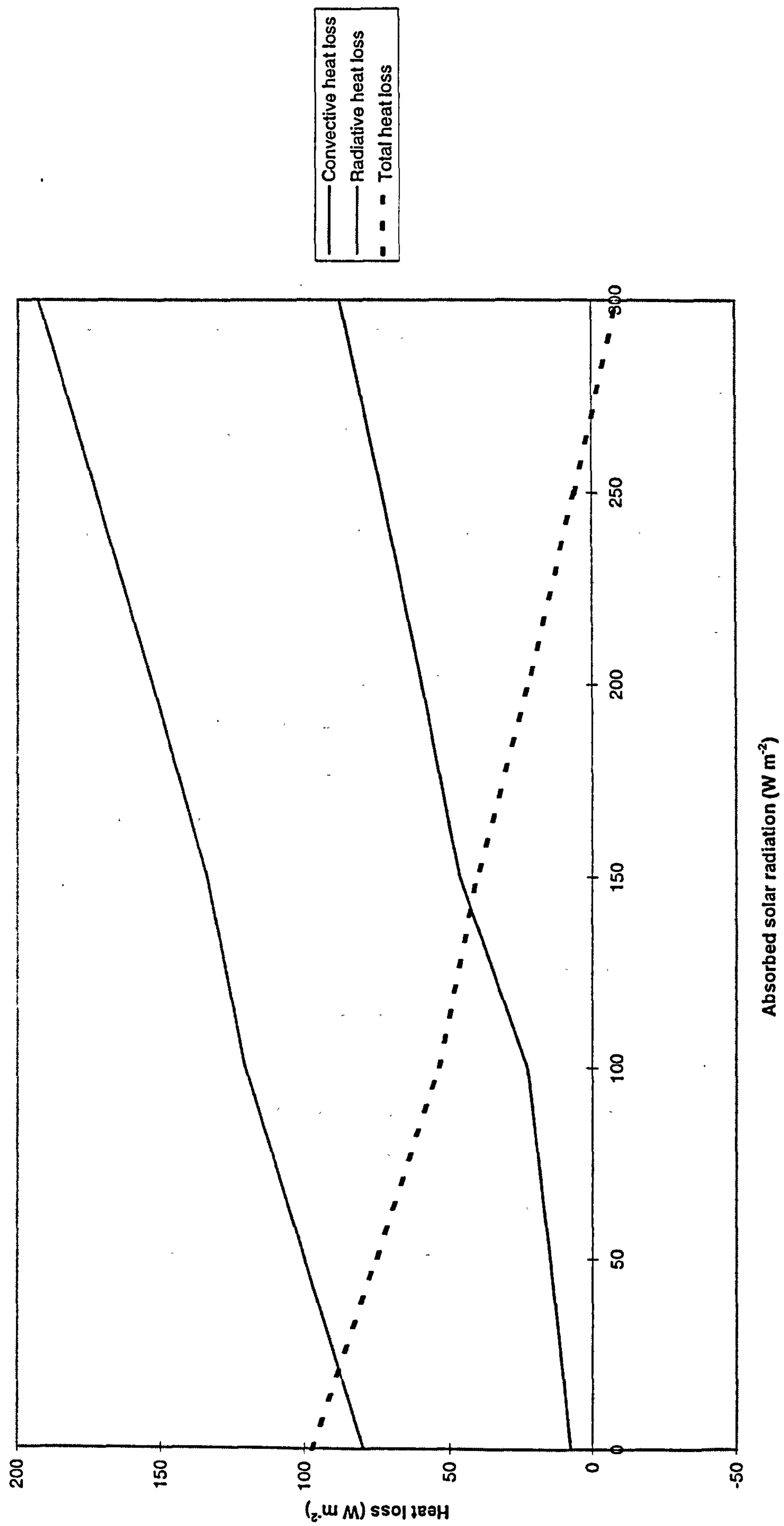
The second part of the test examined the effect on total heat loss of increasing S_{abs} from 0 to 300 W m^{-2} . The air temperature was held constant (20°C) and, again, wind speed was 0.2 m s^{-1} , evaporative heat flux 10 W m^{-2} and coat length 5 mm. The results are shown in Fig 2-7. The total heat loss decreases almost linearly with increasing solar load from about 100 W m^{-2} with no solar radiation to about zero when $S_{\text{abs}} \approx 275 \text{ W m}^{-2}$. The cylinder gains heat at solar loads above about 275 W m^{-2} . The change in the convective and radiative heat losses at S_{abs} between 100 and 150 W m^{-2} is an artefact of the model, caused by a transition from mixed convection at low solar radiation levels to free convection at higher levels. This transition occurs when the temperature difference $T_c - T_a$ exceeds a particular value as coat surface temperature T_c increases with increasing solar radiation.

The preceding tests were run in the absence of enhanced evaporative heat loss through panting, or vasodilation. A real animal would respond physiologically and behaviourally to the environments used in these tests. The next sections discuss the effects of changes in coat wetness through rain, and also enhanced evaporation and vasodilation.

2.8 Rainfall

Wetting the coat by rain (Holmes 1981, McArthur 1991a) or condensation (McArthur 1991b) reduces its thermal resistance by increasing conductivity through the air

Fig 2.7: Components of heat loss from the cylinder in Fig 2.6, as a function of solar load. $T_a = 20^{\circ}\text{C}$



spaces. Rain also reduces resistance by compacting the coat (Gates 1980). In addition, the water evaporating from the coat can produce a large latent heat loss (Gatenby 1983b). Alexander (1974) and Poczopko (1981) showed that metabolic heat production in lambs can double when an animal is water-covered. Coat evaporation is especially relevant in the spring in the UK, when rain and high wind can combine with low temperatures to cause severe cold stress in new-born lambs (Joyce et al, 1966). Similar problems have also been observed in Australia (Glass & Jacob 1991). Mount and Brown (1982) calculated that a completely wet coat decreased the external insulation (coat plus boundary layer) by a constant factor, given as about 30%. This figure varies with wind speed (McArthur 1991a), but no comprehensive data exist.

The wet coat also affects the heat loss for a period after the rain has stopped. McArthur & Ousey's (1994) experiments with a physical model of a calf with a few millimetres of hair found that the completely wet coat stayed wet for about two hours after wetting stopped, but became completely dry within a further hour. The effects of drying time on heat loss from cattle coats were modelled by Higgins & Dodd (1989) as an exponential decrease in coat wettedness following wetting. However, their parameterisation overestimated the time a coat stayed wet.

The current model employed Mount and Brown's value of a 30% reduction in external resistance to simulate the effects of rain. All external resistances were multiplied by a factor $(1 - 0.3t_w)$ where t_w represents the degree of coat wetness. The term t_w is related to precipitation amount in the following way: if total precipitation total since the start of rain, P_h , is less than 1 mm then $t_w = P_h$, but if P_h is greater than 1 mm the coat is assumed completely wet, and $t_w = 1$. Drying time was included in the model by following McArthur & Ousey's observations: t_w was set to 1 for the first two hours after rain stopped, and then reduced to zero in the next hour.

2.9 Appendages

Initially, the unicorn was modelled as a single round-ended cylinder. The energy balance analysis was then extended to include surfaces representing a head and four legs because of the importance of these regions as routes for heat loss. The legs were modelled as flat ended cylinders and the head as a round-ended cylinder. The proportions of length to width of each appendage were assumed constant throughout the animal's life. Relationships were derived between surface area of the whole body and the lengths and widths of each appendage, given typical dimensions of each body part (eg. Davidson, 1966; McArthur & Monteith, 1980a; Porter, 1991). The model included the ability of the head and legs to change the tissue resistance r_t in response to the thermal environment (Section 2.10.1). Convective heat loss from the legs was modelled using values of A , B , m and n (in Eq 2.23 and 2.24) appropriate to vertical cylinders.

2.10 Physiological response to environment - thermoregulatory response of homeotherms

In the thermoneutral zone an animal has to achieve a minimum rate of heat dissipation, corresponding to that produced by metabolization of its food intake (Chapter 1). If an animal cannot dissipate heat at this rate by the methods of heat transfer already discussed (ie. $\text{Heat loss} < M$), it responds in a number of ways. These include changes in peripheral blood flow (vasomotor control), panting and sweating. Experimental data (eg. Blaxter et al, 1959) and analysis (eg. Mount, 1974) indicate that animals will regulate sensible heat loss in preference to evaporative heat loss. This implies that an animal will use vasomotor control before sweating or panting, as increasing evaporative heat loss involves loss of water and/or an increase in metabolic rate, both of which are costly to the animal. In the cold, when the thermoneutral heat

production is lower than the environmental demand for heat, the animal will respond by increasing its metabolic rate (eg. by shivering, or by movement), or by vasomotor control to increase body insulation. In severe cold, vasodilation may occur to prevent freezing of tissue. The purpose of this section is to outline the general principles of thermoregulation rather than provide specific information for different animals. Each species' response to heat or cold is considered separately in Chapters 3 and 4.

2.10.1 Vasomotor control

Vasomotor control of peripheral blood flow is achieved by dilation or constriction of the blood vessels. Dilation allows more blood to flow near the skin surface, reducing the tissue resistance and allowing more sensible heat to be dissipated. Different species use this mechanism in different parts of the body. For example, Blaxter et al (1959) found that dilation in sheep occurs mainly in the extremities (eg. legs and ears) rather than on the trunk, but in other animals (eg. pigs) the main changes in peripheral blood flow occur on the trunk (eg. Mount, 1968) and in cattle vasodilation occurs on both legs and trunk (Whittow, 1962).

In the present model, tissue resistance r_t was initially set to some maximum value corresponding to vasoconstriction. If this tissue resistance was too high to dissipate the required heat, a new value was calculated which would increase the heat loss to equal M . If the resistance required was less than the minimum value, corresponding to fully dilated blood vessels, r_t was set to the minimum value and the animal increased evaporative heat loss, as described in the following two sections.

2.10.2 Sweating

Animals such as cattle increase the evaporative heat loss through the skin in hot conditions to allow their metabolic heat production to be dissipated. In modelling a sweating animal, the latent heat loss required for the animal to maintain homeothermy was calculated. The maximum sweat rate was then determined as in Section 2.4.2. If the required sweat rate exceeded the maximum, the animal was required to use other physiological responses to maintain homeothermy.

2.10.3 Panting

As stated earlier (Section 2.5.3) evaporative heat loss occurs through the respiratory tract. Animals with limited sweating ability, such as sheep, pant to increase evaporative heat loss in hot conditions. These animals also lose heat by convection through panting, but Mitchell (1974) and Alexander (1974) deduced that respiratory convective heat loss was small enough to be ignored. Panting is an inefficient form of heat dissipation, as in many animals (eg. the cow, McArthur 1987) the metabolic heat production is raised due to the extra work being done in respiration, which increases the amount of heat to be dissipated. The panting response varies widely between species, and discussion of each animal's response, and the parameterisation in the model, is given in Chapters 3 and 4.

2.10.4 Response to cold conditions

The effect of shivering is to reduce the trunk tissue resistance, r_{st} , but the benefit from the accompanying increase in heat production (by up to six times thermoneutral in Man (Parsons, 1993)) outweighs the increase in heat loss caused by the fall in r_{st} .

Blaxter et al (1959) found that in sheep, maximal shivering reduced r_{st} by approximately 30%, and this figure seems to be fairly typical for most shivering domestic livestock species (McArthur 1987). In Blaxter et al's experiments on shorn sheep, shivering began just below the lower critical temperature (about 23°C), and reached a constant high intensity at 18°C. In the experiment, the heat loss at 18°C was approximately 1.5 times the thermoneutral level (Graham et al, 1959).

In the unicorn model, the assumption that shivering starts at a fixed air temperature would be over-simplistic, as many factors other than T_a affect the thermoregulatory response of a homeotherm (eg. coat length, wind speed, solar radiation). It was assumed, therefore, that shivering intensity was a function of the rate of heat loss above the thermoneutral level. The non-shivering heat loss G was calculated, and then modified in the following way. Blaxter's experimental findings on sheep were assumed true for the unicorn, and shivering was assumed to start at the lower critical temperature, and to be fully established when heat loss reached 1.5 times the thermoneutral level. In summary, if thermoneutral heat production = M then:

If $G < M$, then no shivering. $r_{st} = r_{stmax}$

If $G \geq 1.5 M$, then maximum shivering. $r_{st} = 0.7r_{stmax}$

Between the two extremes, r_{st} was assumed to decrease linearly with increasing heat loss.

Under extreme conditions, when there is a danger that the tissue temperatures of the legs and head will fall near to 0°C, the blood vessels in these extremities will dilate, increasing heat loss, but preventing freezing of the tissue. Cold induced vaso-dilation was introduced in the model when surface temperatures on the head or legs fell below 5°C, forcing the heat loss from these appendages to a value which maintained skin temperature at 5°C.

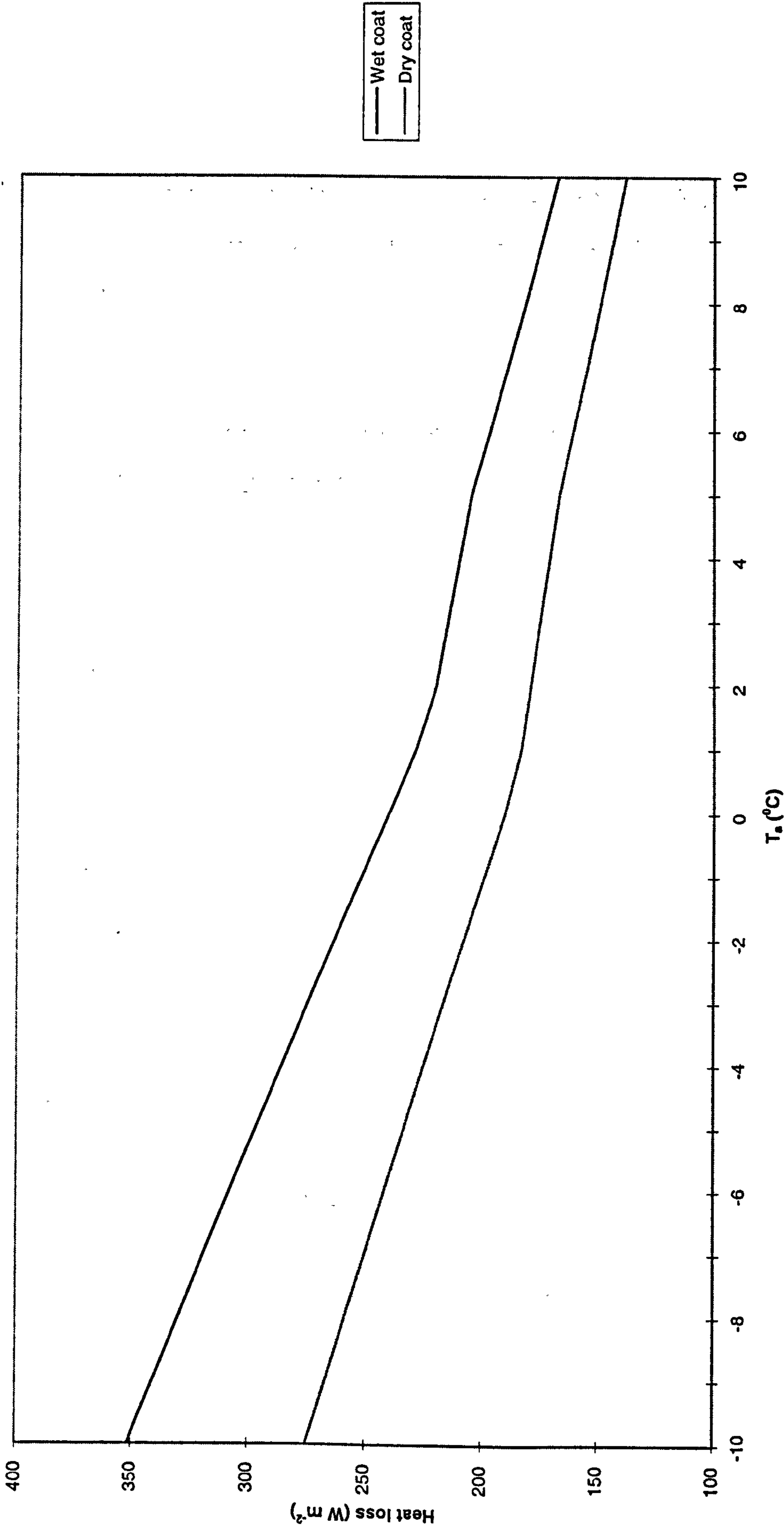
2.10.4.1 TEST 4: Cold wet conditions

Fig 2-8 shows the effect of low temperatures and high wind combined with wet and dry conditions on the heat loss from a unicorn. The model was run to simulate extreme winter conditions - a combination of high wind speed (15 m s^{-1}), low solar load (zero direct, $S_d = 100 \text{ W m}^{-2}$), total cloud cover and a coat length of 20 mm. The 'wet coat' results were obtained assuming the coat was thoroughly wet. Based on a maintenance thermoneutral metabolic rate of 70 W m^{-2} and an assumed summit metabolism three times thermoneutral (see Chapter 1), the animal is in danger of death from hypothermia at 4°C when wet, and -2°C when dry. The change in gradient of the lines just above 0°C marks the onset of dilation of blood vessels in the legs, which increases heat loss but avoids the possibility of freezing of leg tissues. These conditions represent some of the most extreme combinations of wind and rain an animal would face in the UK, and illustrates the importance of shelter from rain.

2.11 Discussion and conclusions

An energy balance model based on the physics of heat transfer has been designed to predict heat loss from a homeotherm (the 'unicorn'), given standard meteorological data as input. The unicorn model gave a mathematically reasonable output for the partition of heat loss over all conditions tested. Some assumptions were necessarily made in the construction of the unicorn model, one of which is that each hour was modelled independent of all preceding hours. Virtually no data exist describing the dependence of heat loss on the heat losses of the previous n hours, where n depends on the species and mass of the animal, as well as environmental conditions. A real animal will store heat during hot conditions in the middle of the day to be dissipated over the cooler night (Section 1.2.1.3). Estimating how much heat is stored during a hot day and

Fig 2.8: Effects of coat wetting on total heat loss from a unicorn as a function of ambient temperature



how much lost as increased evaporative fluxes has not been fully researched. As such, the current model assumes that all energy produced each hour must be dissipated as convection, conduction, evaporation or radiation. The result of the assumption is the model may overpredict instances of heat stress in hot conditions. The next two chapters discuss application of the unicorn model to simulate heat balance of different species of farm animal, including consideration of the species' differing responses to the thermal environment.

APPENDIX 2.1: SUMMARY OF INPUTS TO AND OUTPUTS FROM LIVESTOCK ENERGY BALANCE MODEL

Inputs from:

1) Meteorological data:

- Temperature
- Wind speed
- Radiation
- Humidity
- Rainfall
- Cloud cover

2) Scenario data:

- Increase in mean temperature
- Occurrence of extremes (changes in return period)
- Rainfall patterns & type of rain (convective/frontal?). Links with increased/decreased cloudiness, hence radiation changes

3) System data:

- Type of livestock
- Importance of latent heat transfer
- Effect of various coats
- For sheep - date of shearing, annual wool growth cycle

4) Livestock nutrition model:

- Thermoneutral metabolic heat production from total energy consumed (lactation, pregnancy, growth & maintenance)

5) Housing model:

- Ambient temperature/humidity/air speed maintained in a building

Outputs to:

1) Risks:

- Heat stress: patterns of heat stress - which hours of the day, how often will heat stress occur relative to now?, severity of stress
- Cold stress should be less of a problem in a warmer world

2) Livestock nutrition model:

- Energy required for maintenance either in $W\ m^{-2}$ or as a daily energy requirement (MJ)
- Increase/decrease in food intake due to stress

3) Housing model:

- Energy balance of animals - hourly heat output to the building energy balance
- Latent heat output of indoor animals

APPENDIX 2-2: PROCEDURE FOR CONVECTION ASSESSMENT

Assessment of the type of convection present in a system involves calculation of two dimensionless numbers: the Reynolds (Re) and Grashof (Gr) numbers. Re indicates the relative importance of inertial and viscous forces in the flow, and is estimated for a flow regime by:

$$Re = \frac{u d}{\nu} \quad [2-A]$$

where u = wind speed, d = diameter of trunk, ν = kinematic viscosity of air.

Large values of Re (corresponding to high wind speeds) indicate inertial forces which promote convection dominate, while a low Re indicates convection-inhibiting viscous forces are dominant.

Grashof number (Gr) is a measure of the relative importance of buoyancy and viscous forces, and is estimated for a dry system from T_s and T_a :

$$Gr = \frac{g d^3 (T_s - T_a)}{\nu^2 \bar{\beta}} \quad [2-B]$$

where g = acceleration due to gravity (9.8 ms^{-2}), $\bar{\beta}$ is the inverse of the coefficient of thermal expansion for ideal gas.

Large Gr, corresponding to large temperature gradient, indicates vigorous convection, as the buoyancy forces caused by the temperature gradient are dominant.

The relative magnitude of Gr and Re gives an indication of the type of convection that dominates in a flow regime. If Gr is much larger than Re, the convection is primarily driven by temperature gradient (free convection), and if Re is much larger than Gr the convective heat flux is mainly due to flow velocity (forced convection). The relative importance of Gr and Re can be characterised by another dimensionless number, the Richardson number (Ri), which indicates whether convection is free or forced. Ri is defined as:

$$Ri = \frac{Gr}{Re^2} \quad [2-C]$$

$Ri \leq 0.1$ indicates pure forced convection, $Ri \geq 10$ indicates pure free convection and $0.1 < Ri < 10$ implies mixed convection (A.Ibbetson, pers. comm.)

Once the convection type has been determined, Eq 2.23 or 2.24 is used to calculate boundary layer resistance (Section 2.5.1)

APPENDIX 2-3: SHAPE FACTOR EXPRESSION

For a round-ended cylinder with a layer of coat, the shape factor for interception of solar radiation is given by the area of shadow cast divided by the total area available for interception (ie. coat surface area):

$$\frac{A_h}{A} = \frac{(d + 2\ell)(y - d)\operatorname{cosec} \alpha [1 - \cos^2 \alpha \cos^2 \theta]^{0.5} + \pi \left(\frac{d}{2} + \ell\right)^2 \operatorname{cosec} \alpha}{\pi(d + 2\ell)(y - d) + 4\pi \left(\frac{d}{2} + \ell\right)^2}$$

[Equn 2-D]

where θ = orientation of animal to solar beam (0° = head on, 90° = side on)

α = solar elevation

d = diameter of bare animal trunk (m)

y = total length of bare animal trunk (m)

ℓ = coat length (m)

(Suarez, 1988)

CHAPTER 3 - MODELLING THE HEAT BALANCE OF ANIMALS OUTDOORS

3.1 Introduction

This chapter describes the refinement and extension of the unicorn model to simulate the thermal balance of ruminant livestock outdoors. The animals considered are sheep, dairy and beef cattle, all of which spend a large part of the time outdoors in the UK, where they are exposed to a wide range of environmental conditions. The adaptation of the unicorn model is discussed for each animal, and the choice of input parameters for the model is justified. Aspects of heat transfer unique to each animal are discussed, and the way these are included in the computer model are described. The chapter relates closely to concepts introduced in Chapter 2 and follows a similar section structure. An overview of the sheep model and some validation results were presented by Turnpenny, Clark & McArthur (1997), and a briefer description of the thermal balance models of animals outdoors, along with links to grass growth and feeding models can be found in Parsons et al (1997b).

3.2 General considerations for animals outdoors

The energy balance of animals outdoors cannot be determined simply from the air temperature alone (McArthur, 1990). The heat transfer depends strongly on wind speed, solar radiation and rainfall. The impact of these variables is then altered by the animal in the field as it seeks protection from adverse weather conditions in the form of shade or shelter (Bruce & Broadbent, 1989). There are two fundamental types of shelter:

- 1) Livestock buildings where animals are kept for part of the year, usually winter
- 2) Shelters where an animal *chooses* to go when out in the field (eg. hedges, purpose-built structures etc.)

3.2.1 Winter housing

In the UK, many ruminants are housed only in winter. This housing regime is in contrast with that in which animals employed in intensive production, such as pigs and poultry, are kept indoors all year round; the effects on animal energy balance of this type of environment are considered in Chapter 4.

Winter housing is expensive, both financially and in its effect on animal health and behaviour (Redbo et al, 1996). Several studies have produced contrasting assessments of the value of winter housing from a shelter viewpoint. Bruce & Broadbent (1989), using physical models of calves, found that a period spent in a simple uninsulated building reduced climatic energy demand by 20% in winter and 13% in autumn and spring. This form of shelter produced a weight loss over the winter of only 2 kg, compared with a loss of 40 kg in unsheltered animals. Redbo et al (1996) showed that steers overwintering indoors in Sweden grew better than steer outside in the winter, but that those wintered outside grew better the following summer, giving no net effect overall. Kubisch et al (1991) found that shelter was only useful in very cold temperatures (-10 to -20°C) but this study was made in Canada, and acclimatisation to the cold may at least partly explain the result. Vandenheede et al (1995) found little evidence of benefit from housing beef calves over winter in Belgium as the animals outside only spent about 5% of their time sheltering from rain. Overall, it appears that keeping outdoor animals indoors over the whole winter in the UK is largely unnecessary from a thermal balance point of view, as the low lower critical

temperatures of ruminants combined with generally mild winters mean most of the potential weight loss occurs over short periods. However, additional considerations such as the prevention of poaching of the pasture, ease of control over livestock feeding and reproduction and ease of observation of animals for disease, especially during lambing or calving, usually makes the use of winter housing more cost effective than leaving the animals outside. If animals are left outdoors over winter, however, it is important to allow access to a simple shelter when it is needed (Charles, 1991).

3.2.2 Shelters

The benefits of allowing ruminants shelter outdoors have been quantified in a number of studies. Doney (1963) found that a group of sheep without shelter finished winter between 1 and 5 kg lighter than a similar group allowed access to a simple shelter. Another benefit was noted by Lyth (1996), who reported that the use of shelterbelts allowed stock to be finished at higher altitudes. A discussion of shelterbelt benefits and construction is included in the extensive review by Gregory (1995).

Numerical models of wind flow around shelterbelts (Wang & Takle, 1995, 1996) show a complicated flow structure, the primary features being wind overspeeding above the shelter but a speed reduction behind. The position and magnitude of the speed reduction varies with shelter porosity and width, but a width about twice the height and a porosity of about 0.5 provide the largest speed reductions. Low porosity shelters (eg. walls) produce a turbulent reverse flow close behind them, which is of little benefit to the sheltering animal.

As well as reducing wind speed, a shelter affects the energy and water balance of the ground nearby (Oke, 1987). Turbulence is decreased behind a porous shelter, resulting in a larger diurnal ground temperature cycle, except in the shade of the

shelter where the cycle is reduced (Shao & Lister, 1994). Reduced turbulence also results in reduced sensible and latent heat fluxes. Precipitation deposition is increased in the lee of a shelter due to the lower wind speed, and the reduced evaporation results in moister ground.

These complicated interactions between variables have not been modelled comprehensively in the current work. Rather than concentrating on the energy balance of the ground near a shelter, a simple parameterisation of reduction in wind speed behind obstacles has been used to assess the effects of reduced wind speed on animal energy balance. This method is discussed further in Section 3.3.2.

Animals also use shelters to reduce the solar load in hot conditions, and studies have shown that an animal's respiratory rate and body temperature are significantly lower as a result (eg. Silanikove, 1987). However, the type of shade provided/used is important. For a shade to be efficient it must be of sufficient height to cut out the direct solar radiation but still expose the animal to the lower radiative temperature of the sky to aid longwave radiative loss. The optimum height for artificial shade for cows is about 3.6 m (Bianca, 1965; Garrett et al, 1967). The roof must be made of material which does not re-radiate too much of the heat gained from solar heating on to the animal as thermal radiation. One way to minimise this re-radiation is to paint the top side of the roof white (Bianca, 1965). Natural shade such as trees or hedges are best for minimising re-radiation; the radiant temperature of the underside of a leaf canopy can be approximated to air temperature.

In summary, for an animal outdoors the availability of some form of shelter is essential, and in the UK it is especially important to provide protection from wind and rain in winter.

3a SHEEP

Sheep are present in both lowland and upland terrain in many parts of the world, and are thus exposed to a wide variety of climatic conditions. Tolerance of a wide range of climates is largely achieved by using breeds with varying coat length, since external insulation has a major influence on the sheep's energy balance. In the current work, only UK breeds have been considered, as the concern is to examine the impact of climate change in the UK.

Hill breeds (eg. Cheviot, Scottish Blackface) have more insulation than lowland breeds (eg. Dorset Down, Hampshire, Shropshire), both in the form of fat (higher tissue resistance) and wool (Hart, 1985). They are also able to withstand higher rainfall and softer ground, and do not need as much food all year round. However, for simplicity, the current model represents a 'composite' sheep. The input parameters such as tissue resistance and fleece length represent an average of the values of the most common breeds, and can be used under UK conditions. Section 3a sets out the model parameters for the ewe, initially under thermoneutral conditions, and then discusses the responses during thermal stress.

3a.1 Dimensions

Animal size is usually expressed as the mass of the live animal ('live weight'). For analysis of heat flux densities, the surface area of each part of an animal must be known. There are empirical relationships linking total skin surface area, A_s , (m^2) to liveweight m_b (kg); for example Gates (1980) used:

$$A_s = 0.09 m_b^{0.67} \quad [3.1]$$

for a 'standard' allotropic series of animals (ie. the ratios of lengths of body parts stay constant as the animal grows). This assumption was adopted for the sheep in the present work. From the assumption of allotropy, the ratios of length and diameter of legs, head and trunk can be determined for a sheep of any age can be assumed true throughout the animal's life. From data given by McArthur & Monteith (1980a) and McArthur (1980), the following relationships were established for sheep:

$$A_t = 0.71 A_s \quad [3-2a]$$

$$A_{he} = 0.09 A_s \quad [3-2b]$$

$$A_L = 0.20 A_s \quad [3-2c]$$

$$y_t = 2.49 d_t \quad [3-2d]$$

$$y_h = 2.50 d_h \quad [3-2e]$$

$$y_L = 5.00 d_L \quad [3-2f]$$

where the t, h, L subscripts denote trunk, head and leg respectively (he for area of head), y is the total length of the body part (including hemispherical ends on trunk and head), and d is the diameter of each part. Note that A_L is the combined surface area of four legs. All lengths were calculated in metres. From Equations 3-2a to e, unique relationships were established relating the dimensions of the component body parts to the total skin area. The dimensions were used to calculate the shape factor for solar radiation and to determine the convection heat transfer from each body part.

Under thermoneutral conditions, the deep-body temperature of sheep is about 39°C (Blaxter et al, 1959; Mount, 1979). This value varies slightly between individual animals, and is mainly determined by food intake (Mohr & Krzywanek, 1995). The variability is small, however: within $\pm 0.5^{\circ}\text{C}$ of 39°C , with a rise in T_b corresponding to feeding times. Thus, in the model, T_b was assumed constant at 39°C , under thermoneutral conditions.

Tissue resistance r_s varies considerably over the animal and with different environmental conditions. Under thermoneutral conditions, trunk resistance, r_{st} , values vary widely between individual animals of the same species (Alexander 1974), in the approximate range 85 to 220 s m^{-1} both for adult sheep and lambs (Alexander, 1974). Tissue resistance changes with the size of an animal (Bruce and Clark, 1979), but the changes in tissue insulation with a sheep's age appear to be secondary to the changes in fleece insulation with age. Tissue resistance of the head, r_{sh} , varies considerably between different areas of the head, as some parts (eg. the ears) have almost no tissue insulation at all. Blaxter et al (1959) noted that in sheep vasomotor control occurs primarily in the legs, so r_{sL} varies considerably between warm and cold conditions.

In the current model, r_{st} was assumed constant at 100 s m^{-1} for sheep (Blaxter 1967), chosen as a typical non-shivering value. It was assumed that r_{st} was independent of age. For the head, r_{sh} was taken as 400 s m^{-1} (McArthur 1980), and this represents a thermoneutral mean value over the whole head. The concept of vasodilation in cold conditions to prevent tissue freezing was introduced in Section 2.10.4. This phenomenon was included in the sheep model, which allowed tissue insulation to be decreased to maintain T_{sh} at 5°C in the cold. The inclusion of vasomotor control in the legs of the sheep model, along with typical values for r_{sL} , is discussed in Section 3a.5.1.

3a.3 Heat flow through coat

3a.3.1 Sensible heat transfer

The tissue resistance of the trunk of a sheep is relatively constant, so the fleece forms a large part of the trunk insulation. Since the trunk of a sheep typically represents about 70% of the total skin area of the animal, it is therefore critical to represent the fleece resistance of the trunk correctly in modelling the heat balance of sheep. One of the most important variables in determining fleece resistance is the depth of wool. The equations in Section 2.4.1 show the relationships between the various components of resistance (eg. resistance to free convection, conduction through the trapped air etc.) and coat depth. The wool length varies considerably throughout the year, from a few millimetres after shearing to several centimetres a year later. It is important to model this annual cycle. Wool growth is affected by many factors, including seasonality, diet, hormonal changes and photoperiod (Ryder 1973). The work of Slee & Carter (1961), Ryder (1975) and Nagorcka (1978) in midlatitude conditions suggested that moderate warmth stimulates wool growth, but that heat stress depresses growth. However, Bottomley (1978) found that heat stress has to be prolonged to depress wool growth, which is unlikely under UK conditions. For the present model, the wool depth over the year was incorporated using data collected in the UK by Slee & Carter (1961), on the Wiltshire Horn breed. These data were assumed to represent the results of a typical annual cycle of diet, photoperiod, and thermal conditions encountered in the UK. Appendix 3.1 has a table of these wool growth rates and cumulative wool depth throughout the year. Data points at monthly intervals were linearly interpolated in the model to give the daily fleece depth. It was assumed that shearing takes place at the end of May (day 151). For the lamb, the function of wool depth against day has to be shifted to allow for birth around mid March, when their coat is a similar depth to the ewes' just after shearing.

The head and legs have a much less uniform covering of fleece; the legs are well insulated near the trunk but are almost bare near the feet, while the head has patches of bare skin and fleece. For simplicity, following McArthur (1980), a single mean value of coat depth for the whole appendage was assumed for head and legs; these are 5 mm for the head and 3 mm for each leg (McArthur 1980). These coat depths do not change much over the year.

The thermal resistance of the fleece, and hence the rates of convective and thermal radiant heat transfer, are also affected by the density and diameter of the coat fibres. The sheep's fleece is rather coarse and relatively sparse (around 1000 hairs per cm^2 compared with between 4000 and 10 000 per cm^2 for foxes and rabbits). The result is that the longwave radiation penetration parameter of the coat, p (see Section 2.4.1.4) is lower than for other livestock, at about 500 m^{-1} . The value of p varies from about 400 m^{-1} in Welsh Mountain sheep to about 550 m^{-1} for lowland sheep, such as Dorset Down (Cena & Clark, 1973). In the model, which represents a 'composite' of the breeds found in the UK, a value of 500 m^{-1} was used. The quantity c' , an empirical constant of proportionality in the equation relating the thermal diffusivity of the coat to wind speed, is independent of coat depth and wind speed (Section 2.4.1.1), but varies between breeds and species. A high value of c' indicates that a given wind speed will force more heat transfer through the coat than when c' is low. For sheep, a representative value of $c' = 9.1 \times 10^{-6} \text{ m}$ was chosen (from data in Campbell et al, 1980 and McArthur & Monteith, 1980b).

3a.3.2 Latent heat transfer

In sheep, the respiratory evaporative component dominates; sheep do not sweat much except at high temperatures (greater than about $30 - 35^\circ\text{C}$). Evaporation as a result of vapour diffusion through the skin, E_c , is reported to be relatively constant at about 10

W m^{-2} (Alexander & Williams 1962). This value was therefore assumed for skin evaporation in the model under all conditions.

3a.4 Heat flow to the environment

3a.4.1 Convection

The resistance of the boundary layer to convective heat transfer, r_H , was determined using the theory and values outlined in Section 2.5.1. As explained in that section, McArthur (1980) established an empirical relationship between Nusselt and Reynolds numbers for sheep, so McArthur's relations were used in the current model to predict r_H from wind speed and animal size. However, relationships between Nusselt and Grashof numbers have not been established for a live sheep or a hair-covered cylinder, and the established relationships for a bare horizontal cylinder were used (Monteith & Unsworth, 1990).

3a.4.2 Evaporation

In sheep, the evaporative heat flux from the respiratory tract, E_r , is much more variable than that from the skin. Under thermoneutral conditions and below the lower critical temperature, when respiration rate is minimal, E_r can be assumed constant (Hales & Webster, 1967; Hales & Brown, 1974), in the range $5 - 10 \text{ W m}^{-2}$, the exact value depending on environmental vapour pressure. Sheep have the ability to increase their respiration rates to more than 300 min^{-1} , and there is a corresponding increase in E_r . The relationship between evaporative heat flux and respiration rate is discussed in Section 3a.5.2. In summary, total evaporative heat loss to the environment below the lower critical temperature is E , the sum of E_r and E_c (Section 3a.3.2): approximately $15 - 20 \text{ W m}^{-2}$ in the model.

3a.4.3 Solar radiation

The solar radiation absorbed by the head and trunk of the sheep was calculated as in Section 2.5.4, using the following parameters. Ground albedo, ρ_g , was assumed to be 0.25, the value for grass given by Monteith & Unsworth (1990). Fleece albedo is usually quoted in the range 0.5 - 0.8, obtained from measurements in the laboratory on samples of cleaned cured fleece. Stafford Smith et al (1985) measured a lower coat albedo of 0.26 on sheep in the field, when the fleece was dirty and greasy. In the model, the field value of 0.26 was used. In the calculation of the shape factor (Appendix 2.3) the animal orientation to the solar beam, θ , was assumed initially to be 180° , ie. the animal is tail-on to the beam. This orientation is usually observed in conditions of high direct solar radiation (Section 3a.6).

Determination of the solar load on the legs of an animal outdoors is an extremely complicated calculation, since each leg is shielded by the trunk and other legs by differing amounts depending on the solar elevation, animal orientation and animal posture. In the current work it was assumed that solar load absorbed by the four legs was a constant fraction of that absorbed by the trunk: S_{abs} on the legs was S_{abs} on the trunk multiplied by 0.4. The constant 0.4 is an approximate figure based on the relative surface areas of legs and trunk, and allows for the large variation in exposure of the legs with solar altitude. The legs are only likely to receive significant amounts of direct solar radiation when the sun is at a low elevation, as when the sun is high, most of the leg area will be shielded by the trunk from exposure to direct solar radiation. At low elevations the solar loads are low, and therefore accurate calculation of solar radiation impacting on each leg is probably unnecessary.

3a.5

Physiological response to environment

3a.5.1

Vasomotor control

In sheep, most of the vasomotor control occurs in the extremities, especially the legs.

In the model, the leg tissue resistance, r_{sL} , was initially set to a maximum value, corresponding to vasoconstriction, taken as 800 s m^{-1} (McArthur 1980). If this tissue resistance was not low enough to dissipate the required heat, a new value was calculated by iteration, seeking a balance between heat loss and metabolic heat production. However, r_{sL} was allowed to fall only to a minimum value, corresponding to blood vessels fully dilated, which was 125 s m^{-1} (McArthur 1980).

Blaxter et al (1959) plotted T_b as a function of trunk skin temperature, and found that T_b only starts to rise in response to hot conditions when T_a exceeds about 33°C . Lowering of the feeding level due to such high temperature exposure will probably prevent T_b rising much above 40°C . For UK conditions, T_b has thus been assumed constant.

3a.5.2

Panting

Panting increases the evaporative heat flux from the respiratory tract and allows an animal to dissipate its metabolic heat production under hot conditions. The sheep's panting response to hot conditions is well documented (eg. Hales & Webster, 1967; Hofmeyr et al, 1969). The animal increases its respiration rate, F (breaths min^{-1}), in response to increasing heat stress, which lowers the resistance to water vapour transfer, in turn increasing the evaporative loss. As F rises, the amount of air exchanged per unit time (usually expressed in l min^{-1}) increases, though the tidal volume (amount of air inhaled per breath) initially decreases. This is known as *first*

phase panting, and occurs under mild heat stress. First phase panting continues until the animal reaches its maximum respiration rate, taken as 320 min^{-1} (Hales & Brown 1974). If heat stress increases further, the animal then enters a *second phase* of slower, deeper panting, in which the minute volume still rises, but respiration rate falls. In the second phase, air is exchanged much deeper in the lungs, resulting in a loss of carbon dioxide from the blood, causing respiratory alkalosis which is eventually fatal. Clearly, respiration rate provides a good index of the severity of heat stress.

In the model, the respiration rate was calculated from the evaporative heat flux required to achieve heat balance. The equation relating latent heat flux density to vapour pressure gradient (introduced in Section 2.5.3) was rearranged to calculate the resistance to vapour transfer:

$$r_v = \frac{\rho c_p \Delta e}{\gamma E_r} \quad [3.3]$$

Calculation of Δe required the vapour pressure of the expired air, which was assumed saturated at the temperature of the upper respiratory tissue. This tissue is usually at a lower temperature than the body core, except possibly in birds, which have a different upper respiratory system to mammals (Mount, 1979) consisting of a series of chambers where air may reach body temperature before being expired. Using the evaporative heat loss data of Knapp & Robinson (1954) a value for the temperature of respiratory tissue was deduced. For sheep this was about 36.5°C , about 2.5°C below normal body temperature. The corresponding saturated vapour pressure of the air at this temperature is about 6100 Pa.

A relationship between respiration rate (breaths per minute) and resistance to water vapour transfer was established, based on work by Hales & Webster (1967). Hales & Webster's data relate the volume of air respired (or *minute volume*, $l \text{ min}^{-1}$) to the respiration rate. The minute volume was converted to a resistance to vapour transfer r_v (s m^{-1}) by dividing the surface area of the animal A_s (m^2) by the volume respired per unit time V_r ($\text{m}^3 \text{ s}^{-1}$):

$$r_v = \frac{A_s}{V_r} \quad [3.4]$$

Analysis of Hales & Webster's data revealed linear relationships between respiration rate and the reciprocal of resistance for first and second phase panting. Equation 3.5 is the relationship for first phase panting, and Equation 3.6 is that derived for the sheep in second phase panting:

$$\frac{1}{r_v} = 1.29 \times 10^{-6} F + 1.2 \times 10^{-4} \quad [3.5]$$

$$\frac{1}{r_v} = -9.45 \times 10^{-7} F + 9.88 \times 10^{-4} \quad [3.6]$$

Equations 3.5 and 3.6 were used in the model as follows. Equation 3.3 was used to calculate the resistance required to allow an evaporative heat loss E_r , where E_r is determined by the difference between heat loss and heat production. Equation 3.4 was then used to calculate the corresponding respiration rate. The animal was identified as being in either first or second phase panting; if F was less than 320 min^{-1} , first phase panting was assumed. If F from Eq 3.4 was greater than this, Eq 3.5 was used to calculate second phase respiration rate from the resistance. The onset of second phase panting is a sign of severe heat stress. If the required respiration rate is more than the animal can deliver, the sheep will die of hyperthermia.

Panting is an inefficient form of heat dissipation, as in many animals (eg the cow - McArthur 1987) the metabolic heat production is raised due to the extra work being done in respiration. However, in the sheep, panting efficiency seems to approach 100 % (Hales & Brown 1974) in slight and moderate stress. The metabolic cost of first phase panting has thus been ignored in the model. However, this assumption is not true for sheep in severe heat stress, where the fraction of metabolic heat production attributable to the effect of panting rises from 5% at the limit of first phase panting to 25% at the upper limit of second phase panting.

3a.6 Comparison of model results with measurements on real sheep

An important part of model design is the testing of its predictions. A model must produce a reasonable match with measured data obtained under the same input conditions (IPCC, 1994b). The two main methods of model testing are sensitivity analysis and validation. Sensitivity analysis involves assessing the sensitivity of model outputs to changes in input variables or model parameters, and is considered in Chapter 6. Validation involves comparing the model with observed data, and the

thermal balance models for each species are validated in this and the following chapters.

The errors in the model prediction, when compared with measured data, were assessed using a method described by Quinn (1996), who defined the *Overall error*, O , as:

$$O = \frac{\sum |(model\ value - measured\ value)|}{\sum |measured\ value|} \quad [3.7]$$

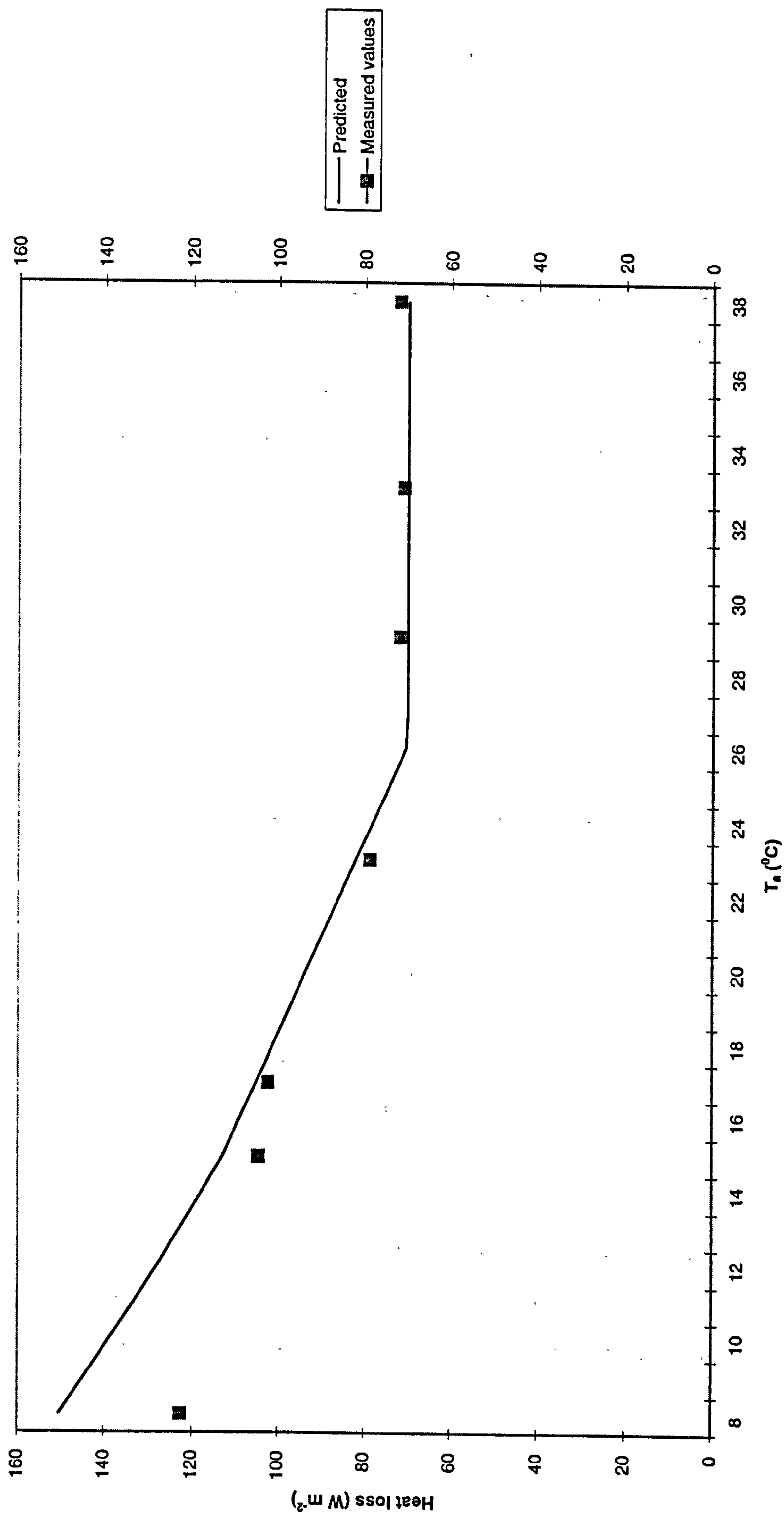
The method allows the errors over a range of points to be combined in one number independent of the sample size. The error O was computed for each of the comparisons in the current model.

3a.6.1 TEST 1: Heat loss from a shorn sheep

Fig 3.1 shows a comparison of total heat loss predicted by the model with measured data from a shorn sheep in a calorimeter obtained by Graham et al. (1959). The model was run for the calorimeter conditions recorded by Graham, ie. wind speed of 0.1 m s^{-1} , no solar radiation and equal radiant and dry bulb temperatures. The fleece depth was a uniform 1 mm over the whole body, and relative humidity remained at approximately 50% for the whole temperature range. A thermoneutral metabolic heat production of 70 W m^{-2} was assumed, corresponding to a medium feed intake.

The lower critical temperature is well-modelled at 26°C , as is the rise in heat loss with decreasing air temperature down to about 16°C . However, the model overpredicts heat loss below 16°C . It is likely that a live animal will adopt a compact

Fig 3.1: Predicted heat loss vs. ambient temperature compared with heat loss measured by Graham et al (1959)



posture to reduce heat loss under cold stress, thereby reducing the surface area available for heat loss. Further analysis has shown that the reduction in effective surface area necessary to make the model and measurements agree would be about 19% at 8°C. As the model considers each body part in thermal isolation, compaction of the posture is a reasonable explanation for the discrepancy between the model predictions and the measurements. The model was therefore tuned to include the effect of a reduced effective area. The fractional discrepancy between the modelled (G_{mod}) and measured (G_{meas}) values of heat loss in Fig 3.1 ($\Delta G/G_{\text{mod}}$), where $\Delta G = G_{\text{mod}} - G_{\text{meas}}$, was expressed as a function of modelled heat loss as multiples of thermoneutral heat production, M (G_{mod}). The data gave an approximately linear response:

$$\text{Fractional discrepancy} = \frac{G_{\text{mod}}}{4M} - 0.35 \quad [3.8]$$

The model then calculated heat loss as before, and if the heat loss was greater than metabolic heat production, Eq 3.8 was used to calculate a new heat loss assuming the animal reduced its effective area for heat loss. This approach is far from ideal. The discrepancy between model and measurement could be almost completely removed if reduction of r_{st} due to shivering was not included in the model. However, such tissue insulation reduction *does* occur, and including it in the current model may have highlighted the process of posture compaction which acts in the opposite sense and is not usually modelled.

The overall error of the model, O , was 7.4% before the allowance was made for posture changes. This figure disguises the relatively large individual errors of approximately 20% at lower T_a , and the very small errors at temperatures greater than 16°C.

3a.6.2 TEST 2: Effects of fleece length and wind speed on heat loss

The ewe model was run for realistic combinations of fleece length, air temperature and wind speed, and the results compared with data obtained by Joyce & Blaxter (1964). The thermoneutral metabolic heat production was not specified by Joyce and Blaxter, so a value of 70 W m^{-2} was used, corresponding to a medium feed intake by a non-lactating ewe (Graham et al, 1959). The measurements were made under calorimeter conditions (ie. $T_r = T_a$ and no solar radiation). The results of the comparisons are shown in Table 3.1. The first part examined the effect on heat loss of different fleece depths at constant air temperature and wind speed. The second part examined the effects of changing fleece depth at low temperatures, under a constant high wind speed. The third part investigated the effects of increasing wind speed while keeping the other variables constant.

Table 3.1: Heat loss to the environment from sheep, G_e (W m^{-2}), measured and modelled for a range of conditions. Discrepancy = (Modelled value - Data)/Data]

T_a ($^{\circ}\text{C}$)	u (m s^{-1})	l_f (mm)	G_e : Model prediction (W m^{-2})	G_e : Measured data (W m^{-2})	Discrepancy, %
10	0.4	25	79.6	78.0	2.1
		98	57.6	59.7	-3.5
-3	4.3	39	129	122	5.7
		12	204	226	-9.7
5	0.4	89	66.8	69.7	-4.2
	4.3		83.0	80.6	3.0

Table 3.1 shows that the model performed well. At 10°C and low wind speed a change in fleece length from 98 to 25 mm (such as might be experienced after shearing) produced an increase in heat loss of approximately 20 W m⁻². The effect on heat loss of a change in fleece length by a given amount is largest when the fleece depth is short. For example, the model predicts that reducing fleece length from 39 to 12 mm at temperatures around 0°C will increase heat loss by nearly 60%. Increasing the wind speed from 0.4 to 4.3 m s⁻¹ while keeping the fleece length constant at 89 mm resulted in an increase in heat loss of about 25% due to decreased coat insulation.

The model predicted lower values heat loss than the measurements under very cold windy conditions combined with a short fleece, but the overall error, O , as calculated from equation 3.7, is only 6.0%. Individual errors are 10% or less, which is within acceptable accuracy for modelling in environmental physics (Monteith & Unsworth, 1990). There was generally a very good match between model and data over a wide range of fleece depths, temperatures and wind speeds. The analysis also shows that fleece length is the most important variable for governing heat loss under cold conditions. The sensitivity of the heat loss to coat length is greatest with the short coat, due to the inverse relationship between heat loss and coat length. Because measurements of coat length are subject to the greatest errors when the coat depth is small, it is to be expected that the largest errors in the model predictions occur when the coat is short. The effects of breed differences on heat loss were examined briefly by Joyce & Blaxter, who compared the heat loss from a Down Cross and a Cheviot under the same conditions, and found little difference in heat loss. They also investigated the effect of orientation of the sheep to the wind. In high winds and low temperatures, an animal is observed to align its tail to the wind to reduce local cooling of the face. Joyce & Blaxter found that this orientation may only reduce overall heat loss by 1 - 5%, which in the current work is the quantity modelled. Therefore the effects of changing orientation to the wind was not considered in the present model.

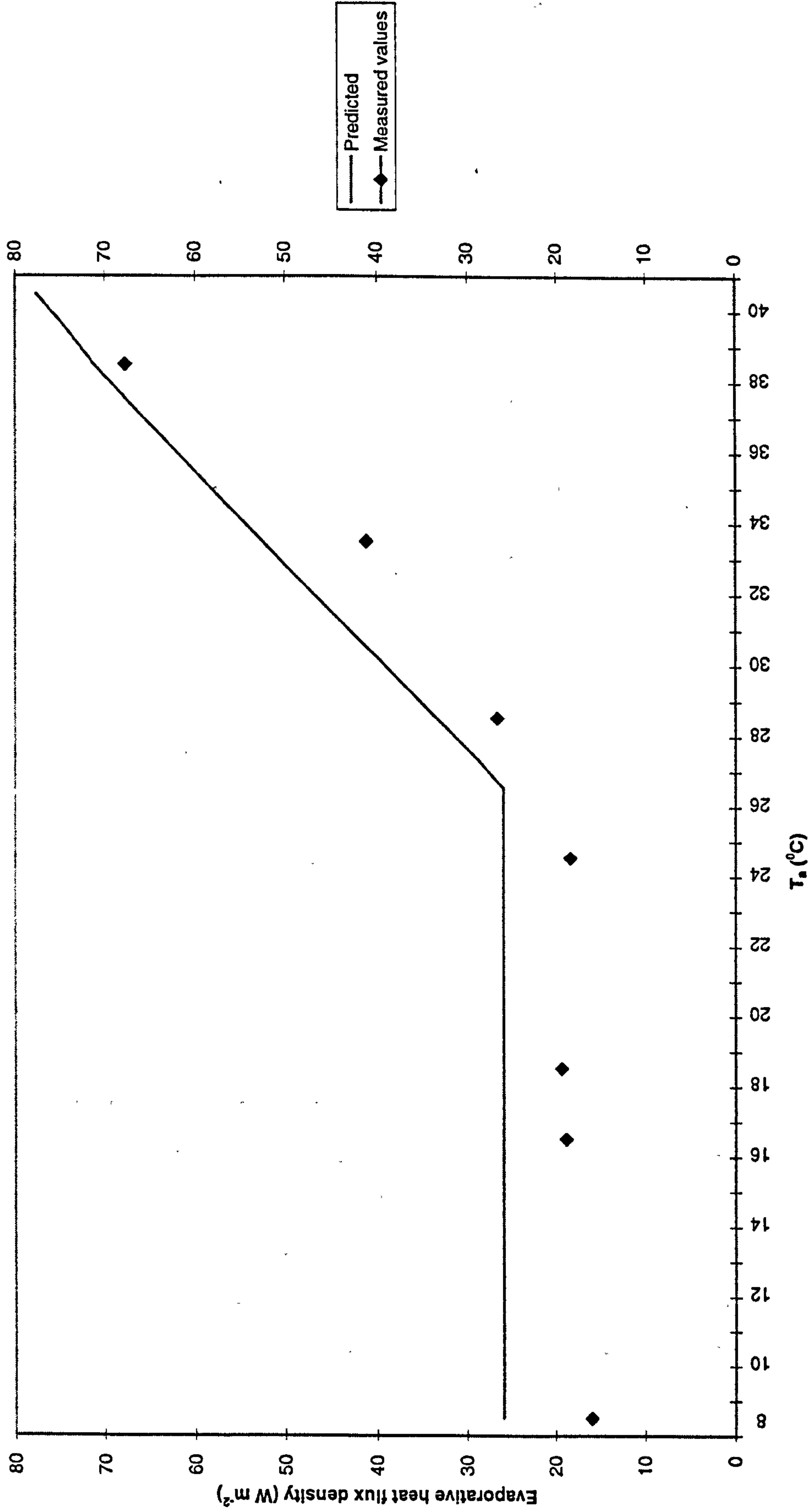
3a.6.3 TEST 3: Physiological response to thermal stress

Fig 3.2 shows the predicted skin temperature of the legs plotted against dry bulb temperature, compared with the skin temperatures of the ears measured in an experiment by Blaxter et al (1959). The plot of these two variables allows assessment of the vasomotor response of the animal. The environmental and animal conditions were the same as in Fig 3.1. Ear surface rather than leg surface temperatures were measured by Blaxter et al due to experimental complications, but since dilation occurs in both in response to the same thermal signal, it was assumed that the surface temperature behaviour will be similar.

Below thermoneutrality, there is a linear rise in skin temperature, T_s , with air temperature of about 0.8 K per K air temperature rise. The onset of vasodilation in the extremities, indicated by a sharp increase in skin temperature, occurs at 25°C, and is accurately modelled. The range and magnitude of dilation in the model ewe are less than in the real animal, for which there appears to be two stages to the increase in T_s . However, Blaxter's measurements showed a wide degree of variability in the range of air temperatures over which dilation occurs, and in the rate of increase of T_s after dilation, even between the two ears of the same animal. Therefore the discrepancy between model and measurement may not be significant.

Fig 3.3 compares the evaporative heat loss from skin and respiratory tract ($E_c + E_r$) predicted by the model with measurements by Blaxter et al. The graph was obtained for the same animal and environmental conditions as Fig 3.2. The air temperature for the onset of panting (LCT), indicated by the rise in evaporative heat flux, is predicted by the model to be 26°C; the measured data indicate about 24°C, though there are not enough experimental data to be certain of this value. Below $T_a = 24^\circ\text{C}$ the measurements of the evaporative heat flux vary between 15 and 20 W m⁻²; the variability is probably due to different levels of activity in the animals and cannot be

Fig 3.3: Predicted and measured (Blaxter et al, 1959) total evaporative heat flux density vs. air temperature

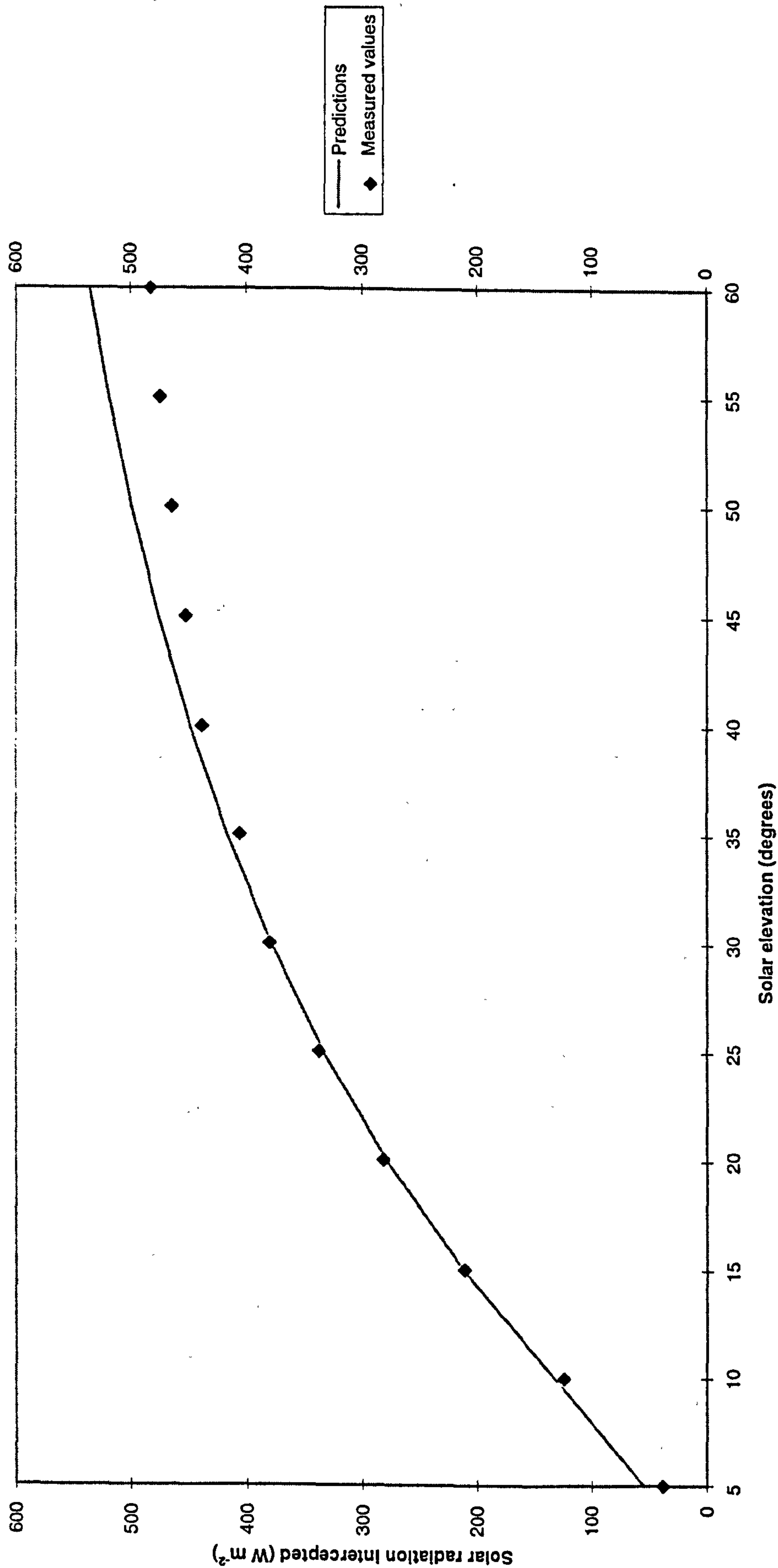


reproduced by the thermal model. Above 24°C, the evaporative heat flux increases by about 4 W m⁻² per K air temperature rise, and there is a good match between model and measurement in the prediction of this gradient. The overall error for the comparison was 26%, but this figure was obtained, by definition, by summing the errors of each point. Thus the presence of a consistent offset error will seem to give a poor validation. The model, in fact, overpredicts evaporative heat loss by 5 - 10 W m⁻² consistently. This is probably due to two main factors. The assumed resting respiration rate from Hales & Webster (1967) was rather high (38 min⁻¹); Hales & Webster noted the usual value is around 20 min⁻¹, but some of their animals were agitated when the measurements were made. Putting the resting respiration rate $F_r = 20 \text{ min}^{-1}$ below LCT as input to the model accounts for about 3 W m⁻² of the difference. Another assumption in the model was that E_c is always 10 W m⁻². This value is only a rule of thumb, and the value may vary with breed and age.

3a.6.4 TEST 4: The effect of solar radiation

The total solar radiation impacting on a sheep in the field was obtained from the model for a range of solar elevation angles. Fig 3.4 compares the model results with measurements made by Clapperton et al (1965) for an animal standing side-on to the sun in clear sky conditions. This comparison tests the accuracy of the model's geometrical method of calculating solar radiation load on the animal (Section 2.5.4). The model output and measurements are in very good agreement for elevations below 45°, which covers most conditions in the UK. Above this elevation, the assumption that the sheep trunk approximates to a cylinder breaks down - in reality, it is a cylinder with a slightly elliptical cross-section. The area of the sheep exposed to direct solar radiation at high elevations is therefore greater in the model, which explains the overprediction of the intercepted radiation by the model. The overall error for the validation is 5.2%.

Fig 3.4: Total solar radiation intercepted by a sheep under clear skies as a function of solar elevation. Predictions and measurements by Clapperton et al (1965)



Solar radiation is an extremely important component of animal energy balance outdoors even at high latitudes (eg. Suarez, 1988). For example, at a solar elevation of 30°, which corresponds to noon around mid-March or mid-September in the UK, the solar load incident on a sheep is around 400 W m⁻². With a coat albedo of 0.26, about 300 W m⁻² is absorbed, which is three to four times maintenance thermoneutral heat production. This illustrates the importance of providing shade for an animal under hot conditions.

3b CATTLE

Dairy and beef cows are present all over the world. From a thermoregulatory perspective, the main problem faced by cattle in warm climates is the very high metabolic rate, which can result in heat stress at relatively low temperatures, especially in productive dairy cows. Cattle in the tropics are usually of breed *Bos indicus*, which have lower metabolic rates than the mainly temperate *Bos taurus* breed. *Bos indicus* also have a shorter coat and sweat more readily (Mount, 1979).

The price of heat tolerance in *Bos indicus* is lower production, both of meat and milk.

Conversely, in the cold cattle are very rarely thermally stressed. Dairy cattle in particular can have lower critical temperatures below -30°C (Webster, 1974), giving them few problems in most locations. This project is concerned with heat loss from cattle in the UK, so the *Bos taurus* breeds found in the UK were used in the model.

In the UK, dairy cattle are mainly confined to lowland areas, as the wetter uplands generally have softer ground and provide poor grazing. The dominant UK dairy breed is the Holstein or the Holstein-Friesian. Beef cattle are hardier, lighter and have lower metabolic rates, and so are more common in upland areas. Angus beef cattle are an example of a breed that originated in the upland parts of Eastern Scotland (Briggs & Briggs, 1980). Other beef breeds in the UK include the Shorthorn, the

Hereford, the Limousin and the Charolais. From the perspective of modelling thermal balance, there are few differences between beef and dairy cattle. The main ones are the weight, thermoneutral metabolic heat production and coat albedo. In the following sections, the model operations outlined refer to both dairy and beef cattle, unless otherwise stated.

3b.1 Dimensions

The total skin area of a cow was taken as

$$A_s = 0.09 m_b^{0.67} \quad [3.9]$$

by Webster (1974), which is the same formula as for sheep (Section 3a.1), with the 0.67 power indicating an allotropic series. The implication is, therefore, that the ratios of the dimensions of each body part are constant with age. However, ASAE Standards (1987) gave standard curves for changes in body dimensions with age. In the dairy cow, for example, the trunk length to width ratio hardly changes throughout the animal's life, but the animal height to leg length ratio decreases by about 35%. In other words, the legs become much shorter in relation to trunk width as the animal matures, so growing cattle are not an allotropic series according to the ASAE. Webster's use of Eq 3.9 was therefore probably a simplification. Strictly, therefore, the assumption made for the sheep that ratios of all the body parts stay the same as the animal grows is not valid for the cow. However, including the detailed ASAE standards in the model rather than assuming the ratios remain constant results in a difference of at most a few centimetres in any particular dimension. The simplifications inherent in representing a cow as a system of cylinders mean that the

increased accuracy gained by including the ASAE standard curves would have been unrealistic. In summary, therefore, Webster's simplification in Eq 3.9 was used in the current model, and the ratios of the body parts were assumed constant throughout the animal's life. The ratios used were:

$$y_t = 2.2 d_t \quad [3.10a]$$

$$y_h = 2.0 d_h \quad [3.10b]$$

$$y_L = 4.0 d_L \quad [3.10c]$$

(combined from ASAE Standards, 1987 and Porter, 1991). The notation is the same as that adopted in Eq 3-2d to 3-2f (Section 3a.1).

3b.2 Heat flow through tissue

The thermoneutral body temperature of cattle is about 38°C (Mount, 1979; McArthur, 1987). Unlike the sheep, a cow's body temperature may rise considerably (eg. by a degree or so) at air temperatures encountered in the UK (25 - 30°C: Mount, 1979) due to their high metabolic heat production. The response of rectal temperature to environmental conditions is discussed further in Section 3b.5.

The tissue resistance of the trunk, legs and head of cattle varies in response to environmental conditions in the same way that resistance of the legs varies in sheep. The constricted value of trunk resistance, r_{stmax} , was calculated using the relation proposed by Ehrlemark & Sallvik (1996):

$$r_{smax} = 20.7 m_b^{0.41} \quad [3.11]$$

For large animals, this relationship produces rather higher resistances (eg. 265 s m⁻¹ for a 500 kg cow) than those given by Blaxter (1967) or Blaxter & Wainman (1964), which are about 170 s m⁻¹. The difference may be due in part to changes in body composition of cattle over the past 30 years, due to genetic improvement. In young calves, Ehrlemark & Sallvik's relationship is more consistent with previous data. Gonzalez-Jiminez & Blaxter (1962) calculated vasoconstricted tissue resistances of about 115 s m⁻¹ on three week old calves, which is approximately in agreement with Ehrlemark & Sallvik's value of 100 s m⁻¹ for calves of a similar age. The trunk resistance corresponding to vasodilation was taken as 30 s m⁻¹ for dairy cattle and 50 s m⁻¹ for beef cattle, and the values do not change with age of the animal (Holmes, 1970; Ehrlemark & Sallvik, 1996). The vasodilated values vary with breed.

Whittow (1962) observed that vasodilation occurs on the limbs of cattle as well as the trunk, but gave no data on the maximum and minimum values of tissue insulation. Holmes (1970) observed that, with increasing environmental temperature, vasodilation occurred first on the ears at about 15°C, then on the legs, then the trunk at about 20 - 25°C. Again, no limb tissue insulation data were given, and the temperatures at which dilation occurs will vary with metabolic rate and other conditions. Due to the lack of data, it was assumed in the current model that values of head and tissue resistance were similar to those of sheep (ie. r_{sh} and $r_{sL} = 400 \text{ s m}^{-1}$), and the vasomotor response of the legs and ears was not modelled. The cow's trunk is approximately 75% of its total surface area, and changes in tissue resistance on the trunk will have a greater effect on heat loss than changes in the extremities, so modelling the resistance of extremities is not as important as modelling the trunk correctly. As in the sheep, the responses to avoid freezing of the tissue were built in to the model.

3b.3 Heat flow through coat

3b.3.1 Sensible heat transfer

As in the sheep, the cattle coat plays two important roles: to protect the animal from solar heat gain and to interfere with heat dissipation (Bianca, 1965). Protection from heat gain is largely provided by a high coat albedo. Cattle coats vary in density and length on seasonal timescales; in the winter, the long thin coat reduces heat loss more effectively than the short summer coat. Berry & Shanklin (1961) found that the insulation of a cattle coat is proportional to the hair weight per unit area. However, data on the physical properties of cattle coats are much rarer than for the sheep's fleece, and the current model used coat depth as the main input variable. Properties such as the ability of wind and longwave radiation to penetrate the coat (indicated by the values of c' and p , respectively) were assumed constant throughout the year in the absence of any contradictory data. The value of p adopted in the model was 1800 s m^{-1} , given for cattle by Cena & Clark (1978). A value of c' for cattle is not given in any literature, so the value for caribou of $2.4 \times 10^{-5} \text{ m}$ was used in the model (Campbell et al, 1980). Caribou, deer and cattle have similar hair fibres (Cena & Clark, 1978; Monteith & Unsworth, 1990).

The cattle coat growth cycle over the year was investigated by Dowling & Nay (1960). The breed studied were beef cattle (Shorthorns). The summer hair is about half the length, and half the weight per unit area, of the winter coat, but the average fibre diameter of the summer coat is about 30% greater. Dowling & Nay's data give a minimum length of 10 mm in spring, 12 mm in the summer and 14 mm in the autumn, rising to 22 mm in late winter, prior to shedding. For the model, a linear interpolation was assumed between these seasonal figures in the absence of more detailed data. The data were used for the dairy and beef models.

3b.3.2 Latent heat transfer

Below the lower critical temperature, evaporative heat loss is limited to water vapour diffusion through the skin and water vapour exchange from the respiratory tract at thermoneutral respiration levels. McArthur (1987) assumed that water vapour diffusion through the skin resulted in a minimum value of E_c of 10 W m^{-2} . Blaxter & Wainman (1964) and Webster (1974) separately measured the minimum total evaporative heat flux (skin plus mouth) as 17 W m^{-2} . From these data, the resting respiratory evaporative heat flux was assumed to be 7 W m^{-2} . Above the lower critical temperature the evaporative heat loss rises. In cows this is principally as a result of sweating (ie. increasing E_c) rather than by panting, so the analysis must include consideration of the transfer of water vapour through the coats (outlined in Section 2.4.2). The operation of the sweating response of the model is discussed in Section 3b.5.

3b.4 Heat flow to the environment

3b.4.1 Convection

Measurements on heat transfer from live cattle made by Wiersma & Nelson (1967) yielded relationships between Nusselt and Reynolds numbers and between the Nusselt and Grashof numbers for forced and free convection respectively. These data were subsequently used by Higgins & Dodd (1989) and Ehrlemark & Sallvik (1996) in their computer models of heat transfer from cattle. The relationships are: for forced convection:

$$Nu = 0.65 Re^{0.53} \quad [3.12]$$

and for free convection:

$$Nu = 6.85 Gr^{0.137} \quad [3.13]$$

In forced convection, Eq 3.12 indicates that as wind speed (represented by Reynolds number) increases, the rate of increase of Nusselt number (which is directly proportional to heat flux density) decreases. This dependence is shown by the power of 0.53. In other words, at higher wind speeds, increasing the wind speed still further makes less difference to the heat transfer. This dependence on wind speed contrasts with the Nusselt/Reynolds number relationship for sheep (Section 2.5.1) which shows an almost linear dependence. The wind speed at which a cow's coat insulation is almost destroyed (for example reduced to 10% of its still air value) is less than for the sheep's fleece, which would be expected since cows usually have much shorter coats than sheep.

The processes occurring in free convection from a rough surface are complex and are as yet largely unresearched. Achenbach (1977) showed that a rough surface increased turbulence, and hence the heat transfer in wind was increased relative to a smooth surface. However, at low Reynolds number another process acts in the opposite sense: a rough surface will increase the boundary layer thickness, and hence impede heat transfer. Table 3.2 compares typical values obtained from the Nusselt/Grashof number relationship given by Wiersma & Nelson (1967) with those for smooth cylinders (Section 2.5.1) for a range of temperature differences.

ΔT (K)	Grashof number	Nusselt number (smooth cylinder)	Nusselt number (rough cylinder)
1	2.32×10^6	19	51
5	1.16×10^7	28	64
10	2.32×10^7	33	70
15	3.48×10^7	37	74

[Table 3.2: Nusselt numbers measured from smooth and rough cylinders under free convection. ΔT is the temperature difference between the surface and the air, Grashof number was calculated as $2.32 \Delta T \times 10^6$, assuming air temperature of 20°C and characteristic length scale of 0.25 m (Appendix 2.2)]

As the Nusselt number is directly proportional to heat flux density, the rough surface acts to increase heat transfer, ie. the decrease in laminarity dominates over the increase in boundary layer thickness. Consequently, a smooth-cylinder assumption for free convection from cattle is likely to underestimate heat transfer at low wind speed. The difference in heat loss from the whole animal modelled using the rough and smooth cylinder assumptions has been assessed in the sensitivity analysis in Chapter 5. Wiersma & Nelson's empirical relationship was obtained from a physical model of a cow, with a Hereford pelt attached, and no comparable measurements have been made on real cattle. Consequently, no assessment of the effects of breed and coat length may be done. One possible source of error in Wiersma & Nelson's data is their use of thermocouples to measure coat surface temperature. The temperatures obtained will be less accurate than those obtained for a solid surface as the position of a rough surface is less well-defined.

3b.4.2 Solar Radiation

Kovarik (1964) showed that coat colour affects the absorption of solar radiation by influencing both the amount reflected and the depth at which absorption takes place. These two effects work against each other. Coats with low reflectance (eg. black) have high radiation absorptance, which increases the amount of solar radiation, and hence heat, absorbed, but the heat absorption takes place near the surface of the coat.

The result is that much of the absorbed heat is re-radiated to the environment, so the net thermal load at the animal skin is relatively low. White coats reflect much of the incident solar radiation, but the radiation which is absorbed penetrates much deeper into the coat, thus giving a higher thermal load on the animal. Kovarik found that, for a real animal, with radiation penetrating the coat, the thermal load on the animal was minimised with an optimum albedo which uses the advantages of both effects. The value of the optimum varies with coat depth and type of hair.

In the current model, solar radiation is assumed not to penetrate the coat, therefore white coats will minimise the thermal load absorbed by the animal. The effects of assuming non-penetration of the coat by solar radiation are considered in Section 3b.6. Dairy cows in the UK are usually Friesian-Holstein, which are piebald. It was assumed that half the animal's surface was black (albedo 0.05) and half white (albedo 0.5). In sunlight, the energy balance of the light and dark parts will differ, but in considering the energy balance for a whole animal, as in the current model, a whole animal albedo was used. The value chosen for the Friesian-Holstein cattle was the arithmetic mean of the black and white albedos, approximately 0.3. Beef cows are usually brown, with an albedo of about 0.1 (Mount, 1968). The solar radiation on the legs was calculated in the same way as for sheep (Section 3a.4.3).

3b.5 Physiological response to environment

Cattle employ more physiological mechanisms for thermoregulation than the sheep. The sheep's responses to heat consist almost entirely of vasomotor control and panting, but a cow may pant, sweat and vasodilate at the same time (McArthur, 1987), following which the body temperature rises. Panting is employed to a smaller extent than sweating, and this response raises the cow's metabolic rate significantly (McArthur, 1987). This complicated system of responses occurring in parallel was not modelled in the current work, following the example of Ehrlemark & Sallvik (1996), who followed the principle of least thermoregulatory effort (Section 2.10). This assumes that thermoregulatory mechanisms are deployed preferentially, in order of least metabolic cost. Vasomotor action occurs first, followed by sweating, then panting. Body temperature rises only when the maximum sweat rate is reached.

The current work is concerned primarily with the use of the model to investigate the impact of climate change. It was assumed that the model output for the cow should simply indicate the likely level of thermal stress. This approach was chosen in preference to a detailed analysis of the heat balance, including the increases in respiration rate, metabolic rate and body temperature, which would be extremely difficult to model accurately. In running the model for thirty years of hourly meteorological data, such a complicated model would be slow, and much of the output would not be used. Hence, vasomotor control and sweating, the main responses of cattle to the thermal environment, were modelled and the assessment of the stress experienced was based on the degree to which these were employed.

3b.5.1 Vasomotor control

Since cows are usually above their lower critical temperature in the UK, vasomotor control is used more to reduce heat loss in the cold than to increase heat loss in warm conditions (Thompson, 1973). Vasomotor control has been observed on all parts of the body, including trunk, legs and tail, but the current model included only vasodilation and constriction occurring on the trunk. More details, and the values used in the model for fully dilated and constricted blood vessels, are given in Section 3b.2. As in the sheep, vasomotor control was assumed to occur before water-costly sweating, which was modelled to begin only when the blood vessels were fully dilated.

3b.5.2 Sweating

Most of a cow's sweat glands are on the upper body, possibly to counteract the effects of solar load in this region (Bianca, 1965). The raised evaporative heat flux resulting from sweating therefore varies considerably between different areas of the body. However, for simplicity, the current model considered the thermal balance of the animal as a whole, so the spatial variation of E_c was not modelled.

The model calculated the required evaporative heat loss by sweating as the difference between thermoneutral metabolic heat production and heat loss with full vasodilation and minimal evaporative heat loss. The program was run again with the new value of E_c when this value exceeded 10 W m^{-2} . However, as a higher evaporative heat loss reduces T_s , the required evaporative heat loss for equilibrium was lowered. This procedure continued until stable values of T_s and E_c were obtained. The theoretical maximum evaporation rate (based on physical principles), E_{\max} , was calculated as in Section 2.4.2. The value of E_{\max} could not be used on its own, as it approaches

infinity as the coat length falls to zero, and the maximum sweat rate for real animals is limited by physiological factors, including water availability. Thompson (1973) and Webster (1974) state that the highest observed evaporative heat flux from the skin of a cow is about 120 W m^{-2} . In the model, the calculated E_{max} was compared with the physiological maximum; the lower of the two was taken as the maximum evaporative heat flux under given conditions. Atmospheric humidity has little effect on the evaporative heat flux, as when ambient humidity is high, skin wetness (ie. the ratio of evaporative heat loss to E_{max}) increases to compensate. In other words, the theoretical value of E_{max} falls when humidity is high, and the animal sweats at a greater fraction of the maximum possible. The animal is therefore more stressed at higher humidities. The degree of stress is expressed as the ratio of actual to maximum possible evaporative heat flux. When E_c exceeds E_{max} the evaporation of sweat is restricted, and metabolic rate, respiration rate and body temperature start to rise. High respiration rates in cattle are a last resort response to hot conditions (Bianca 1965) as the metabolic cost is significant. However, when high humidity and high temperatures combine, the respiration rate and body temperature may increase rather than the animal suffering a drop in evaporative heat flux (McLean & Calvert, 1972). Body temperature and respiratory responses have not been parameterised in the current model for reasons already discussed. When E_c exceeds E_{max} the model simply flags the conditions as causing severe heat stress in cattle.

3b.5.3 Responses to cold conditions

As already mentioned, responses to cold conditions play a less frequent role than the responses to warm conditions for cattle in the UK. The dilation of the blood vessels in the extremities to prevent tissue freezing in severe cold was parameterised as for the unicorn (Section 2.10.4). Cattle also use piloerection in the cold to increase the coat insulation. Thompson (1973) quoted an increase in coat insulation of almost 50% when the coat was fully erect, but this figure varies widely between breeds. The

relationship between increase in coat depth and increase in insulation is non-linear; Monteith (1973) stated that when calves double the coat thickness they achieve only a 35% increase in insulation. In part, this non-linearity is due to the effects of curvature of the body, and is most noticeable in animals such as the chicken, which uses feather fluffing to minimise heat loss (see Chapter 4). Piloerection was included in the current model by allowing the coat resistance to rise in response to cold in an attempt to match heat loss to heat production. Thompson's figure of a maximum coat resistance of 1.5 times the non-erect value was used as the upper limit.

3b.6 Cattle model validation

3b.6.1 TEST 1: Effect of coat length and wind speed on heat loss

The model was run for different coat lengths, wind speeds and temperatures, and the results compared with measurements by Blaxter & Wainman (1964). The data were obtained from beef steers, with a thermoneutral metabolic heat production of approximately 100 W m^{-2} , and a mean mass of 336 kg. Solar radiation was zero, and $T_r = T_a$. Initial tests showed a marked underprediction of heat loss by the model, which was corrected by modifying the tissue resistance of the trunk. The quantity r_{stmax} in the original model was calculated as approximately 230 s m^{-1} for a 350 kg cow (using Ehrlemark & Sallvik, 1996), but this was larger than the value of 170 s m^{-1} given by Blaxter (1967) for vasoconstriction. The difference may be due to changes in muscle/fat composition of a typical animal over the past 30 years. The model was then run with $r_{\text{stmax}} = 170 \text{ s m}^{-1}$, with facility for shivering if necessary, for comparison with Blaxter & Wainman's data. The results are shown in Table 3.3.

Table 3.3. Effects of wind speed, air temperature and coat length on heat loss from steers. E = respiratory + cutaneous evaporative heat flux per unit skin surface area,

$W\ m^{-2}$, G_H = sensible heat flux, $W\ m^{-2}$. Discrepancy = (Modelled value - Measured data)/Measured

T_a (°C)	l_t (mm)	u (m s ⁻¹)	E: data	E: model	G_H : data	G_H : model	Discrepancy, %
0	28	0.2	20	26	87	74 ¹	30
		0.7	20	17	93	89	-4.3
1.0	4	0.2	18	17	145	125 ³	-13.8
9.0	22	0.2	28	37	69	63	32.1
9.6	23	0.7	23	29	78	71	26.0
19.0	6	0.7	29	30	72	70	3.4
	9	0.2	42	42	78	58 ²	0.0
	22	0.2	46	53	55	47	15.2
		0.7	45	49	57	51	8.9

See text for cases marked 1, 2 and 3.

For conditions above the LCT (ie. E greater than the resting value of $17\ W\ m^{-2}$), the discrepancy refers to *evaporative* heat flux measurements versus model predictions. Above the lower critical temperature (LCT), which covers all data apart from those at 0° and 1.0°C, a major assumption of the model is that evaporative heat loss is calculated as the value needed to force total heat loss to equal metabolic heat production ($100\ W\ m^{-2}$). In Table 3.3, the total heat loss ($E + G_H$) measured at 9.0, 9.6 and 19.0°C was equal to $100 \pm 3\ W\ m^{-2}$, so it can be assumed that the real animal was above its LCT for measurements made at these temperatures. A successful validation result for these conditions is therefore indicated when the model predicts the latent heat flux correctly. Although some of the percentage errors are high, the absolute errors are acceptable, given that the assumed E below the LCT in the model may be in error by up to $5\ W\ m^{-2}$ due to differences in breeds and age. Blaxter's measurements of components of heat production varied by about $3\ W\ m^{-2}$ between different animals under the same environmental conditions.

In the case marked 2, the measured total heat loss was 120 W m^{-2} , while the model continued to predict the value as 100 W m^{-2} . It is evident, therefore, that in reality, measured data do not always conform to the model's rigid simplification that heat loss = thermoneutral heat production above the LCT.

Below the LCT ($E \leq 17 \text{ W m}^{-2}$), the discrepancy was calculated from the modelled and measured *sensible* heat fluxes. The model sets evaporative heat loss to a minimum value, obtained from measurement (Section 3b.3.2) and calculates sensible heat loss. Therefore, below the LCT a successful validation result is indicated by the model predicting sensible heat loss correctly. In case 3, both model and measurement agree that the animal is below its lower critical temperature, ie. total heat loss exceeds thermoneutral metabolic rate. In case 1 (ie. 0°C , 28 mm coat and 0.2 m s^{-1} wind), the measured data suggest the animal was just below its lower critical temperature but this result was not indicated by the model. At 0°C , 28 mm coat and 0.7 m s^{-1} wind, the sensible heat loss was predicted to within 5%, but when the coat was reduced to 4 mm (clipped) the model underpredicted sensible heat loss by 14%. A very short coat is subject to large relative errors of measurement, and as was noted for sheep (Section 3a.6.2), the predicted heat loss is sensitive to such errors. The model underprediction at 4 mm coat length is therefore probably within errors of measurement on the real animals. In addition, at coat length of 4 mm, there will be bare parts of the skin showing through the coat, and some parts of the body may be completely bare. Exposure of the skin will enhance heat losses by thermal radiation and convection. Such enhancement is not predicted by the model, which assumes a uniform covering of coat, with radiant and convective exchange taking place at the coat top.

3b.6.2 TEST 2: Heat loss from Friesian calves

This test examined the effects of wind speed and air temperature on young cattle. The test was made in conjunction with Test 1 in the previous section, with the aim of

testing the model's accuracy over a wide range of animal ages. The model predictions were compared with data measured by Holmes & McLean (1975) on Friesian calves. The calves were aged between 7 and 60 days, and had a mean mass of 37 kg. The measured metabolic heat production was 81 W m^{-2} for a maintenance feed intake, and 108 W m^{-2} for twice maintenance. The measurements were taken in a calorimeter, so solar radiation was zero, and the radiant and air temperatures were assumed equal. Coat length was not measured by Holmes & McLean, in spite of the importance of this parameter in determining heat loss. The model assumed a value of 15 mm for the coat length of a young calf.

The comparison was made for maintenance feed level to allow assessment of the performance of the model for animals below the LCT. Four temperatures and two wind speeds were used: 3, 8, 12 and 20°C and 0.2 and 1.6 m s⁻¹. The results are shown in Table 3.4.

Table 3.4. Comparison of predicted total heat loss (G_e , W m^{-2}) from Friesian calves with data by Holmes & McLean (1975). Discrepancy = (Modelled value - Data)/Data

T_a (°C)	u (m s ⁻¹)	G_e model:	G_e measurement:	Discrepancy, %
3	0.2	103	100	3.0
3	1.6	140	107	30.8
8	0.2	89	94	-5.3
8	1.6	122	103	18.4
12	0.2	80	87	-8.0
12	1.6	105	92	14.1
20	0.2	81	88	-8.0
20	1.6	82	85	-3.5

Lower critical temperatures: $u = 0.2 \text{ m s}^{-1}$ Model LCT = 11°C
Measured LCT = 12°C

$u = 1.6 \text{ m s}^{-1}$ Model LCT = 19°C
Measured LCT = 16°C

The overall error, O (Eq 3.7) for all data was 12%. The model and measurement agreed to within 10% for the low wind speed conditions. The LCT was well-modelled at low wind speed, to within a degree of the measured value. However, at high wind speed the model over-predicted heat loss, and the discrepancy increased as temperature fell. The behaviour of the model was similar to the sheep model below the lower critical temperature (Section 3a.6.1) where the model over-prediction was probably due to the real animal adopting a compact posture, and hence reducing heat loss. In sheep, the relatively low metabolic rate may cause the animal to be below its lower critical temperature reasonably frequently in winter, and it was important to model posture changes. However, the growing calf usually has a metabolic rate of at least 140 W m^{-2} (Mount, 1979), 1.75 times the value used in the current test. The high metabolic rate means that cows in the field will seldom be below their LCT in UK conditions. For this reason, postural changes were not incorporated in the cow model below the LCT.

3b.6.3 TEST 3: Penetration of the coat by solar radiation

This test was different to Tests 1 and 2, as it compared predictions from the current model with those from another model. McArthur (1987) developed a general thermal balance model and used parameters for cattle for the validation. McArthur's model allowed for penetration of solar radiation into the cattle coat, which the current model

did not. The aim of this test was to compare the effects on heat loss of including and ignoring solar radiation penetration.

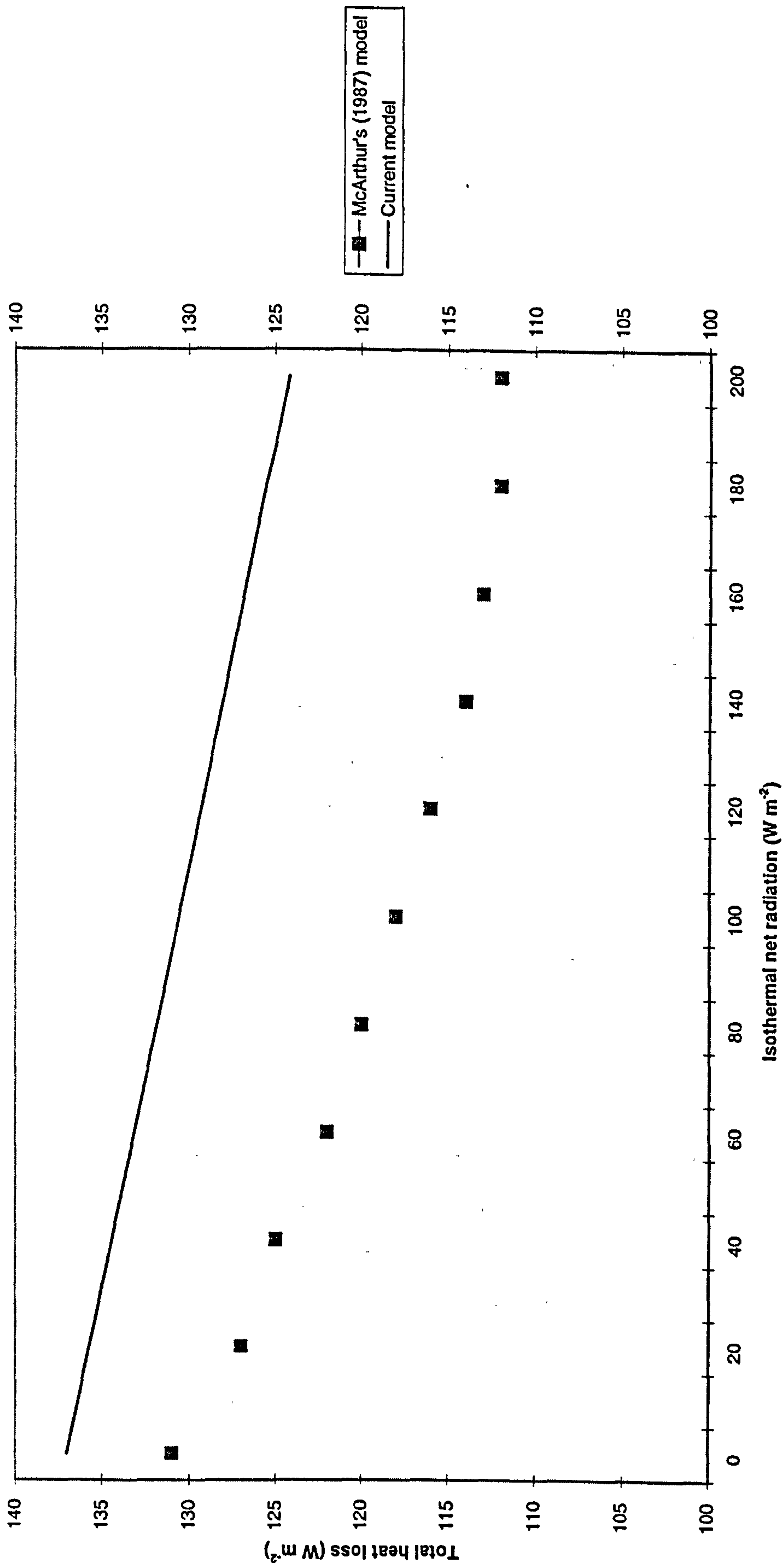
Fig 3.5 shows the heat loss from the model cow plotted against the solar load for a 10 mm coat length, the shortest usually found in animals in the field. The air temperature was assumed to be 10°C, coat reflectivity 0.66, wind speed 0.5 m s⁻¹ and vapour pressure 1000 Pa. Fig 3.5 shows that as expected, penetration of solar radiation into the coat decreases the heat loss from the animal. Without a solar load, the two models agree to within 5%, but as solar radiation increases, the discrepancy becomes greater. The current model overpredicts heat loss by approximately 10% by ignoring radiation penetration. This error is acceptable, and the advantage gained in model simplicity by ignoring solar radiation penetration seems not to produce severe problems.

3.3 Behavioural responses of outdoor animals

As well as physiological responses to the environment, animals also respond to hot or cold conditions by changing their behaviour. For animals outdoors, such behaviour may involve moving to a more comfortable thermal environment, or changing their posture to alter the heat loss. Baldwin (1974) reviewed studies of behavioural thermoregulation, and the responses are summarised as follows:

- 1) High ambient temperature
 - * Increase surface area for heat loss
 - * Shade-seeking
 - * Wallowing or bathing
 - * Group dispersion

Fig 3.5: Total heat loss from model sheep as a function of isothermal net radiation. Comparison of current model predictions with predictions from McArthur's (1987) model.



2) Low ambient temperatures

- * Huddling in groups
- * Reduce effective surface area for heat loss (eg. by adopting a compact posture)
- * Doing mechanical work (eg. walking etc.)

Some of these responses have already been discussed. This section covers aspects such as modelling the effects of shade and shelter and quantifying their effects on heat balance.

3.3.1 Animal choice

It is commonly observed that, when the air temperature is high, sheep and cattle in a field without shade under high solar radiation usually stand 'tail-on' to the direct solar beam, both to reduce the local heating of the head and to minimise the amount of solar radiation impinging on the body. Alternatively, a group of animals will stand in a row, side-on to the beam, each animal shading the next. However, most animals not feeding will seek shade when provided. Animals exposed to wind and rain will shelter behind fences and walls, unless their food needs are great enough to overrule their desire for shelter. These simple observations introduce the complex subject of animal choice.

Wathes (1997) outlined the three types of choice an animal can make: environmental, nutritional and social. Nutritional and social choices have been reduced by intensive farming, so for outdoor animals, environmental choice dominates. An animal has to decide on the optimum environment, given several other factors, such as hunger or the desire to mate. Nicol (1997) proposed three 'goals' that may determine animal choices. First, to *maximise* some quantity, maybe energy gain or thermal comfort. Second to *optimise* some value; usually for homeotherms this involves maintaining a

constant deep-body temperature. Third, as a *trade-off*, for example, lying down and sacrificing physical comfort but benefitting by avoiding drafts, or walking across a field in hot sunshine to reach food in preference to staying hungry in the shade. It has been suggested that food demand is the primary choice over all others, but this is not always the case, especially in the short-term. Modelling which choices or trade-offs an animal will make, and when, is a very complex process, and has not been considered in the current work. However, it is important to quantify the effects of shade and shelter, and to this end the outdoor energy balance model has been run to comparing the thermal balance of the unicorn with and without shade and shelter.

3.3.2 Shelter from wind

The effects of shelter from rain have already been demonstrated in Fig 2.6. This section outlines how shelter from wind was incorporated in the model. Bruce & Broadbent (1989) used a series of 'climate modifiers' to calculate effective values of wind speed and rainfall in a selection of shelter types. For example, 10 m inside a forest, the wind speed was found to be 0.55 of the unsheltered value, and the corresponding climate modifier for rainfall was 0.8. These values were found from observation, and vary considerably with type and dimensions of the shelter, as shown by the models of Wang & Takle (1995, 1996). Two types of shelter have been considered here:

- 1) A Wall, 1.5 m high, porosity = 0.1

A sheep (height 0.5 m) sheltering in the region of minimum wind speed will experience a wind speed of approximately 5% of the open ground value (Wang & Takle, 1995).

- 2) A dense group of young trees, or tall hedge, porosity = 0.4

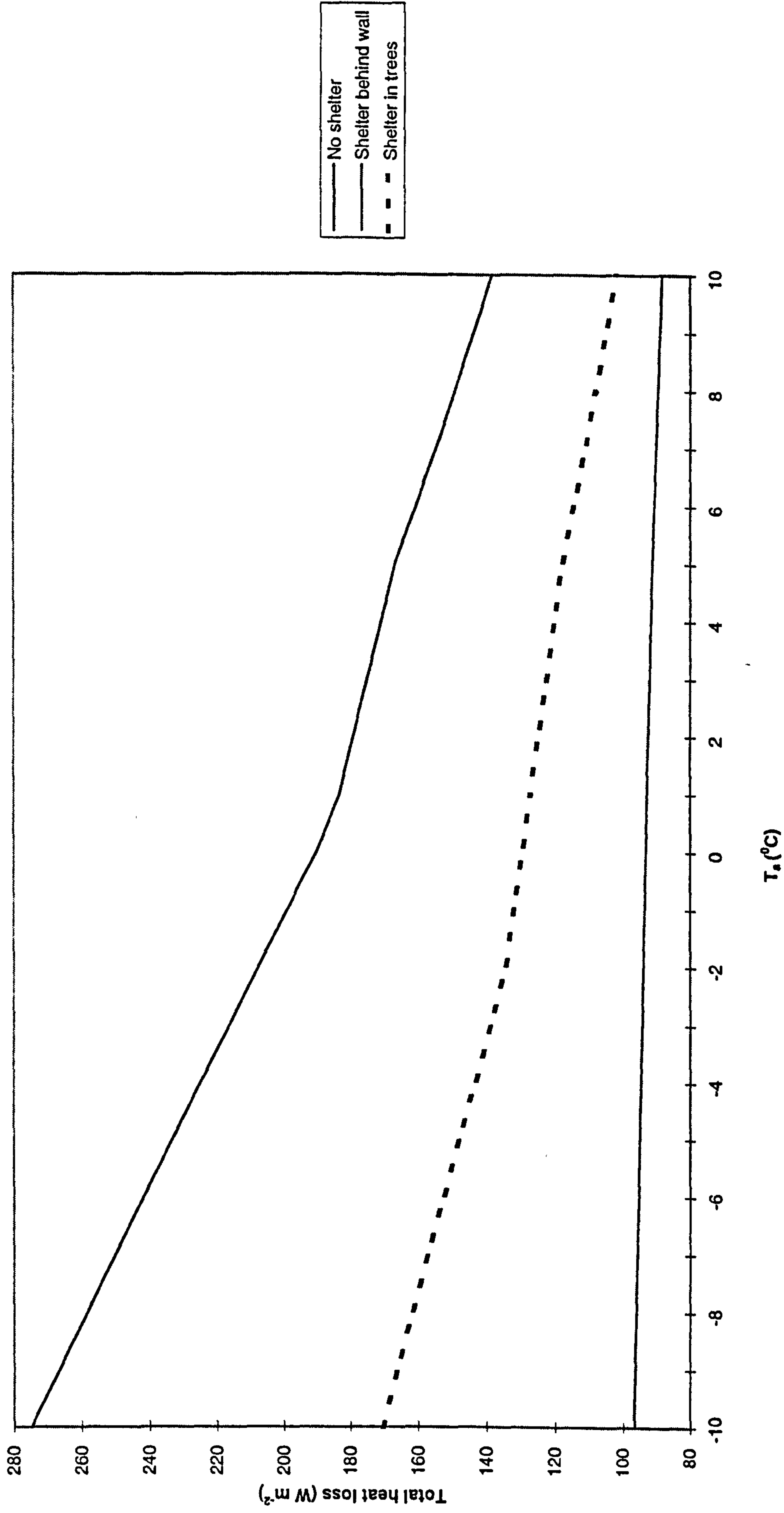
A sheep or cow which is 0.3 times the shelter height will experience a wind speed approximately 35% of the open ground value (Wang & Takle, 1995) when sheltering in the region of minimum wind speed.

The conditions used in producing Fig 2.8 were used in the model runs for both shelters. The coat was assumed to be dry. The effects of shelter can be seen in Fig 3.6. Sheltering behind a stand of young trees, which reduces the wind speed by 65%, an animal can reduce its heat loss by 25% at 10°C and 38% at -10°C. The change in gradient of heat loss with temperature, associated with the dilation of blood vessels in the legs to stop the tissue freezing, occurs at an air temperature of about -2°C for the animal sheltering near the trees, compared to 2°C for the unsheltered animal. The increase in heat loss with decreasing temperature is modified by increasing shelter. For unsheltered animals, heat loss increases by approximately 8 W m⁻² per K temperature fall below the point of maximum dilation. This value falls to 4.4 W m⁻² per K for the animal behind the trees, and for the animal behind the wall the change is 0.5 W m⁻² per K. The animal behind the wall does not need to vasodilate to prevent tissue freezing, and the heat loss remains relatively low. This test shows the importance of providing shelter for animals at high wind speeds, and that the benefit increases as temperature falls.

3.3.3 Shade

The only estimate of the effects of shade on the heat balance of livestock outdoors is found in Stafford Smith et al (1985). Their approach assumes that the diffuse solar component striking the animal in shade (including that reflected from the ground) is 40% of the open ground diffuse radiation. None of the direct solar component is assumed to strike the animal in shade. The equation for solar radiation incident on the animal (Eq 2.31) therefore becomes:

Fig 3.6: The effects of different types of shelter on modelled heat loss from the unicorn



$$S_i = (1 - 0.6Z) \left[\frac{\rho_g (S_b + S_d)}{2} + \frac{S_d}{2} \right] + (1 - Z) \frac{A_h}{A_c} S_b \quad [3.14]$$

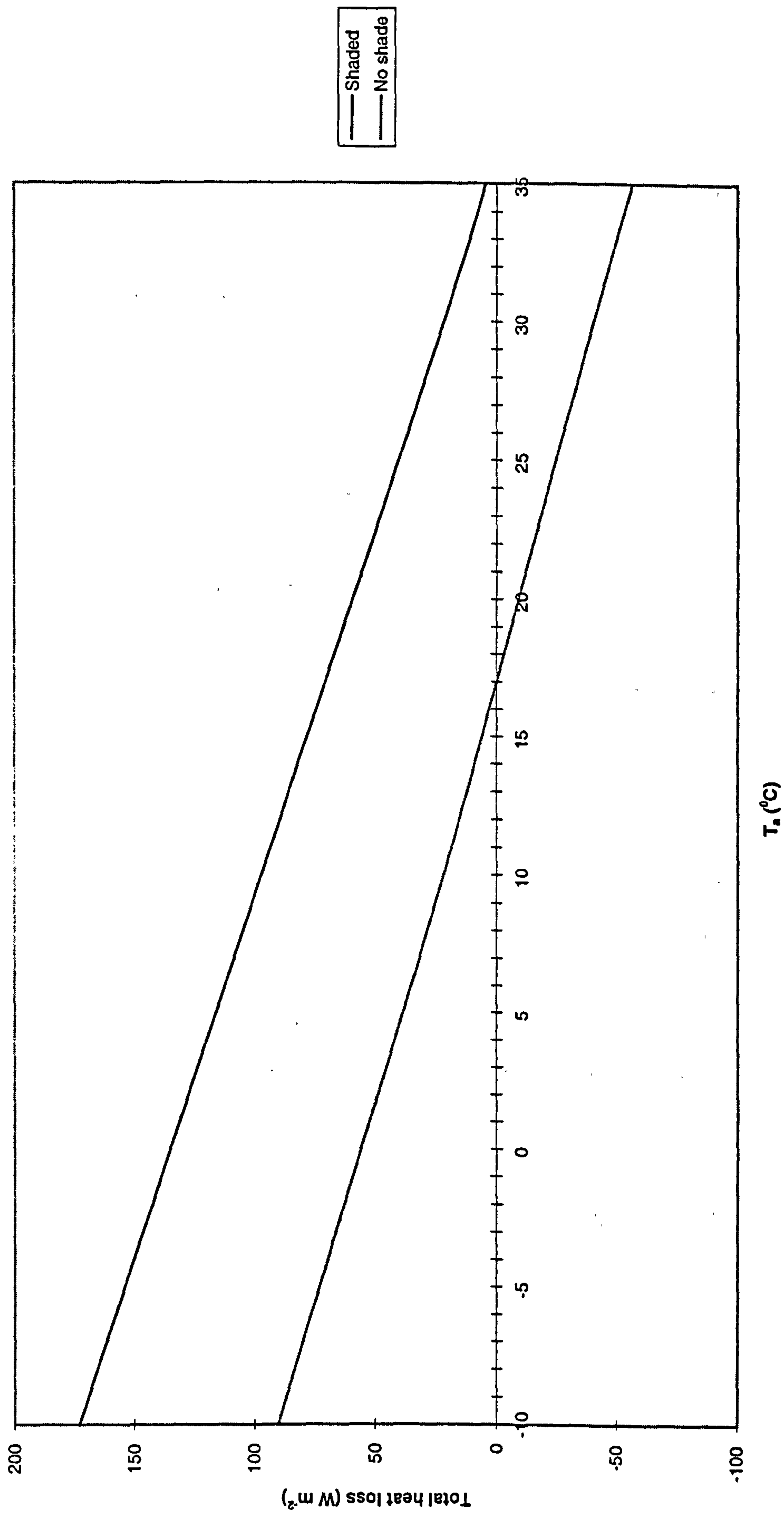
where $Z = 1$ if the animal is in shade and 0 if in the open.

Shade also affects the longwave radiation exchange. Stafford Smith assumed that, for an animal standing under a tree, the radiant temperature of the sky, T_{sky} , was equal to T_a , so that the radiant temperature of the environment, T_r , is given by:

$$T_r = \left[\frac{T_g^4 + T_a^4}{2} \right]^{0.25} \quad [3.15]$$

The conditions used in Fig 2.6 were used again to examine the effects of shade on the energy balance of a unicorn, taken here as an inanimate cylinder. Fig 3.7 compares the total heat loss from an animal in the open and in shade under a tree at noon on a clear day in mid-summer. The unshaded animal absorbed about 300 W m^{-2} of solar radiation. The animal in shade absorbed 45 W m^{-2} , all from diffuse radiation. Over the whole temperature range, shade increases the rate of heat loss from the unicorn by more than 70 W m^{-2} , which is approximately the rate of thermoneutral heat production at maintenance feed intake. Although an absorbed solar radiation of 300 W m^{-2} is impossible at the lower end of the temperature range in the UK, the graph illustrates the importance of solar radiation as a component of the energy balance. At high temperatures, an increase in the heat loss by 50 W m^{-2} as a result of shade would be equivalent to a significant decrease in the respiration rate of a sheep, for example. Blaxter et al's (1959) data suggest that the reduction in the respiration rate of sheep due to shade at high temperatures is between 100 and 200 breaths per minute,

Fig 3.7: Predicted total heat loss from a unicorn in direct sunlight and in shade



indicating a significant lessening of heat stress. Conversely, at low temperatures, an animal may use solar radiation to alleviate cold stress. Solar load can be maximised by standing side-on to the direct beam, and even at low solar elevations, standing in the sun can reduce cold stress significantly (Vandenheede, 1995).

3.4 DISCUSSION AND CONCLUSIONS

The unicorn model was adapted to model the thermal balance of ruminants outdoors, and in general the models of each species performed well in comparison with experimental data. One of the problems in the model validation was the scarcity of recent measured data of components of heat loss, thermoneutral metabolic heat production and body insulation. For cattle and sheep, the available data were generally obtained before 1970, and usually under carefully controlled calorimeter conditions. In the field, the environment is highly variable, for example animals are subjected to gusty wind and wet coats, and also to variable solar loads. Much of the work on cattle was done on beef calves or steers; accurate heat loss data across a range of temperatures for pregnant or lactating dairy cows or ewes is not available. The model validations (Sections 3a.6 and 3b.6) used the best data available in comparing the output of the model cow with real measurements, but some measurements omitted important variables such as coat length. In order for future models to be useful, more data are needed, and need to be obtained under specified conditions. Observations should include the coat length of the animal, humidity and air speed which were not always mentioned in the data used above. In spite of such problems, the models, especially the sheep, produced predictions within 10% of the measurements under the same environmental conditions. This error is acceptable for a model of environmental processes, especially when considered in conjunction with the likely errors in experimental data.

Many of the assumptions in the cattle and sheep models have already been discussed; the main shortcomings of the models are now discussed. Some parts of the models (especially for the cow) used breed-specific relationships which have been assumed to hold for all breeds. Some examples include the modelled coat growth cycle for cows (which employs data from Shorthorns), and the Nusselt/Reynolds and Nusselt/Grashof number relationships for sheep and cattle. There are other instances where the model has used a single parameterisation, usually assuming a 'standard' animal, for a process which may vary between breeds (eg. choice of r_{stmin} and the vasomotor response). Such assumptions may cause errors when the model is applied to a particular breed. However, the validation has shown that the resultant errors are relatively small. The animal's choice of environment, for example when to go into shade or shelter, and also the mechanical work done by an animal, have not been modelled due to the excessive complexity which would be required. The effects on heat balance of the presence of other animals has not been included, although in the field, sheep especially will huddle together in the cold. All these points may be included in future modifications of the model, although the model developments will have to be done in conjunction with relevant data collection.

APPENDIX: WOOL GROWTH RATES

Data from Slee & Carter (1961), Wiltshire Horn breed:

MONTH	WOOL GROWTH DURING MONTH (mm)	CUMULATIVE WOOL LENGTH AT END OF MONTH (mm)
Jan	3	69.5
Feb	3	72.5
Mar	4.5	77
Apr	5	82
May	5.5	87.5 / 5 after shearing
Jun	6.5	11.5
Jul	8	19.5
Aug	9.5	29
Sep	12	41
Oct	10.5	51.5
Nov	9	60.5
Dec	6	66.5

NOTES:

Shearing occurs at the end of May, reducing the coat to 5 mm length.

CHAPTER 4: MODELLING ANIMALS IN INDOOR ENVIRONMENTS

4.1 Introduction

This chapter describes the adaptation of the unicorn model to simulate the thermal balance of livestock indoors. The animals modelled were pigs and broiler chickens, which spend most of the time indoors in the UK. The chapter follows a similar structure to Chapter 3, emphasising the special aspects unique to each species rather than giving a full analysis of the heat balance. Some of the developments described in this chapter are included in Turnpenny et al (1997), combined with models of feed intake and housing thermal balance.

4.2 General considerations for animals indoors

Animals such as pigs and poultry are usually kept indoors all year round in the UK. Pigs and poultry, unlike ruminant livestock, have a much narrower thermoneutral zone (Charles, 1994), and as such are usually kept in controlled environment houses to maximise productivity. Such houses maintain the thermal environment (eg. temperature and humidity) within certain limits depending on the age and species of livestock by controlling the ventilation rate (Randall & Boon, 1994). For poultry, the optimal temperature is about 31°C for newly-hatched birds, falling to about 20°C at two to three weeks old (Mount, 1979; Charles, 1986). The temperature inside the house is usually chosen by balancing costs of fuel for the ventilation fans and feed with productivity of the animals, ie. the house is run at a financially optimal temperature, which usually but not always lies close to the lower end of the animals' thermoneutral zone. Young pigs are susceptible to cold while tissue insulation is low, but mature pigs are susceptible to heat as their thermoregulatory capacity is limited (Section 4a.4). New-born piglets, even fed at three times maintenance, have a lower

critical temperature around 29°C, though mature fat sows would be severely hyperthermic at this temperature (Mount, 1979). However, the pig's capacity for behavioural adaptation to the thermal environment usually prevents severe problems in the UK.

An animal in a controlled environment house is not exposed to direct solar radiation, and efficient building design makes the solar radiation load approximately zero in windowless poultry houses (Clark & McArthur, 1994). The small windows in some pig houses (Smith, 1994) have little effect on the net radiation between the animals and their surroundings. In addition to protection from rain, air speed is controlled, thus removing two of the major causes of cold stress at low temperatures. However, the increase in humidity and temperature caused by many animals in one space is significant (Clark & McArthur, 1994), and in hot conditions may aggravate heat stress.

Within the animal house there can be considerable non-uniformity of variables such as air speed and temperature. D'Alfonso et al (1996) measured the dry bulb temperature field in different building types, and found considerable stratification, especially in cold conditions. The centre of the house was approximately 3 - 4°C warmer than round the walls, and air near the ceiling was also about 3 - 4°C warmer than near the floor. Heber et al (1996) made measurements, and Christenen (1993) used computational fluid dynamics, to predict the air movement pattern within an animal house. Heber et al showed the flow to be complex and turbulent, with a circulation originating from the air intake and promoted by convection induced by the warm animals. The turbulence was found to be non-isotropic, and thus predicting the air speed within an animal house is extremely difficult analytically.

The variability of temperatures and air speeds within structures is most important for broiler chickens when they are being transported. Mitchell & Kettlewell (1994) reported that 40% of mortalities occurring in animal transport are due to thermal stress. Even when not fatal, thermal stress can cause tissue damage and affect

hormone levels and blood chemistry, affecting production quality as well as the animal's welfare. Mitchell & Kettlewell used thermal mapping to show the heterogeneous nature of the temperature field within a chicken transporter. Large thermal gradients occur between the carrier containers and the edges of the transporter. Humidity is an important factor: increasing the relative humidity from 20 to 80% at 28°C raised body temperature at a rate of 0.4°C hr⁻¹. Webster et al (1993) exposed a physical model of a chicken to different wind speeds and temperatures on a lorry. The mean temperature inside the transporter varied from 6 - 8°C above outside temperature when the lorry was moving, to 8 - 14°C above when the lorry was stationary. They found that in the vast majority of conditions birds will be uncomfortable some of the time when being transported. However, increasing the air speed by vehicle motion had a large effect. The maximum outside temperature at which the animals will be comfortable (on the basis of mean interior temperature) rose from 13°C when the lorry was stationary to 26°C when the lorry was moving, indicating that controlling air movement inside animal transporters will have a significant beneficial effect.

4a PIGS

The response of the pig to its thermal environment changes considerably as it grows, principally due to the increase in tissue resistance with age. The coat is generally sparse (except on some mature animals), and since the coat insulation provides such a small part of the total body insulation, it was assumed in the current model that the pig is hairless. This assumption considerably simplifies the computation necessary to reach stable solutions of the heat balance equation. The pig has also been modelled as a cylindrical trunk with round ends incorporating the head, and four legs. The representation of the pig's combined trunk and head as a round-ended cylinder is almost an exact fit, as shown by the image analysis experiments of Schofield & Marchant (1996).

4a.1 Dimensions

Brody (1964) measured the following relationship between pig mass and skin surface area:

$$A_s = 0.10 m_b^{0.63} \quad [4.1]$$

The 0.63 power indicates the pig does not grow as an exact allotropic series; the surface area increases less per unit mass gain than for allotropic series. Standard data indicate that the pig grows in a similar way to cattle. Animal height to leg length ratio decreases by about 25% as the animal grows (ASAE Standards, 1987), though to a lesser extent than in cattle (Section 3b.1). However, as in cattle, the increased complexity of including such variations would produce false accuracy, given the assumption of the pig as a system of cylinders. An allotropic series was therefore assumed. The formula for sheep, Eq 3.1, predicts a surface area which is up to 8% above Brody's equation, Eq 4.1. An allotropic formula was therefore derived for use in the current model for pig surface area, which gave a similar surface area to Brody's for typical pig weights (up to 100 kg):

$$A_s = 0.086 m_b^{0.67} \quad [4.2]$$

Petherick (1983) showed that the linear body dimensions of pigs were proportional to the 0.33 power of live weight. The constant of proportionality was provided for the trunk but not the legs, making the data incomplete for use in the current model. The current model used the combined measurements of Davidson (1966), ASAE Standards (1987) and Schofield et al (1997) to deduce the following relations between lengths

and diameters of body parts in the pig. With similar notation to that in Section 3a.1, the relations are:

$$y_i = 2.6 d_i \quad [4.3]$$

$$y_L = 3 d_L \quad [4.4]$$

4a.2 Tissue insulation

In pigs, the tissue is the primary source of insulation. Tissue insulation varies considerably with the age of the animal; up to a week old, when its subcutaneous fat layer starts to build, a pig is very vulnerable to cold stress, with a lower critical temperature around 34°C (Mount 1979). Conversely, mature sows can have lower critical temperatures around 0°C. Based on the analysis of Bruce and Clark (1979) and data from Ingram (1964b) and Mount (1968), the model relation between maximum tissue resistance of the trunk (constricted blood vessels) and live weight is:

$$r_{stmax} = 40.0 m_b^{0.33} \quad [4.5]$$

with r_{stmax} in $s m^{-1}$ and m_b in kg. The same sources yielded the relation between dilated resistance (r_{stmin}) and live weight as:

$$r_{stmin} = 24.2 m_b^{0.33} \quad [4.6]$$

Unlike sheep, vasodilation in pigs occurs mainly on the trunk (Ingram 1964b); there are few data for heat transfer from the legs, so it was assumed that leg tissue resistance was a constant, unaffected by weight and environmental conditions. The value of r_{sL} chosen for the model was 400 s m^{-1} , which represents the average value of constriction and dilation for a similar sized sheep's leg (McArthur 1980).

4a.3 Heat loss to the environment

4a.3.1 Convection

The convective heat transfer was calculated for the pig in the same way as for the unicorn (Section 2.5.1). A relationship between Nusselt and Reynolds number for a hairy model pig was established by Gannon (1996):

$$Nu = 0.0016 Re^{0.963} \quad [4.7]$$

At all wind speeds in the forced convection regime, Gannon's relationship gives a lower Nusselt number, and hence lower heat transfer, than the relationship for the bare cylinder derived by McArthur (1980):

$$Nu = 0.095 Re^{0.68} \quad [4.8]$$

However, Gannon's observations that heat transfer from rough cylinders in the forced convection regime is less than from a bare cylinder contrasts with the observations of Achenbach (1977), who showed that convective heat transfer from a rough cylinder was greater than from a smooth cylinder due to increased turbulence.

The pig indoors is generally subject to low wind speeds (less than 2 m s^{-1}), and therefore more likely to be in the free convection regime than the forced. However, a Nusselt/Grashof number relationship has not been estimated for hairy pigs, and therefore the equation for a bare cylinder in Section 2.5.1 was used in the current model to calculate heat transfer from pigs in free convection. The relationship for smooth cylinders [Eq 4.8] was used in the current model to describe forced convection. Eq 4.8 was chosen in preference to Gannon's relationship [Eq 4.7] for three reasons: consistency with the available data for free convection, the rarity of forced convection from indoor pigs, and the contradiction of Gannon's relationship with previous observations.

4a.3.2 Evaporation

Like the sheep, the pig does not actively use sweating as a method of heat loss (Ingram, 1964b; Ingram & Legge, 1969). However, unlike the sheep, it does not normally use panting either. The pig can hyperventilate under extreme heat stress (eg. at air temperatures greater than 35°C) but the associated evaporation is not sufficient to completely dissipate the heat produced by metabolism. In the current model, evaporation from the skin was taken as a constant 10 W m^{-2} (Ingram 1974), and the respiratory loss was taken as a constant 20 W m^{-2} at air temperatures below 30°C , increasing linearly to 40 W m^{-2} at 45°C (Morrison et al, 1967; Ingram 1964a).

4a.3.3 Conduction to the floor and other animals

The pig can lose 15% of its heat through conduction to the floor (Mount 1967). The effects on animals of different floor types has been examined in several studies. For example, Stansbury et al (1987) found that pigs kept on expanded metal had a significantly lower mortality rate than pigs kept on concrete. The weaning weight was 13% higher for the pigs on the metal floor. Sallvik & Wejfeldt (1993) made measurements on groups of 16 pigs of mean mass 34 kg subject to different degrees of embedding in straw. The lower critical temperature fell from about 10°C when 20% of the pig surface area was immersed in straw to -22°C for 70% immersion. The results show that providing sufficient insulation extends the range of tolerable temperature considerably.

Bruce & Clark (1979) parameterised conduction by representing heat lost (watts) to the floor, H_f , by:

$$H_f = A_f \frac{\rho c_p}{r_s + r_f} (T_b - T_a) \quad [4.9]$$

where r_s and r_f are the resistance of pig tissue and floor material respectively, and A_f is the area of the animal in contact with the floor. Mount (1967), observing the behaviour of new-born pigs, classed them into two positions: 'fully stretched out' or 'supported' (where the limbs, but no part of the trunk, were in contact with the floor).

The criteria for deciding which posture or intermediate posture the animal was in were based on Mount's observations. For T_a greater than 25°C, the animals were assumed to be fully stretched out to increase heat loss. For T_a less than 20°C all the animals were assumed to be supported to minimise heat loss to the floor. Between the two air temperatures a linear interpolation was used to describe the variation of

contact area with T_a . This is a simplification of Bruce & Clark's original parameterisation of the animal-floor interaction, made to limit complexity in the model. The quantity A_f is difficult to measure (Mount, 1967), and there are an almost infinite number of variations of pig posture. In the current model, 20% of the total skin area was assumed to be in contact with the floor when the animal was fully stretched out, and 10% when the animal was supporting itself (Bruce & Clark, 1979).

The thermal resistance of a floor varies widely between different materials. Since this resistance is a function of the area over which heat transfer occurs, r_f is also a function of A_f . This area depends on the size and posture of the animal, and on the number of animals in the group. The calculation of r_f as a function of body mass and number of pigs in the group is given in Appendix 4.1.

The area in contact with other pigs increases non-linearly with number of animals in the group. Bruce and Clark give:

$$\frac{A_o}{A_s} = 0.15 \left(1 - \frac{1}{N}\right) \quad [4.10]$$

where A_o/A_s is the ratio of area in contact with other animals to whole surface area of the pig, and N is the number in the group. It was assumed that all pigs are at the same surface temperature, therefore no net heat transfer occurs from pig to pig. Bruce & Clark's analysis was adopted in the current model.

4a.4 Responses to the environment

4a.4.1 Body temperature changes

As stated in previous sections (4a.2, 4a.3.2) the pig will vasodilate on the trunk to

increase heat loss in warm conditions, but cannot physiologically increase evaporative heat loss efficiently to aid heat dissipation. A pig may wallow in mud or water to aid evaporation, and this behavioural response is discussed in Section 4.3. If a wallow is not provided, and the pig cannot dissipate the thermoneutral heat production appropriate to the food intake, then the body temperature must rise to increase heat loss. Ingram (1964a) found the deep body temperature of the pig increased from 39°C at $T_a = 30^\circ\text{C}$ to 40.6°C at $T_a = 35^\circ\text{C}$. This increase occurred in conjunction with the rapid increase in breathing rate. The present model calculates the body temperature required to dissipate the metabolic heat, and raises the temperature accordingly. The body core can reach 43°C (Ingram & Legge 1969); above this, a pig without a wallow will die of hyperthermia very quickly.

4a.4.2 Shivering

The shivering response of a unicorn was introduced in Section 2.10.4, based on the experiments on a shorn sheep. In the absence of data giving environmental conditions which induce shivering in the pig, it was assumed that the shivering response was the same as for the shorn sheep. In other words, shivering began at temperatures below the LCT, and reached a maximum when the heat loss was 1.5 times thermoneutral heat production. It was assumed that shivering reduced tissue resistance to 70% of the non-shivering value.

4a.5 Comparison of model with measured data

4a.5.1 TEST 1: Effects of environmental temperature on heat loss

The model was run for young pigs exposed to different air temperatures at fixed wind speed, and the results are compared in Table 4.1 with measurements from several studies collated by Verstegen et al (1973). In all cases the measurements were made

in a calorimeter: solar radiation was zero and $T_r = T_a$. Verstegen et al's measurements were made on eight groups of four pigs of approximate mean mass 30 kg. Metabolic heat production was 116 W m^{-2} . Some other studies in the collation used slightly different combinations of group size and mass. The air speed was minimal in all cases (taken as 0.1 m s^{-1}).

Table 4.1. Effects of environmental temperature on heat loss from groups of growing pigs. G_e = total heat flux density. Discrepancy = (Modelled value - Measured data)/Measured

T_a (°C)	G_e Model (W m^{-2})	G_e Measured (W m^{-2})	Discrepancy, %	Source of data/notes
7	170	142	20	Close & Mount (1971). 3 expts, group of 3, mean mass 22 kg
8	165	133	24	Verstegen et al (1973)
9	161	130	24	Holmes & Mount (1967). 5 expts, group of 6, mean mass 20 kg
10	156	126	24	Verstegen (1971) (cited in Verstegen et al (1973)
12	146	126	16	Close & Mount (1971). 3 expts, group of 5, mean mass 32 kg
14	136	116	17	Verstegen (1971)

All pigs described in Table 4.1 were below the LCT. The results show a marked overprediction of heat loss by the model of between 15 and 25%. Although the model includes the effects of shivering, and the effects of animals touching each other (Section 4a.3.3) it does not include the effects of huddling in tight groups as a behavioural response to low temperatures. Holmes & Mount (1967) and Mount (1968) observed that huddling is essential for the thermal comfort of very young pigs, which have lower critical temperatures as high as 34°C. Huddling effectively reduces the surface area available for heat loss, in the same way that compacting the posture

reduces heat loss from a single animal. Mount (1968) showed that at 10°C a newborn pig reduced heat loss by 35% by huddling, and even a 60 kg pig reduced heat loss by 20% by huddling.

The increase of heat loss with decreasing temperature below the LCT changes with group behaviour. The model results in Table 4.1 show an increase in heat loss at a rate of about 5 W m^{-2} per °C fall in temperature. This compares with a measured increase of about $3.5 \text{ W m}^{-2} \text{ °C}^{-1}$ where huddling occurs - a difference of about 30%. A similar relative decrease in heat loss rise was reported by Mount (1979) to be due entirely to huddling.

It is reasonable to suggest the model discrepancy can be accounted for entirely by the lack of huddling in the model. The overall error, O (see Section 3a.6) was 21%, which is well within the differences in heat loss expected between a huddling and a single animal. A huddling response model would be dependent on temperature and other environmental conditions as well as on group size and the mass of each animal.

Such a model is not currently available. In the current project, the pigs were assumed to be in controlled environments, usually with high metabolic rates, and cold stress is not likely to be encountered regularly; it is the responses to hot conditions, which under a changed climate may be encountered more frequently, which are of more concern. Consequently, no attempt was made to devise a temperature-dependent huddling scheme for the current project. It should be noted that the model may therefore over-predict the frequency of cold stress especially in young animals when outside temperatures are low. Another possible reason for the overprediction of heat loss below the LCT by the model is that the animals in the experimental studies were kept in the calorimeter for up to three weeks before measurements were taken, and had thus had the time to acclimatise. They would therefore lose less heat at a given environmental temperature than animals exposed to the same conditions instantaneously, as in the model's predictions.

4a.5.2 TEST 2: Effects of air speed on heat loss

Mount (1966) measured the effects of air speed on heat loss from single new-born piglets. Heat loss was determined from whole-body calorimetry, which is more likely to give realistic results for the energy balance of the whole animal than heat flow disc measurements (eg. Mount & Ingram, 1965). Mount's (1966) results were compared with model predictions in this test. Again, solar radiation was zero and $T_r = T_a$ in the calorimeter. The results are given in Table 4.2.

Table 4.2. Effect of air speed on heat loss from new-born piglets. G_e = total heat loss to environment. Discrepancy = (Modelled value - Measured data)/Measured

T_a (°C)	Mass (kg)	wind speed (m s ⁻¹)	G_e model (W m ⁻²)	G_e measurement (W m ⁻²)	Discrepancy, %
20	1.75	0.05	152	125	22
20	1.75	0.34	152	142	7
20	1.58	0.82	174	145	20
20	2.01	1.58	199	151	32
30	1.82	0.05	73	79	-8
30	1.82	0.34	78	89	-12
30	1.62	0.82	88	92	-4
30	2.08	1.58	98	109	-10

Each measured data point is the mean of measurements on five or six pigs. All conditions in the experiment were below the LCT for a piglet (Mount, 1966). The table shows that the model overpredicts heat loss by between about 7 and 30% at 20°C. This temperature is approximately 12 - 14°C below the LCT, and a single piglet will compact its posture to reduce heat loss. In current husbandry practice, piglets are never kept singly, and they will huddle together to minimise heat loss (see previous section). At 30°C the model predictions are in agreement with the measurements to within 4 - 12%, with an overall error of 9%, which is acceptable given the assumption of the pig as a smooth cylinder, with no coat insulation.

4a.5.3 TEST 3: Thermoregulatory responses to the thermal environment

This test examined the ability of the model to predict the thermoregulatory responses of the pig. The two variables chosen for comparison were the skin temperature of the trunk and the deep body temperature, both of which are direct indicators of the animal's response to its thermal environment. The model results were compared with

data from Ingram (1964a), who made measurements on 25 kg pigs fed on a maintenance diet (metabolic heat production 70 W m^{-2}). The measurements were taken at air temperatures from $-5 - 35^{\circ}\text{C}$ in a climate room with no solar load and $T_r = T_a$. Air speed was 0.1 m s^{-1} . The results are presented in Tables 4.3 and 4.4.

Table 4.3. Comparison of model predictions and measurements of deep body temperature of pigs for a range of environmental temperatures.

$T_a (^{\circ}\text{C})$	T_b modelled ($^{\circ}\text{C}$)	T_b measured ($^{\circ}\text{C}$)	Discrepancy ($^{\circ}\text{C}$)
-5	39.0	39.4	-0.4
10	39.0	39.2	-0.2
25	39.0	39.0	0.0
30	39.0	39.1	-0.1
35	40.6	40.6	0.0

The results justify the model assumption that the body temperature of pigs varies little below the lower critical temperature. The model also correctly predicted the body temperature rise at air temperatures above about 30°C for animals with a maintenance feed intake. For normal growing pigs, with metabolic rates approximately 50 W m^{-2} above maintenance, body temperature rise will occur below 30°C in the absence of a wallow.

Table 4.4. Comparison of modelled and measured skin surface temperature on the trunk of pigs (T_{st}) for a range of environmental temperatures.

T_a (°C)	T_{st} modelled (°C)	T_{st} measured (°C)	Standard deviation on measured data (°C)	Discrepancy, (°C)
-5	20.2	23	2.5	-2.8
10	26.2	27	2.0	-0.8
25	32.2	33	1.0	-0.8
30	33.4	36	1.0	-2.6
35	38.1	38	< 1.0	0.1

Table 4.4 shows predicted and measured skin temperatures of the trunk as environmental temperature changes. Ingram (1964a) found that above $T_a = 25^\circ\text{C}$, the skin temperature increased linearly with air temperature at about 0.5°C per degree air temperature change. Below 25°C , the gradient decreased to approximately 0.3°C per degree air temperature change. The air temperature at which gradient changes was well-modelled at about 25°C , which corresponds to the onset of shivering. Shivering increases the skin temperature by decreasing the tissue resistance, so below about 25°C the skin temperature will be higher in a shivering than a non-shivering animal - hence the shallower gradient below the LCT. The maximum discrepancy between modelled and measured skin temperatures was less than 3°C . The measured data were the means of measurements on seven animals, and the large standard errors on the skin temperatures show the variability between individual animals even of the same breed under the same conditions. The model showed acceptable accuracy in predicting skin temperature of the pig, and thus justified the assumption that the shivering response of the pig was the same as that of the sheep.

4a.5.4 TEST 4: Conduction from piglets to the floor

Mount (1967) measured heat conduction to the floor for new-born pigs, mass 1.5 kg, in a climatic chamber with low air speed (0.1 m s^{-1}). Concrete and wood were used

for floor material (see Appendix 4.1 for thermal properties of these materials). The model predictions were compared with Mount’s data in Table 4.5. The quantity G_f refers to the heat loss by conduction per unit total skin surface area.

Table 4.5. Conductive heat loss from new-born pigs, G_f , for three environmental temperatures.

T_a (°C)	Floor type	G_f modelled (W m ⁻²)	G_f measured (W m ⁻²)	Discrepancy, %
19.5	Concrete	34	22	55
	Wood	23	9	61
25.2	Concrete	44	25	76
	Wood	26	13	100
29.9	Concrete	30	17	76
	Wood	17	9	89

The model overpredicts conductive heat loss by between 50 and 100%. However, the model correctly predicted the rise in conductive heat loss when temperature rose from 19.5 to 25.2°C, and the smaller fall in heat loss as the temperature rose to 29.9°C. At the lowest temperature, most of Mount's animals were standing or supported on their legs, so although the floor was cool the heat loss was less than at 25.2°C. At 29.9°C most animals were fully stretched on the floor to maximise heat loss, but the warm floor resulted in a lower heat loss than at 25.2°C. The broadly correct predictions of the changes in conductive heat loss with temperature, while still showing a large discrepancy in the absolute values, suggests a problem with estimating the area of the animal touching the floor. It has already been stated that accurate measurement or prediction of the contact area is extremely difficult (Section 4a.3.3). The discrepancies between model and measurement could easily be due to differences between model assumptions about pig posture and the measurements made by Mount. The wide variety of possible pig postures means that, in spite of these discrepancies, there are no grounds for discarding the current model scheme. However, it must be noted that the floor conduction component may be virtually impossible to predict accurately.

4b BROILER CHICKENS

Young chicks have no definite thermoneutral zone and as such have only a small range of environmental conditions which provide optimum comfort and productivity (Richards, 1974, Van Kampen, 1974; Misson, 1976). Misson found that day-old chicks are heterothermic, ie. they cannot maintain a constant body temperature or minimum metabolic rate when environmental conditions depart from the optimum. The result, even with older birds, is that chickens can suffer severe thermal stress or death under conditions encountered reasonably frequently in the UK (MAFF, 1996). Climatic change may therefore have more effect on chickens than the other species.

4b.1 Dimensions

The energy balance of poultry has been modelled mathematically by Bouchillon et al (1970) and physically by Wathes & Clark (1981a). In both cases, the body of the bird was represented by a sphere, and Wathes & Clark used three cylinders of the same size to represent the neck and legs. The relationship between feather surface area and mass for poultry was given by Walsberg & King (1978) and Mitchell (1985) as:

$$A_c = 0.081 L_w^{0.67} \quad [4.11]$$

The growing chicken forms an allotropic series, indicated by the 0.67 power. Mitchell's relationship was used in the current model. The ratios of the dimensions of the body parts assumed by Wathes & Clark (1981a) were then assumed constant throughout the chicken's life. The ratios of the dimensions of the various body parts were:

$$d_t = 11 d_L \quad [4.12]$$

$$y_L = 5.7 d_L \quad [4.13]$$

where d_t and d_L are the diameters of the body and legs respectively, and y_L is the length of the legs. The neck was assumed to have the same dimensions as the legs.

4b.2 Heat flow through the body

The thermoneutral body core temperature of poultry is about 41°C (Richards, 1977). Unlike the other species of livestock, T_b in poultry rises progressively with air temperature in hot conditions, as a consequence of panting (Hutchinson, 1954; Misson, 1976; Mount, 1979). The response of T_b to hot environments is described in Section 4b.4.2.

The chicken's body consists of two layers: the tissue, with thermal resistance r_{tt} , and the feathers, with thermal resistance r_{pt} . Richards (1977) found that the skin temperature under the feathers changes by a maximum of 4°C over the T_a range 15 - 40°C, taking a mean value almost the same as deep-body temperature. Richards concluded, therefore, that nearly all the insulation on the feathered parts is provided by the feathers. Richards also found that the tissue resistance under the feathers was constant with age. Therefore, modelling the response of the skin surface temperature in a three layer model similar to the sheep would introduce an unnecessary complication; in the current model, the combined insulation of tissue *and* feathers in series ($r_{pt} + r_{tt}$) was considered. The result was a two-layer model, which greatly simplified the analysis. The change with age of the combined tissue and feather resistance (called r_{st} for consistency with previous species models) observed in broiler chickens by Wathes & Clark (1981c) was attributed to changes in feather cover with age. Up to 30 days old, while the chick is covered with down, Wathes & Clark

observed r_{st} values of about 100 s m^{-1} . The resistance then rose linearly with age to reach a maximum of about 500 s m^{-1} at 53 days old, or approximately 2 kg body mass. Lower resistance values were reported by other sources, notably Davis et al (1973) and O'Neill & Jackson (1974) who obtained 300 and 350 s m^{-1} , respectively, for 2 kg birds. In the current model, Wathes & Clark's observations of the change of r_{st} with age were used, but the maximum r_{st} value was taken as a compromise between Wathes & Clark's and Davis et al's measurements, namely $r_{stmax} = 400 \text{ s m}^{-1}$.

The condition of the coat in laying hens is an important determinant of the insulation.

Plumage can be severely damaged by poor living conditions, or by birds pecking themselves or others (Olson et al, 1974; Clark et al, 1982). Richards (1977) found that the heat flux from poorly feathered birds was more than twice that from well-feathered animals. Wathes & Clark (1981b) found that r_{st} for a bird with a severely degraded coat can be as little as a quarter of the value for a perfect coat. However, problems of feather loss are usually confined to battery-housed laying hens, and broiler chickens kept in barns do not usually suffer significant feather loss.

The insulation of the neck and legs of the chicken varies considerably from one part of the appendage to another. The base of the neck and top of the legs are fully feathered, but the feather cover becomes thinner nearer the extremities, and some parts such as combs and feet are bare. The appendages, especially the combs, wattles and feet of poultry play a very important role in thermoregulation. These regions are used to dissipate excess heat in hot conditions, but modelling the spatial variation of insulation and heat loss over the extremities is difficult. In the present work, the insulation of the extremities, r_{sL} , was determined from measurements of the *thermal circulation index*, TCI, reported by Richards (1974). The TCI is the ratio of thermal resistance to radiant and convective heat transfer through the boundary layer, r_a , to thermal resistance to heat transfer through the body:

$$TCI = \frac{r_a}{r_{st}} \quad [4.14]$$

From the TCI, bulk values of r_{sL} for the whole appendage were estimated. Richards found the TCI of the comb, neck, feet and shank rose by a factor of about ten between full constriction and full dilation of the peripheral blood vessels. Assuming an external resistance of 150 s m^{-1} from the air speed conditions given in Richards (1971), the maximum and minimum values of r_{sL} were 800 and 80 s m^{-1} . These values were adopted in the current model for the whole neck and legs. The consequences of the uncertainty inherent in these values due to the spread of Richards' data is considered in the sensitivity analysis in Chapter 6.

4b.3 Heat flow to the environment

Measurements of heat transfer from a model chicken were made for air speeds ranging from 0.09 to 2.7 m s^{-1} (Wathes & Clark, 1981a). In all cases, the convection was in the mixed regime, and they derived the following relation:

$$Nu = 2 + 0.79 Re^{0.48} \quad [4.15]$$

Since poultry indoors are unlikely to encounter air speeds outside the range tested by Wathes & Clark, Eq 4.15 was used in the current model to calculate convective heat transfer for all conditions. The chicken's small size means that air speed has to be extremely low for free convection alone to occur, and forced convection is unlikely indoors.

Evaporation in chickens is an important route for heat transfer in hot conditions (Hutchinson, 1954; Richards, 1976). There are no sweat glands, so, as in the sheep, most of the evaporative heat loss occurs through panting. Evaporation from the skin is limited to water vapour diffusion through the pores, which rises as air temperature increases but the absolute values are small: less than 10 W m^{-2} at 5°C and $15 - 18 \text{ W m}^{-2}$ at 30°C (Richards, 1976), although different experiments yield different value. The total evaporative loss (cutaneous plus respiratory) below the LCT varies between different sets of measurements. For example, Richards (1977) measured total evaporative heat losses of less than 10 W m^{-2} below the LCT (see Section 4b.5.2). In the current model, total evaporative heat loss E was assumed to be a constant 10 W m^{-2} below the LCT. The use of panting, and the effect on body temperature, is discussed in Section 4b.4.2.

4b.4 Physiological responses to thermal environment

4b.4.1 Vasomotor control

As in the other livestock species (Sections 3a.5.1, 3b.5.1, 4a.4.1) the chicken uses vasomotor control in preference to other, more costly, forms of thermoregulation. In the current model, the blood vessels in the neck were assumed to dilate and constrict at the same time as those in the legs, thus simplifying the model; effectively, the model chicken consisted of a body with three legs. As for the other animals considered earlier, the tissue resistance in the appendages took its maximum value unless the total rate of heat loss was less than the metabolic rate, when the resistance needed to achieve thermal balance was calculated.

4b.4.2 Panting and body temperature rise

In birds, unlike sheep, the body temperature rises as the animal's respiration rate

increases (Bouchillon et al 1970). Birds can tolerate body temperature rises of up to 4°C in the short-term (Mount, 1979), and T_b is allowed to rise to offset the metabolically costly mechanism of panting. Hutchinson (1954), taking measurements from chickens, found an almost linear relationship between body temperature and evaporative heat flux from the respiratory tract. As humidity rises, the gradient of the evaporative heat flux versus body temperature graph falls. For example, Hutchinson measured the total evaporative heat flux as 69 W m⁻² at a deep-body temperature of 44°C when vapour pressure was 860 Pa. The evaporative heat flux density fell to 42 W m⁻² when the vapour pressure increased to 3720 Pa. Hutchinson's data were used in the current model to derive the following empirical relationship between evaporative heat flux, body temperature and vapour pressure:

$$E = (-3.5 \times 10^{-3} e_a + 23) (T_b - 314) + 10 \quad [4.16]$$

where T_b is in Kelvin, and vapour pressure in Pascal. In the model, if the tissue resistance of the legs and neck was minimal, and metabolic heat production still exceeded heat loss, the evaporative heat flux necessary for heat balance was calculated as the difference between heat loss and heat production. Eq 4.16 was then used to calculate a new body temperature, and the process was repeated until stable values of T_b and E were found. The upper lethal limit for T_b in domestic birds is about 46°C, but the animal will be in severe heat stress when T_b exceeds about 44°C.

4b.4.3 Feather fluffing

Fluffing of feathers in cold conditions is an important mechanism for reducing heat loss from birds. Bouchillon et al (1970) state that the thickness of feathers can increase three-fold when the feathers are fluffed. However, the effects of curvature of the chicken's body give a corresponding increase in thermal resistance of about 70% (Monteith, 1973). In the current model, the chicken increased its feather resistance

below the LCT to achieve thermal balance, up to a maximal resistance of 1.7 times the value with preened feathers.

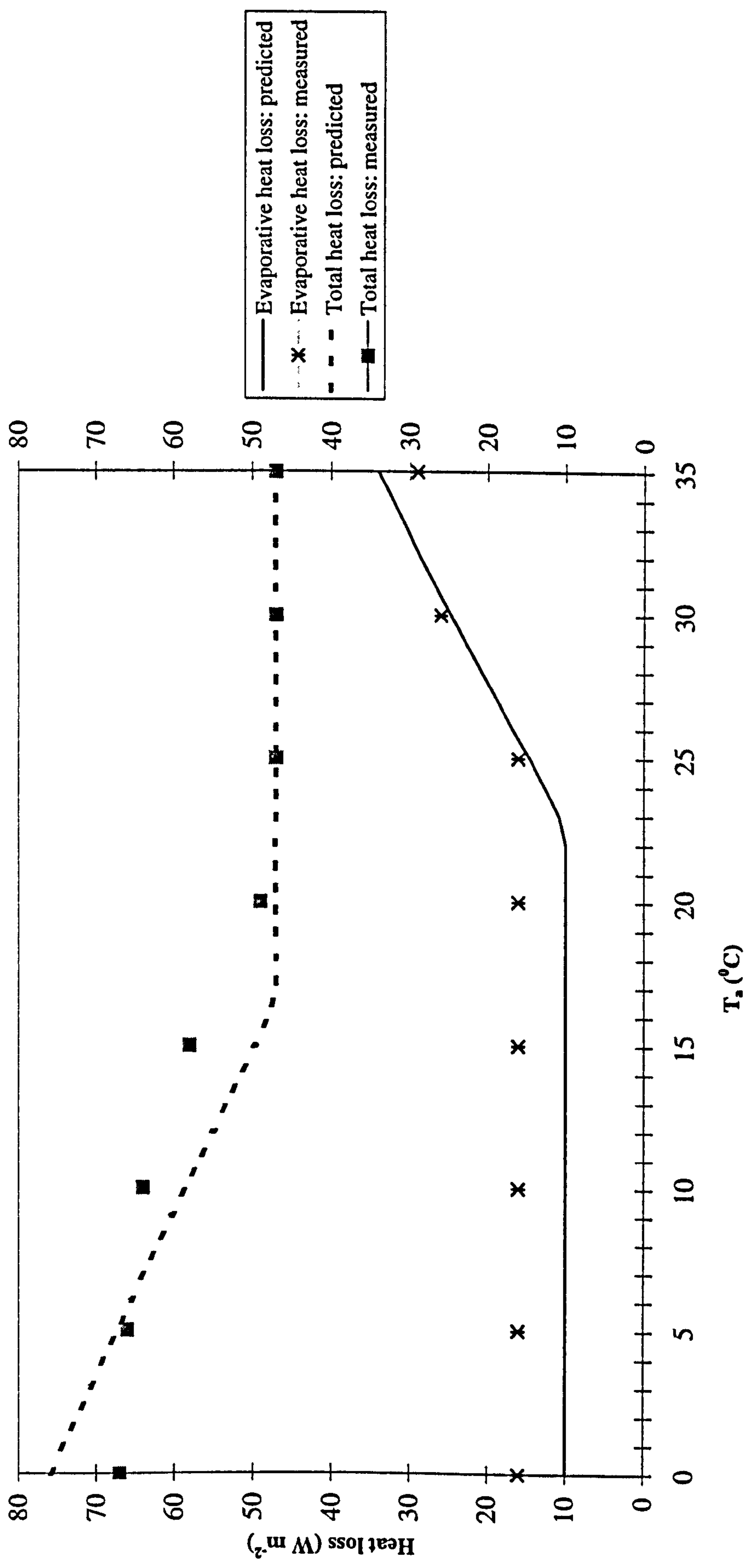
4b.5 Comparison of chicken model with measured data

4b.5.1 TEST 1: Effects of air temperature and humidity on heat loss

The first test compared predictions of heat loss from the chicken model with measurements made by Romijn & Lokhorst (1966). The test was in two parts: the first investigated the effect of changing environmental temperature on the heat loss, and the second investigated the effects of changing humidity at high ambient temperature. The measurements were made on North Holland Blue hens, with an average mass of 3.5 kg, in a respiration chamber with $T_r = T_a$. Wind speed was minimal (0.1 m s^{-1}).

In the first part of the test, the temperature ranged from 0 - 36°C. Relative humidity varied between 64 and 87% over the temperature range. Fig 4.1 shows the total heat loss G_e and the evaporative component E . The measurements displayed on Fig 4.1 are mean values of up to ten individual results; the variability was $\pm 5 \text{ W m}^{-2}$, or up to $\pm 10\%$ of the mean. The air temperature at which evaporative heat flux started to rise was well-predicted as 23°C, compared to the measured value of about 25°C. The total heat loss was also well-predicted, with an overall error of 6%. Below the LCT the measured values of G_e are non-linear with decreasing temperature but the model does not predict the observed behaviour. A real bird will compact its posture in the cold. One example of this behaviour is a bird putting its head under its wing, thus reducing heat loss (Deighton & Hutchinson, 1940). However, the discrepancy between model and measurements, especially given the variability of the measurements, is acceptable.

Fig 4.1: Predicted and measured (Romijn & Lokhorst, 1966) total and evaporative heat loss from chickens v. ambient temperature



In the second part of the test, the model was tested at air temperatures of 24.2 and 33.8°C, and relative humidities (rh) of 40 and 90% in each case. The results are given in Table 4.6.

Table 4.6. Modelled and measured evaporative heat losses and body temperatures for chickens at moderate and high ambient temperatures and humidities.

T _a (°C)	Vapour pressure,Pa (rh, %)	E modelled (W m ⁻²)	E measured (W m ⁻²)	Discrepancy, %	T _b modelled (°C)	T _b measured (°C)
24.2	1200 (40)	22	22	0	41.0	40.6
	2400 (90)	22	10	120	41.0	40.7
33.8	2120 (40)	41	38	8	42.2	41.4
	4760 (90)	36	19	89	43.4	42.3

Table 4.6 shows that at 24.2°C and rh = 40%, the evaporative heat loss of 22 W m⁻² is predicted exactly. However, at 90% humidity, the predicted evaporative heat flux remains at 22 W m⁻², compared with a measured value of only 10 W m⁻². The lack of response from the model to the increase in humidity was due to the assumption that evaporative heat flux is a function of body temperature as well as vapour pressure (Section 4b.4.2). When the conditions are not hot enough for body temperature to change (eg. at T_a = 24.2°C in the current example), Eq 4.16 predicts that changes in humidity will have no effect on the evaporative heat flux. This response is an artefact of the model - a consequence of assuming the evaporative heat flux below the LCT is independent of humidity. The table shows that at 33.8°C, the evaporative heat flux at low humidity was well-predicted at about 40 W m⁻². However, at high humidity (rh = 90%) the prediction was poor - the measured values of E are half of those at rh = 40%, a result which would be expected since evaporative heat flux is proportional to the vapour pressure difference. The model overprediction of E = 36 W m⁻² is due to the way the model calculates latent heat loss. The required evaporative heat flux is assumed to be the difference between sensible heat loss and metabolic heat production. The required evaporation is, therefore, independent of humidity, so raising humidity will not alter the water loss *required* for heat balance. However, the model does calculate the ease with which the animal can achieve the required water

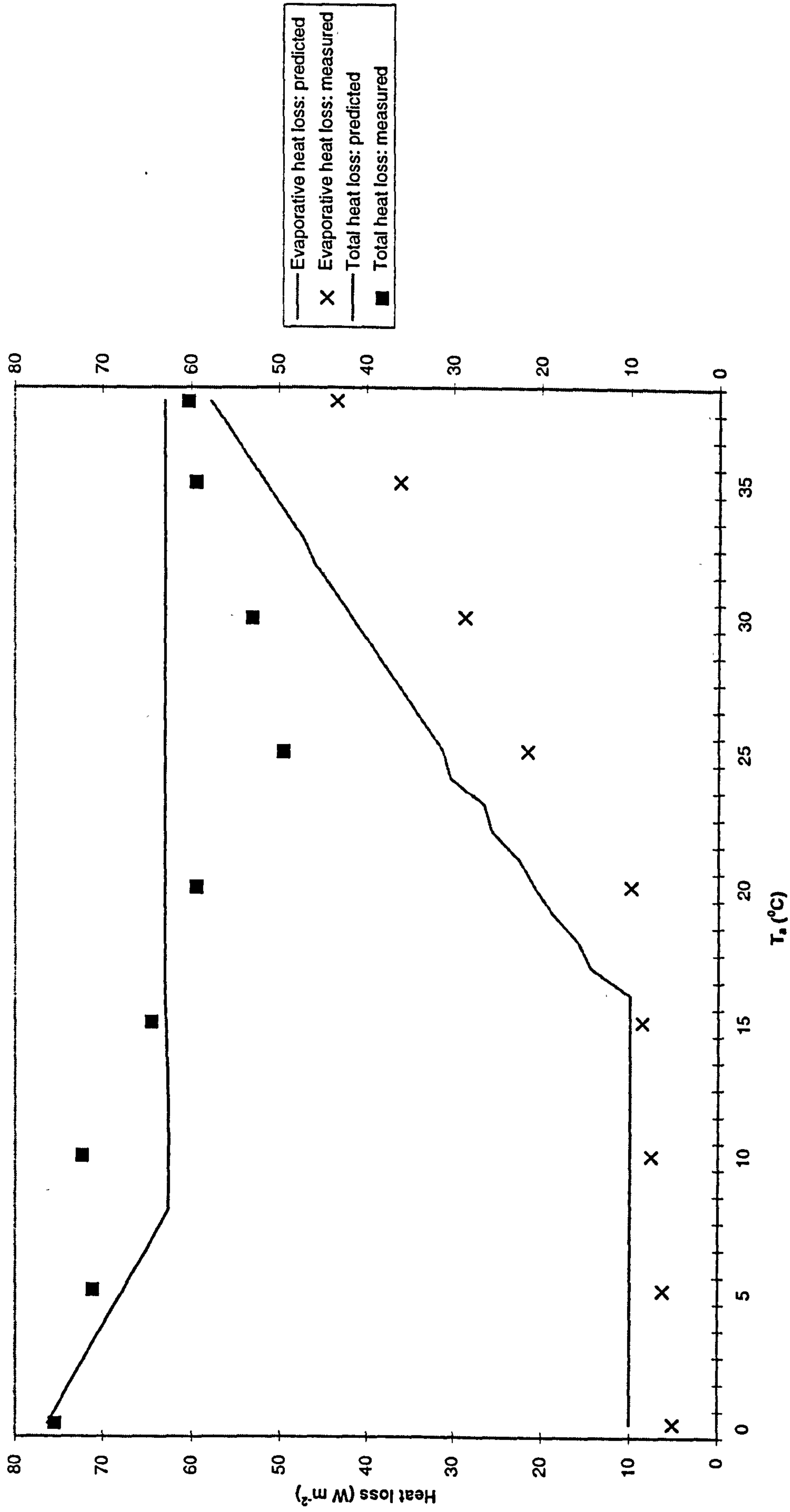
vapour loss. Given the evaporative heat flux, Eq 4.16 was used to predict the accompanying body temperature rise, which is dependent on the humidity. Therefore, in the current model the raised body temperature is a better indicator than E of the stress experienced. At 33.8°C, the predicted body temperature was 1.2°C higher at $rh = 90\%$ than at $rh = 40\%$. The corresponding measured figure was 0.9°C. It was concluded that the model can represent reasonably well the effects of raising humidity on a chicken's body temperature at high temperatures.

4b.5.2 TEST 2: Effects of air temperature on components of heat loss, skin and body temperature

Richards (1977) measured the heat loss from twelve Babcock hybrid hens over a wide range of environmental temperatures. The mean mass of the birds was 2.3 kg, and the measurements were conducted in a metabolism chamber, with $T_r = T_a$ and air speed was approximately 0.1 m s^{-1} . Unlike the set of measurements in the previous section (Romijn & Lokhorst, 1966), the model's assumption of a thermoneutral zone, as for the other species, does not appear to be valid in this case, possibly due to the acute nature of the exposure of the birds. In the absence of an obvious thermoneutral heat production, the feed-related metabolic rate observed by Richards (63 W m^{-2}) was assumed as a thermoneutral value for the model. Relative humidity was 30% at all temperatures. The model output was compared with Richards' observations, and the results are given Figs 4.2 and 4.3.

Fig 4.2 shows the variation of total and evaporative heat loss from the mean of the twelve birds as a function of environmental temperature. One indication of the accuracy of the model is the prediction of air temperature above which evaporative heat flux starts to rise. The model's prediction is 16°C, whereas the measurements show the rise begins at about 20°C. Although the predicted values of E exceed the measured values by about 10 W m^{-2} when T_a is greater than 20°C, the rate of increase of evaporative heat flux with increasing air temperature is predicted almost exactly by

Fig 4.2: Total and evaporative heat losses of chickens (predicted and measured by Richards, 1977) vs. air temperature

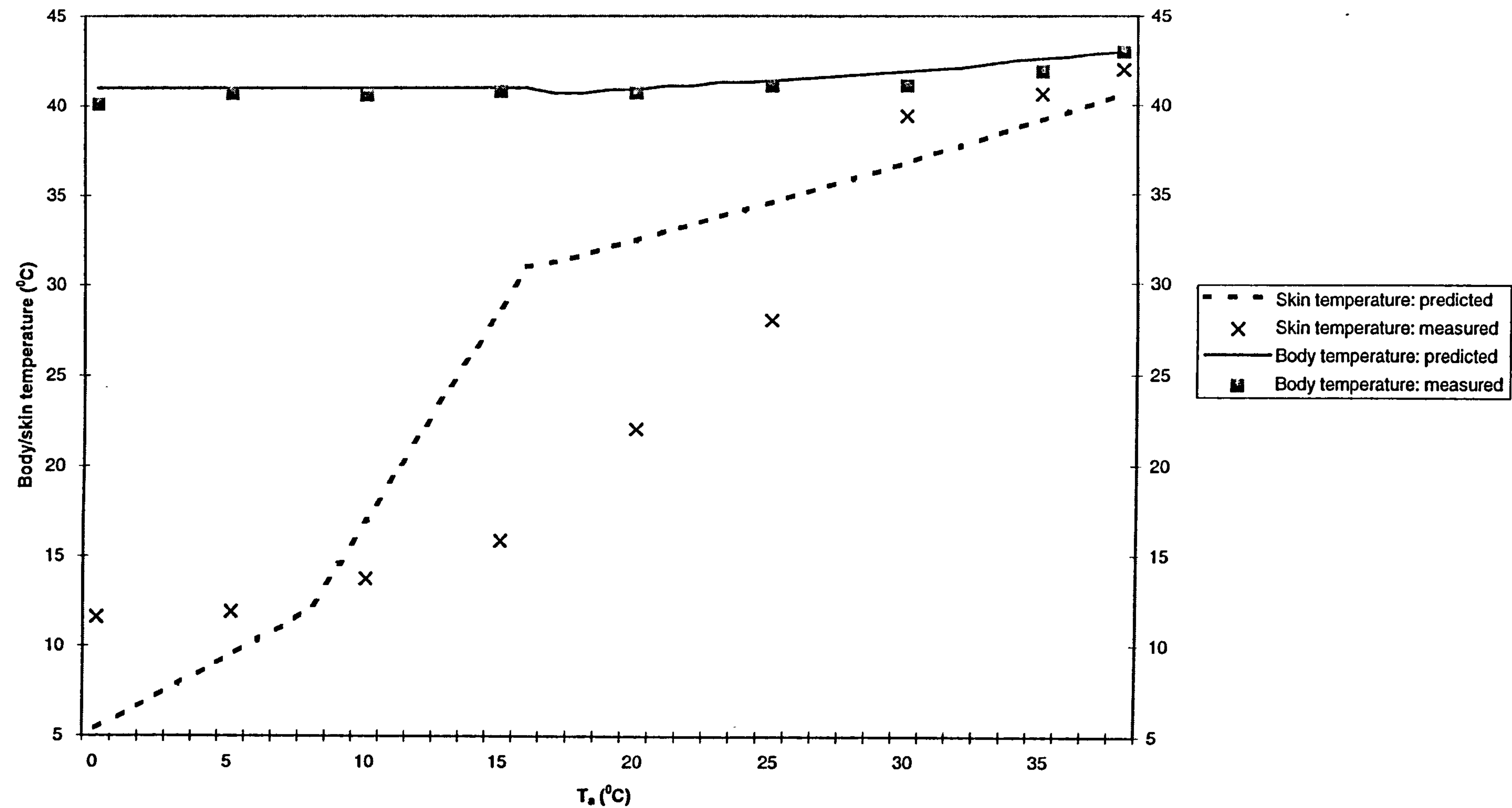


the model: 1.9 W m^{-2} per $^{\circ}\text{C}$ temperature rise. The values of G_e are predicted well. The overall error of the model's total heat loss predictions was 7%, but the standard error on the measurements of G_e given by Richards was $\pm 5 \text{ W m}^{-2}$, or up to 8%. Given the assumption of a thermoneutral metabolic rate in the model, the model predictions are acceptable.

Fig 4.3 shows skin temperature measured on the comb and deep body temperature plotted against air temperature. The model predictions are also plotted, with the skin temperature of the 'leg' used by the model as an indicator of vasomotor response. The body core temperature is well predicted, with each model value of T_b within 0.8°C of the corresponding measured value. The standard error given for the measurements was approximately 0.3°C , due to the variability between the six hens used in the study. The effect of the model feedback between T_b and evaporative heat flux (Eq 4.16) is evident on the graph at air temperatures between 16 and 25°C . When evaporative heat flux starts to rise, in this case at 16°C (Fig 4.2), the feedback causes body temperature to fall initially. The body temperature rise is therefore restrained by increasing evaporative loss.

Skin temperature on the appendages is not well predicted by the model, in contrast to the sheep (Fig 3.2). The air temperature at which dilation starts is unclear from the measurements, but appears to be about $6\text{-}8^{\circ}\text{C}$ above that predicted by the model. The range over which dilation occurs is much wider in the real animal: approximately 15°C , whereas the range predicted by the model is about 7°C . The real chicken obviously uses evaporative heat loss, body temperature rise and vasomotor control in parallel, and simultaneous prediction of all the variables is impossible in the current model, driven by the principle of least metabolic cost. The important conclusion is that while extremity temperature is not well modelled, the total heat loss and body temperature, which drive thermal stress, provide good predictions.

Fig 4.3: Predicted and measured (Richards, 1977) skin and body temperature of chickens vs. air temperature



4b.5.3 TEST 3: Effects of extremely hot conditions on components of heat loss

The third test examined the effect of increasing wind speed on heat loss from poultry at very high ambient temperatures. In experiments by Timmons & Hillman (1993), three or four unacclimatized White Leghorn hens were exposed to air temperatures of 37.8 and 40.4°C, and air speeds of 1.0 and 2.0 m s⁻¹, and the convective, radiative and evaporative heat losses were measured separately using a novel calorimeter design. The vapour pressure was approximately 3000 Pa and T_r was equal to T_a. The hens had a mean mass of 1.8 kg. Table 4.7 compares the results of Timmons & Hillman's experiments with model predictions for the same conditions.

Table 4.7. Components of heat loss from chickens at high ambient temperatures. Measured data are the range of values observed in three or four birds. * = range greater than 40 W m⁻²

T _a (°C)	u (m s ⁻¹)	E mod (W m ⁻²)	E meas (W m ⁻²)	C mod (W m ⁻²)	C meas (W m ⁻²)	L mod (Wm ⁻²)	L meas (W m ⁻²)
37.8	1.0	45†	32 - 54	6†	-7 to 10	4†	-3 to 15
	2.0	45	21 - 43	8	-40 to 40*	4†	-10 to 15
40.4	1.0	51†	49 - 62	2	-47 to -80*	2†	-1 to 13
	2.0	51†	40 - 69	3	-25 to -76*	2	0 to -28

Table 4.7 shows the often large variability between individual birds' responses to the same environment under extreme conditions. Cases marked † are those where the model prediction is within the range of the measured data. The model predicts the correct magnitudes for the partition between convective (C), radiant (L) and evaporative heat loss at T_a = 37.8°C. At 40.4°C, Timmons & Hillman found no clear pattern in the partition of heat transfer, and the model could not predict heat losses with any accuracy. However, these extreme conditions are unlikely to be encountered in the UK, even under climate change. The conclusion is that at very high temperatures, it is very difficult to predict heat stress levels for chickens as each bird varies widely in its response to the thermal environment.

4.3 Behavioural responses to indoor environment

Many behavioural responses used by outdoor animals (Section 3.3) are employed by indoor animals. In the cold, animals compact their posture to reduce the effective surface area available for heat loss. For example, Deighton & Hutchinson (1940) found that chickens could reduce their heat loss by 12% by putting their heads under their wings. In open plan broiler houses chickens regulate their thermal balance by seeking out the thermal environment to suit their individual preferences. The variations of temperature and air speed within animal houses (Section 4.2) allow each animal to choose a thermally comfortable area. Radiant heaters are sometimes used to widen the range of thermal environments (Alsam & Wathes, 1991b).

Grouping and dispersion of animals is an important thermoregulatory mechanism indoors. As indicated earlier (Section 4a.6) young pigs use grouping as one of the main methods of preventing cold stress. Misson (1976), in experiments on groups of twenty newly-hatched chicks, measured a reduction in heat loss of 12 - 15% and a reduction of 2°C in the lower critical temperature due to huddling of the flock. Huddling is also employed under cold conditions outdoors. LeMaho et al (1976) found that penguins reduced heat loss by 37% by huddling in groups. In contrast, in hot conditions, animals stay as far away as possible from each other (Mount, 1968). Pigs in hot environments need to wallow to increase evaporative heat loss, due to their poor sweating ability (Ingram, 1965; Mount, 1968; Gannon, 1996). Mud provides a better wallow than clean water as the mud holds the water for longer, providing longer periods of increased evaporation (Mount, 1979; Gannon, 1996). Estimates by Ingram (1964a) indicate a loss of 500 W m^{-2} can be achieved from wallowing. This will keep the pig from being heat stressed in the most hostile environments; conversely, in the absence of a wallow, the pig may die of heat stress even at air temperatures below 35°C. As in the case of the outdoor animals, modelling behavioural responses and animal choice is difficult, and in the current model the

behaviour of pigs and chickens was not modelled. In the case of pigs it was assumed that the animal will wallow, if one is available, after full vasodilation occurs.

4.4 Discussion and conclusions

The unicorn model was adapted to predict the thermal balance of pigs and broiler chickens indoors. In both cases, the unicorn model was reduced to a two-layer approximation. The geometry of these animals was different from the unicorn - in the case of the chicken substantially so. The pig model generally performed well in comparison with measured data, except in the cold, where the lack of a suitable scheme to account for behavioural mechanisms such as huddling resulted in overpredictions of heat loss. The model may therefore overpredict the frequency of cold stress, but in a changed climate the frequency of heat stress is the more important quantity. Omission of a cold-induced huddling response was therefore justified in the current work. Generally, however, behavioural responses of pigs are at least as important, if not more so, than physiological responses, so a simple thermal model including physiological responses alone predicts a very narrow range of tolerance. Boon (1981) found that the ratio of number of pigs lying down and touching other pigs to the total number lying down was inversely proportional to the difference between LCT and air temperature. Future models will be greatly improved by further research on the effects of air temperature and other variables such as animal weight and group size on the contact area between animals.

The chicken model predicted the total and evaporative heat loss well in relation to air temperature at low humidities, but at high humidities and hot conditions the evaporative heat loss was overpredicted. However, T_b , which is an effective stress indicator, was predicted reasonably well by the current model.

The evaporative heat flux required by chickens for thermoneutrality was related to T_b and vapour pressure by Hutchinson's (1954) data. Richards (1976) linked evaporative

heat flux with respiratory frequency but the consequent increase in T_b was not measured. Overall, the important variable in the current work is T_b , which is used to determine the severity of heat stress in chickens. Hutchinson's data were therefore used, and assumed reliable, in spite of their age. More recent measurements are needed which relate evaporative heat loss to respiratory frequency, vapour pressure, *and* the resultant rise in deep-body temperature. In summary, the chicken model produced a good match with available data at low humidities despite the model's assumptions. However, at high humidities, heat stress may be overpredicted.

APPENDIX 4.1 CALCULATION OF THERMAL RESISTANCE OF FLOOR

Bruce & Clark (1979) expressed the resistance of a floor in $s\ m^{-1}$, r_f , as the resistance for a standard sized pig (mass = 45 kg) with 20% of its surface area in contact with the floor (r_{f45}), multiplied by correction factors to account for different mass, posture and group size:

$$r_f = r_{f45} \left(\frac{L_w}{45} \right)^{0.33} \left(\frac{A_f}{0.2 A_s} \right) N^{0.5} \quad [4.17]$$

The power of 0.33 results from the assumption that floor resistance is directly proportional to a characteristic length scale for the animal, ie. the cube root of the mass. The floor resistance was also assumed proportional to the square root of the total contact area provided by N pigs. The A_f scale factor allows for variations in pig

posture. 20% of the total skin area was assumed in contact with the floor when the animal was fully stretched out, and 10% when the animal was supporting itself (Bruce & Clark, 1979). r_{f45} is an intrinsic property of a floor, and typical values for common materials used in pig houses are:

Wood:	280 s m^{-1}
Straw:	600 s m^{-1} (50% embedded - Sallvik & Wejfeldt, 1993)
Concrete:	85 s m^{-1}

CHAPTER 5 : MODELLING THE IMPACT OF CLIMATE CHANGE ON LIVESTOCK ENERGY BALANCE

The models of the thermal balance of livestock have been presented and validated in Chapters 3 to 5, and in this chapter outlines the use of the models to assess the impact of climate change on these livestock. The estimation of the input parameters such as weather data and metabolic rate are described in relation to other models used in the overall assessment of climate change on UK agriculture. A necessary step for the present analysis was the development of a subsidiary model to generate hourly weather data. This chapter also outlines the scenarios and initial conditions used in the model runs, and the standard principles followed for any impact assessment are described.

5.1 Climate change and the need for downscaling

The broad issue of climate change has already been discussed in Chapter 1. This section considers the use of the climate change scenarios in assessing the impact of climate change on livestock energy balance. The main problem in the impact assessment lies in the relation between the climate change scenarios and realistic daily weather. The scenarios provide predictions of monthly mean temperature and precipitation, but changes in the probability of extreme values are also important. For livestock the solar radiation load, wind speed and humidity are at least as important as temperature and precipitation. In addition, the General Circulation Model (GCM) output is on a coarse spatial scale, with as few as five grid points for the whole UK.

The need for reducing large temporal and spatial scale model output to smaller scales ("downscaling") is thus an important one in order for impact assessments to take place (eg. Wilks, 1992; Semenov & Porter, 1995). Downscaling techniques generally fall into two categories: *nested model downscaling* or *empirical downscaling* (Hewitson, 1995). Nested model methods involve using a fine-resolution model for the region in question, using as input the coarse resolution GCM output. This method has the advantage of being mechanistic, but is extremely computer-intensive, and limited to one particular region. Empirical downscaling involves deriving relationships between large-scale circulation data and small scale variables such as temperature and precipitation. One assumption implicit in this method is that the relationships between large and small-scale variables will remain constant under climate change conditions. Hewitson (1995) proposed this to be a valid assumption, as any change in climate will most likely appear as changes in persistence, intensity and frequency of large scale circulation patterns, rather than as changes in the basic dynamics. Examples of the use of empirical-statistical downscaling methods include the work of Fuentes et al (1995) and Gyalistras & Fischlin (1995), who downscaled GCM output to predict monthly mean temperature and precipitation under changed climate conditions for the whole of Switzerland, on a very fine (2.5 km) grid. Jones & Conway (1995) used similar methods to downscale large-scale circulation patterns in the form of Lamb weather types (Lamb, 1972).

The reduction of temporal scale was the principal aim of the work described in this chapter. Different applications require data at different timescales. Mean daily values of the weather variables can be used as inputs to models such as grass growth, in which changes over timescales less than a day are not significant. However, models of the thermal balance of livestock and buildings (Chapters 2, 3 and 4) require data at hourly intervals, as the energy balance changes significantly hour-by-hour. In this chapter, methods for producing hourly values of the necessary input variables are presented.

5.2 Generation of hourly weather data from climate change scenarios

In this project, the downscaling of data from monthly mean values was achieved using a mixture of empirical and mechanistic methods. The use of mathematical models to synthesise meteorological data has increased dramatically since about 1980, with the advent of more sophisticated models which require daily or hourly meteorological data as input, such as models of disease spread, insect population dynamics and soil water content (Jones & Phelps, 1996). The so-called "weather generators" are usually used to fill in gaps in current data, where collection of comprehensive weather data sets is too expensive and time-consuming. Weather generators can also be used to create data sets for projected conditions, such as those predicted by climate models or to produce realistic synthetic data with the same statistical properties as the long-term means. The stochastic weather generator, such as that designed by Richardson (1981), generates sequences of random numbers which have the same statistical properties as meteorological data (Parsons et al., 1995). The numbers, which represent a daily data series, are generated from input values of long-term means, variances, frequencies and extremes, and the correlations between variables such as rainfall and solar radiation. These correlations are obtained from observations at particular sites, and are included when the model is calibrated. In the current work, the Erosion/Productivity Impact Calculator (EPIC) weather generator, designed by Richardson & Nicks (1990), was used to generate a sequence of daily data for current and climate change conditions at various sites in the UK. Full details of the daily data generator can be found in Richardson & Nicks (1990), and Matthews et al (1997).

For the thermal balance model, hourly weather data were required. The following section describes the generation of hourly data from the daily values.

Outputs received from EPIC for each day were:

- Total precipitation (mm)

- Vapour pressure (Pa)
- Total of global solar radiation, S_{gt} (MJ)
- Maximum and minimum dry bulb temperature, T_{max} and T_{min} (°C)
- Wind speed ($m\ s^{-1}$)

The thermal balance models require the following variables at hourly intervals:

- Precipitation (mm)
- Direct and diffuse components of solar radiation,
 S_b and S_d ($W\ m^{-2}$)
- Dry bulb temperature, T_a (°C)
- Radiant temperature of the sky, T_{sky}
- Temperature of the ground surface, T_g
- Wind speed ($m\ s^{-1}$)
- Vapour pressure

Downscaling can be done in a number of ways from the very complicated statistical techniques to the very simple. Examples of statistically-based models include Degelman (1976) and Knight et al (1991). The downscaling methods used in this project, which requires the generation of many years of hourly data, and are consequently limited for computer time, have tended to be the simplest where possible. In assessing climate change impacts, the difference between current and predicted future conditions is the most important indicator. While ensuring that hourly data matches current patterns where possible the accuracy of this match was sometimes sacrificed for a simpler but less accurate method. Such an approach gives an accurate climate change impact assessment, provided data used in determining current baseline conditions are analysed in the same way as those from the climate change scenario.

5.2.1 Rainfall

Several methods for generating hourly rainfall data from daily totals have been proposed. These are either stochastic point process models (Cowpertwait, 1994 & 1995), or empirically based random generators which divide days into different types according to when rain falls (McGechan & Cooper 1995). Both approaches were too computationally expensive for use in this project, and it was considered unrealistically detailed to introduce detailed hourly variations when forecasting for sixty years hence.

A simpler method was chosen, based on the observation that the maximum rainfall intensity in the day (I_{\max} , mm hr⁻¹) is related reasonably well (A.C.Armstrong, pers.comm.) to the total rainfall in the day (P_d , mm) by:

$$I_{\max} = 0.3P_d \quad [5.1]$$

In the procedure adopted in the current work it was assumed that the maximum rainfall intensity occurs at noon and that the rainfall intensity is distributed as a triangular function. The start and end times of the rainfall event were calculated by forcing the area under the triangle to equal the total rainfall for the day (Fig 5.1). Knowing the rainfall intensity at each hour, the total rainfall for each hourly interval was calculated by assuming the rainfall intensity to be constant over the hour. This method is artificial but is a reasonable start.

5.2.2 Cloud cover and diffuse and direct solar radiation

Solar radiation and cloud cover are the most difficult variables to generate. All that is known is the daily total of global radiation; from this the partition between diffuse and direct solar radiation and cloud cover for each hour must be calculated. Accurate methods of partitioning the radiation receipt into its two components are very sensitive

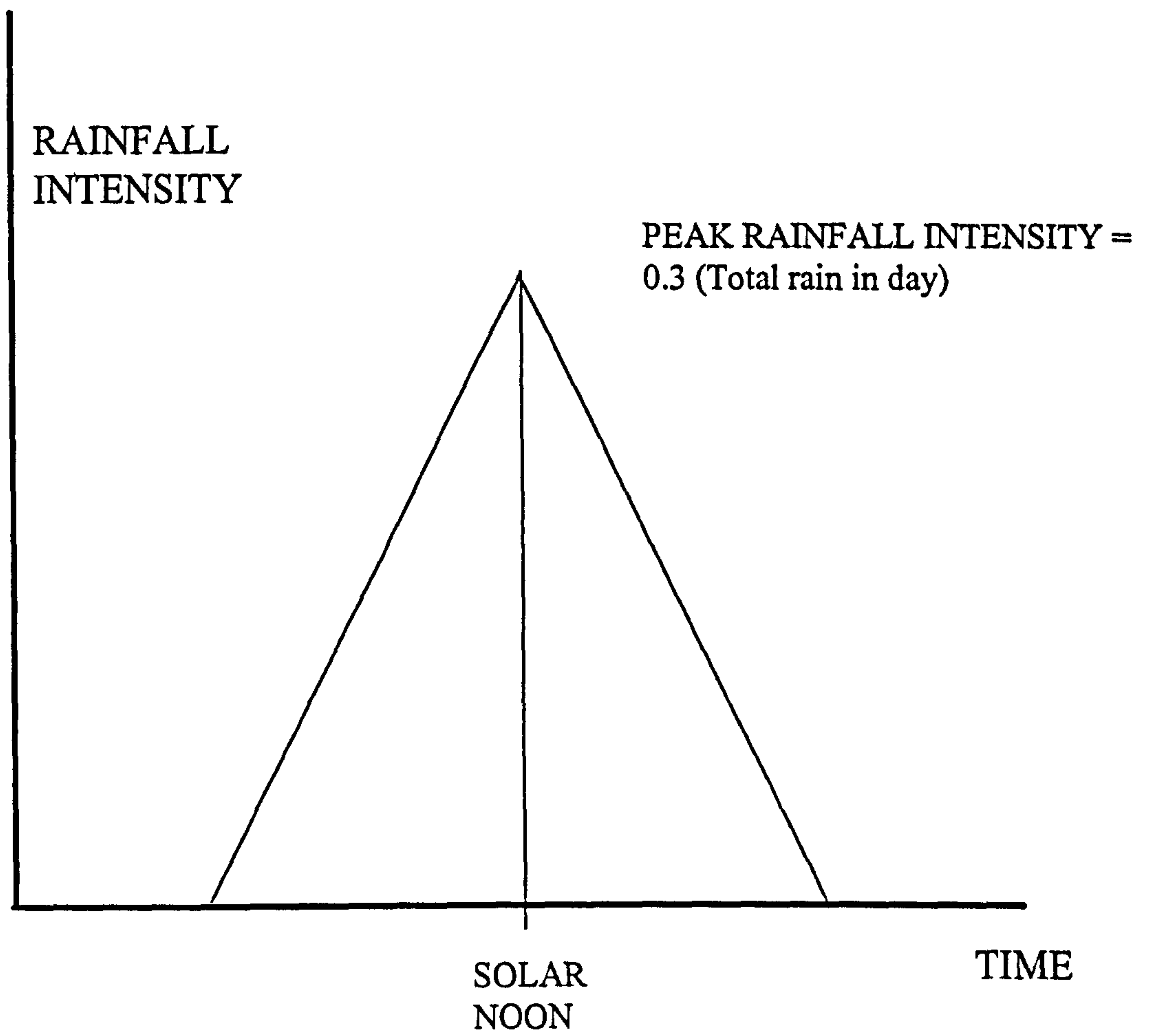


Fig 5.1: Distribution of rainfall intensity over time of rainfall

to the clear-sky radiation transmittance, which is not routinely measured. As for rainfall, there are several stochastic methods for reducing solar radiation data to hourly values (eg. Knight et al, 1991; Aguiar & Collares-Pereira, 1992).

The first step is to calculate the total radiation for the day on a horizontal surface at the top of the atmosphere S_{TOA} (MJ). This energy input was determined from astronomical variables, and is dependent on the day of the year and latitude of the site. The value of S_{TOA} is given by:

$$S_{TOA} = \frac{86400}{\pi \times 10^6} D_o S_o (h_s \sin \phi \sin \delta + \cos \phi \cos \delta \sin h_s) \quad [5.2]$$

with

$$\cos h_s = -\tan \phi \tan \delta \quad [5.3]$$

where ϕ is the latitude of the site, and h_s is the azimuthal angle of the sun from the zenith at sunrise (see also the symbol list at the beginning of the thesis). In the current work an effective atmospheric transmittance, τ , was defined by:

$$\tau = \frac{S_{gt}}{S_{TOA}} \quad [5.4]$$

where S_{gt} (MJ) is the daily receipt of solar radiation (total) at the ground. The quantity τ has been defined elsewhere as the Daily Clearness Index (Knight et al 1991), and small values of τ indicate low radiation penetration. Knight et al used

complex statistical-empirical methods to reduce daily clearness index to hourly clearness index; in this model, clearness index is assumed constant through the day.

The quantity τ does not correspond to the usual definition of atmospheric transmittance, which refers only to the effects of attenuation by atmospheric aerosol in a cloudless sky (Gates, 1980). The Daily Clearness Index, however, contains implicit reference to atmospheric scattering *and* cloud cover. The value of τ given by Eq 5.4 was used in an empirical relationship to deduce a cloud cover fraction. Iqbal (1980), from measurements in mid-latitudes, found that a value of τ less than about 0.35 corresponds to complete cloud cover. τ greater than about 0.75 corresponds to clear skies (Orgill & Hollands, 1977; Iqbal, 1980). Spencer (1982) reported that values of τ between 0.35 and 0.75 correspond to partly cloudy skies in Australia, showing Orgill & Hollands' work to be applicable over a wide range of latitudes. The preceding empirical results were used in the current model to deduce cloud cover fraction:

When $\tau > 0.75$ then attenuation can be accounted for entirely by scattering, and cloud cover was assumed zero.

When $\tau < 0.35$ the sky was assumed to be completely overcast.

When τ was between 0.35 and 0.75, a linear interpolation was used to determine cloud cover fraction.

The value of τ for overcast skies does not vary much with solar elevation, but it varies with cloud type. A typical value for thick stratocumulus is $\tau = 0.3$, though high cirrus may give a value of 0.6 - 0.7. In the current model, a single value of 0.35 was used for τ since detailed cloud type predictions are not available for climate change scenarios.

For each hour, the global solar radiation at the Earth's surface (S_g , W m^{-2}) was then calculated from:

$$S_g = S_o D_o \sin \alpha (\tau^{\frac{1}{\sin \alpha}}) \quad [5.5]$$

where raising τ to the power of $1/\sin \alpha$ accounts for the change in transmittance due to increased atmospheric path length at low solar elevations. Solar elevation α depends on the latitude, time of day and the day of the year, and the calculation for α is given in Appendix 5.1.

The final stage involves partitioning the solar radiation at the ground between its direct and diffuse components. This is extremely complicated analytically as the ratio of diffuse to direct radiation varies with cloud cover and type, and with solar elevation. Orgill & Hollands (1977) used data from Toronto (at a similar latitude to the UK) to relate τ to the ratio of diffuse radiation to global radiation at the surface. They found:

$$S_d = S_g (1 - 0.249 \tau) \quad [5.6]$$

for $\tau < 0.35$, which corresponds to total cloud cover. For partly cloudy skies (τ ranging from 0.35 to 0.75) the following relation was obtained:

$$S_d = S_g (1.557 - 1.84 \tau) \quad [5.7]$$

and for totally clear skies ($\tau > 0.75$):

$$S_d = 0.177 S_g \quad [5.8]$$

Orgill & Hollands recommended the use of Eqs 5.6 - 5.8 between latitudes 43° and 54°N, and these equations were therefore adopted for the current model. The effect of solar elevation on the partition between direct and diffuse radiation was assessed by Orgill & Hollands and Iqbal (1980). Iqbal found that solar elevation affected the maximum ratio of diffuse to total at the ground. At elevations below 30°, the diffuse to total ratio was greater than the values obtained from Eqs 5.6 - 5.8, given the same cloud cover. However, the effects of elevation produce maximum errors of only 0.05 in the value of τ , and since the errors due to assuming a constant cloud cover through the day, and constant cloud type, are larger than 0.05, the altitude dependence was ignored, and Eqs 5.6 - 5.8 were used directly in the current work. Since S_g and S_d/S_g are known, it was trivial to calculate S_d , and $S_b = S_g - S_d$.

5.2.3 Ground, sky and air temperatures

5.2.3.1 Air temperature

In the current work a simple relationship between maximum (T_{\max}) and minimum (T_{\min}) air temperatures and time of day was developed and used to estimate hourly values of air temperature. Values of daily maximum and minimum dry bulb temperature were interpolated with a sine function of time, with the maximum temperature displaced two hours behind solar noon. In the model, the maximum temperature is therefore always at 2 pm and the minimum at 2 am. The equation developed was

$$T_a = \overline{T_a} + (T_{\max} - \overline{T_a}) \sin\left[\frac{2\pi}{24}(t - 8)\right] \quad [5.9]$$

where t is the hour of the day (eg 15 = 3 pm) and the mean temperature $\overline{T_a}$ is given by:

$$\overline{T_a} = \frac{T_{\max} + T_{\min}}{2} \quad [5.10]$$

5.2.3.2 Radiant temperature of the sky

The radiant temperature of the sky, T_{sky} (Kelvin) is nearly always significantly below the air temperature; even for skies totally covered with low cloud T_{sky} has been measured 11 K below T_a (Unsworth & Monteith, 1975). The current work used a combination of existing relationships of the effects of vapour pressure and temperature on the emissivity of the sky to deduce a value for T_{sky} (Cole, 1976).

The relevant equation is:

$$T_{\text{sky}} = \{T_a^4(YZ + (0.84c))\}^{0.25} \quad [5.11]$$

where Y and Z are dimensionless functions given by:

$$Y = 1 - (0.84c) \quad [5.12]$$

and

$$Z = 1 - 0.261 \exp[-7.77 \times 10^{-4} (T_a - 273.15)^2] \quad [5.13]$$

Idso & Jackson (1969) derived Eq 5.13, which is the emissivity of a clear sky as a function of T_a (Kelvin) alone, and validated the equation for a wide range of latitudes and seasons. Unsworth & Monteith (1975) used observations made in Oxfordshire to include the effects of a partly cloudy sky, and Eq 5.11 was formed from the results of Unsworth & Monteith's work. The inputs for calculating hourly T_{sky} are hourly air temperature and cloud cover, as obtained by the procedures in Section 5.2.3.1 and 5.2.2 respectively. Since cloud cover is assumed constant over the day in the current model, the difference ($T_a - T_{sky}$) is also constant over a day.

5.2.3.3 Ground surface temperature

Under clear sky conditions, the temperature of the ground, T_g , can be significantly different from air temperature. A new method was developed here to solve the energy balance of the ground for the surface temperature:

$$S_a = Q_g + C_g + E_g + L_g \quad [5.14]$$

where S_a is the total solar radiation absorbed by the ground, Q_g is the ground heat flux, and C_g , E_g and L_g are the convection, evaporation and thermal radiation heat fluxes at the ground respectively. Ground heat flux was taken as positive downwards, in the same direction as solar radiation, so in Eq 5.14, the value of Q_g on the right hand side is negative. Substituting for the various terms in the energy balance equation 5.14, and rearranging for T_g (Kelvin), the following expression was obtained, details of which can be found in Appendix 5.2:

$$T_g = \frac{S_a - \frac{k}{\Delta z} T_{deep} + \rho c_p \left(\frac{T_a}{r_H} + \frac{T_{sky}}{r_R} \right) - E_g}{\rho c_p \left(\frac{1}{r_H} + \frac{1}{r_R} \right) - \frac{k}{\Delta z}} \quad [5.14a]$$

The resistances r_H and r_R have the same meaning as in Chapters 2-4 but refer here to the ground surface. The Bowen Ratio for the ground surface is defined as C_g/E_g (Monteith & Unsworth, 1990), and has a value of about 0.65 for Europe (after Oke, 1987), ie.

$$E = \frac{\rho c_p}{0.65 r_H} (T_g - T_a) \quad [5.14b]$$

The thermal conductivity of the ground, k , was assumed to be $1.0 \text{ W m}^{-1} \text{ K}^{-1}$, which corresponds to clay soil with 20% water content or sandy soil with 10% water (van Wijk & De Vries, 1963). The soil temperature T_{deep} was assumed constant at 283 K at a depth $\Delta z = 1 \text{ m}$. Substituting these simplifications into Eq 5.14a and rearranging for T_g gives:

$$T_g = \frac{S_a - T_{\text{deep}} + \frac{2.53 \rho c_p}{r_H} T_a + \frac{\rho c_p}{r_R} T_{\text{sky}}}{\frac{2.53 \rho c_p}{r_H} - 1 + \frac{\rho c_p}{r_R}} \quad [5.15]$$

where

$$S_a = (1 - \rho_g)(S_b + S_d) \quad [5.16]$$

5.2.4 VAPOUR PRESSURE AND WIND SPEED

Vapour pressure is related to airmass, taking higher values for moist tropical airmasses, such as those behind warm fronts, and taking low values for cold air of continental origin. Vapour pressure can be assumed constant through the day

(McGechan & Cooper 1995), since air masses are generally large and reasonably uniform in humidity. Departures from this assumption will occur if fronts pass the site during the day, but allowance for this is beyond the scope of the project. The current analysis used the vapour pressure calculated from the 0900 GMT relative humidity supplied from the daily data and assumed that the vapour pressure remained the same over the day.

Chou & Corotis (1981) developed methods for generating hourly wind speed using the Weibull distribution parameters with autocorrelation functions for various sites. These functions relate the wind speed at hour i to the wind speed at any subsequent hour. Mean values of wind speed at 10 m (standard height) for different times of day are listed for various sites (Troen & Petersen 1989). The form of the hourly variation changes with time of year and site, but in general the wind reaches a maximum in early afternoon and the minimum value is just before dawn. This diurnal variation is most pronounced in summer, when strong solar heating occurs. Corotis et al (1977) showed that the diurnal variation in summer over the US Midwest (where solar heating is intense) was $\pm 30 - 40 \%$ of the daily mean. However, data for Waddington, Lincolnshire, show that all three-hour mean wind speeds 10 m above the ground are within $\pm 1 \text{ m s}^{-1}$ of the daily mean wind speed. A difference of 1 m s^{-1} at 10 m translates to a difference of about 0.5 m s^{-1} at a height 0.5 m above the ground, which is equivalent to the mid-trunk height of a standing sheep. Given the errors involved in estimating ground roughness and the assumption of the logarithmic wind profile, such diurnal variations are small enough to be ignored. Hence, in the present work, wind speed was taken to be constant through the day.

Standard weather data will overestimate wind speed at the height of the animal. In calculating the wind speed at animal height, a logarithmic wind profile was assumed. A mixture of experiment and theory has established that the wind speed $u(z)$ at height z is given by:

$$u(z) = \frac{u_*}{k} \ln \left[\frac{z - d'}{z_o} \right] \quad [5.17]$$

where u_* is the friction velocity (m s^{-1}), z_o is the roughness length (m), d' is the effective height of the surface above ground level (m) and k is von Karman's constant, with a value of about 0.41. The friction velocity u_* increases as vegetation height increases, but is independent of height in the surface layer. The roughness length z_o is the height at which mean wind speed is zero, if the logarithmic profile is extrapolated towards the surface. The type of substrate affects the values of z_o and d' , and in the current model representative values for rough pasture of 0.01 m for z_o and 0.06 m for d' were used (McIntosh & Thom, 1969). Mikami et al (1996) showed that values for z_o and d' given in the literature are usually measured over flat planes, and over complex hilly terrain the velocity profiles needed to determine z_o and d' are difficult to obtain, and prone to errors. However, no better estimates were given for these two parameters over hilly rough pasture, so McIntosh & Thom's values were used in the current analysis.

5.3 Validation of the hourly weather data generator

The generation methods divide the variables into two main categories:

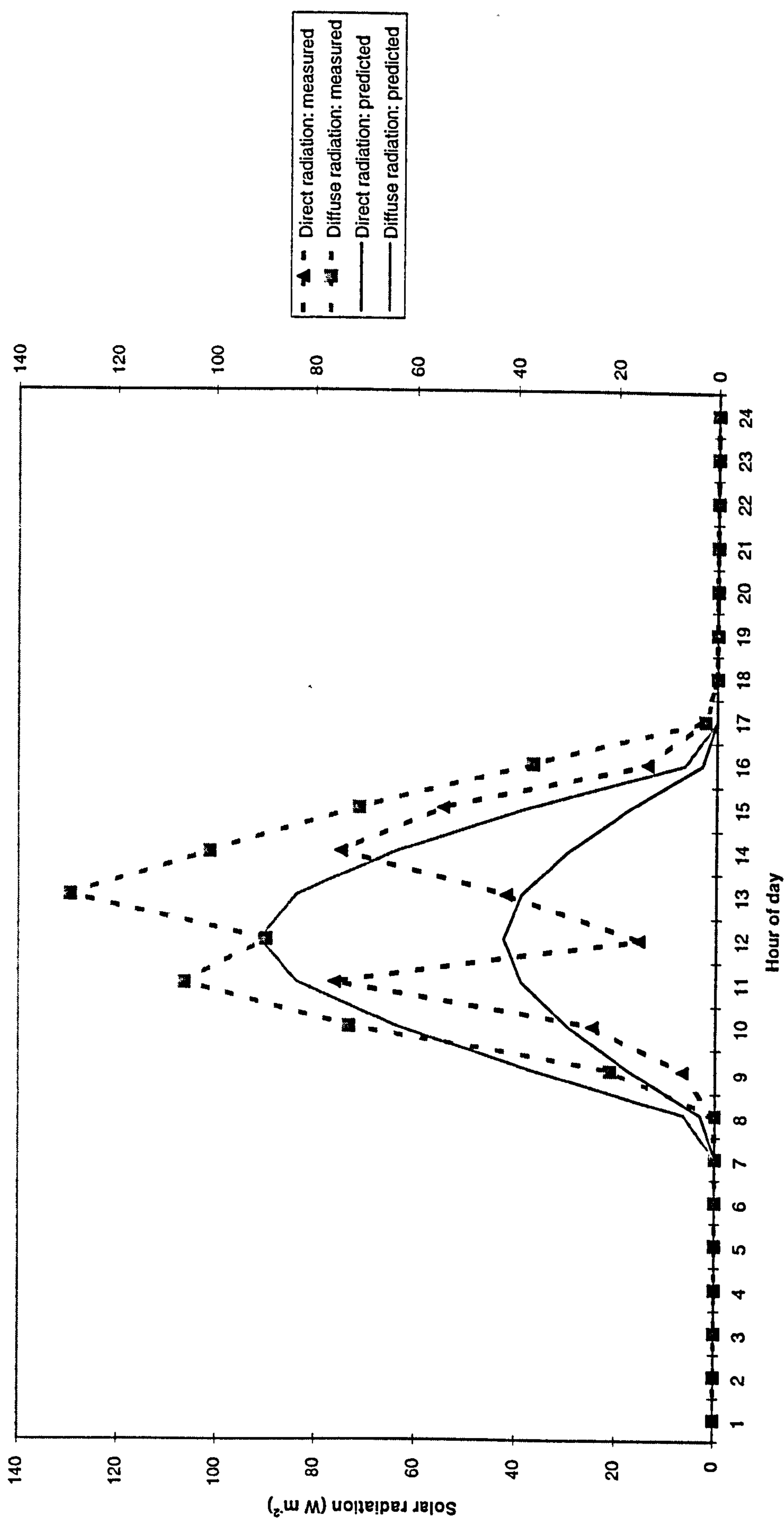
- 1) Those which aim (physically or empirically) to duplicate as nearly as possible current hourly patterns (solar radiation, T_a , T_g , T_{sky})
- 2) Those which are determined by arbitrary interpolation, with an empirical basis (wind speed, vapour pressure, rainfall)

The first category of variables can be compared with recorded data; the recorded daily values are inputs to the generator, and the outputs were compared with the recorded hourly values.

5.3.1 Solar radiation

Fig 5.2 shows one of the days chosen for comparison, 26 January 1996 at Sutton Bonington. The partition between direct and diffuse solar radiation is reasonable, with diffuse radiation greater than direct, as expected even on sunny winter days. The assumption of constant cloud cover over the day gives good results for days which stay totally cloudy or totally clear, but for days with variable cloud (as in this case) the hour-by-hour comparisons are poor, as expected. The maximum S_b (which is the clear sky value) is underestimated, while the solar load in the cloudy periods is overestimated. The daily total of global radiation predicted (S_{gt}) does not necessarily exactly equal the measured amount. This is because the value of τ used (Eq 5.4) includes attenuation by clouds as well as by atmospheric aerosol, and the use of Eq 5.5 to calculate global radiation at each hour is only strictly valid for clear sky values of τ . The errors resulting from this assumption on four test days are given in Table 5.1:

Fig 5.2: Predicted and measured direct and diffuse solar radiation, 26 January 1996 (sunny winter day)



DAY	S _{gt} (measured) (MJ)	S _{gt} (predicted) (MJ)	Error: (predicted - measured)	error (%)
Cloudy winter (12.1.96)	1.2	1.8	+0.6	+50
Sunny winter (26.1.96)	3.4	2.5	-0.9	-26
Sunny summer (5.8.95)	23.8	22.3	-1.5	-6
Cloudy summer (18.8.95)	15.9	15.5	-0.4	-2.5

Table 5.1: Analysis of errors in comparing measured global radiation totals with generated totals.

The worst errors are at low solar elevations, but in these cases the solar load is small, and has a minimal effect on the animal heat balance. A worst case error (eg. 1.5 MJ over a day) corresponds to an average error of about 40 W m^{-2} for the solar radiation receipt on a horizontal surface over a 10 hour light period. The amount actually absorbed by the animal depends on the geometry and skin/coat reflectance, but 5 W m^{-2} per hour is a reasonable approximation. This amount is small enough to neglect.

5.3.2 Air temperature

Air temperature is well-modelled by the sine curve when cloud cover is constant. On cloudy days (eg. 31 August 1970, Fig 5.3), the phase lag of temperature behind solar noon is predicted correctly. However, the generated temperature peak occurs about

Fig 5.3: Predicted and measured air temperature at Sutton Bonington, 31 August 1970 (cloudy summer day)

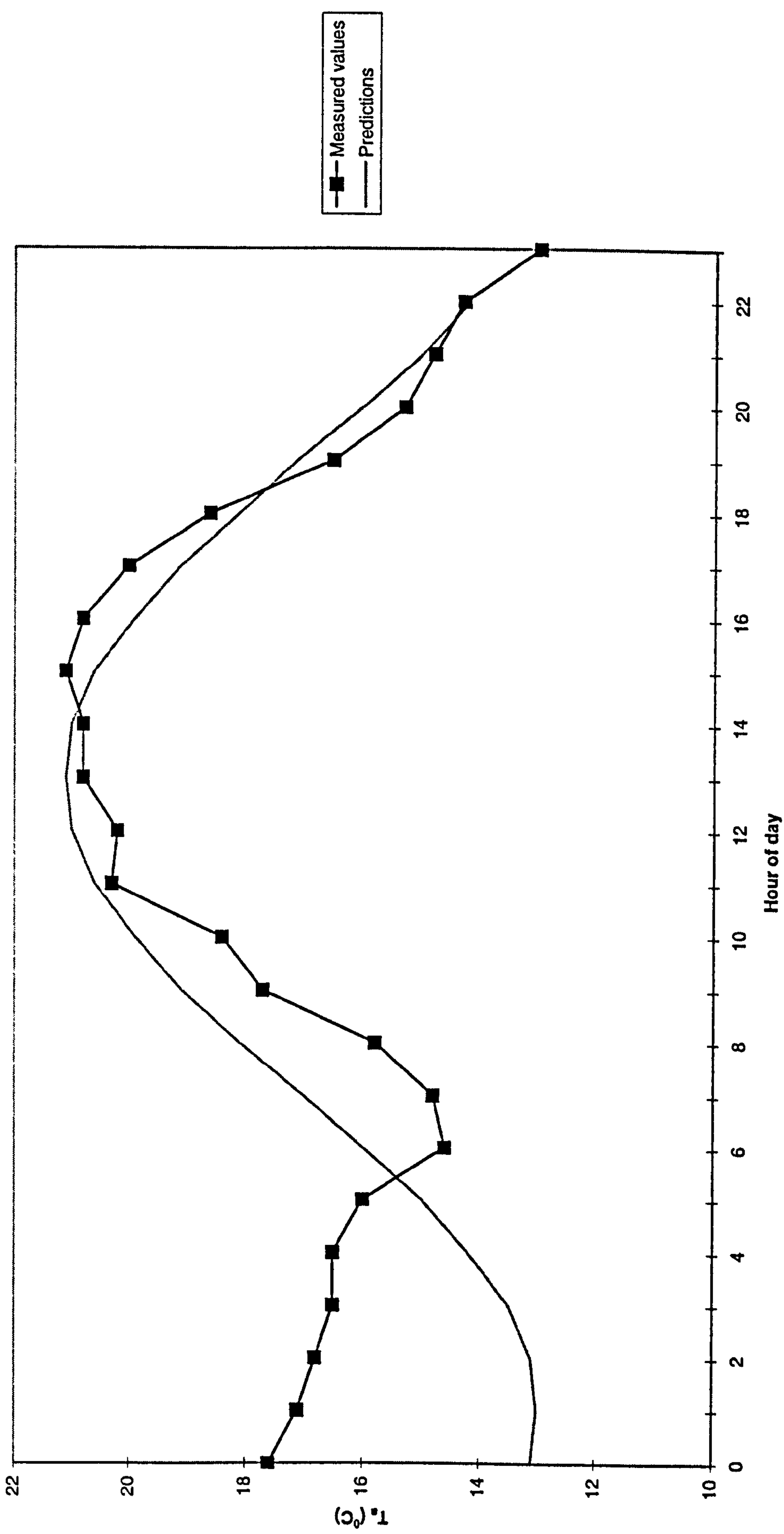
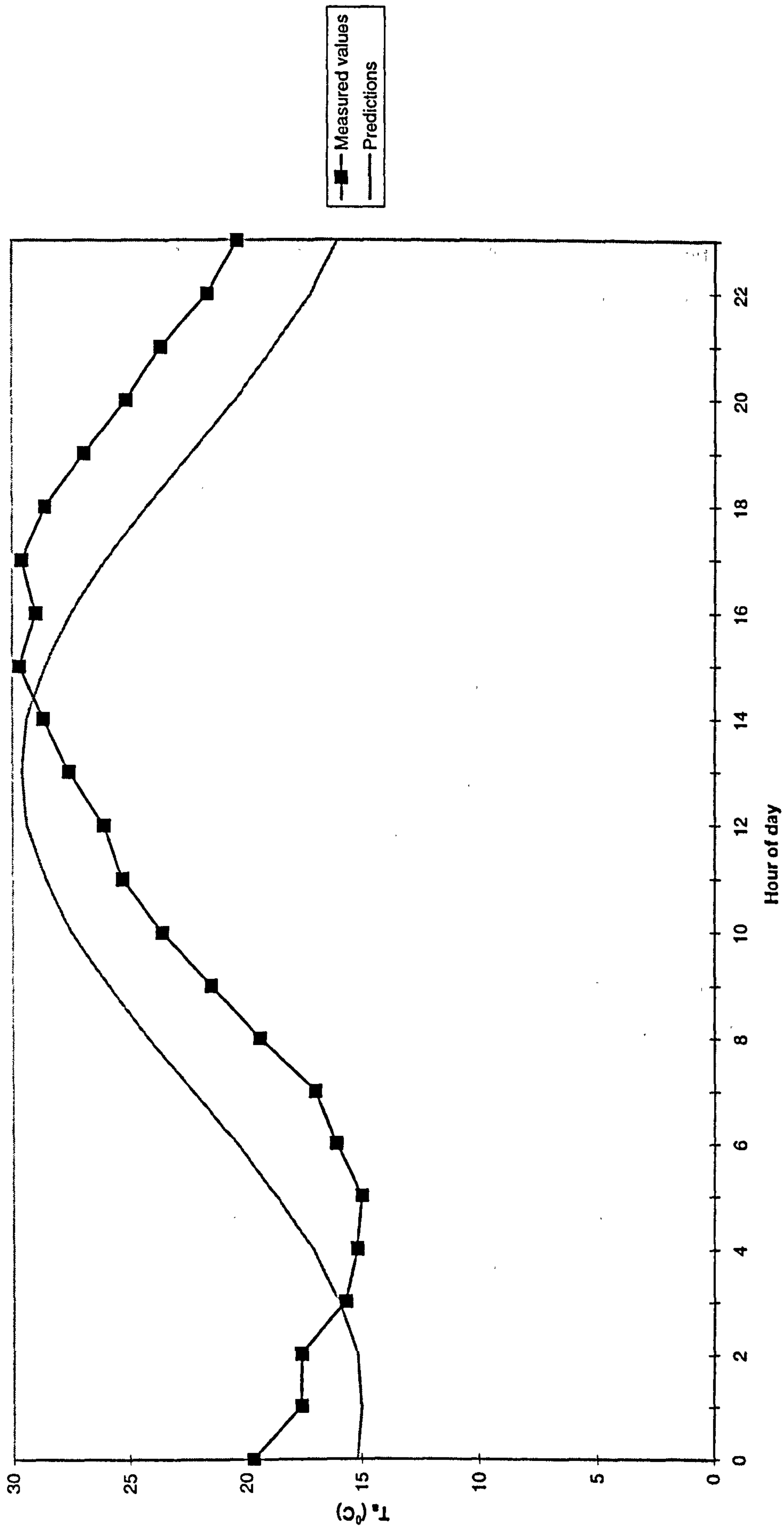


Fig 5.4: Predicted and measured air temperature at Sutton Bonington, 7 July 1970 (clear summer day)



an hour too early on clear days (eg. 7 July 1970, Fig 5.4). One possible remedy is to change the phase lag on the generator depending on the amount of cloud cover, but this would introduce unnecessary complexity. The shape of the modelled curve matches well with the measurements, except in frontal situations (eg. early morning on 31 August 1970, Fig 5.3). The modelled time of occurrence of T_{\min} (2 am) is rarely true (on clear nights the minimum is usually just before dawn), but since the radiation environment is constant through the night, the time of minimum temperature is not important in the current analysis.

5.3.3 Ground surface and sky temperatures

Under cloudless, windless summer daytime conditions, T_g can be more than 10°C above air temperature. Similarly, on clear nights T_g can be more than 10°C below air temperature. Sample calculations of T_g for a clear day and night are given in Appendix 5.2. These predictions are reasonable compared with observations. The assumption of ground heat flux as dependent on a fixed temperature at 1 m T_{deep} is a simplification; in reality the ground heat flux depends much more on the temperature a few cm below the surface, which changes with time. In reality, the evaporative heat flux E_g will depend on soil moisture and type, as well as on solar radiation and temperature, rather than being a constant fraction of C_g . However, the modelled heat loss from the animal was not found to be as sensitive to T_g as to other variables such as wind speed (see chapter 6), hence the calculation of T_g using the simple energy balance presented here is sufficient for use in the thermal balance model.

Observations have shown that the value of T_{sky} can be more than 20°C below the air temperature when skies are clear, but can approximate to air temperature under low thick cloud (eg. Stafford Smith et al, 1985). Sample calculations using Eqs 5.11 - 5.13 to calculate T_{sky} are given in Appendix 5.2. The results are in broad agreement with observations.

5.3.4 Other variables

The second category of variables cannot sensibly be compared hour-by-hour with measured data; the method of assessment was to check that the departures from what could be expected from real data stayed within acceptable limits (eg. $\pm 15\%$).

The vapour pressure, when assumed constant through the day, was usually within $\pm 15\%$ of the measured values. Variations in vapour pressure of this magnitude are not likely to significantly affect the energy balance of a homeotherm, unless the air temperature is close to T_b . Consequently, this assumption was deemed reasonable.

Rain was poorly predicted by the triangular function scheme, as expected. Rainfall is essentially a random event series, and comparison of the scheme used in the current model with any given day's data would be spurious. Other methods of generating hourly rainfall data may be examined in the future - for the present work the triangular function is the best simple prediction available.

Wind speed data for Sutton Bonington confirmed the observation by Troen & Petersen (1989) that the maximum deviation from the daily mean value was less than 1 m s^{-1} on the vast majority of days, especially at inland sites. The present assumption about wind speed was therefore considered acceptable.

5.4 Modelling the impact of climate change on the thermal balance of livestock

5.4.1 Inputs to the thermal balance model

This section shows how the present heat balance model for livestock fits into a suite of models developed to assess the impact of climate change on UK agriculture. The relationships between models are shown in Fig 5.5. The detailed workings of the other models are given elsewhere (eg. Parsons et al 1997b, Turnpenny et al, 1997). Fig 5.5 shows that, in addition to the weather input, there are two direct links between the present model and other models: first with a livestock energy nutrition model, and second with a housing model (both developed at Silsoe Research Institute, Bedford). The housing model output, which specifies the thermal environment in the building, replaces the weather data as input to the energy balance model for animals indoors. One modification which was included when running the present model with many animals in one house was to include the effects of increased humidity caused by water loss from the animals. The latent heat loss from the animals was converted to the equivalent hourly water loss (kg of water per kg of air in the building), and this value was fed back into the ventilation calculations to modify the humidity in the building (Parsons et al, 1997b).

The nutrition model, which deals with the conversion of food intake to energy output and storage, outputs the liveweight of each animal and the metabolic heat production on daily time steps. These values are used as input to the thermal balance model, as described in Chapters 3 and 4. In heat stress, it is commonly observed that animals reduce feed intake, and hence metabolic heat production (eg. Bianca, 1965; Senft & Rittenhouse, 1985; Wiernusz & Teeter, 1996). Reduction of feed intake was parameterised in the nutrition model by reducing the feed intake for a day by 2% for each hour of severe heat stress noted in the previous day. The definition of severe

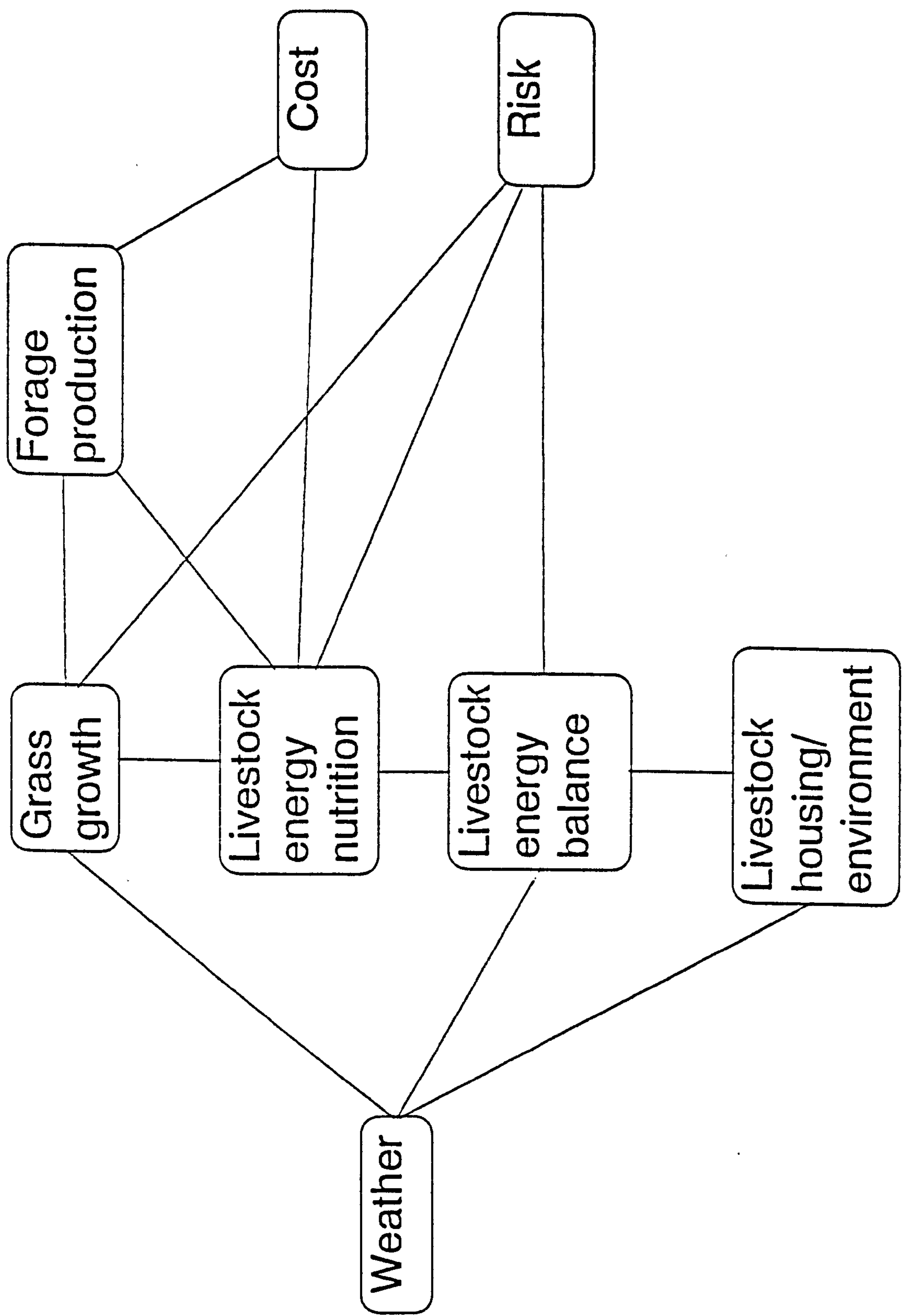


Fig 5.5: Interrelationships between component models in the Grassland-Livestock Integrated Model System (Parsons et al, 1997c)

heat stress for each species is given in Chapter 6. The maximum feed intake reduction was taken as 16% (from the data of Senft & Rittenhouse, 1985).

The weather data were generated separately from the other models and accessed each hour by the thermal balance model from a system of files. Weather data was also supplied to the grass growth model and the housing model. In this way, climate change impact on thermal balance of livestock was assessed using as inputs both weather predictions and modelled changes to other parts of the agricultural system.

5.4.2 Principles of impact assessment

The Intergovernmental Panel on Climate Change (IPCC) produced extensive guidelines for projects involved with climate change impact assessment (IPCC, 1994b). These identify seven steps in any assessment project. These steps are summarised in this section, along with an outline of the way these steps were approached in the current project.

The first two IPCC steps, the definition of the problem and the selection of the method, have been described in Chapter 1. The definition of the problem "involves identifying the goals of the assessment....the spatial and temporal scope of the study, the data needs, and the wider context of the work." The method, the use of mechanistic models (as far as possible) to predict the thermal heat balance of the animals, is justified in Section 2.1. Step three is the testing of the method, and is mainly covered in the current work by the individual model validations in Chapters 3 and 4. Part of this step included gathering measured data for comparison with the model output. Another part is the sensitivity analysis, which assesses the impact of changing input parameters on model output. The sensitivity analysis is presented in Chapter 6.

When the models were designed and validated, step four of the IPCC recommendations was reached - the selection of the scenarios. Scenario selection included a definition of the present situation in terms of a standard baseline climatology. This was chosen as the 1961-1990 World Meteorological Organisation standard data set (Viner & Hulme, 1994). The selection of the climate change scenario was made by MAFF, as part of the contractual obligations of the project. The emission scenario chosen was the IPCC scenario 92a, generated from the UKHI model (see Chapter 1 for discussion of the range of scenarios). IPCC 92a corresponds to a continuation of current usage of fossil fuels (but with restrictions on CFC emissions), with a doubling of world population by 2100. The present impact assessment was made for several combinations of sites and species. Dry lowland and upland sites were considered, represented by Boxworth (Cambs) and Pwllpeiron (Gwynedd), respectively. The species modelled at each site were:

SPECIES	DRY LOWLAND SITE	UPLAND SITE
Sheep	✓	✓
Dairy cow	✓	-
Beef calf	✓	✓
Pig	✓	-
Poultry	✓	-

Table 5.2: Sites and species combinations modelled in the current work.

The intensive (indoor) species were only modelled at one site, and there is very little upland dairy farming in the UK.

Step five is the actual assessment of impacts. In the current model step five involved analysing the differences between the current levels of heat loss and frequency of thermal stress and those predicted to occur under climatic change conditions. Synthetic hourly weather data were produced for the baseline (current) climatology for each site and then the same schemes were used to generate hourly weather data corresponding to a changed climate from the climate change scenario. The predictions of the model, and the accompanying discussion, are presented in Chapter 6. Steps six and seven involve an assessment of the responses to climate change, by the system itself and following human intervention respectively. The effects of thermal stress on livestock have been discussed in previous chapters. Adaptation by an animal to chronic thermal stress can take many forms, and these are discussed in Chapter 7. Examples include reduction of feed intake and metabolic heat production on exposure to chronic heat stress (eg. Berman, 1968) and reduced weight gain in animals exposed to chronic cold stress (eg. Doney, 1963; Bruce & Broadbent, 1989). Mitigation of the effects of climate change by human intervention is also discussed in Chapter 7. Possible mitigation strategies for an increase in mean air temperature may be similar to those used currently in hot climates, for example the provision of adequate shade or water sprays to increase evaporative cooling, or a reduction in stocking or growth rates.

5.5 Conclusions

In this chapter, the design of methods for downscaling GCM output to hourly weather data were presented and validated. For some variables (eg. temperature and solar radiation) the methods chosen produced a good match with the measured data. However, some of the methods (eg. for random events such as rainfall) were too simple to reproduce observed values. Future work could involve adapting more complicated statistical processes for use in generating data for climate change research. In the current project, the simplification of the occurrence of rainfall could

lead to underprediction of cold stress, as the potentially dangerous combination of high winds and rainfall occurring with low temperatures at night cannot occur with the presented rainfall scheme. Similarly, incidence of heat stress could be underestimated if wind speed during the middle of the day is overestimated. The treatment of wind speed as a mean value over the day could also underpredict cold stress, as gusts and hours in the day of significantly high wind speed are not modelled. However, these problems do not mean that results obtained from the impact assessment are invalid. Using the same hourly weather data schemes to generate current and future data sets, the difference in stress incidence between current and future is the important indicator rather than the absolute values.

APPENDIX 5.1: CALCULATION OF SOLAR ELEVATION

The following equations are standard solar geometry and were obtained from Gates (1980). The elevation of the sun above the horizon, α , at a given place, time and date is given by:

$$\sin \alpha = \cos \delta \cos \varphi \cos h + \sin \varphi \sin \delta \quad [5-A]$$

where φ is the latitude (positive in the northern hemisphere, δ is the solar declination, or latitude at which the sun is overhead at noon on the given day (DAY), and is given by:

$$\delta = \frac{\pi}{180} 23.5 \cos \left(\left[\frac{2\pi}{365} \right] (172 - \text{DAY}) \right) \quad [5-B]$$

(Stafford Smith et al, 1985). The term $\pi/180$ converts δ to radians for use in the model, and DAY is the Julian day (eg January 1st = 1). The quantity h is the hour angle of the sun at the given time, and is the azimuthal angle between the sun and the position of the sun at solar noon:

$$h = \frac{2\pi}{24} \times t_n \quad [5-C]$$

t_n is the time from solar noon (eg. -3 = 9 am) so h is zero at solar noon.

APPENDIX 5.2: CALCULATION OF T_g

The energy balance of the ground, Eq 5.14, was expanded by considering each term as follows:

S_a was calculated using Eq 5.16. The ground heat flux density Q_g was written as:

$$Q_g = \frac{k}{\Delta z} (T_{deep} - T_g) \quad [5-D]$$

The convective heat flux density from the ground was written as:

$$C = \frac{\rho c_p}{r_H} (T_g - T_a) \quad [5-E]$$

the heat flux density due to net longwave radiation from ground to sky was written as

$$L = \frac{\rho c_p}{r_R} (T_g - T_{sky}) \quad [5-F]$$

Substituting Eqs [5-D to 5-F] into Eq 5.14 gives

$$(1 - \rho_g)(S_b - S_d) = -\frac{k}{\Delta z} T_g + \frac{k}{\Delta z} T_{deep} + \frac{\rho c_p}{r_H} T_g - \frac{\rho c_p}{r_H} T_a + \frac{\rho c_p}{r_R} T_g - \frac{\rho c_p}{r_R} T_{sky} + E_g \quad [5-G]$$

Gathering terms involving T_g on the left hand side:

$$T_g = \frac{S_a - \frac{k}{\Delta z} T_{\text{deep}} + \rho c_p \left(\frac{T_a}{r_H} + \frac{T_{\text{sky}}}{r_R} \right) - E_g}{\rho c_p \left(\frac{1}{r_H} + \frac{1}{r_R} \right) - \frac{k}{\Delta z}} \quad [5-H]$$

SAMPLE CALCULATIONS OF T_g

Case 1: Clear summer day:

$S_a = 300 \text{ W m}^{-2}$, $T_a = 300 \text{ K (27°C)}$, $T_{\text{sky}} = 280 \text{ K (7°C)}$, $r_H = 300 \text{ s m}^{-1}$ (in a 1 m s^{-1} wind: Monteith & Unsworth, 1990), $r_R = 170 \text{ s m}^{-1}$

Then from Eq 5.15, $T_g = 311 \text{ K (38°C)}$

Case 2: Clear winter night:

$S_a = 0 \text{ W m}^{-2}$, $T_a = 270 \text{ K (-3°C)}$, $T_{\text{sky}} = 250 \text{ K (-23°C)}$, $r_H = 400 \text{ s m}^{-1}$, $r_R = 290 \text{ s m}^{-1}$

Then $T_g = 261 \text{ K (-12°C)}$

SAMPLE CALCULATIONS OF T_{sky}

Case 1: Clear winter night: $T_a = 270 \text{ K } (-3^\circ\text{C}), c = 0$

from Eq 5.11 - 5.13, $Y = 1$ and $Z = 0.74$

$T_{\text{sky}} = 250 \text{ K } (-23^\circ\text{C})$, ie. 20°C below T_a

Case 2: Partly cloudy summer day: $T_a = 300 \text{ K } (27^\circ\text{C}), c = 0.7$

Then $Y = 0.41$, $Z = 0.85$ and

$T_{\text{sky}} = 295 \text{ K } (22^\circ\text{C})$, ie. 5°C below T_a

Case 3: Winter day, total cloud cover: $T_a = 270 \text{ K } (-3^\circ\text{C}), c = 1$

then $Y = 0.16$ and $Z = 0.74$ and

$T_{\text{sky}} = 267 \text{ K } (-6^\circ\text{C})$ ie. 3°C below T_a

CHAPTER 6 - RESULTS AND ANALYSIS

6.1 INTRODUCTION

This chapter presents a selection of the results produced by the unified model and the thermal balance model alone. The thermal balance model was run for several UK sites and scenarios when linked with the feeding and grass growth models, and the results of the 30-year runs are presented in Section 6.3. The thermal model was then decoupled from the feeding and grass growth models and run alone with the assumption that the animal had a fixed metabolic rate above the LCT (but with the growth function still input from the feeding model). These results are given in Section 6.4. The sensitivity of the thermal balance models to changes in the inputs is assessed in Section 6.5.

6.2 INDICATORS OF THERMAL STRESS

In the current work, examining several different species and scenarios with thirty years of hourly data used for each, a scheme had to be designed to reduce the huge amounts of data produced to manageable levels. The main indicator used to describe the thermal status of an animal was the *thermal stress level*. Labels were defined to classify the thermal status of an animal based on various physiological indicators as it responds to its environment. Kerslake (1972) outlined several definitions of thermal stress, both purely in terms of environmental conditions and in terms of the responses by the animal. One definition, based on analysis of heat exchange similar to the current work, defined a heat stress index as the evaporative heat loss required for thermal balance divided by the maximum possible evaporative heat loss. This index is useful for sweating animals such as Man and cattle.

Animals such as chickens where stress severity is best described by body temperature elevation require separate definitions of stress levels.

Alexander (1974) defined the following zones of thermal comfort for sheep:

- "COLD LETHAL" when heat loss exceeds summit metabolism
- "COLD" when heat loss is between basal metabolic rate and summit
- "HOT" when the animal is no longer thermoneutral but the upper critical temperature is not reached
- "HOT LETHAL" above the UCT

These definitions were used as a starting point in the current model. The cold zone was split into "SIGNIFICANT" and "SAFE" cold stress, the transition occurring when the heat loss is approximately double the thermoneutral heat production, chosen as a simpler criterion in the current model than, for example, the temperature of the skin below a certain "comfortable" value, which is hard to determine. In the heat, the UCT is hard to determine, so in the model, "SEVERE" heat stress is flagged when the model animal cannot dissipate the heat using its normal (preferred) mode of dissipation (eg. sweating in cattle, first phase panting in sheep etc.). The transitions between "SAFE" and "SIGNIFICANT" heat stress were defined by dividing the full range of the chosen stress-inducing variable into three roughly equal parts. The stress levels are defined in Table 6.1.

6.3 RESULTS: INTEGRATED MODEL

The results presented here cover a dry lowland site (Boxworth) and an upland site (Pwllpeiron). All four species (Chapters 3 and 4) were considered, though dairy cattle were not modelled at the upland site, consistent with current farming practice, and only the lowland site was used for the indoor animals. Each site and species combination (seven in all) was modelled for the baseline (current) conditions and for

Table 6.1. Definitions of thermal stress levels

	SEVERE COLD	SIGNIFICANT COLD	SAFE COLD	SAFE HEAT	SIGNIFICANT HEAT	SEVERE HEAT
DAIRY & BEEF COW	$Q > 5.5M$	$2M < Q \leq 5.5M$	$M < Q \leq 2M$	$E_{res} < E \leq 0.5E_{max}$	$0.5E_{max} < E < E_{max}$	$E > E_{max}$
PIG	$Q > 4M$ [1]	$2M < Q \leq 4M$	$M < Q \leq 2M$	$39^{\circ}C < T_b \leq 40^{\circ}C$ [2]	$40^{\circ}C < T_b \leq 41^{\circ}C$	$T_b > 41^{\circ}C$ [3]
BROILER CHICKEN	$Q > 2.5M$ [4]	$1.5M < Q \leq 2.5M$	$M < Q \leq 1.5M$	$41^{\circ}C < T_b \leq 42^{\circ}C$	$42^{\circ}C < T_b \leq 43^{\circ}C$	$T_b > 43^{\circ}C$
EWE	$Q > 5.5M$ [5]	$Q \leq 5.5M$ but with maximal posture compaction	$Q > M$, with posture compaction not maximal	$F_{res} < F_1 \leq 270 \text{ min}^{-1}$ [6]	$270 < F_1 \leq 320 \text{ min}^{-1}$	$F_2 > 0$

Notes:

M = thermoneutral heat production; Q = environmental demand (heat loss); E_e = evaporative heat loss; T_b = deep body temperature
 F_1 , F_2 = first and second phase respiration rate

[1]: Pig summit metabolism $\approx 4.5M$ at 1 day, $3.3M$ at 6 days (Poczopko, 1981) [2]: Wallowing starts

[3]: At $T_b = 42^{\circ}C$ the blood pH rises; $43^{\circ}C$ imminent death from hyperthermia (Ingram & Legge, 1969)

[4]: Bennett (1972)

[5]: Whitmore & Young (1986)

[6]: Metabolic rate starts to rise at about 270 min^{-1} (Hales & Brown, 1974)

three climate change scenarios (1992a, c and f - see Chapter 1) for a thirty year run of data. The thirty year series of weather data do not correspond with any specific dates in the present or future, but have statistical properties consistent with the means and standard deviations of current and scenario weather data. For each site/species combination, one year was chosen from each run and a daily running total of hours of stress experienced was plotted for baseline and scenario conditions. In the discussion below, HSHS is the hours of severe heat stress.

6.3.1 Sheep

Figs 6.1 to 6.4 show the model predictions for sheep at Boxworth and Pwllpeiron, based on 100 animals in a 12 ha field. Figs 6.1 and 6.3 show the total HSHS over the 30 year run, for current and climate change scenario conditions. Over the thirty years, the incidence of heat stress is predicted to rise by 15 - 20%, but there is a lot of inter-annual variability. Currently, the predicted mean number of hours per year of severe heat stress at Boxworth is 790, with a standard deviation of about 90 hours per year. Under climate change (the mean of the scenarios), the average rises to 930 hours per year, again with a standard deviation of 90. The inter-annual variability is significant: ten out of the thirty years under 2050 conditions came within one standard deviation above the current mean of heat stress frequency. At Pwllpeiron (Fig 6.3), the pattern is similar to that at Boxworth, but unsurprisingly the hours per year of heat stress is significantly less for the upland site.

Figs 6.2 and 6.4 show the daily running totals of HSHS for year 30 at Boxworth and Year 8 at Pwllpeiron. The years chosen were those in which there was least difference between the three climate change scenarios (see Appendix 6.1). The gradients of the respective curves indicate the mean number of HSHS per day - the steeper the gradient the more frequent is heat stress occurrence. The graphs show that the pattern of occurrence of heat stress is the same through the year under

Fig 6.1: Duration of Severe heat stress in Ewe for 30 year run at Boxworth; Baseline and three scenarios

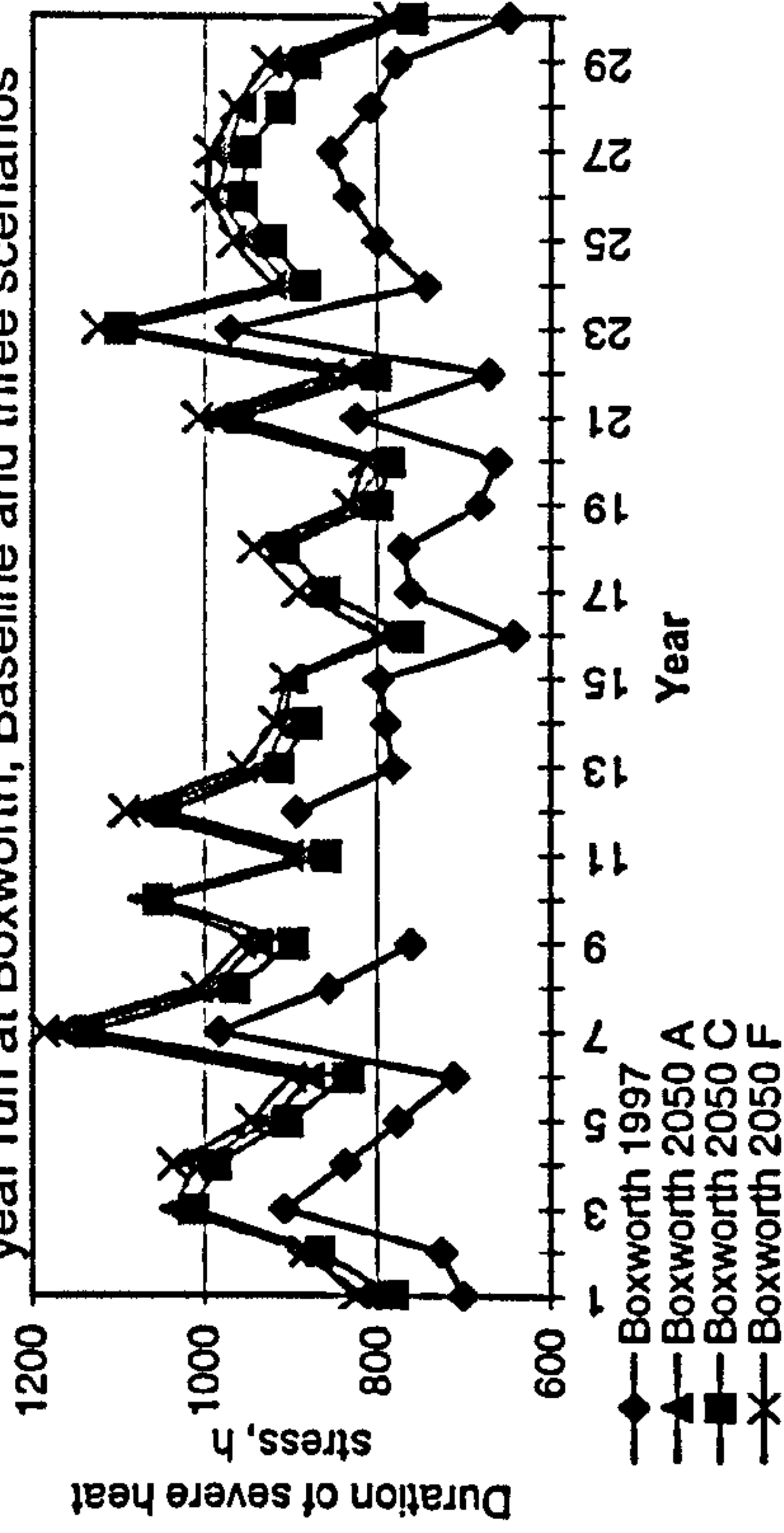


Fig 6.2: Cumulative hours of severe heat stress for Sheep at Boxworth, Year 30

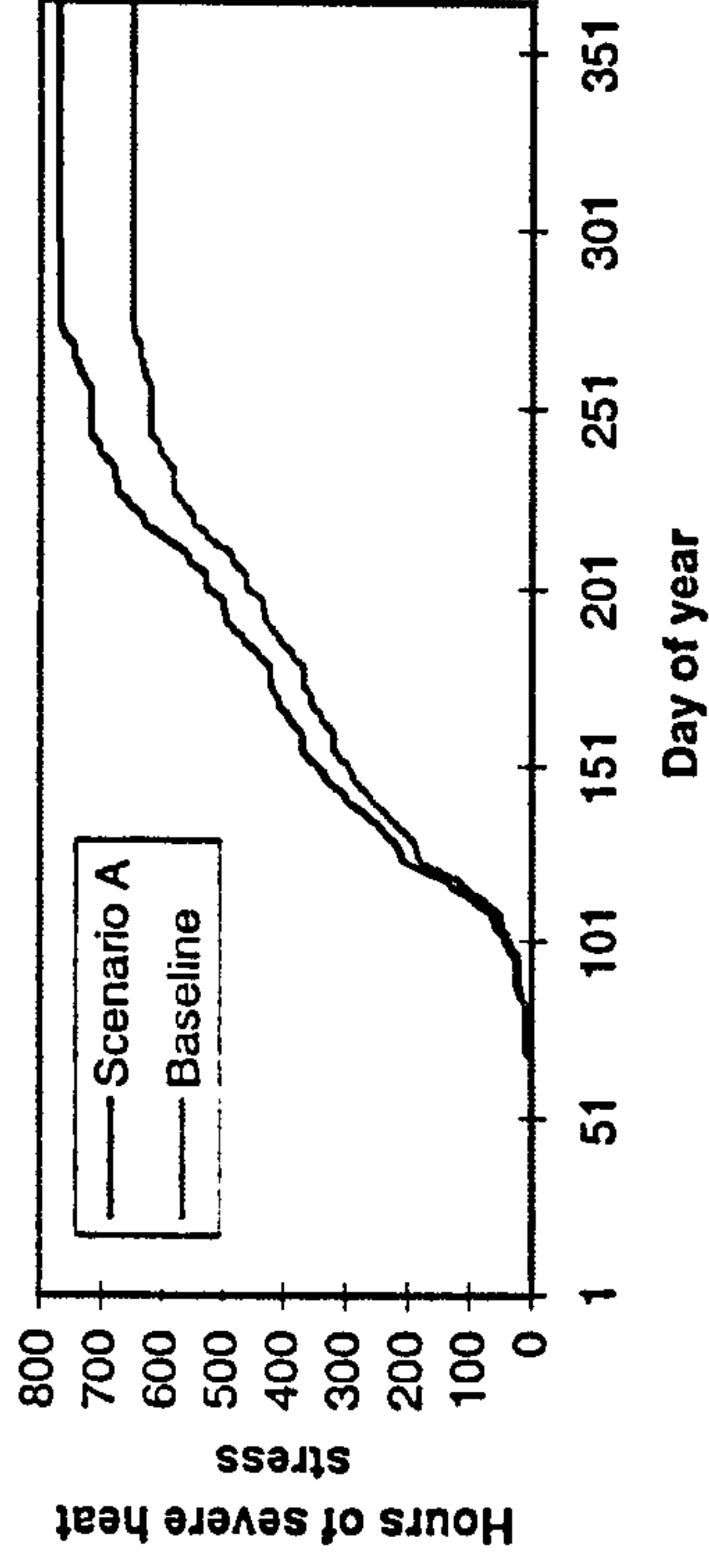


Fig 6.3: Duration of Severe heat stress in Ewe, Pwllpeiron, 30 year run for baseline and three scenarios

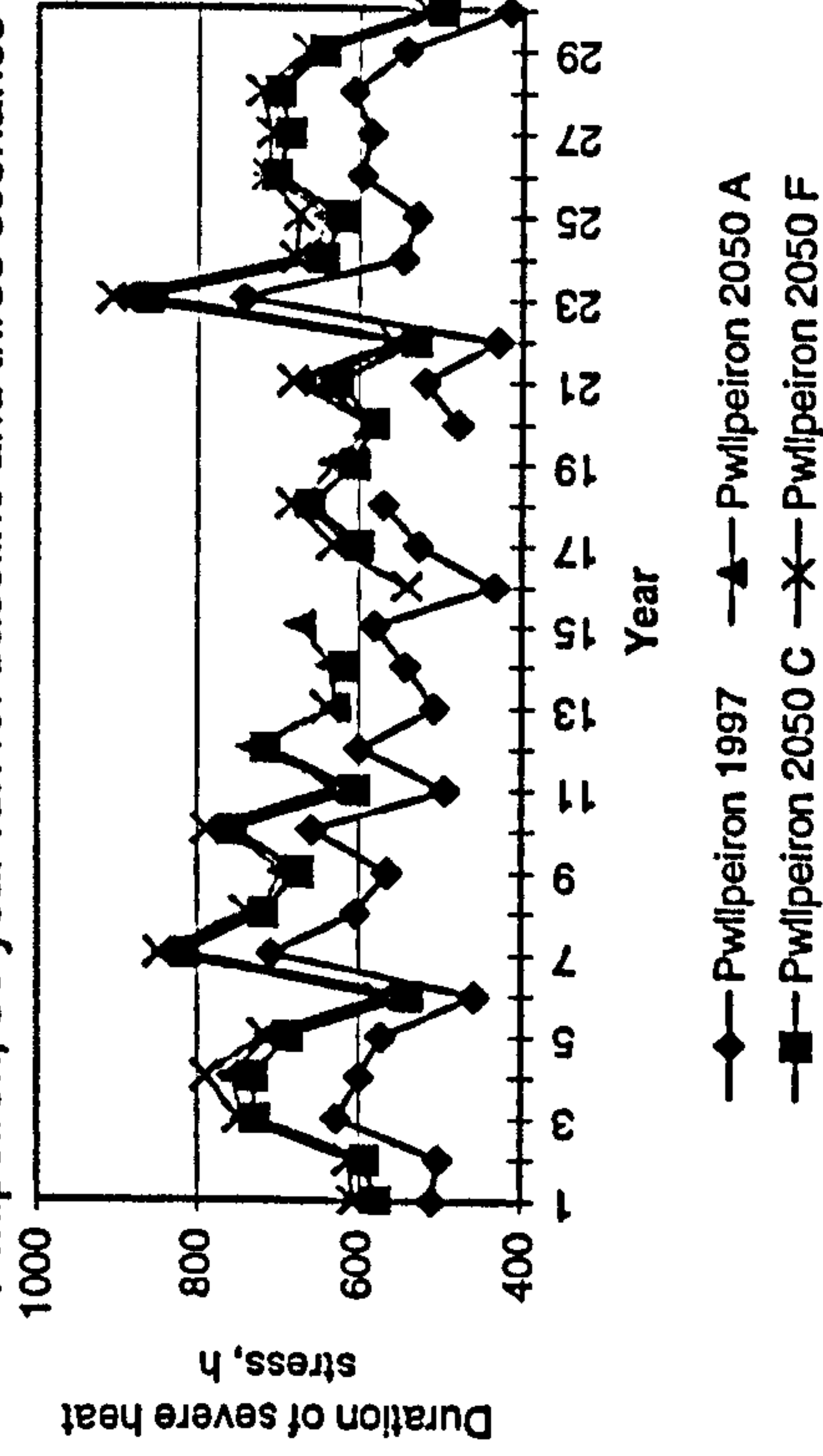
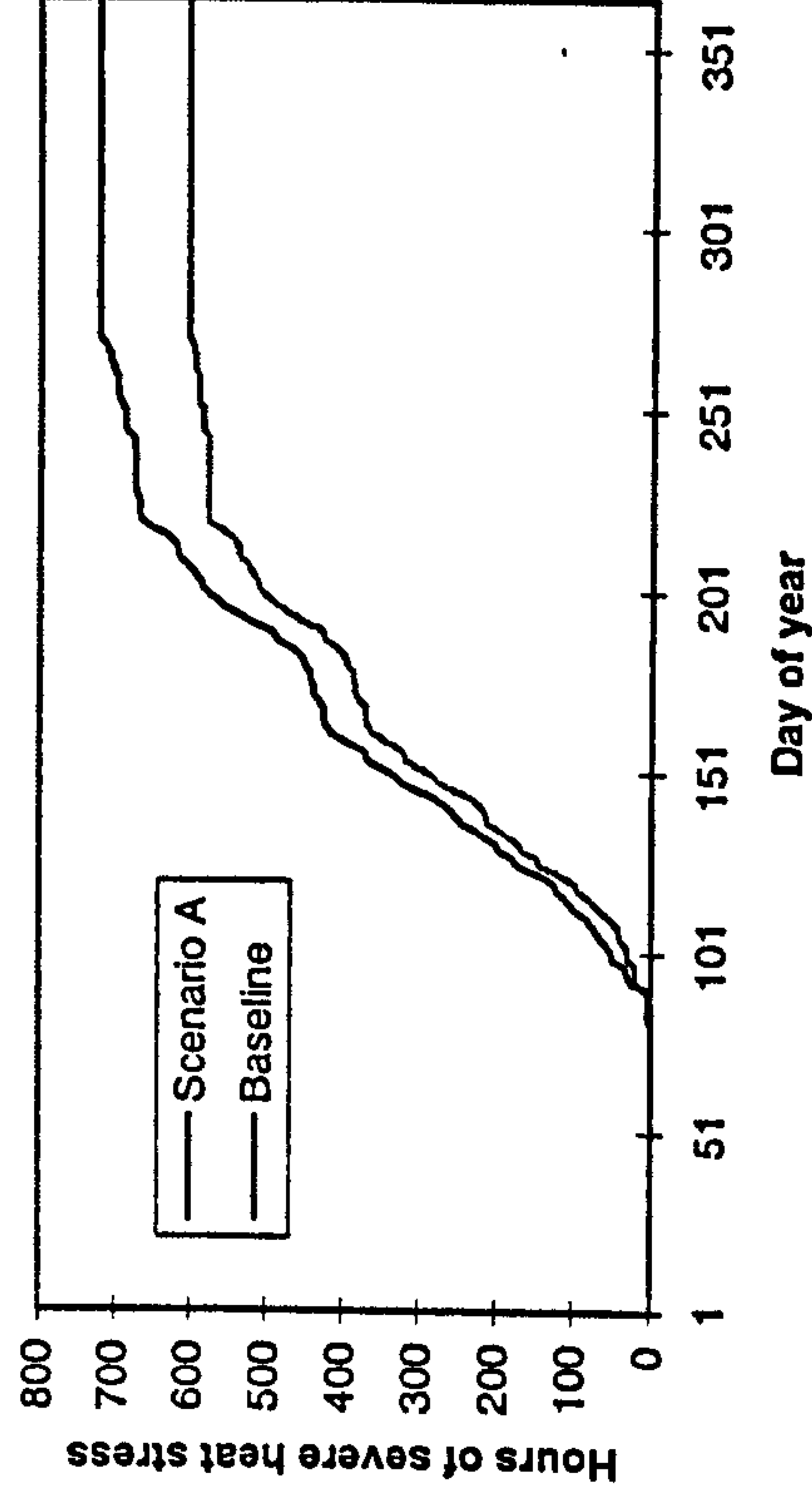


Fig 6.4: Cumulative hours of severe heat stress for Sheep at Pwllpeiron, Year 8



current and climate change conditions, but the number of hours of stress in each 'step' of the graph is higher under climate change, giving a steeper gradient. Under climate change there will be more hours per day with heat stress, rather than more days on which heat stress occurs. This conclusion is drawn from the similar start and end points of stress occurrence for the two scenarios, but the steeper gradient under climate change. At Boxworth (Fig 6.2), heat stress levels are predicted to rise by about 100 hours in the chosen year. At Pwllpeiron, heat stress events start later than at Boxworth (about 20 days).

6.3.2 Beef calves

Figs 6.5 and 6.7 show the yearly totals of severe heat stress for beef calves at Boxworth and Pwllpeiron respectively, based on a stocking density of 240 animals per 60 ha field. The total HSHS per year values are less than those for the sheep, as the beef calves do not lactate and therefore have lower metabolic rates through the year. As for the sheep, the inter-annual variability is important as well as the impact of climate change. At Boxworth, the current mean HSHS per year is 550, with a standard deviation of 70. Under climate change the predicted mean is 640, with a standard deviation of 70. Consequently, the mean duration of heat stress increases by about 15% under climate change but the standard deviation of the mean of the current frequencies is about 13%. Thirteen out of the thirty years under climate change are predicted to be within one standard deviation of the current mean. The climatic change scenario has a detectable, but not severe, effect on heat stress duration in terms of the current inter-annual variability. Pwllpeiron shows a similar variability between years, but with a mean of about 150 hours per year less heat stress (a reduction of about 30% from Boxworth). Climate change at Pwllpeiron has even less effect than at Boxworth, with a range of heat stress hours from 350 - 650 h over the thirty years under climate change, compared to the current range of 300 - 600 h. The lower air temperature at Pwllpeiron under

Fig 6.5: Duration of Severe heat stress in Beef calf at Boxworth, 30 year run: baseline and three scenarios

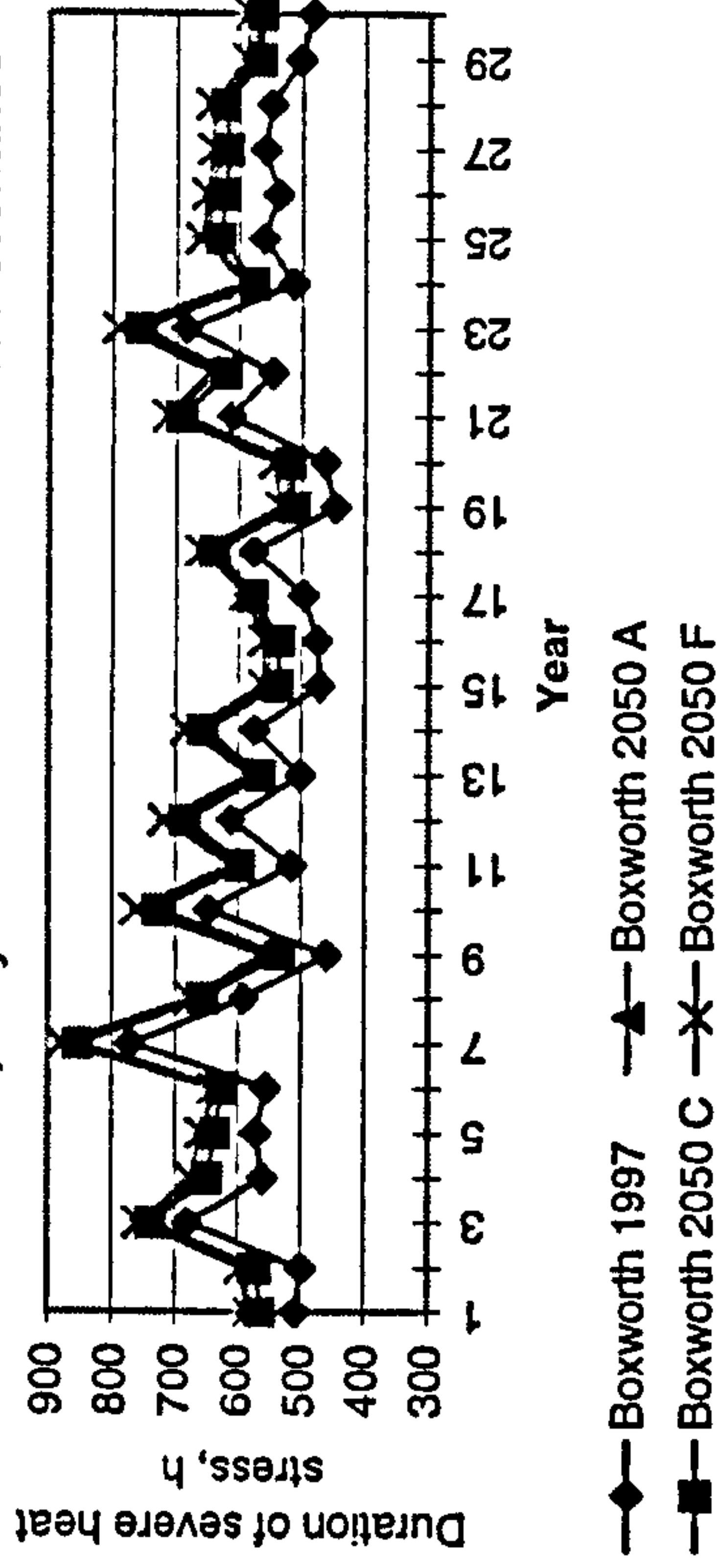


Fig 6.6: Cumulative hours of severe heat stress for Beef cattle at Boxworth, Year 10

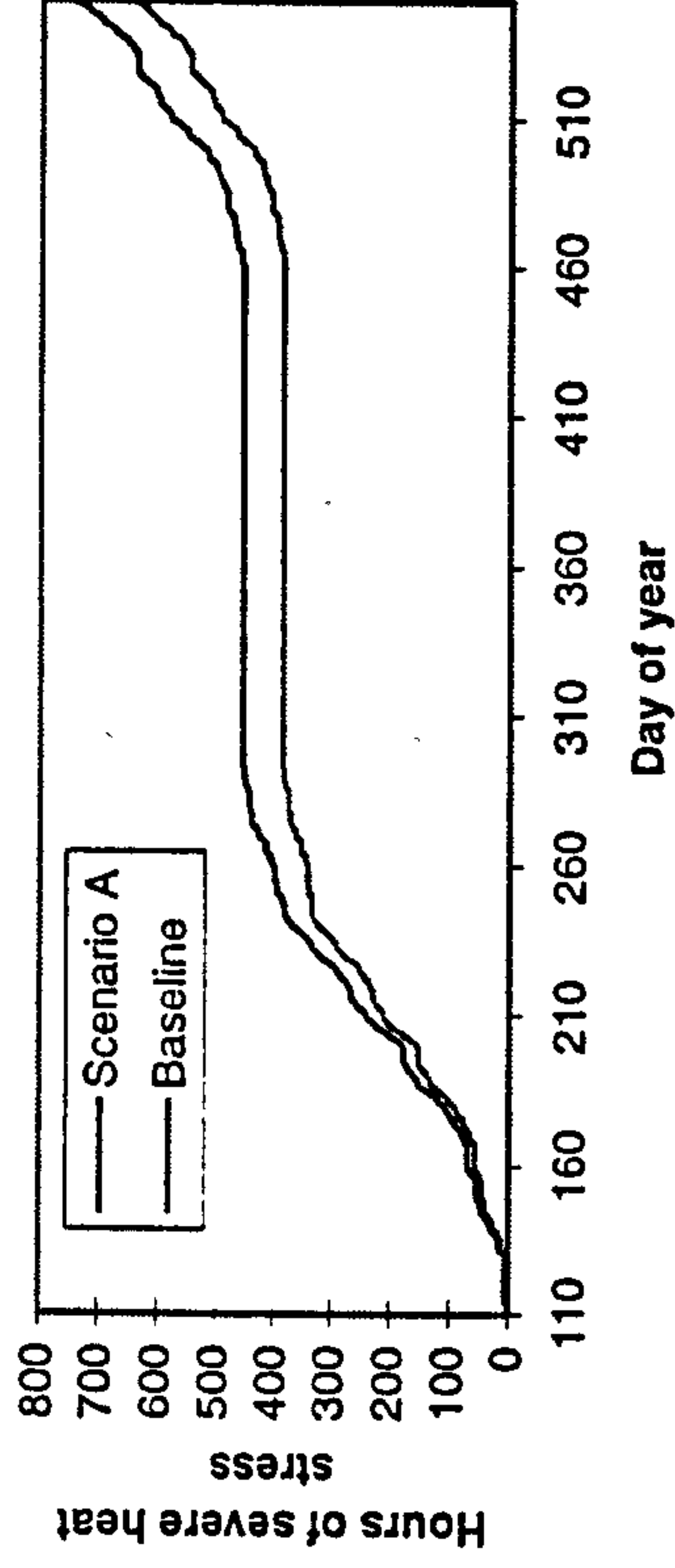


Fig 6.7: Duration of Severe heat stress in Beef calf at Pwllpeiron, 30 year run: baseline and three scenarios

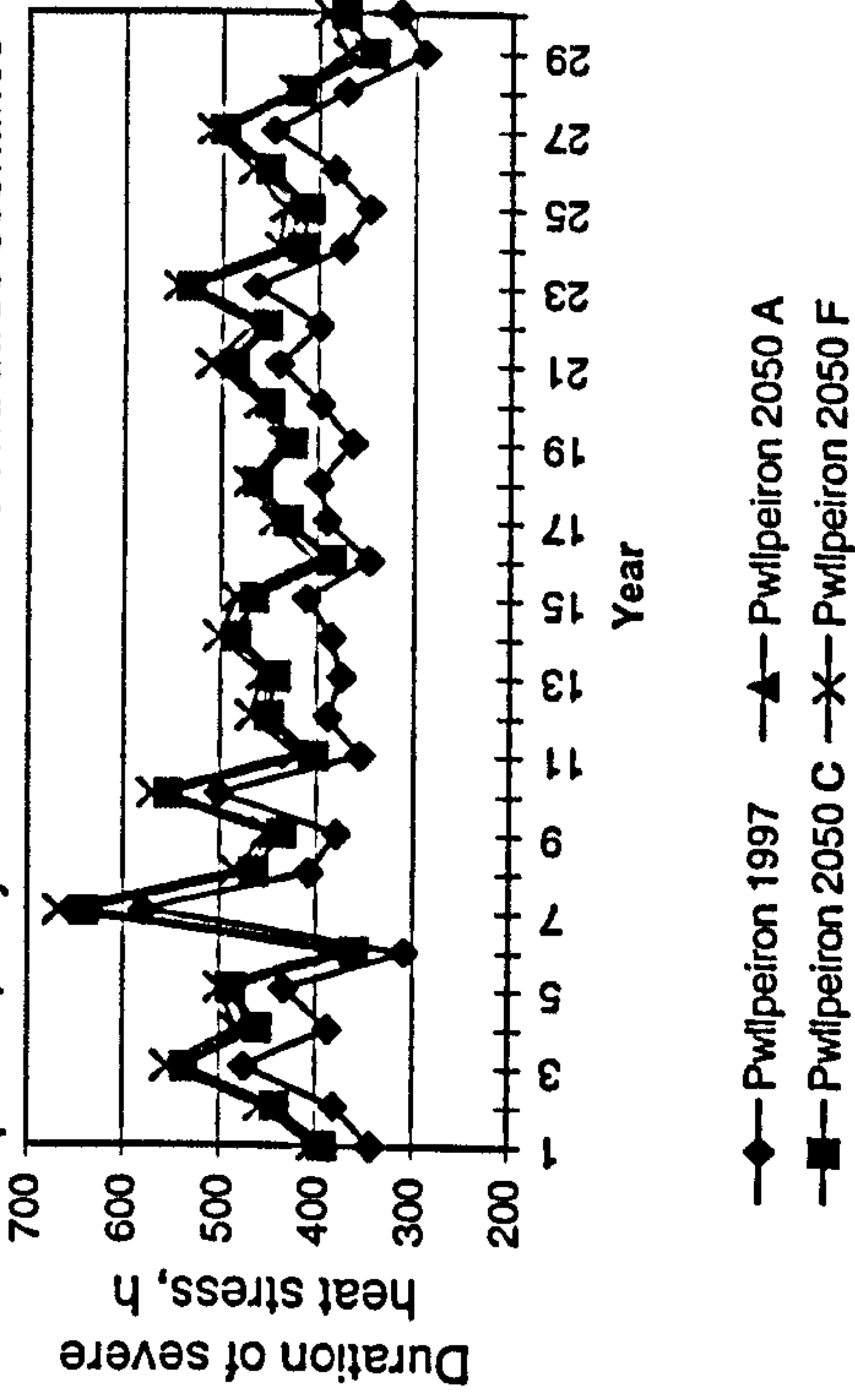
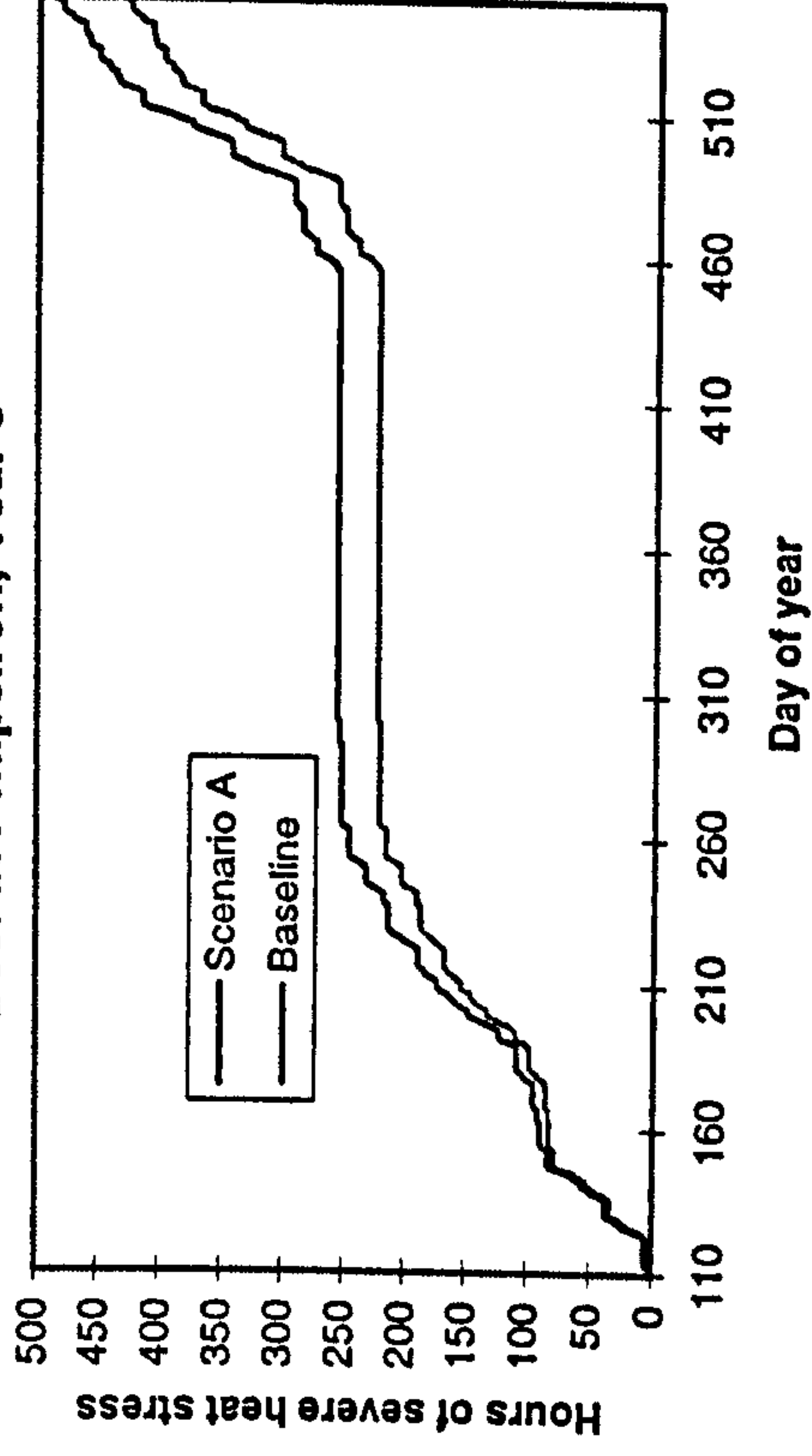


Fig 6.8: Cumulative hours of severe heat stress, Beef at Pwllpeiron, Year 5



current conditions means that any change in the climate will have to be larger than an increase at Boxworth to produce a comparable increase in stress levels on these livestock.

Fig 6.6 and 6.8 are plots of the running total HSHS in typical years at the two sites. The calves are born on Day 110, and the modelled life was 550 d. At Boxworth, the relatively smooth lines indicate an even spread of heat stress events from day to day. At Pwllpeiron, the heat stress events occur in 'steps', indicating a climate where stressful conditions only occur on certain days rather than every day. Heat stress events at Pwllpeiron occur from about early April to mid September, and at Boxworth the stressful period ends about a month later. As in the sheep, the effects of climate change are mainly to increase the number of hours per day of heat stress rather than changing the number of days when stress occurs.

6.3.3 Dairy cattle

Fig 6.9 shows the predictions for dairy cattle at Boxworth, based on 100 animals in a 60 ha field. The total hours of stress are much higher than for beef cattle, due mainly to the very high heat production of a high-yield dairy cow. The current levels of HSHS are between 1100 and 1600 hours per year (hours where metabolically costly panting must be used) for a dairy cow standing in the sun. In practice, cattle will seek shade from the direct solar beam, so these figures are overestimates; nevertheless, it is useful to look at the difference between current and climate change conditions. Climate change increases the heat stress duration by about 10% on average, but as for the other outdoor animals, the inter-annual variability dominates. Ten of the thirty years run for 2050 have HSHS within one standard deviation of the current mean.

Fig 6.9: Duration of Severe heat stress in Dairy cow, Boxworth, 30-year run: baseline and three scenarios

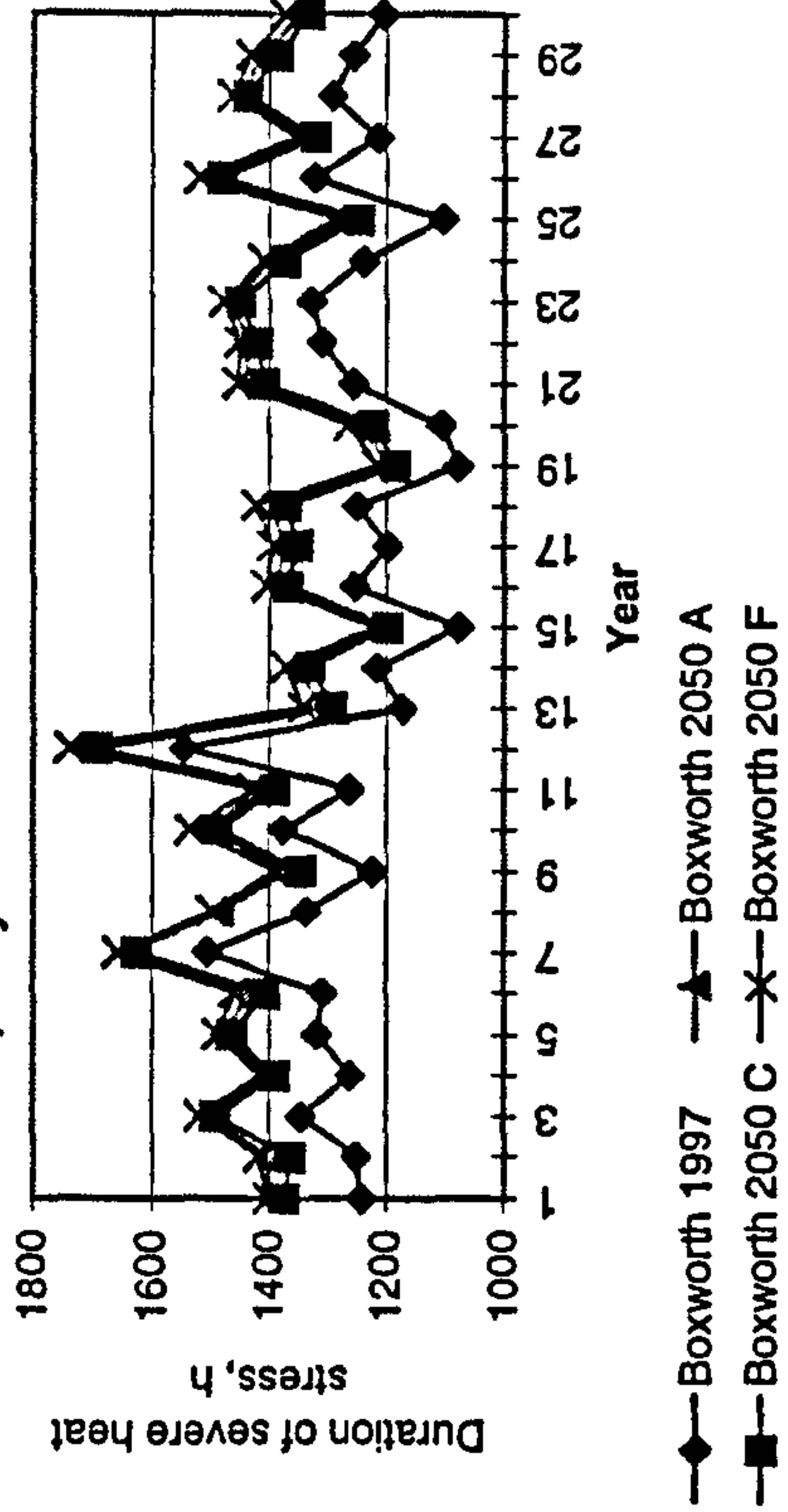


Fig 6.10: Cumulative hours of severe heat stress for Dairy Cattle, Boxworth, Year 4

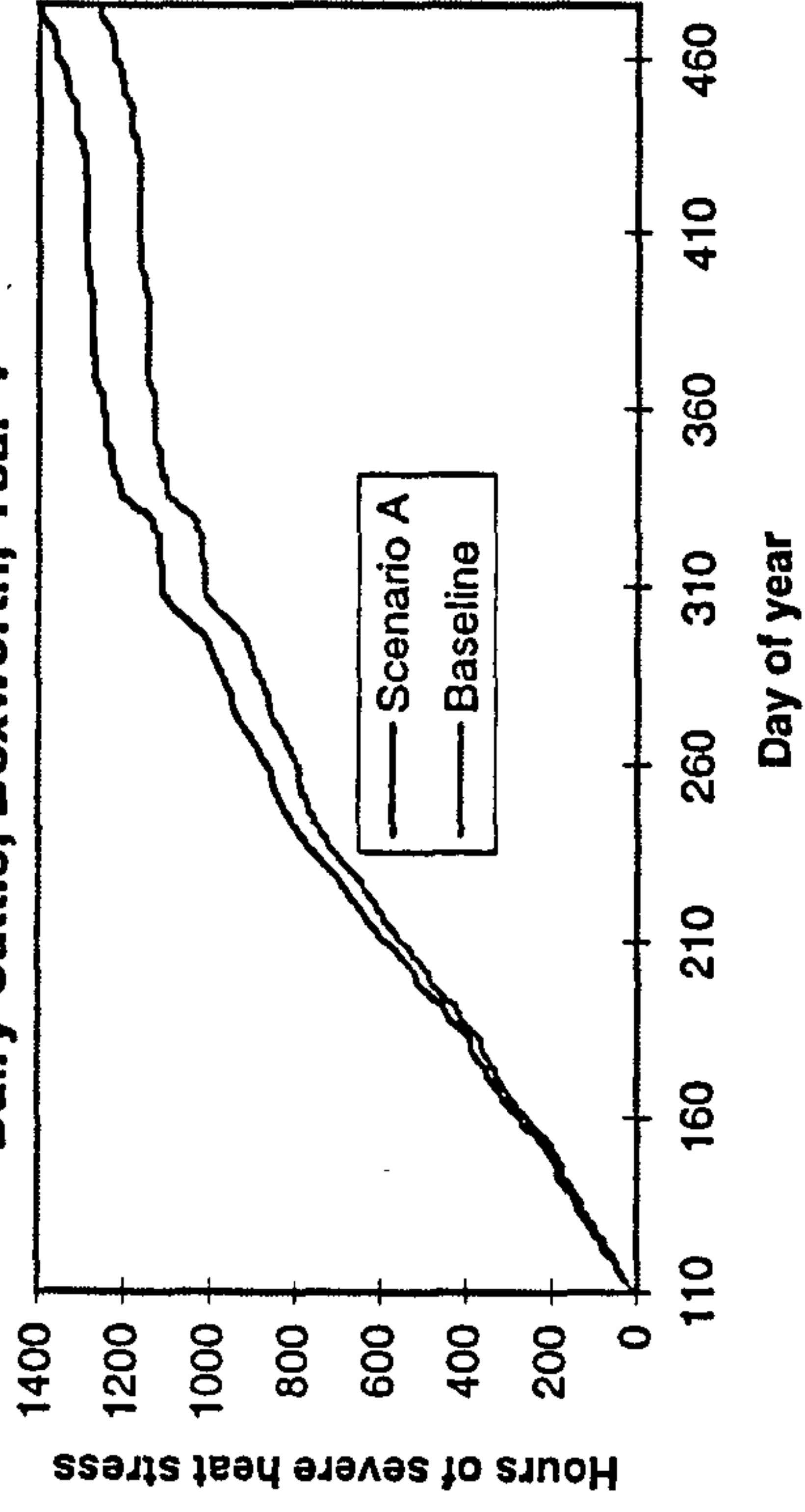


Fig 6.10, for Year 4 of the run, shows that stress will occur throughout the year due to the high metabolic heat production, even averaging half an hour per day during days 340 to 440 (December - March). Climate change makes little difference to the occurrence and severity of stress during the first 150 days of the year (spring and early summer), as seen in the similarity of the gradients during this period. Stress is more frequent in winter under a changed climate than it is at present, which is consistent with the predictions that most warming at high latitudes will occur in the winter.

6.3.4 Pig

The 30 year run results presented for housed pigs in Fig 6.11 show the total HSHS at Boxworth for 640 pigs in a building with a floor area of 480 m². Unlike the outdoor animals, there was more variation between the scenarios, and two Scenarios (A and F) were analysed, chosen as the most likely scenarios of a future change in climate. Appendix 6.1 contains a discussion of the similarity between predictions under different scenarios for outdoor animals and the larger spread of predictions for indoor animals. Fig 6.11 predicts a significant increase in stress levels for the pig with climate change. The current mean HSHS per year is 1020, and for Scenario A this figure rises to 1250, both with standard deviations of about 100 hours per year. The increase in HSHS is therefore 25% under climate change, and 26 of the 30 years under 2050 condition are more than one standard deviation above the current totals.

The distribution of heat stress events through a typical year is shown in Fig 6.12, and the difference between baseline and Scenario A totals for the same year is plotted against day of the year in Fig 6.13. The graphs refer to the approximately 110 day finishing period of the pigs, which are slaughtered at 100 kg; hence the HSHS totals for the year cover three separate pigs' finishing periods, the last ending

Fig 6.11: Duration of Severe heat stress in Pig, Boxworth, 30 year run: baseline and three scenarios

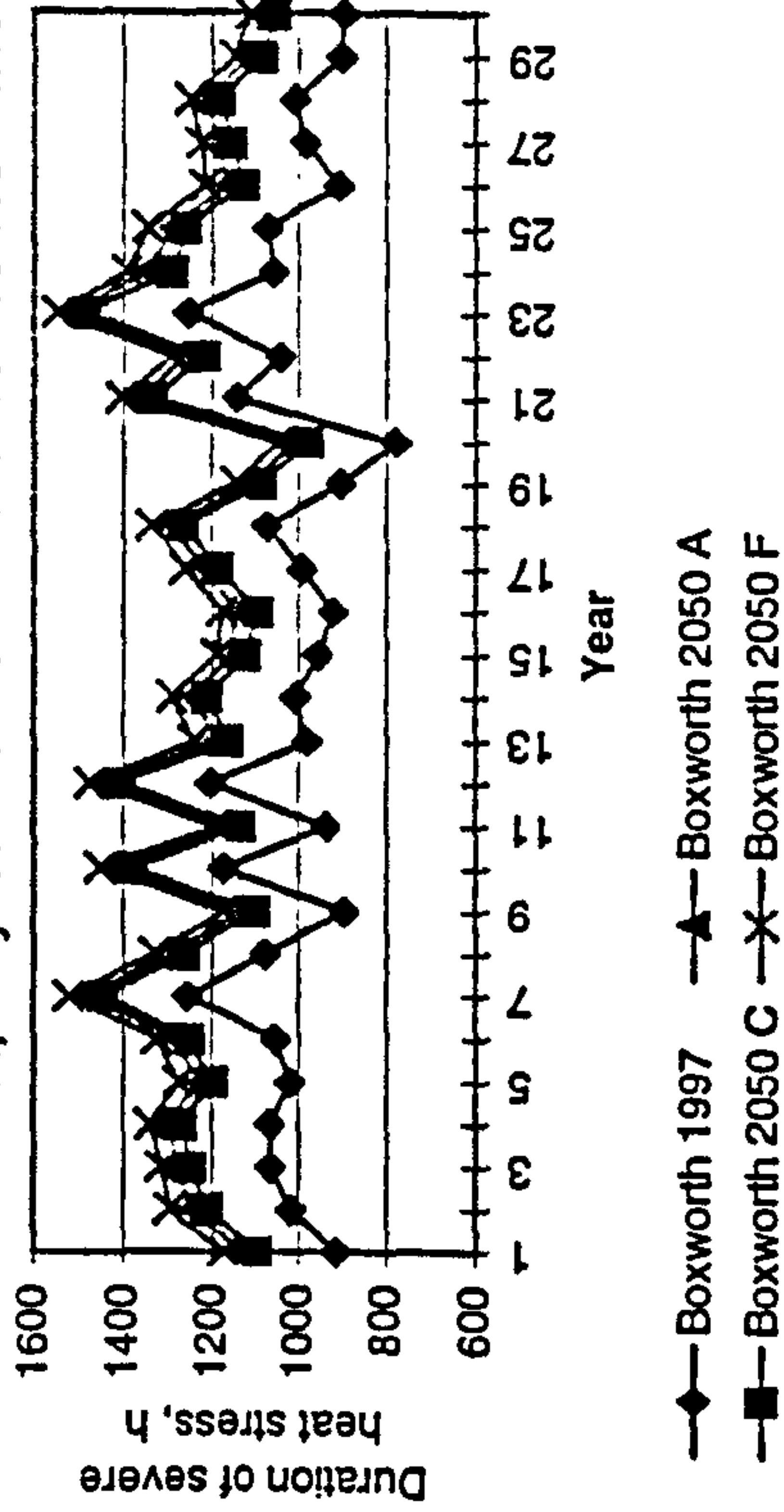


Fig 6.12: Cumulative HSHS, Pig, Boxworth, Year 3

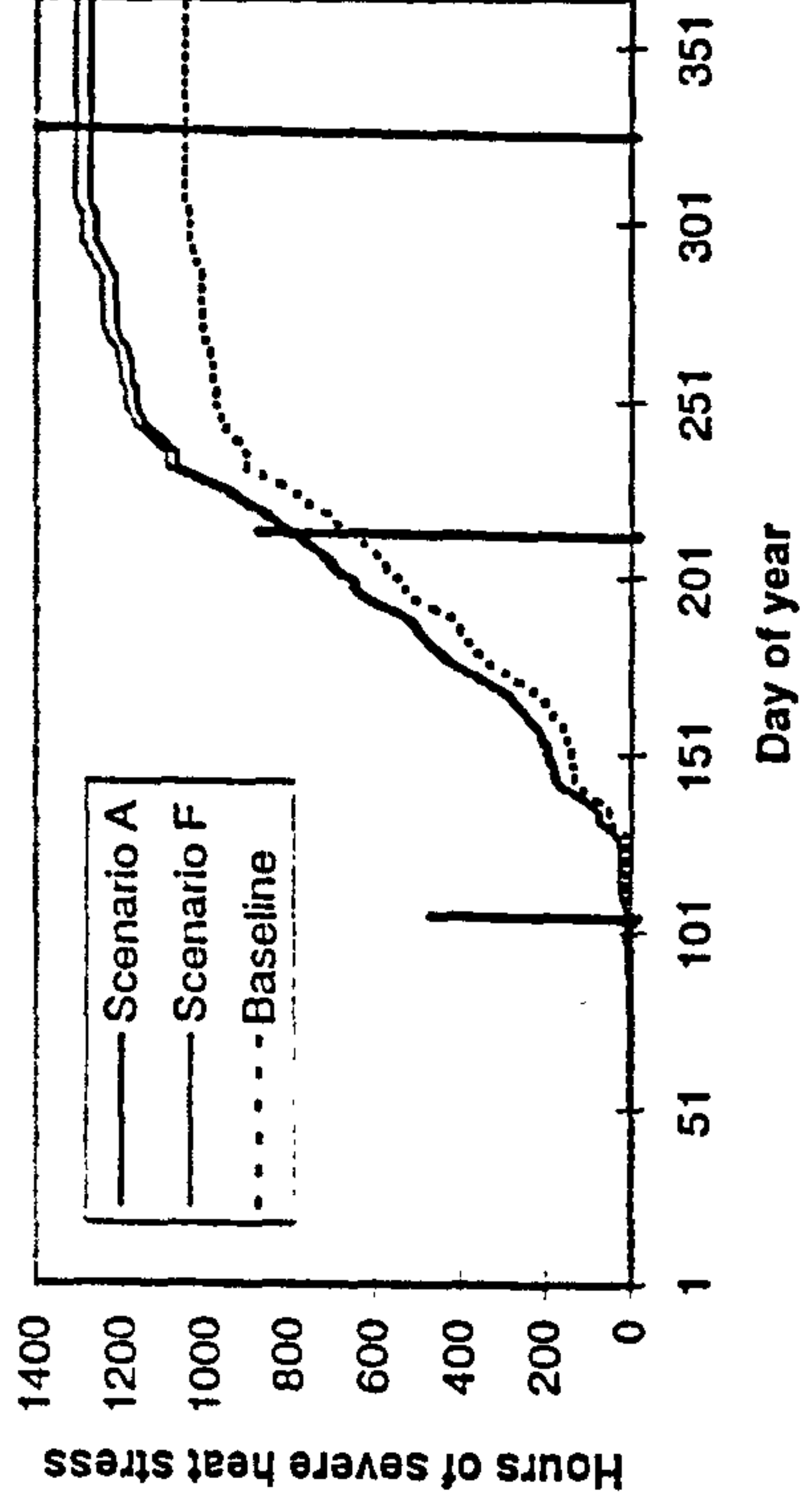
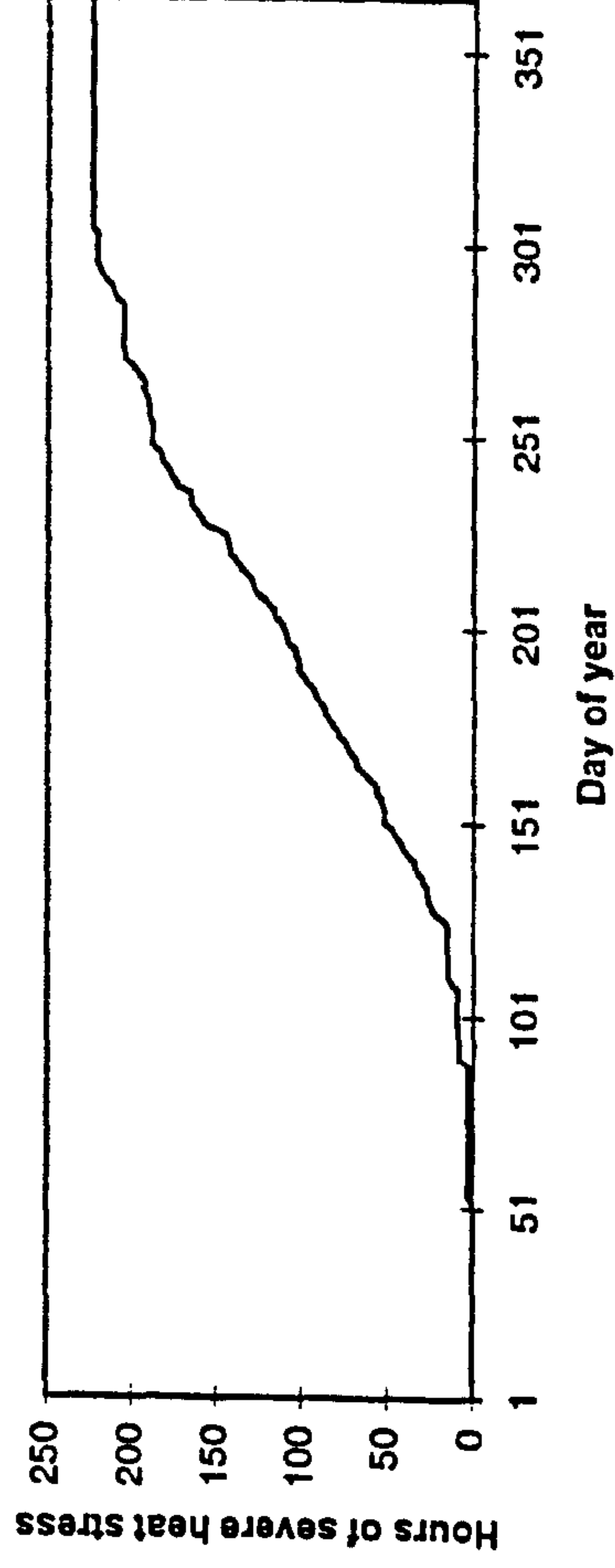


Fig 6.13: Cumulative HSHS: difference (Scenario A - Baseline), Pig, Year 3



on day 321. The first pig of the year has very little problem with heat stress either now or under climate change, but the stress events start about 20 days earlier under climate change. However, climate change will increase the duration of stress during the day. The gradient of the line in Fig 6.13 gives the mean number of extra hours of heat stress under climate change. From about Day 125 to Day 240 (beginning of May to end of August) there is an almost constant difference in HSHS per day: about 1 - 1.5 hours per day extra under climate change. Between Day 240 and Day 300 (to the end of October) the increase is about 0.75 hours per day and from Day 50 to Day 125 (mid February to early May) the increase is approximately 0.25 hours per day. The difference between scenarios (about 35 hours in the chosen year) is relatively small compared with the difference from the baseline (about 230 hours in the chosen year), but larger than for the outdoor species. The effect of the rapidly changing size of the animal (especially when the new animals replace the old) is not obvious. After the second pig starts its finishing period around day 100, the increase in heat stress indicated in Fig 6.12 is small for the first 30 days or so, but this may be purely due to the weather. The third pig experiences more heat stress in the first 30 days than the last 70 days, linked to the cooling weather in autumn, and maybe also to the lack of behavioural adaptation in the model (Chapter 4). A group of live pigs will huddle and separate to regulate their heat balance, so the heat stress predicted for the summer is probably an overestimate.

6.3.5 Broiler chicken

The broiler model was run with 10 000 birds in a house with floor area 480 m² at Boxworth, and the predictions are shown in Figs 6.14 - 6.15. Fig 6.14 shows the 30 year totals of HSHS. The mean totals over the 30 year period are 1590 and 1730 hours per year for current and Scenario A conditions respectively, with standard deviations of about 100 hours. The increase in stress duration under

Fig 6.14: Total hours of severe heat stress for chickens at Boxworth: baseline and three scenarios

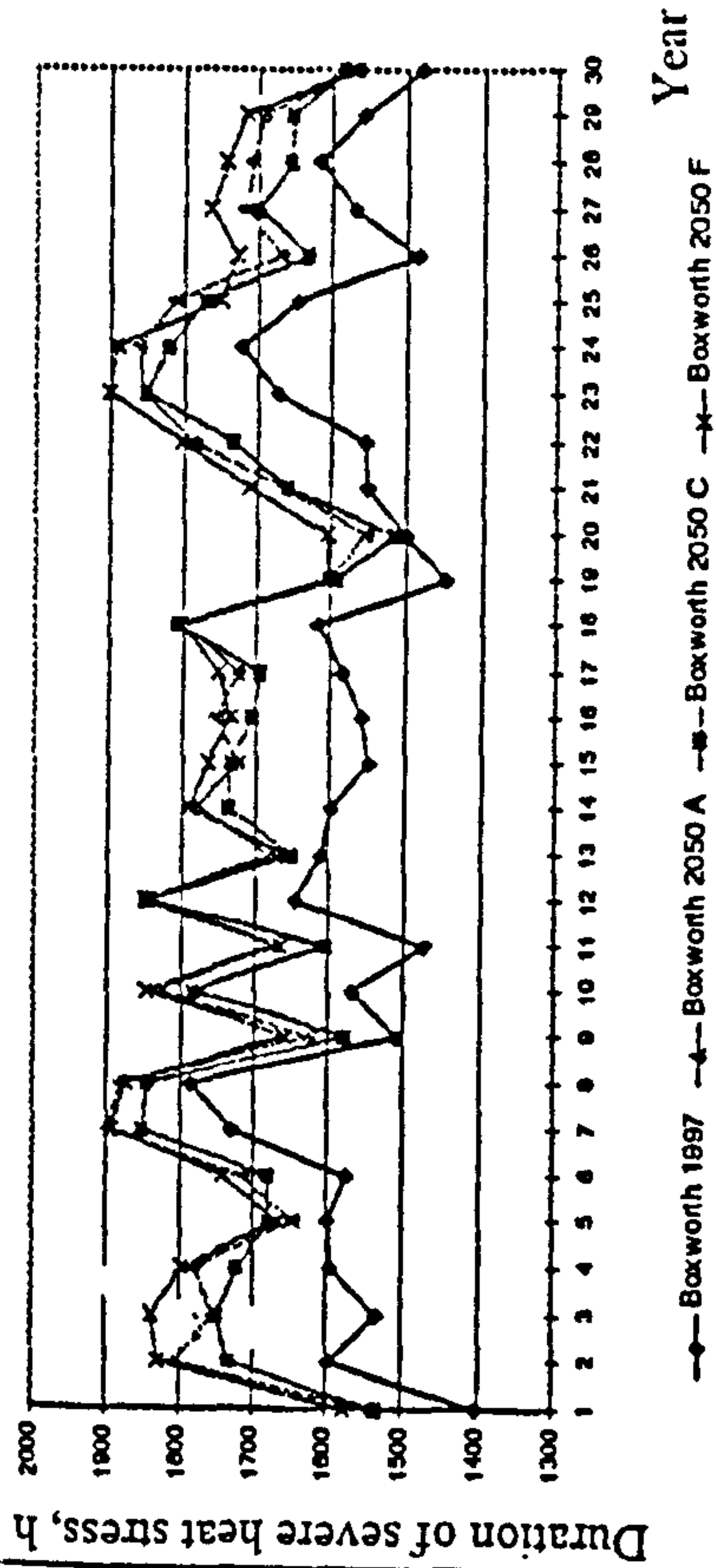
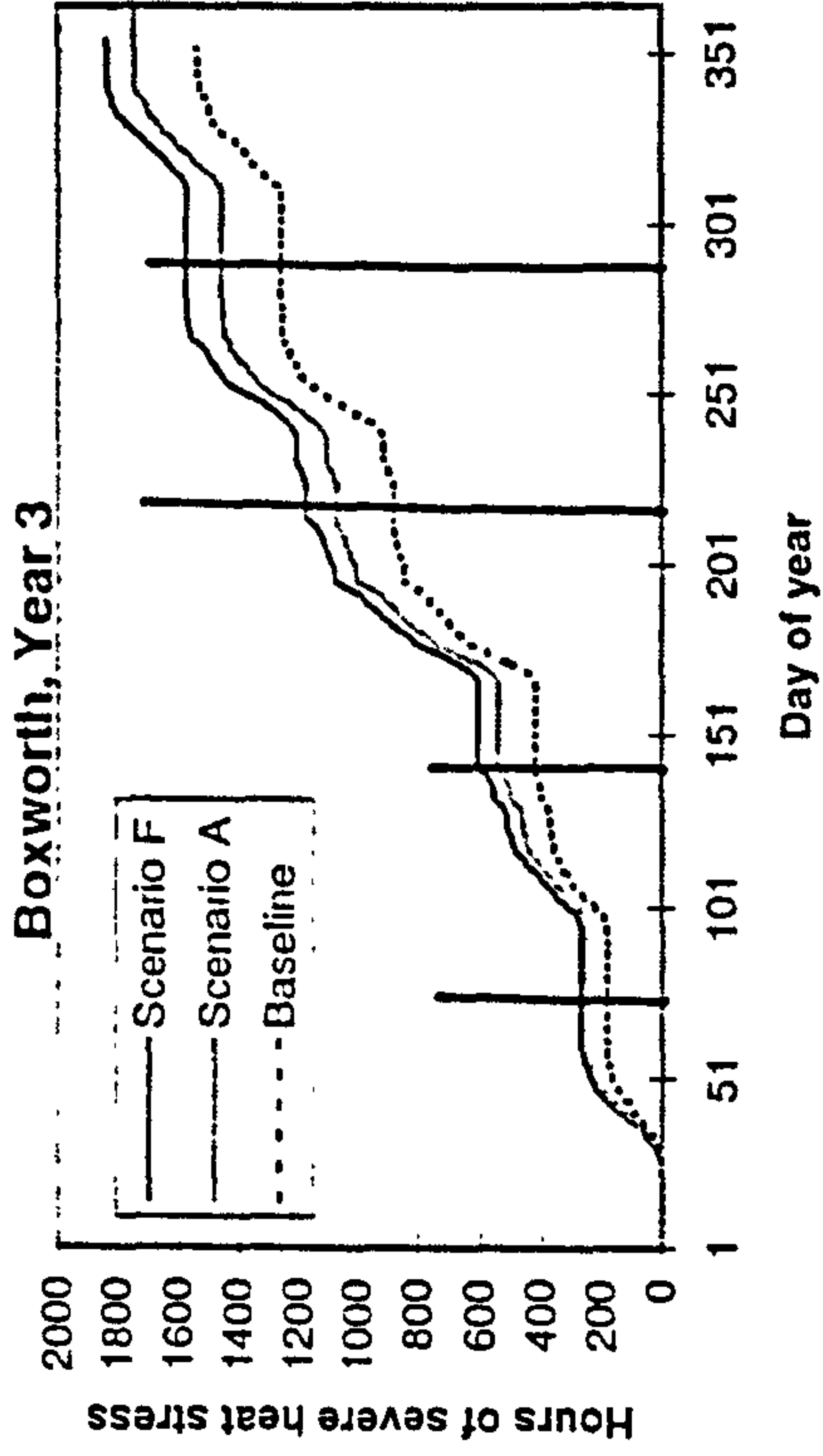


Fig 6.15: Cumulative HSHS for Chickens at Boxworth, Year 3



climate change is therefore less than 10%, and the inter-annual variability is high. In some years (eg year 20) there is no change between current and Scenario C conditions whereas in year 23 the difference is more than 150 hours. For the chicken, the annual totals imply less than for the other species considered, as there are five separate bird lives through the year (indicated by the vertical bars on Fig 6.15). The birds are slaughtered when they reach 3 kg in the current model, which gives a life of roughly 70 days. The cumulative total HSHS in the chosen year (3) is shown in Fig 6.15. The effect of bird age on thermal stress is obvious in the lack of stress experienced during the first 20 days of life (except in mid summer, when the fourth bird of the year experiences around 20 hours of stress in the first 20 days of life). New-born chicks are particularly susceptible to the cold (Chapter 4). There is a larger difference between scenarios than for the other animals: the final total for the year under Scenario F is 85 hours more than for Scenario A, which is nearly 40% of the difference between Scenario A and the current conditions.

6.3.6 Summer heat stress

The mean number of HSHS per day in summer was calculated for the pig and the chicken under current and projected conditions. Summer has two definitions: 'long', from May to October (183 days), and 'conventional', from June to August (91 days). The mean number of stress hours in each definition are presented in Table 6.2.

Table 6.2. Mean hours of severe heat stress per summer day (HSHS) for chicken and pig

ANIMAL	mean HSHS, long summer, baseline	mean HSHS, long summer, Scenario A	mean HSHS, conventional summer, baseline	mean HSHS, conventional summer, Scenario A

ANIMAL	mean HSHS, long summer, baseline	mean HSHS, long summer, Scenario A	mean HSHS, conventional summer, baseline	mean HSHS, conventional summer, Scenario A
CHICKEN	4.9	5.5	5.7	6.5
PIG	5.6	6.8	8.9	10.4

The mean HSHS for chickens is predicted to rise by about 1 hour per day during conventional summer under climate change. The mean HSHS over the long summer in 2050 will be similar to the value in today's conventional summer, ie. heat stress normally restricted to days in June, July and August at the moment could be encountered earlier and later in the year under climate change. However, the patterns are complicated by the fact that the chicken's life is only 70 days; a newly hatched chick has a much better tolerance to heat (see Fig 6.15). The pig's finishing period is about 110 days, and so the number of hours over the summer when the pig is a heat-resistant young animal is less than the chicken; therefore, the number of hours of stress per day is correspondingly higher. Pigs are also less tolerant to heat than chickens and, unless they are provided with a wallow, HSHS could increase by about 1.5 hours per day over the conventional summer (Table 6.2). The total duration of stress would then be very high, and have significant impact on the animal's productivity and comfort. Note that the standard deviation on the above figures is about 6 hours per day due to variable values of HSHS (between zero and about 15) of HSHS and the spread of values driven by the weather data.

6.3.7 Economic impacts

Assessment of the economic impacts of the changes likely to occur to livestock systems in the UK under a changed climate is difficult. Variables such as the price of electricity to drive ventilation systems, or the price of wheat, vary on short timescales, and predicting their behaviour 50 years ahead with accuracy is virtually impossible. Other factors such as trade agreements (eg. GATT) will have much more influence, but again predicting the impact on agriculture is difficult. In the current system of models (Figs 6.17 - 6.19), variable costs such as the price of forage and milk were assumed constant, and the gross margin of the livestock production was calculated (Parsons et al, 1997a). Gross margin, GM, is defined as the surplus of total revenue over total variable costs (eg. grain) (Upton, 1976). Fig 6.17 shows the inter-annual variation of gross margin for dairy cattle under current (Scenario 1) and climate change conditions. Under climate change, the gross margin rises slightly under climate change, probably due to decreased forage intake and buffer use caused by heat stress. Dairy cattle are typical of all the outdoor animals, which show little change or a slight rise in GM under climate change. The increase in heat stress duration, therefore, has little effect on the economic viability of outdoor livestock systems, or on the suitability of the sites studied for livestock use in the future.

For indoor animals, the increased heat stress has a greater economic impact. In the pig, there will be a significant increase in stress, and a corresponding increase in energy used for ventilation under climate change (about 8%), but the food intake will also fall considerably due to increased heat stress. Since most pigs are fed only concentrate, this reduction in food represents a gain economically, and the resulting gross margin is almost identical for climate change as for current conditions (Fig 6.18). In contrast, Fig 6.19 shows a large decrease in gross margin for the chicken, forced by the poorer feed to meat conversion efficiency under hot conditions, and

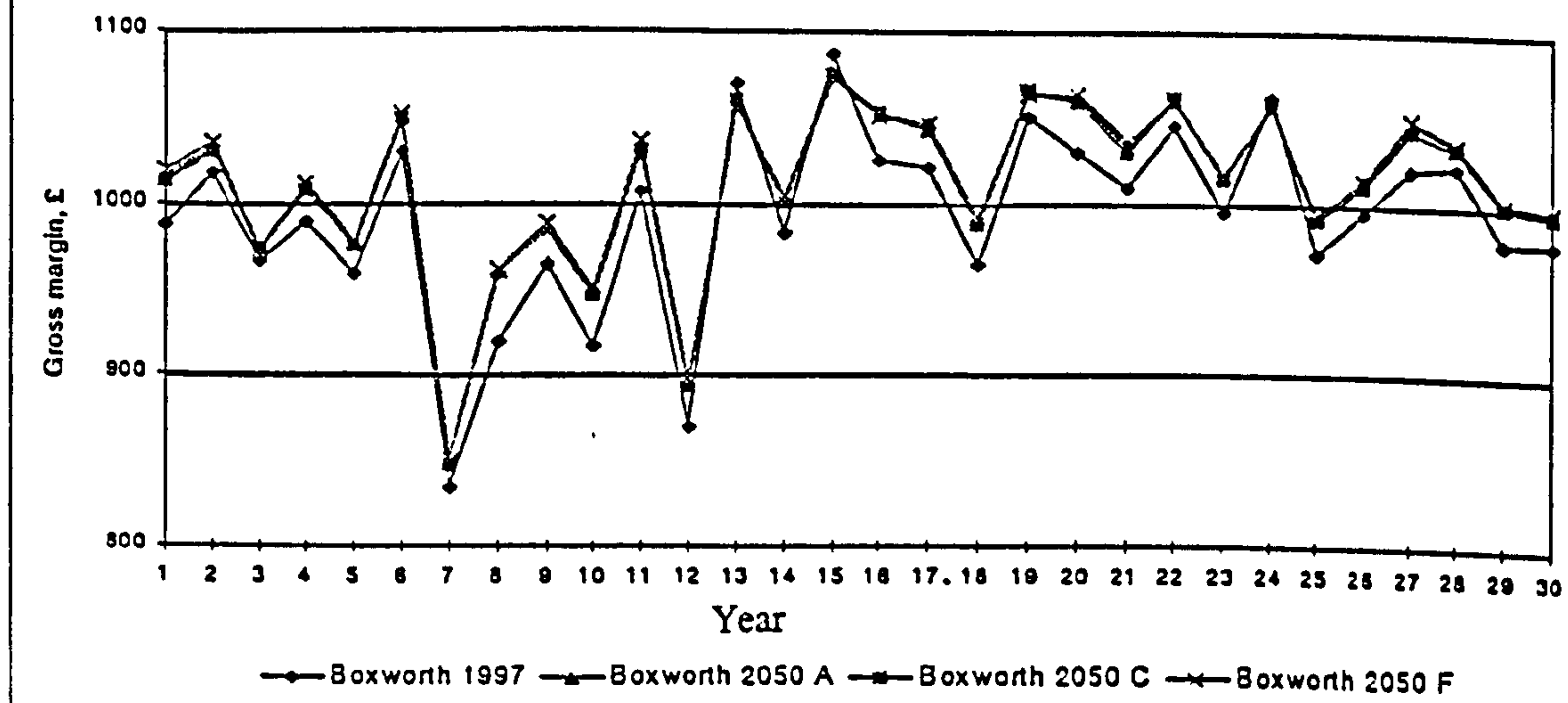


Fig 6.18: Gross margin of pig for 30-year run: baseline and climate change scenarios

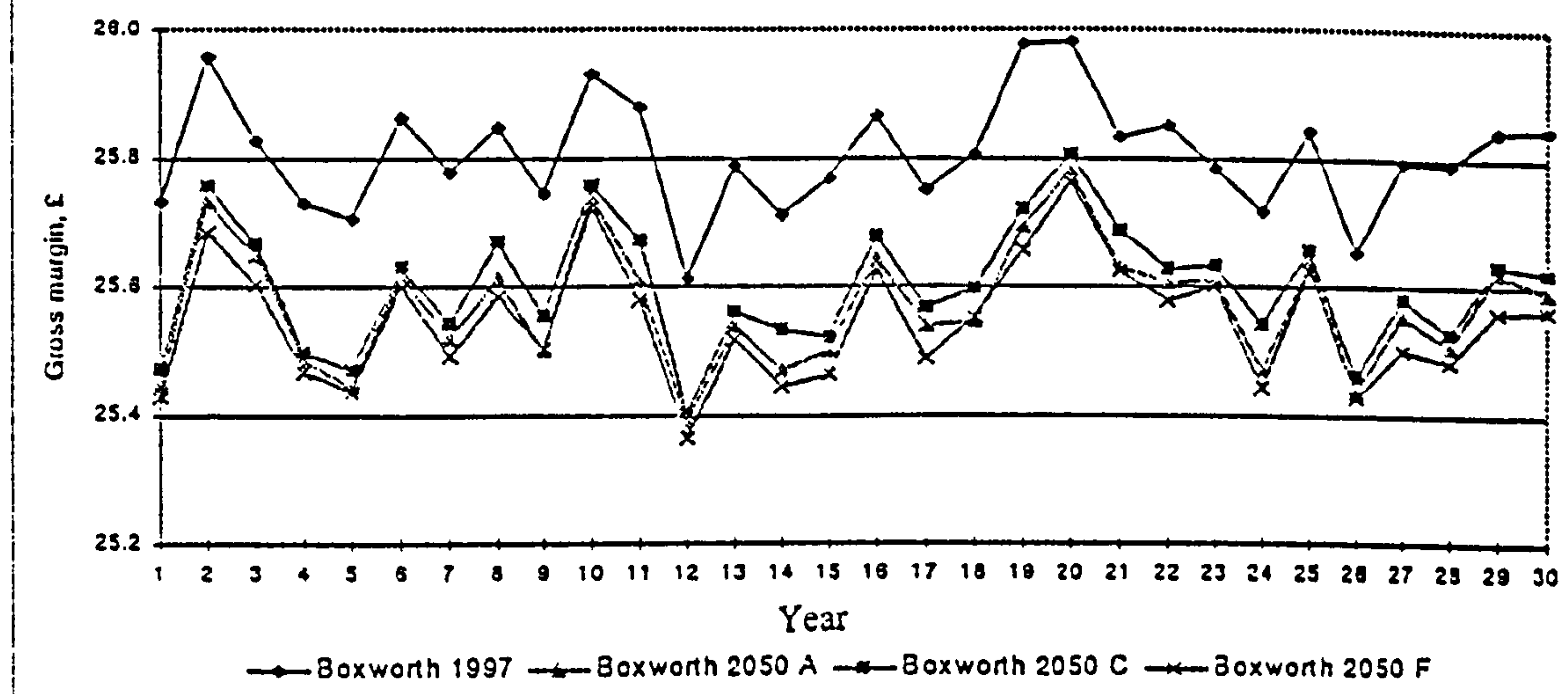
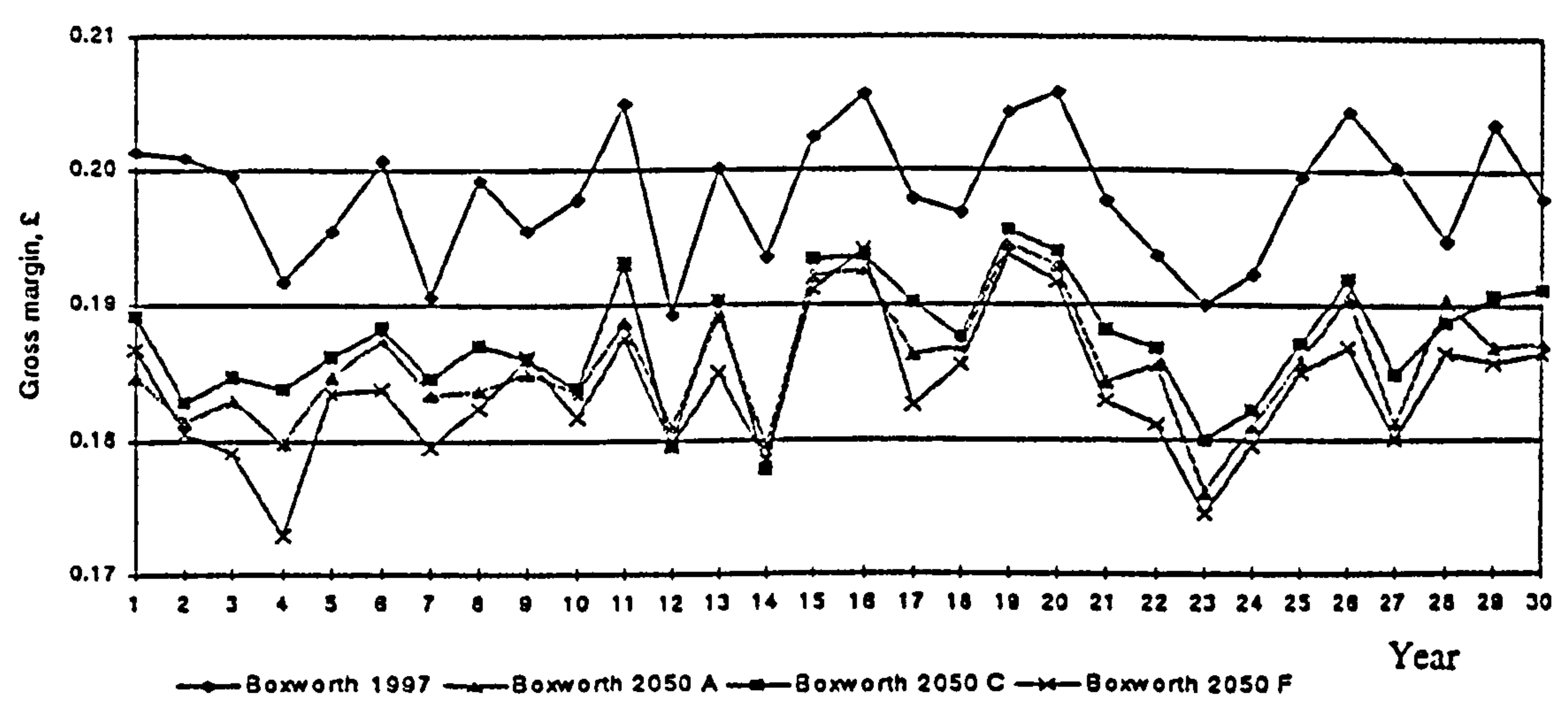


Fig 6.19: Gross margin of chicken for 30-year run: baseline and climate change scenarios



by the increase in fan energy of approximately 10 - 15% required to keep the animals from very high stress frequencies, and prevent significant mortality. Without further, or better designed, alleviation methods, the decrease in gross margin of up to 10% is significant, and represents a serious problem for poultry producers.

6.4 RESULTS: THERMAL BALANCE MODEL EXPERIMENTS

The thermal balance model was decoupled from the rest of the suite (apart from the input of growth over time) and fixed metabolic rates were assumed. The purpose was to test the performance of the model alone, and to examine the effects of feed intake on duration of stress. In the previous sections, high HSHS were predicted by the model even for current conditions, due probably to high metabolic rates. Pigs and chickens were chosen for attention given the possible impact of climate change on their economic performance given in the previous section. The metabolic rates of these animals on a maintenance, and multiples of maintenance, feed intake were calculated using data from the literature and Eq 1.3. This equation provides an approximate relationship between metabolisable energy intake and metabolic rate (Chapter 1). For pigs, Close & Mount (1978) gave metabolisable energy for maintenance, M_m as $\approx 77 \text{ W m}^{-2}$; therefore metabolic rate for n times maintenance feed intake (denoted as nM_m) was calculated from Eq 1.3 and is given by:

$$nM_m = 77 + 0.3 (77n - 77) \quad [\text{Eq 6.1}]$$

In the current model experiment, the animals were assumed to be fed at twice ($2M_m$) and four times ($4M_m$) maintenance to represent low and high growth rates. For pigs, the corresponding metabolic rates are 100 and 146 W m^{-2} respectively.

For comparison, the nutrition model (Parsons et al, 1997a) produced heat productions approximately 2.5 to 3 times maintenance. For broilers, the maintenance energy is about 60 W m^{-2} (from data by MacLeod, 1990 and Gates et al, 1996). The same calculation as for pigs yields metabolic rates of 78 and 114 W m^{-2} for twice and four times maintenance feed intake respectively.

The results for pigs are shown in Figs 6.20 and 6.21. Pigs at twice maintenance are relatively comfortable, with less than 400 hours of severe heat stress per year under current conditions. The main period of stress occurs from the beginning of July to early September. Under climate change, the period of stress starts earlier, in approximately mid-June. The mean daily stress duration seen today through the height of summer (the gradient on Fig 6.20) continues well into October under climate change. However, the total number of hours is relatively manageable. Pigs fed at four times maintenance (Fig 6.21) have about five times the total HSHS of the twice maintenance pigs, even under current conditions. There is less difference (relatively) between current and climate change conditions at this feed level. Heat stress problems start at the end of March and continue through October, with about 13 hours a day of potential stress over the summer.

The results for chickens are shown in Figs 6.22 and 6.23. Fig 6.22 shows the running total of significant *cold* stress events for birds fed at twice maintenance, as at such a low feed level less than ten severe heat stress events were predicted for the year. Cold stress is a problem in the first twenty days of life, before the feathers are fully developed, but the duration of cold stress approximately halves with each successive flock reared. Cold stress in the first twenty days of life is predicted even under climate change, especially in winter when climate change has little effect. However, in the spring and autumn the number of cold stress hours is reduced under climate change, by about 20% for each bird life. Increasing the feed intake to four times maintenance produces a very large increase in severe heat stress events (Fig 6.23). The graph indicates that birds will be reasonably comfortable for the

Fig 6.20: Cumulative HSHS for a Pig fed at twice maintenance

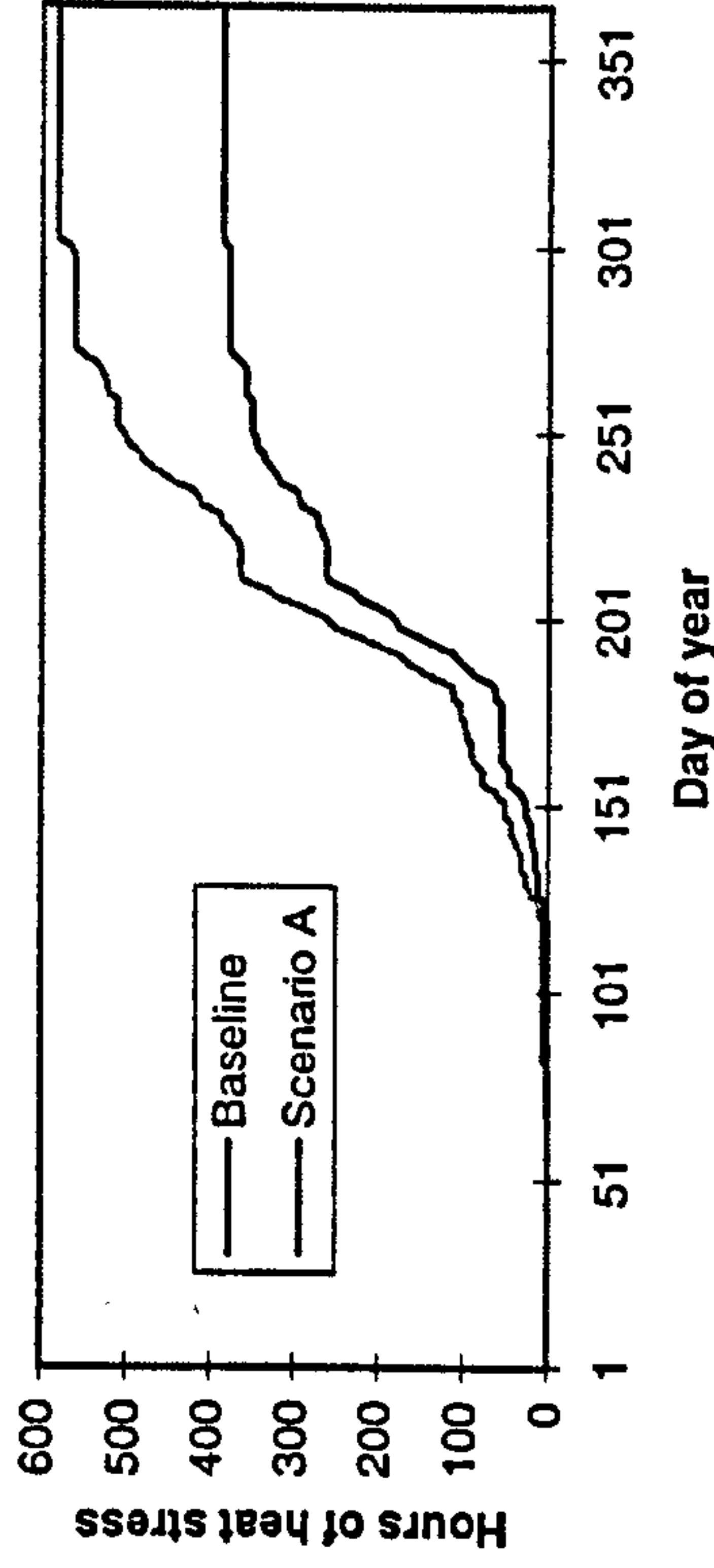


Fig 6.21: Cumulative HSHS for a PIG fed at four times maintenance

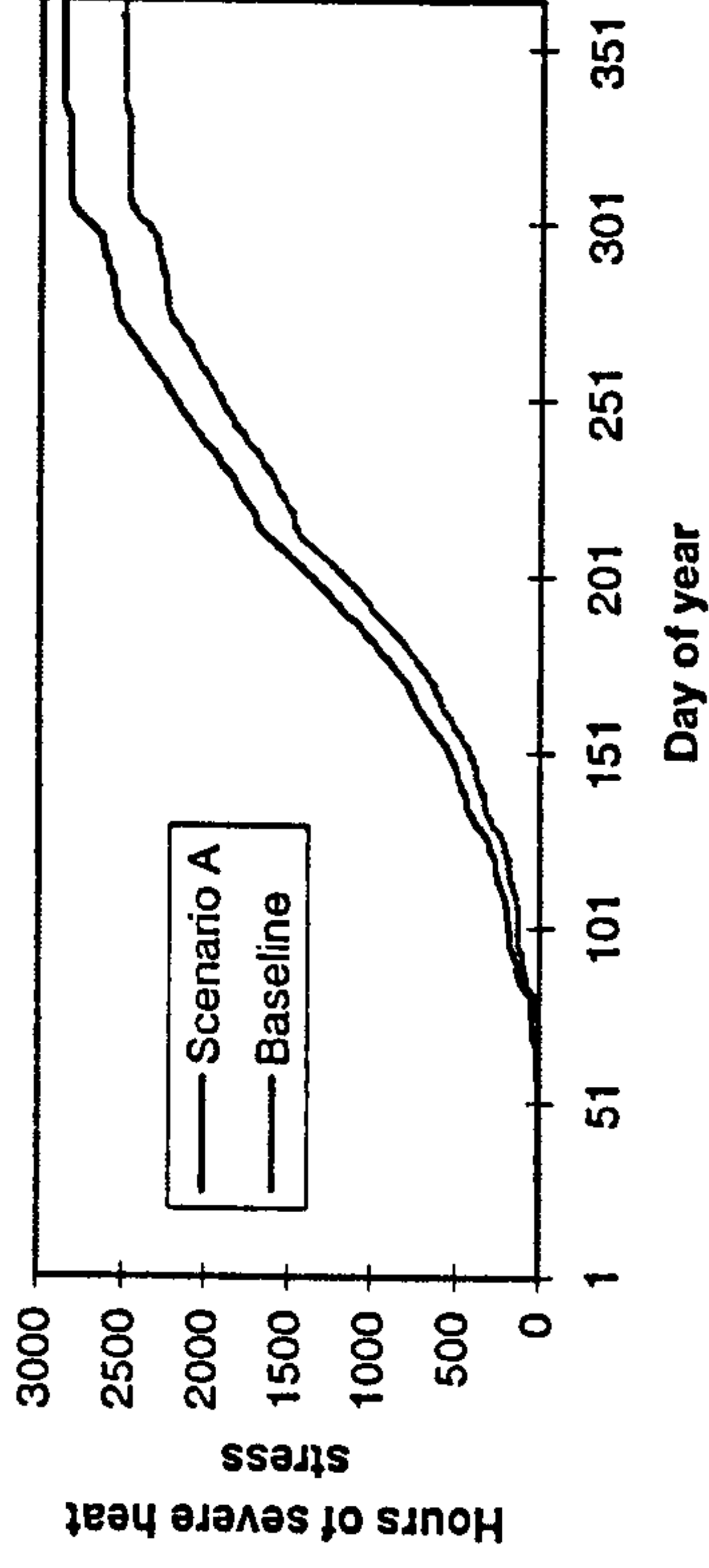


Fig 6.22: Cumulative hours of significant cold stress for a Chicken fed at twice maintenance

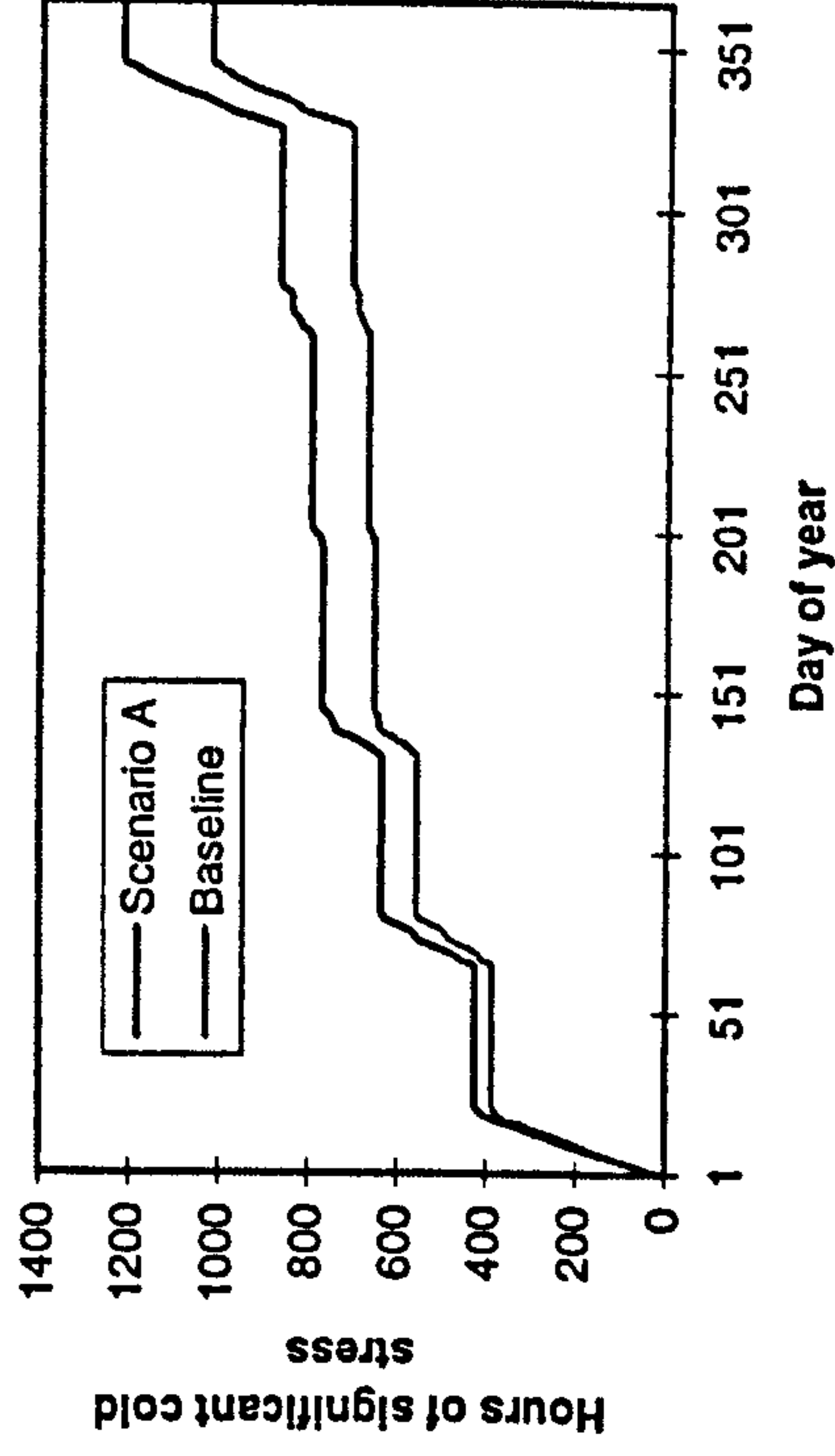
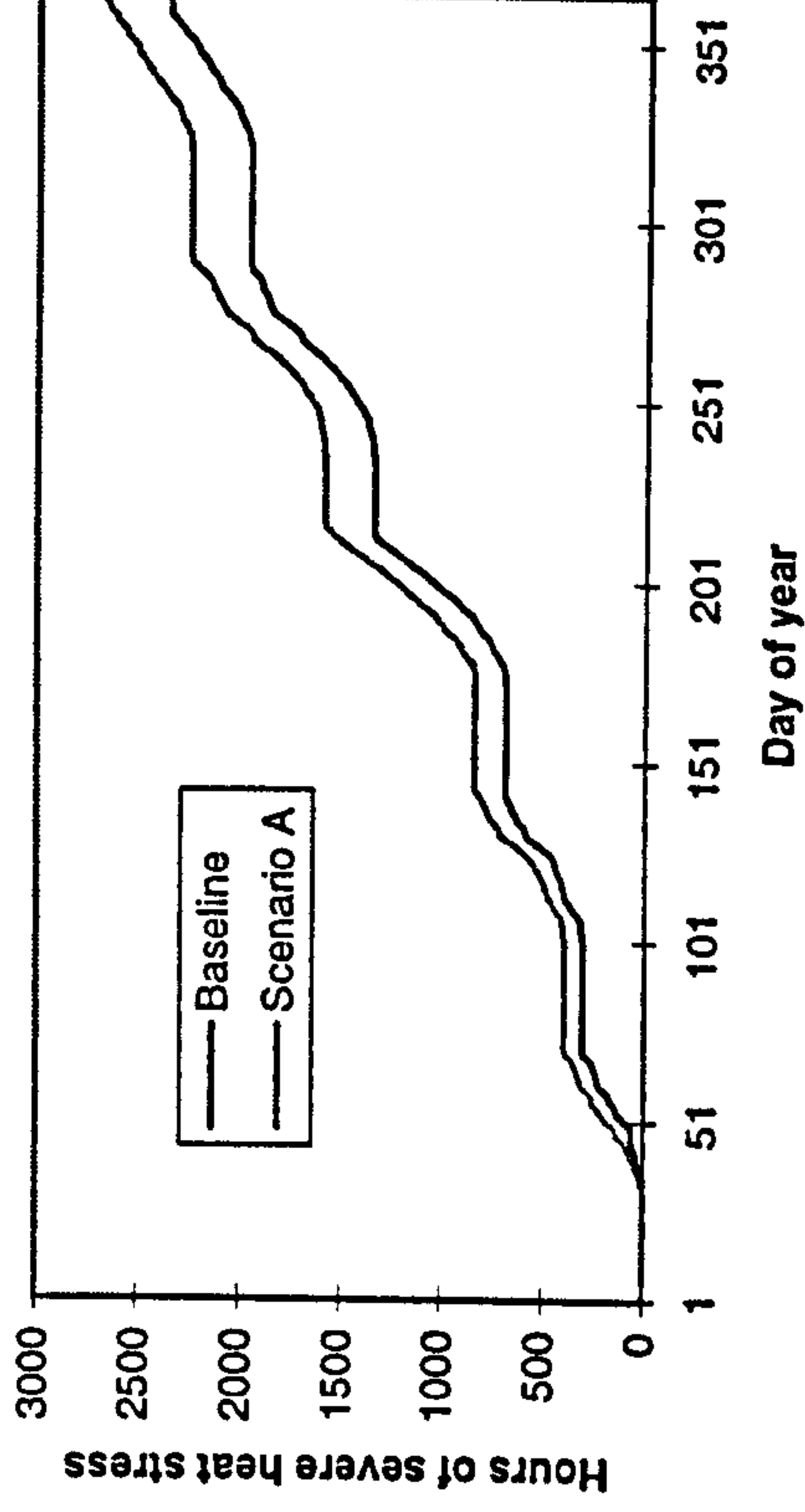


Fig 6.23: Cumulative HSHS for a Chicken fed at four times maintenance



first twenty days of life, but heat stress will be a problem at all times of year. The conclusion is that the thermal comfort, and hence productivity, of the birds is highly sensitive to the feed intake.

6.5 SENSITIVITY ANALYSIS

The sensitivity analysis for a model tests how sensitive the outputs are to changes in the input variables (see Chapter 5). The standard method of keeping all inputs constant and varying one at a time was adopted in the current model, as the large number of inputs make analysis of the system extremely complicated when more than one input is varied at once. The output for the thermal balance models is the total heat loss, or the thermal stress level. Assessing the impact of a change in each input on variables indicative of thermal stress (eg. respiration rate, body temperature) is a useful analysis. The main part of the sensitivity analysis used the unicorn model, with increased respiration rate taken as the main mechanism of enhanced evaporative heat loss; effectively this was the sheep model. The sheep model illustrates the general characteristics of the thermal balance model, but special considerations for other animals were included (eg. effects of ambient humidity on body temperature in chickens and sweat rate in cattle).

The first step in the sensitivity analysis was to define the 'default' conditions; these are the values that all the inputs would have unless they were being tested. The inputs were divided into two broad categories: Weather and Animal inputs. The Weather inputs, and default values, were as follows:

Day of year = 180

Time = 12 noon

$T_a = 20^{\circ}\text{C}$

$S_b = 600 \text{ W m}^{-2}$

$$S_d = 150 \text{ W m}^{-2}$$

$$T_{\text{sky}} = 7^\circ\text{C}$$

$$T_g = 27^\circ\text{C}$$

$$e_a = 1000 \text{ Pa}$$

$$u = 4 \text{ m s}^{-1}$$

$$\text{rain in past hour} = 0.5 \text{ mm}$$

ie. noon on a typical summer day.

The Animal inputs (eg. tissue resistances, body temperature) were taken as for the sheep (Appendix A), with the following additional values:

$$M = 70 \text{ W m}^{-2}$$

$$\text{mass} = 50 \text{ kg}$$

$$\text{coat length} = 20 \text{ mm}$$

Chapters 2, 3 and 4 have illustrated the effects of air temperature and solar radiation on the energy balance of the animals. In this section, the sensitivity to other inputs is quantified. Since there are many inputs, only selected sensitivities are presented here, generally those variables whose sensitivity has most significance.

Sensitivity to weather inputs - general model

Fig 6.24 shows the effect of increasing the ambient vapour pressure from 300 to 2100 Pa at $T_a = 20^\circ\text{C}$, ie. increasing relative humidity from 13 to 90%. The animal is in strong sunlight, and panting considerably ($\approx 200 \text{ min}^{-1}$) even at 300 Pa, though the stress is not severe. The stress level, indicated by the respiration rate, increases non-linearly with vapour pressure, which is expected since respiration rate

Fig 6.24: Sensitivity of predicted respiration rate to vapour pressure

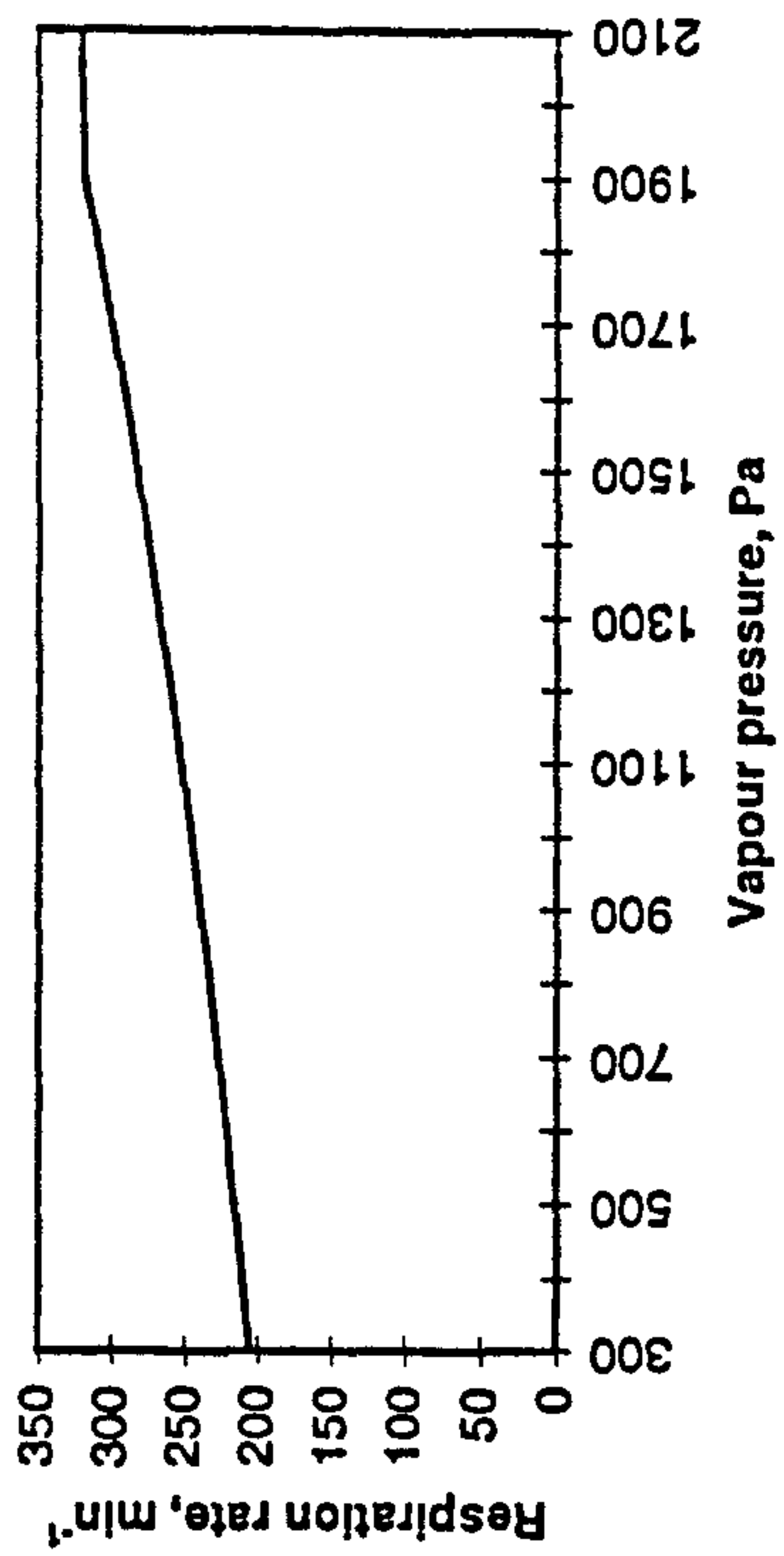


Fig 6.25: Sensitivity of predicted respiration rate to wind speed

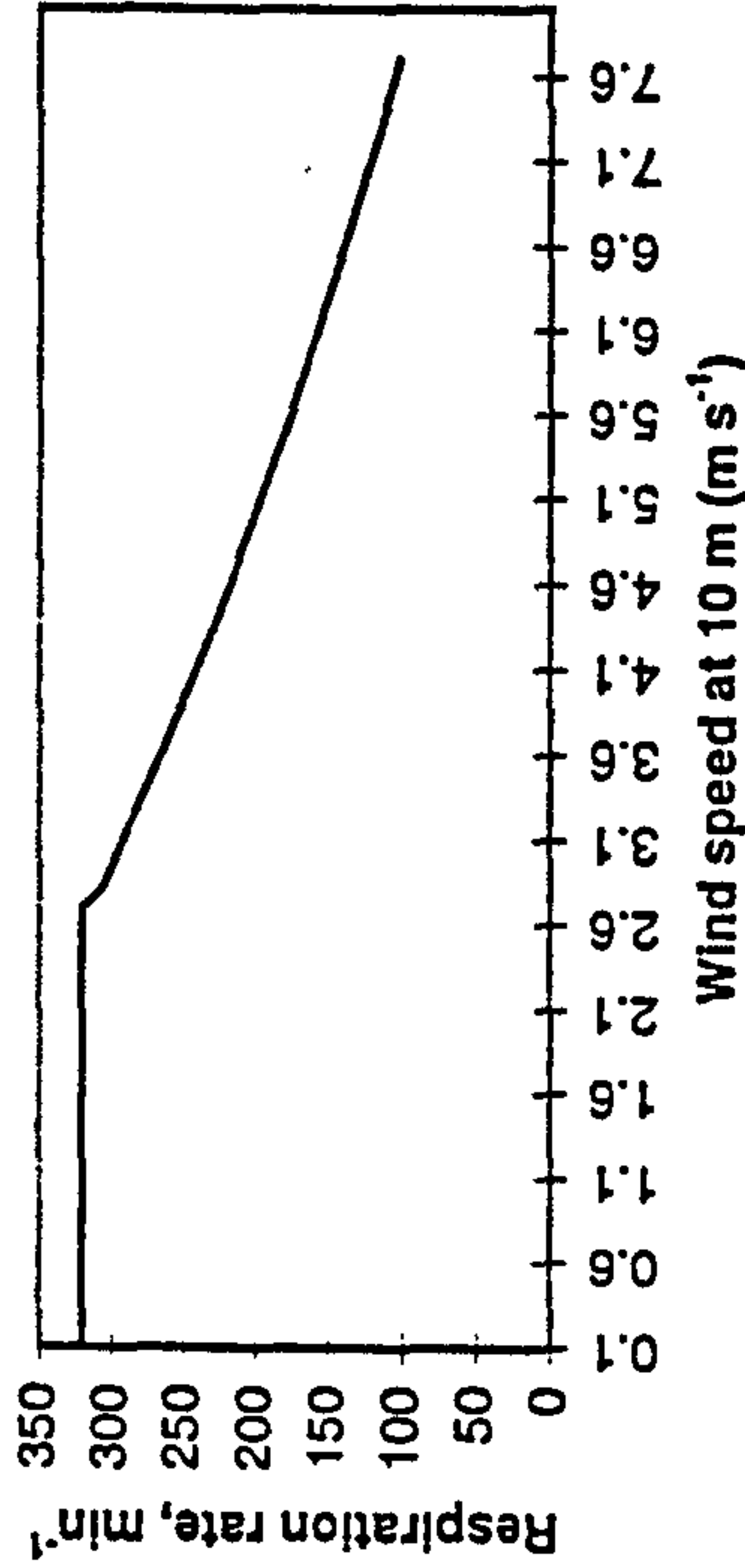
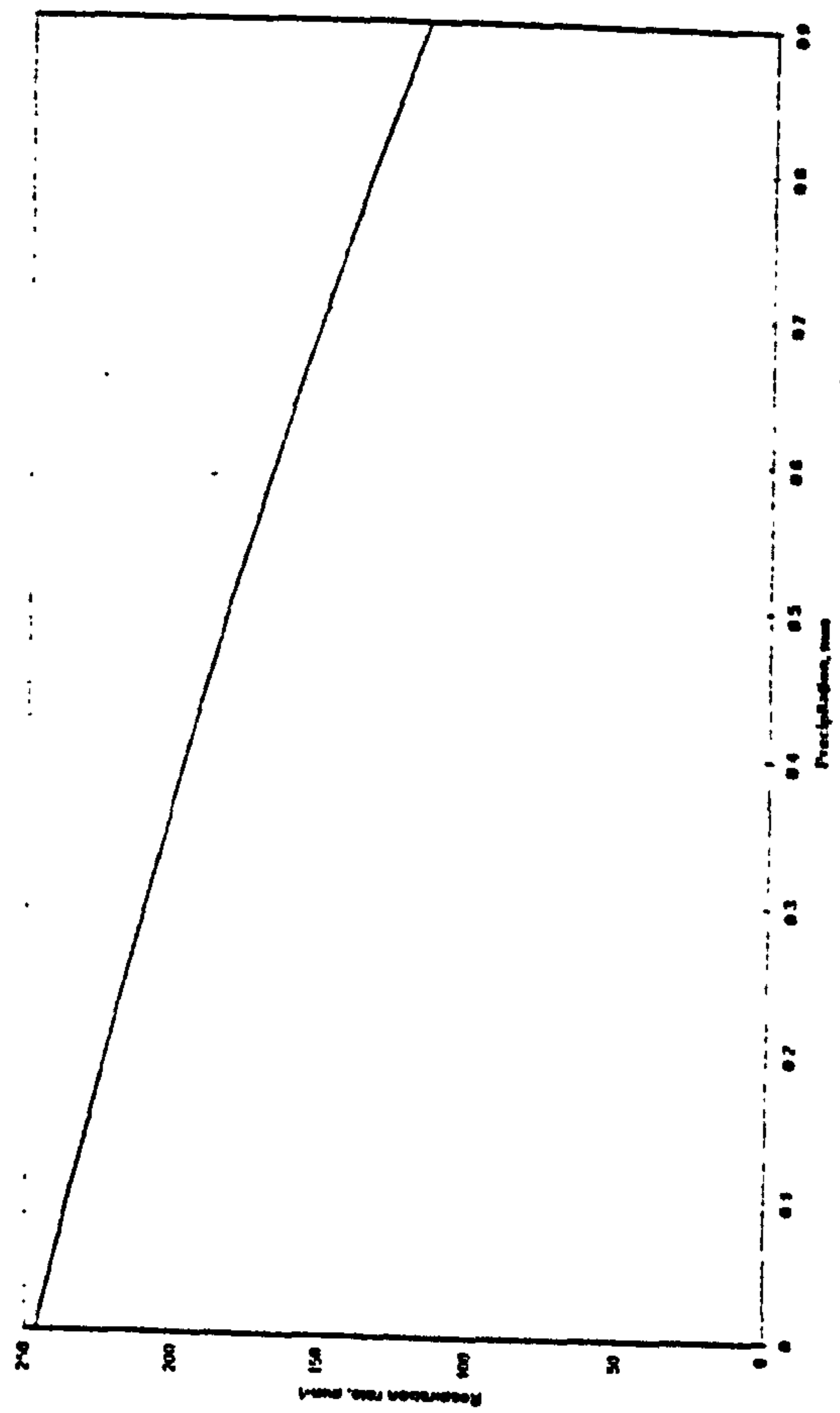


Fig 6.26: Sensitivity of respiration rate to rain amount



is inversely proportional to the vapour pressure difference (Section 3a.5.2). At about 1900 Pa the animal will enter second-phase panting (severe heat stress).

Fig 6.25 is a plot of respiration rate against wind speed at 10 m above the ground. Below about 3 m s^{-1} (which corresponds to about 1 m s^{-1} at animal height) the model predicts second phase panting, indicated by the flat portion on the graph. As wind speed increases, the respiration rate falls non-linearly to a safe 100 min^{-1} at about 8 m s^{-1} . Due to the non-linearity of the dependence of thermal resistances on wind speed, a unit increase in speed at low winds has much more of a cooling effect than the same increase at high wind speed.

The effects of coat wetness were illustrated in Section 2.10.4.1, and Fig 6.26 shows how increasing amounts of rainfall reduce the respiration rate of an animal. The relationship between respiration rate and rainfall is almost linear at about 150 min^{-1} per mm of rain. Above 1 mm of rain, it was assumed that the coat was fully wet, and any further increase in rainfall rate had no effect on the thermal balance. The effects of rain illustrated in Fig 6.26 are probably underestimated, since the solar load stays constant for all precipitation values. In reality, of course, the solar load will be greatly reduced when precipitation is high, increasing the cold stress.

Sensitivity to weather inputs - special considerations

Fig 6.27 shows the body temperature of the chicken plotted as a function of vapour pressure, for two air temperatures: 20 and 30°C . The model was run for chicken parameters (see Chapter 4), and for a bird in a building (ie. solar radiation = 0). The animal was a mature (2 kg) broiler, with a heat production of 110 W m^{-2} . At $T_a = 30^\circ\text{C}$, body temperature rises at approximately 0.05°C per 100 Pa vapour pressure rise. This means that a 40% rise in relative humidity will cause a 1°C rise in body temperature. At 20°C , the gradient is less, with body temperature rising at

Fig 6.27: Sensitivity of body temperature of chicken to changing vapour pressure for two air temperatures

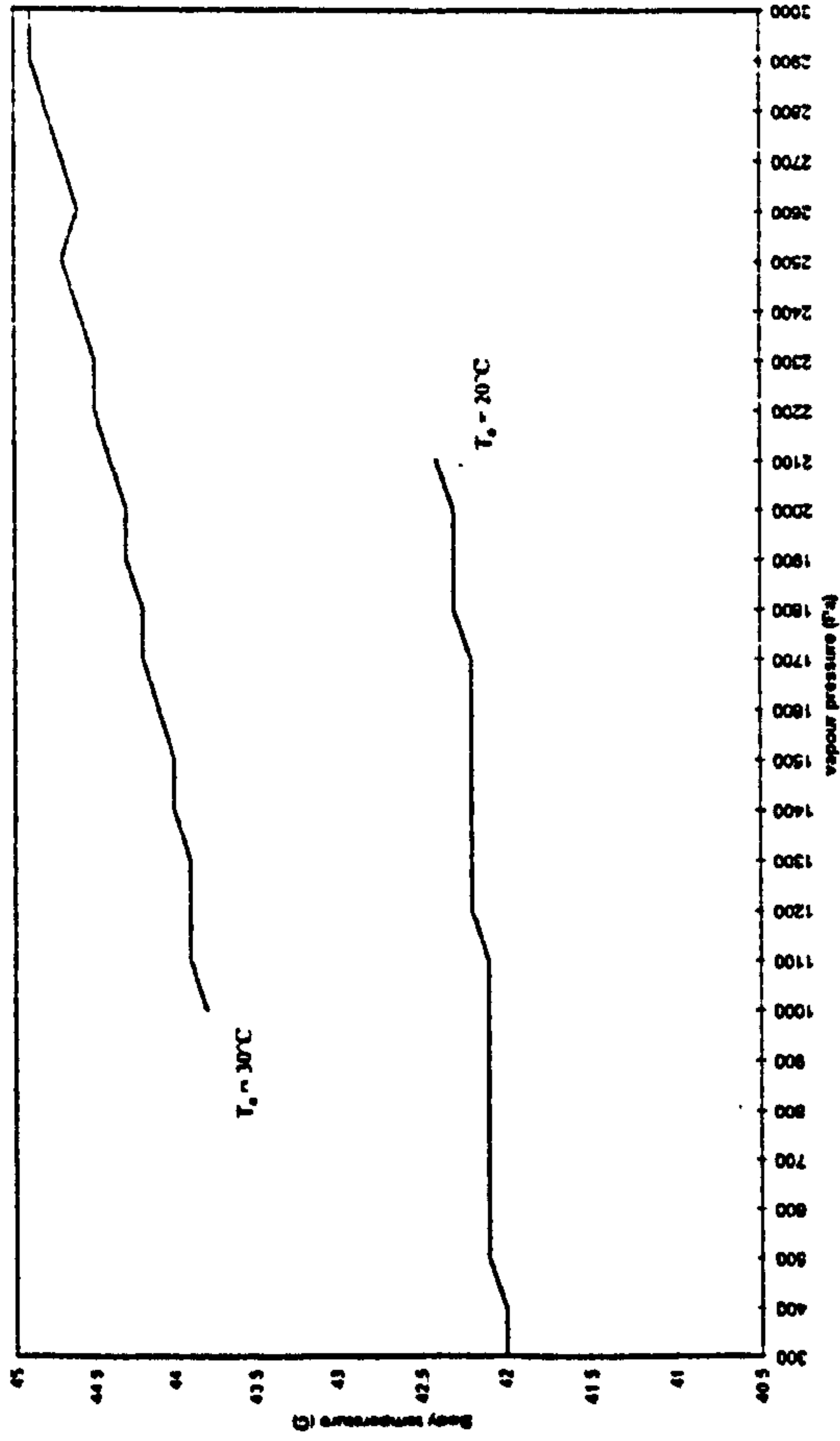


Fig 6.28: Sensitivity of predicted sensible heat loss to coat length

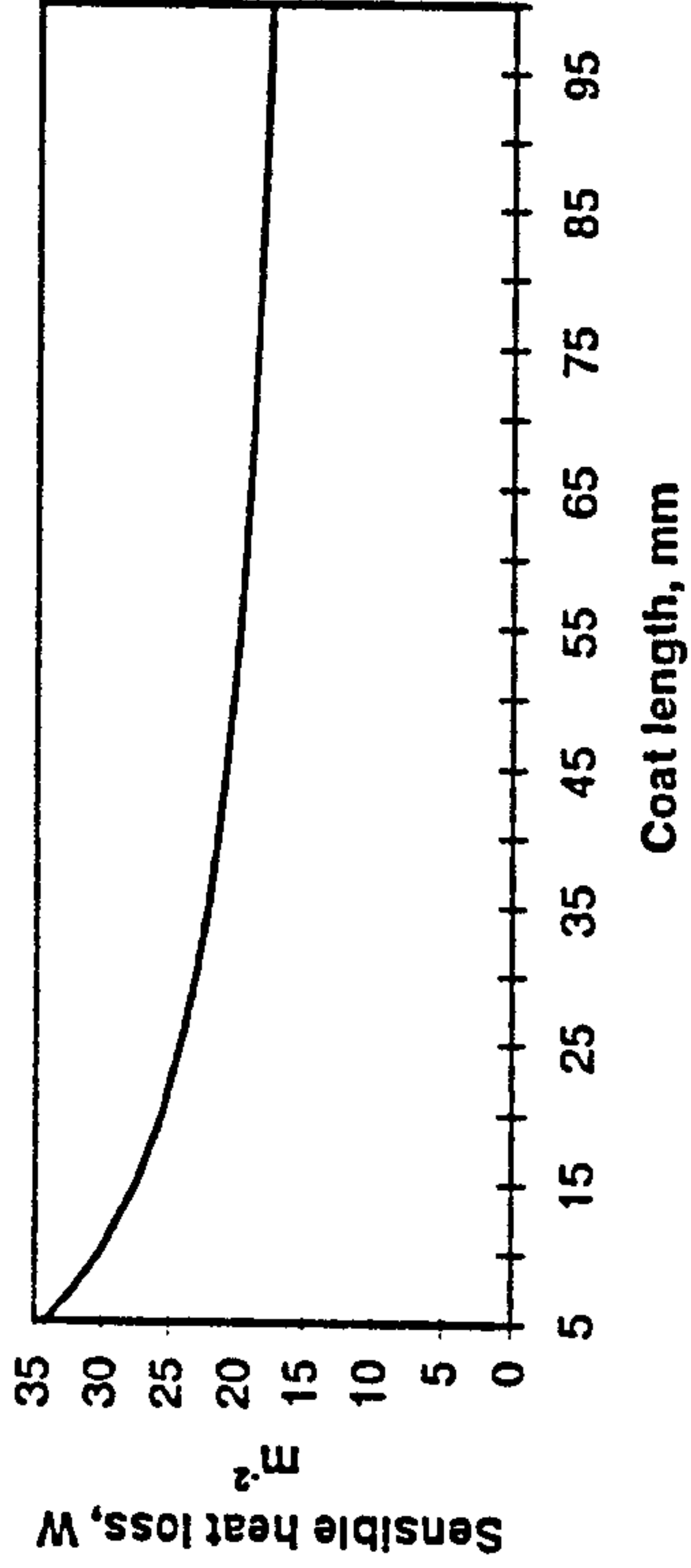
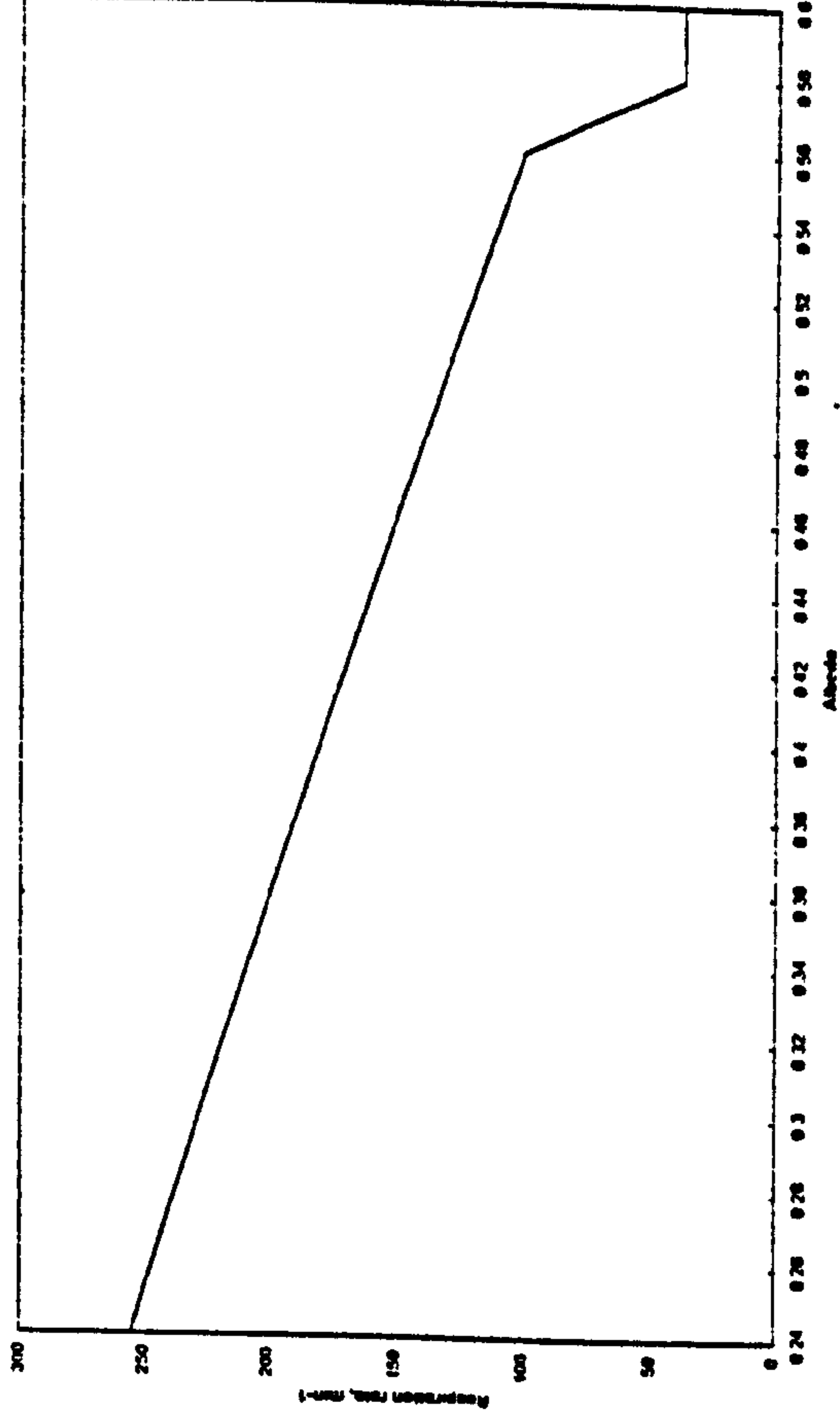


Fig 6.29 Sensitivity of predicted respiration rate to coat reflectivity



about 0.02°C per 100 Pa. Fig 6.27 shows the increased importance of humidity at higher temperatures.

The effect of humidity on the sweating response of cattle was also tested. A 500 kg dairy cow with a metabolic rate of 170 W m⁻² was modelled, with the baseline environmental conditions the same as for the general model sensitivity analysis. At 20°C, the vapour pressure was increased from 300 to 2100 Pa. Over this range, the maximum (theoretical) evaporation rate, based on the vapour pressure difference between animal and environment (Section 2.4.2) was higher than the physiological maximum sweat rate, which is limited by water availability. The evaporation rate was therefore limited by water supply rather than environmental conditions under the conditions tested. In contrast, at 30°C the humidity is predicted to have a significant effect on the thermal state of the cow. The vapour pressure was varied from 1000 to 3000 Pa, and over the upper part of this range the theoretical maximum evaporation rate was below the physiological maximum sweat rate. For example, at 1000 Pa (24% relative humidity) the evaporation rate was 63% of the maximum, giving significant heat stress. Severe heat stress began when the humidity reached 57% ($e_a = 2400$ Pa) and the evaporation rate reached the maximum. Again, the effects of humidity are seen to be greatest at high temperatures.

Sensitivity to other inputs - general model

The general model was run with the default conditions above to test its sensitivity to the other input variables. Fig 6.28 shows the effect of coat length on the sensible heat loss from the model animal. As indicated in Section 3a.6.2, unit changes in length have more impact on sensible heat loss when the coat is short, due to the inverse relationship between insulation and coat thickness. Fig 6.28 confirms the earlier observations. Increasing the coat length 1.5-fold from 40 to 100 mm

(approximately the fleece growth of a sheep from September to shearing) reduces sensible heat loss by only 15%; by autumn, the animals have almost all their insulation for the winter. At low coat lengths the model is sensitive to length. For example, a 5 mm error in an estimation of the coat length can give a 15% error in the predicted sensible heat loss when a sheep has just been sheared.

Fig 6.29 is a graph of the respiration rate as a function of coat albedo. The range of albedo covered represents the range for sheep in the field. The albedo of clean white wool is about 0.6 (Monteith & Unsworth, 1990) but dirty wool has an albedo nearer 0.25 (Stafford Smith et al, 1985). Increasing the albedo of the coat gives a linear decrease in the solar load absorbed, which results in a linear decrease in respiration rate. Dirty sheep may suffer significant heat stress at 20°C standing in the sun, while very clean sheep may be in their cold zone. The step in respiration rate at albedo = 0.56 in Fig 6.29 is due to the onset of vasoconstriction in the extremities.

Animals outdoors may alter their orientation to the sun to maximise or minimise their interception of solar radiation to aid their heat balance (Section 3.3.1). The effect of orientation varies with the angle of elevation of the sun due to the complex geometry, and an example of this effect is shown in Fig 6.30. The 'Summer' day line was modelled using the same conditions as above (Day 180, noon) which gives a solar elevation of about 60°. The 'Winter' conditions used were 31 January at noon (solar elevation about 20°), with clear skies and a typical direct solar radiation on a horizontal surface of 200 W m⁻² and diffuse solar radiation of 40 W m⁻² (Gannon, 1996). Fig 6.30 shows the solar radiation flux absorbed per unit animal surface area. At high elevations orientation makes little difference to the average load on the body. The behaviour of standing tail-on to the sun is probably to minimise local heating of the head. At low elevations, orientation is a significant factor, and the solar load can be increased by about a third (50 W m⁻²) by standing

Fig 6.30: Sensitivity of absorbed solar load to changing orientation to the beam: low and high sun

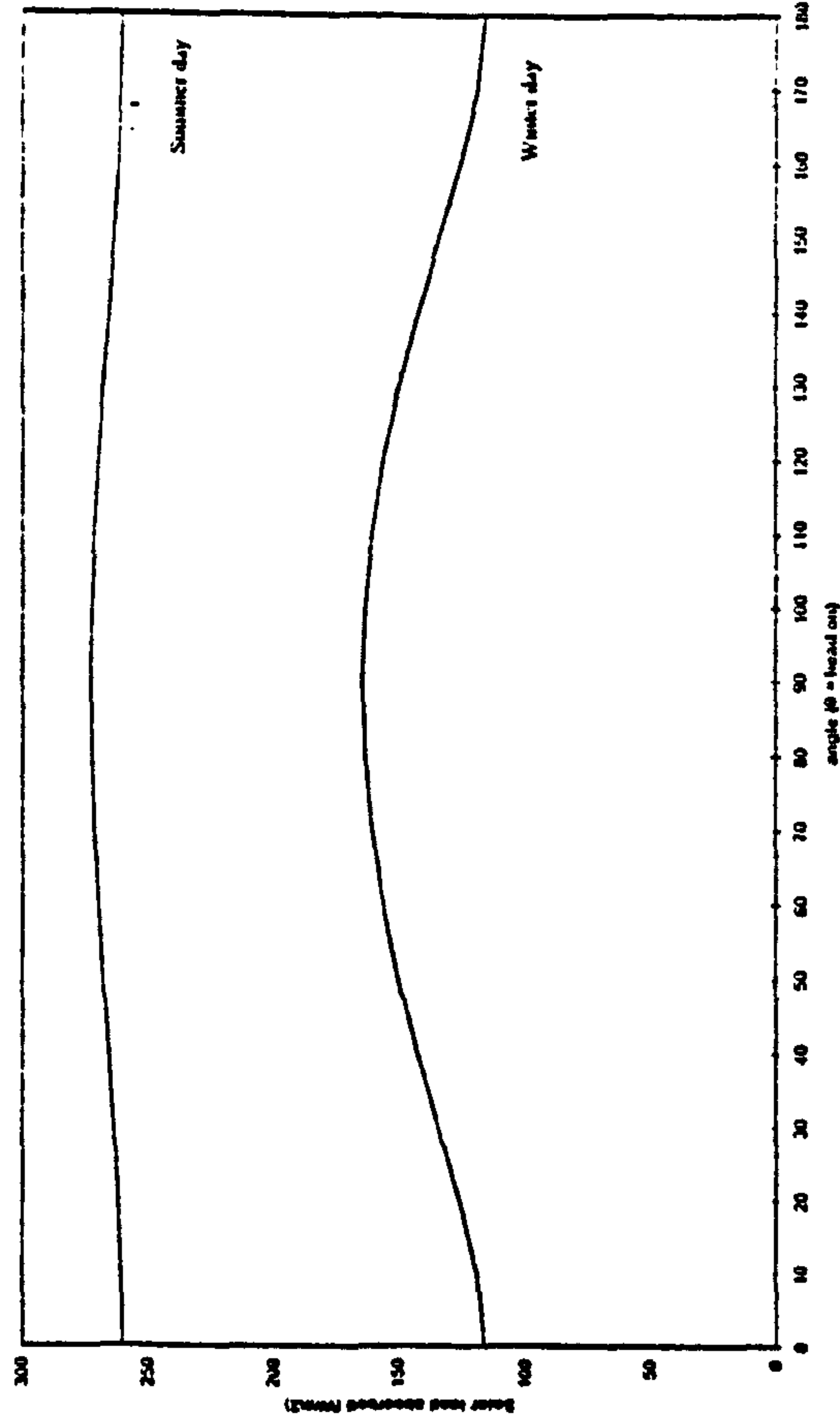


Fig 6.31: Sensitivity of predicted respiration rate to choice of trunk tissue resistance

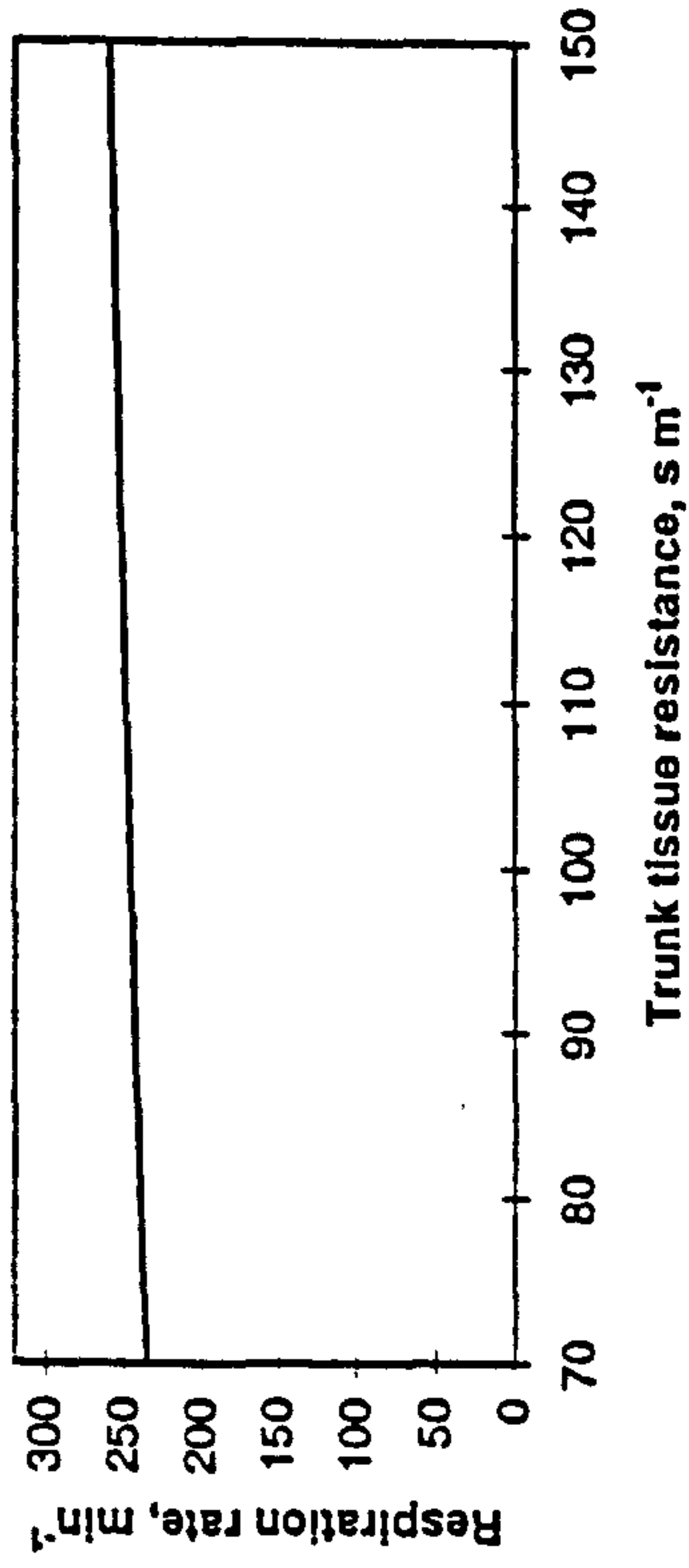
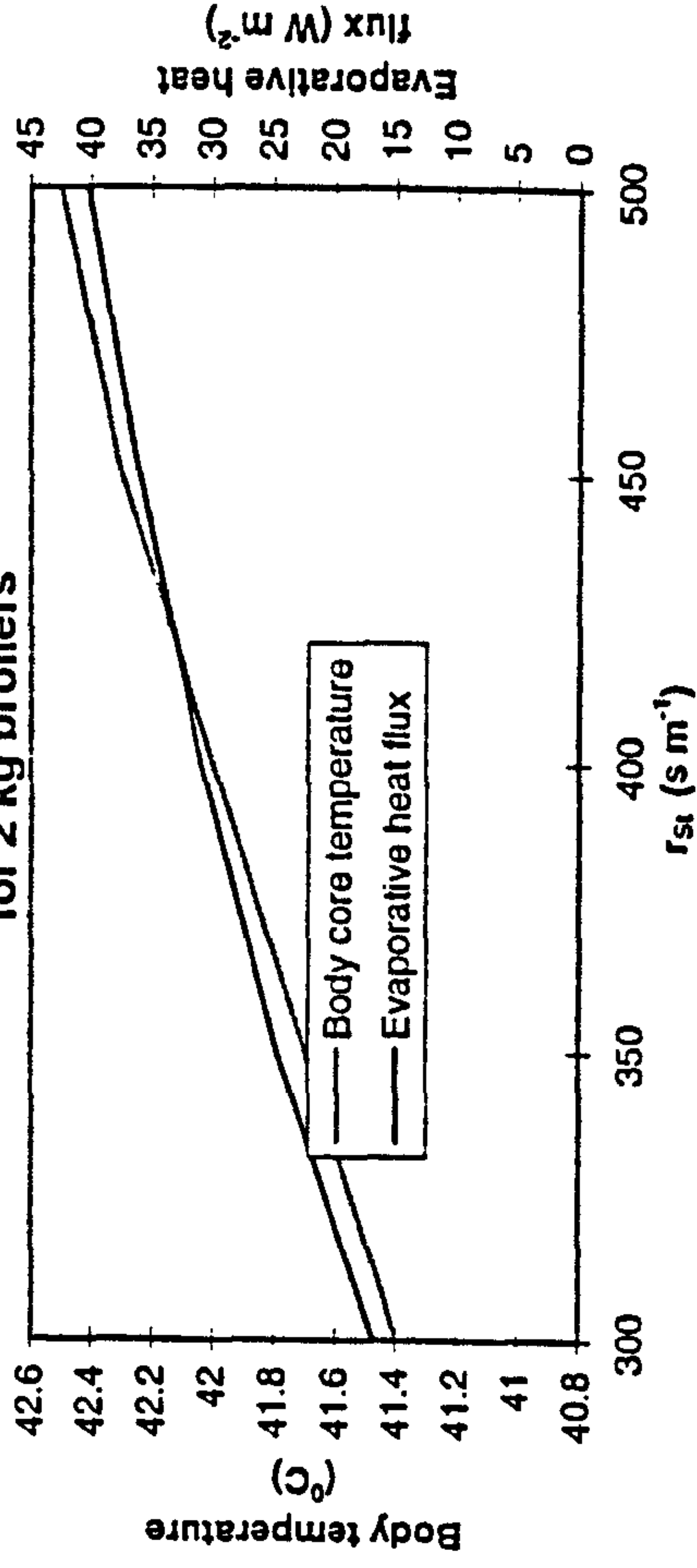


Fig 6.32: Sensitivity of predicted evaporative heat flux and body core temperature to choice of trunk tissue resistance for 2 kg broilers



side-on to the sun. Orientation is often used by animals in the winter to counteract the effects of the cold.

The tissue resistance of the trunk of a sheep, r_{st} , was assumed to remain constant in the current model irrespective of environmental conditions and age. However, r_{st} varies considerably between different individuals, and the assumption of a constant 100 s m^{-1} for r_{st} (Blaxter, 1967) is an approximation. The model was run with a range of r_{st} inputs and the effect on the respiration rate is shown in Fig 6.31. The graph shows that the choice of resistance has little effect on the respiration rate, only 10 to 15 breaths min^{-1} across the range of r_{st} values. Even when the line is extrapolated to an r_{st} of 220 s m^{-1} (Alexander, 1974), the respiration rate will only rise to about 260 min^{-1} . Therefore, due to the insensitivity of respiration rate to r_{st} , a typical value of $r_{st} = 100 \text{ s m}^{-1}$ is reasonable for most sheep and conditions in the UK.

Sensitivity to other inputs - special considerations

There is considerable ambiguity in the literature over the choice of tissue resistances for the appendages of chickens, r_{sL} . Data from the TCI of chicken appendages (Richards, 1974 - see Chapter 4) show that there is a ten-fold increase in the tissue resistance in the appendages during vasoconstriction. However, it is unclear from the data what the exact values of r_{sL} under vasodilation and vasoconstriction are. From the spread of the TCI values, the possible ranges are 50 and 500 s m^{-1} respectively to 100 and 1000 s m^{-1} respectively. Since appendages are important in thermoregulation by poultry, a sensitivity analysis was carried out to see how much effect the chosen values of r_{sL} for dilation and constriction had on the model output. A 2 kg bird with a metabolic rate of 110 W m^{-2} was modelled in an air temperature of 15°C (chosen to correspond to the likely zone of vasomotor action) and 50% relative humidity. Changing the r_{sL} values from 50 and 500 s m^{-1} to 100 and 1000 s m^{-1}

m^{-1} resulted in an increase in body temperature of only 0.4°C . Therefore 'compromise' values of 800 and 80 s m^{-1} as used in the current model were considered to be valid approximations.

The tissue plus pelt resistance of the body of chickens is a major component of insulation (see Section 4b.2), but available data are variable. The model was tested under the same conditions as for r_{sL} with the tissue plus pelt resistance varying across the range of values reported: 300 to 500 s m^{-1} . The results are shown in Fig 6.32. The tests show a high sensitivity to the choice of r_{st} . For example, an r_{st} of 300 s m^{-1} (eg. Davis et al, 1973) gives no thermal problems for a chicken at 15°C , with a body temperature less than 0.5°C above the thermoneutral value. However, an r_{st} of 500 s m^{-1} (eg. Wathes & Clark, 1981c) causes significant heat stress at the same air temperature, with an evaporative loss (mostly from panting) of 40 W m^{-2} , and a body temperature of 42.5°C . Inter-bird variability in this case makes a large difference to the results.

6.6 CONCLUSIONS

There are two main conclusions from the above results (see also Matthews et al, 1997):

- Climate change will have little effect on the heat balance of ruminants outdoors or on the suitability of a site for grazing livestock
- Animals indoors (eg. pigs and chickens) will experience significantly more heat stress under climate change

The present study indicates that outdoor livestock will be relatively insensitive to changes in climate; for example, the change in stress levels in beef calves at

Pwllpeiron predicted for 2050 is not enough to make the mean HSHS per year exceed the current value at Boxworth. However, indoor animals are likely to suffer more thermal stress under a changed climate. The gross margin of pigs will hardly change (assuming a constant meat price), but the significant increase in stress on the animal could become a welfare problem, and will probably affect the quality of the meat, hence a drop in value and gross margin. Both pig and Broiler chicken farms will have to introduce alleviation methods to avoid serious economic and welfare problems in the coming fifty years. In the next chapter, the possibilities for alleviation strategies are discussed and practical recommendations are made for the UK.

APPENDIX 6.1

Figs 6.1, 6.3, 6.5, 6.7 and 6.9 show that for outdoor animals the difference in predictions between the scenarios is small compared to the difference from the current values. However, Figs 6.11 and 6.14 show that this is not the case for indoor animals. The following table indicates a reason for these results. The numbers are the mean daily maximum temperatures for a site in central England, as predicted by the UKHI model. The numbers in brackets are, for Scenario A, the difference between the scenario and the baseline, and for Scenario F the difference from Scenario A.

Table 6.2

Scenario	January	March	June	September
Baseline	6.0	9.2	19.1	18.4
A	9.5 (3.5)	12.2 (3.0)	21.2 (2.1)	20.9 (2.5)
F	10.2 (0.7)	12.7 (0.5)	21.5 (0.3)	21.3 (0.4)

The temperature differences between scenarios are indeed much smaller than between scenario and baseline. The other climatic variables also have an effect. In Scenario F, rain totals and wind speed are predicted to be higher than in Scenario A, but only slight differences in solar radiation are predicted. Outdoors, the effects of wind and rain in Scenario F are therefore likely to modify the increased heat stress caused by higher temperatures and reduce the stress levels to close to Scenario A. Indoors, however, where wind speed is controlled and low, and rain and solar radiation are zero, there are no such modifying effects in Scenario F, and temperature is the principal driver of heat stress. There is therefore a greater difference between scenarios. Appendix B has a table of the full monthly predictions made by the GCM used in the current project.

CHAPTER 7 - DISCUSSION AND CONCLUSIONS

7.1 INTRODUCTION

This Thesis set out to develop a series of models to predict the thermal balance and associated stress levels in different species of livestock, under current and climate change conditions in the UK. This was a complicated and difficult task. The models had to deal with the different species and their widely differing body structures and thermoregulatory responses. The models had to consider the impact of several weather variables, such as rainfall and solar radiation, in addition to air temperature. Overall, the models performed well in their predictions of components of heat loss and thermal stress levels.

The present models incorporated some new features. However, some simplifying assumptions about the physical and physiological processes involved in the animal/environment interaction were inevitable to make the modelling manageable.

The first part of this chapter considers the novel features of the current models. The main assumptions made and the limitations of the present models are also considered.

The implications of the predictions are then discussed, for the animals, for humans and for global ecology generally. The chapter includes a brief review of current methods used to alleviate thermal stress in livestock, and discusses the possible use of such methods in the UK under a changed climate. Finally, further applications of the current models are suggested, with and without modifications, to allow a fuller assessment of climate change impact on livestock.

7.2

NOVEL FEATURES

The current models of livestock thermal energy balance provide a significant improvement on existing empirical models (eg. Mount & Brown 1982) by using as the basis the physics of heat transfer and animal physiology. The full body, including appendages, was modelled for a range of different livestock species, and physiological responses such as vasomotor action, sweating and panting were modelled from a physics rather than an empirical basis where possible. The current models improved on other mechanistic models (eg McArthur 1987) by modelling the heat balance of complete animals in the field, using hourly weather data as input, thus allowing easy assessment of the thermal state of an animal using readily available data. The work also assessed the direct climatic effects on animal heat balance, an area which has received little attention to date.

7.3

MAIN ASSUMPTIONS

The assumptions made in the present models fall into two general categories: those where physical and physiological processes have been included by means of simplified approximations of reality, and those processes which were excluded.

7.3.1

Thermal balance models

Processes simplified in the current models

The assumptions made about physical processes relate mainly to the interaction between climatological variables and the animal surface. Longwave radiation impinging on animals outside was assumed to come from two sources only: the

ground and the sky. Objects such as trees, buildings or nearby animals were excluded as sources of radiant energy (Section 2.5.2). A full analysis would require the use of solid angle geometry to describe "view factors" for each surface in an animal's environment. The view factor is a measure of the relative contribution of a particular surface to the overall radiation balance of the animal, and a complete analysis requires complex integration techniques (Oke, 1987). The likely impact of the radiant energy from these other objects on an animal's overall heat balance could not easily be tested here, as most heat balance measurements have been made on single animals in metabolic chambers, where the radiant temperature of the environment was equal to the air temperature.

The coat depth was assumed to be uniform over an animal's trunk, as was the wind penetration. The assumption of a uniform coat depth around the trunk is reasonable for cattle, but much less so for sheep, which often have a longer fleece on the back than on the underside, possibly evolved as additional protection from high solar loads on the back. The animals were assumed to be always orientated side-on to the wind. Studies have revealed that the effect of wind varies with position around a cylindrical object covered with hair or clothing (eg. McArthur & Monteith, 1980b). However, Joyce & Blaxter (1964) found that heat loss from sheep is only reduced by about 5% by changing orientation, and their finding is supported by other workers (eg. Gebremedhin 1987). Thus, the likely variation in wind penetration into different parts of the animal coat seems to have little impact on the overall energy balance of the animal. For pigs, it was assumed that the coat insulation was negligible. Although this is likely to be a reasonable assumption for indoor pigs, outdoor pigs have a distinct layer of hair over the body surface with measured resistances of about 40 s m^{-1} (Gannon, 1996). Consequently, the hair coat should be modelled if the present pig model is applied to outdoor units.

Wetting of the coat (Section 2.8) was treated simply as a decrease in external resistance. This approach to a complex process has been adopted by other modellers

(eg. Mount & Brown, 1982). The cumulative effects of several hours of low rainfall was not modelled. Validation of the predictions of heat loss from a wet animal is difficult because few measurements have been made in these conditions. The conclusion from the assumptions made is that conditions of cold stress which occur when wind and rain occur simultaneously will not be well-modelled. Therefore the model may be unreliable if required to predict changes in incidence of cold stress. However, this is acceptable as there is not much effect on the prediction of incidence of heat stress.

Solar load was assumed to be uniformly distributed over the whole trunk and head. In reality, there can be large variations in the solar load on different parts of the body. For example, total solar radiation on the backs of sheep can exceed 1000 W m^{-2} and can elevate the wool surface temperature to more than 80°C (eg. Stafford Smith et al, 1985) while the wool surface on the underside, exposed only to radiation reflected from the ground, remains below body temperature. Solar radiation absorption was assumed to occur at the coat surface - the complicated physics of absorption of shortwave radiation within the coat was not attempted. The test in Section 3b.6.3 showed that even at high solar loads, the current model was within an acceptable margin of McArthur's (1987) analysis, which modelled radiation penetration.

In summary, the physical interactions between weather variables and animal have been assumed uniform over the whole body. The implicit assumption of a uniform coat and skin surface temperature is obviously simplistic. In reality, the surface temperatures and heat flux densities will vary with position on the body. However, the validation tests produced good matches between the available measurements and the whole-body heat loss predicted by the model, and therefore the assumption of uniformity is acceptable for the present purposes.

Processes excluded from the current models

The second category of simplifications are those parameters or processes which were excluded from the models. Some processes were omitted from the current models because they cannot easily be parameterised as the relevant variables depend on animal behaviour. For example, the position of an animal outdoors near objects (eg. shelter or shade) will affect the radiation balance as well as the pattern of air movement around the body (see tests in Section 3.3.3). For indoor animals, behavioural methods of thermoregulation such as huddling and group separation by pigs, or spreading the wings by chickens, are important (eg. Osbaldiston, 1968). However, as indicated in Sections 3.3 and 4.3, the modelling of animal choice is extremely difficult and has not been attempted here.

Heat loss from the legs and head was considered significant in this study, confirming the conclusions reached by others (eg. Gonzalez-Jiminez & Blaxter, 1962; Whittow, 1962; Holmes, 1970; Richards, 1974). Although heat loss from appendages was included in the analysis, there was no attempt to model mechanistically the thermal interaction between different body parts. For example, the arrangement of the legs will provide a complicated air movement pattern which will affect the boundary-layer resistance. Similarly, there will be thermal radiation interaction between the body parts, but these interactions were not modelled because the geometry was considered too complicated. Exclusion of such radiative interaction will give overestimates of heat loss in the cold. For example, the test in Section 3a.6.1 shows an overprediction of heat loss from shorn sheep of about 20% at $T_a = 8^\circ\text{C}$ when thermal interaction between body parts obtained by compaction of posture in the cold reduces the effective area for heat loss. Such postural responses were modelled here, when necessary, using an empirical tuning.

The differences in stress duration and gross margin between current and future values

presented in the Thesis represent a worst-case scenario. The models were run with climate change weather data, but there was no allowance for gradual change in climate or physiology over the intervening period. The animals were assumed to react to the changed climate as if the conditions were imposed now, with no opportunity for the animals to adapt. Bianca (1965) defined the process of acclimatization (or acclimation) as:

"With repeated or continuous exposure to extreme conditions, functional and structural changes occur to enable an animal to live without distress"

Short-term acclimatization responses to hot conditions include a rise in both body temperature and sweat rate; also, the rise in respiration rate becomes less pronounced.

These effects usually occur within ten days of the start of the exposure (Bianca, 1959a). The importance of acclimatization is recognised. For example, calves exposed to humid heat for some time will increase their respiration rate more readily than those accustomed to hot dry conditions (Bianca, 1959b). In the long term, coat growth patterns change to allow for hotter conditions, and animals reared at high temperatures have better tolerance to heat than those used to cooler conditions (Bianca, 1965). Observations by poultry farmers reveal that birds born in summer experience less heat stress than those born in spring and subject to heat later on in life (D.J.Parsons, pers. comm.). Tropical breeds and animals born in the tropics fare much better in hot conditions than temperate-raised animals. Kabuga et al (1990) showed that Ghanaian-born cattle suffered no reduction in fertility even in the hottest most humid season. Measurements on sheep in Pakistan by Kaushish et al (1995) showed maximum respiration rates of only 110 min^{-1} , even at $T_a = 40^\circ\text{C}$.

An animal's ability to acclimatise depends on its feed intake, and on the environmental conditions. Wiernusz & Teeter (1996) observed that keeping chicken feed levels high in hot conditions to avoid loss of production results in a poor ability to acclimatise. Thus, short-term gains in productivity may give long-term losses.

Voluntary feed intake is dependent on the acclimated temperature rather than the current air temperature (Senft & Rittenhouse, 1985). Senft & Rittenhouse designed a mathematical model to quantify the effects of extreme conditions on the feed intake of cattle. The acclimatized temperature, T_{acc} , defined as the temperature at which the animal is comfortable, was calculated as the running mean air temperature over the past ten days; the weather before these ten days was assumed not to affect the animal response. If the air temperature on a given day was different to T_{acc} , the feed intake was assumed to drop in proportion to the square of the difference between T_a and T_{acc} . The maximum observed feed intake reductions were about 20%. Senft & Rittenhouse's model was used by Prescott et al (1994) to investigate the effects of sudden cold snaps in the winter. The results show that when animals are used to extreme temperatures (eg. mid-winter) the acclimatization time is less than when temperatures are fluctuating (eg. in the autumn). The current models treat metabolic rate as a constant above the LCT. However, in acute heat stress conditions, the metabolic rate may rise as a consequence of the van't Hoff effect and the increased effort of panting (eg. Whittow & Findlay, 1968). The rise in M is limited to acute exposure to heat stress. Chronic exposure of animals to hot climates results in adaptation, most widely through a decline in metabolic rate (eg. Bianca, 1965 for cattle, Mount, 1968 for pigs, van Kampen, 1974 for poultry).

In summary, animals employ many physiological and behavioural mechanisms to counter the effects of thermal stress, but there are few data from which to quantify the adaptations. Section 5.4.1 described an attempt to modify the short-term animal feed intake in response to high stress levels, based on observations reported by Senft & Rittenhouse. However, long-term adaptations, especially the metabolic rate reductions, were not modelled and the heat stress predictions for climate change may be less severe than predicted.

7.3.2 Hourly weather data generator

The reduction of daily weather data to hourly values, described in Sections 5.2 and 5.3, was subject to many assumptions which were incorporated to keep the model as simple as possible. Hourly values of solar radiation were difficult to generate from the daily global totals, and assumptions such as the isotropy of diffuse radiation, and the definition of a Daily Clearness Index (Section 5.2.2) were used. The Daily Clearness Index, which quantified the effects of clear sky atmospheric transmission and cloud cover, was assumed constant over the day. The equations used to calculate global radiation at the Earth's surface, which depend on atmospheric transmittance alone, used Daily Clearness Index instead as the only value available.

The division of global radiation between direct and diffuse depends on cloud cover and transmittance, and an empirical scheme was used to relate Daily Clearness Index to diffuse radiation. The result was that cloud cover had to be assumed constant through the day in generating hourly solar radiation. This assumption is valid when the days are uniformly clear or cloudy, but on days of variable hour-by-hour cloud cover, especially when the sun is alternately obscured and clear, which covers many days in the UK, the model's hourly predictions are poor. The thermal balance models are sensitive to solar radiation, and therefore the hourly predictions of heat loss may be affected significantly by the assumption of constant cloud cover. Further work should involve more accurate modelling of solar radiation and the relationship between cloud cover and direct and diffuse radiation at the ground. The empirical relation between Daily Clearness Index and cloud cover fraction, is independent of cloud type and base height; for the current model the Daily Clearness Index corresponding to total cloud cover was 0.3, which is typical for stratocumulus. Corresponding figures for other cloud types could be included (eg. 0.13 for fog, 0.4 for cirrocumulus, 0.7 for cirrus - Gates, 1980). Using Daily Clearness Index rather than clear sky transmittance to calculate the radiation at the ground (Section 5.2.2)

produces only small errors, and those principally at low elevations (Table 5.1).

Hourly values of wind speed were assumed constant over the day (Section 5.2.4). This assumption is simplistic. However, the errors inherent in reducing 10 m wind speed to that at animal level relied on assumptions about ground roughness, and were assumed to dominate over the small variation in mean hourly wind speed over the day in inland UK (Section 5.2.4). In addition, the wind was assumed to be non-turbulent, ie. the effects of gusts were not modelled, as the hourly timescale of the model is much larger than the average time of a gust (seconds). Indoors, the wind profile was assumed uniform, though in reality there is a complex turbulent flow pattern inside buildings (Section 4.2).

The assumptions made about hourly rainfall data are discussed in Sections 5.2.1 and 5.3.4. The simple triangular method assumed that the maximum rainfall intensity in a day is 0.3 times the total precipitation, and that maximum intensity occurs at noon. One consequence of this method is that the rain starts and finishes at the same time each day, and the effects of sudden sharp showers, for example cannot be modelled. In reality, rainfall durations and intensities are almost random on timescales from a few minutes to several days (Ward & Robinson, 1990). The increase in heat loss due to wetting of an animal may be important when combined with low temperatures and high winds, combinations which are not addressed by the current model. A statistical treatment is necessary for improvement.

A value for ground surface temperature T_g was calculated from a heat balance equation (Section 5.2.3.3) assuming that no heat was stored in the ground. The specific heat capacity of dry soils are less than $1.0 \text{ kJ kg}^{-1} \text{ K}^{-1}$ (eg. Van Wijk & de Vries, 1963), as compared to $3.48 \text{ kJ kg}^{-1} \text{ K}^{-1}$ for body tissue (eg. Tzschentke et al, 1996). Soils will store less heat than animals over a given time, so the assumption of non-storage taken for animals is valid for soils. However, wet and peaty soils have higher heat capacities, since the specific heat capacity of water is $4.2 \text{ kJ kg}^{-1} \text{ K}^{-1}$, and

so will store more energy. Another important assumption in calculating surface temperature was that latent heat flux was always a fixed fraction of the sensible heat flux, from Bowen ratio data for Europe. This assumption ignores the effect of ground wetness on the temperature, and on the fluxes of moisture to and from the animal, but since the animal thermal balance models are not as sensitive to T_g as to variables such as wind speed, the approximate determination of T_g used in the current model is acceptable.

To summarise, the weather generator performed well under most conditions, but some variables (eg. rain) may be predicted with considerable uncertainty.

7.4 IMPLICATIONS OF RESULTS

This section considers some of the wider implications of the increased thermal stress predicted to occur under climate change.

7.4.1 Effects of climate change on thermal balance

Outdoor animals

This Thesis predicts that outdoor ruminants will be fairly insensitive to changes in climate. The results generally show a tolerance by these animals to changes predicted for 2050. The mean dairy herd-wide drop in milk production due to climate change in the UK was predicted to be about 1%, which corresponds approximately with predictions for dairy cattle in the northern US Rockies (Klinedinst et al, 1993). One possible aid to reducing stress is to increase the coat reflectivity. The sensitivity analysis has shown a strong dependence of solar heat load on albedo, and the difference between a dirty animal and a clean one may be significant enough to cancel out the effects of climate change on beef, wool and milk production.

Indoor animals

For pigs and poultry, the implications of the predictions are more serious. Heat stressed pigs and chickens give poorer meat and egg quality and have a reduced conception rate (Section 1.3.2.2). Figs 6.22 and 6.23 confirm that the chicken's thermal balance is sensitive to feed intake. The current normal feed intake of about 3.5 times maintenance (eg. Gates et al, 1996) is close to the limit of survival, as shown by the relatively high mortality in chickens (Chapter 1 and Section 4.2). The problems of stress in transporters outlined in Section 4.2, which are already only just tolerable, will become more serious should climate change. The increase in heat stress in pigs will produce poorer quality meat, and less of it, as feed intake falls. Figs 6.20 and 6.21 show a marked effect of feed intake on stress, though not as severe as for the chicken. An energy intake of four times maintenance is too high, even under current conditions. Three times maintenance intake, which is the approximate value used in the main model runs (Figs 6.11 - 6.13), is about the intake limit for current conditions and may have to be reduced under climate change to avoid a 25% increase in the duration of stress (Section 6.3.4).

7.4.2 Economic considerations

The effects on gross margins (GM) of the various livestock systems are presented in Section 6.3.7. For chickens, a reduction of 10% in GM would be serious - enough to put many poultry producers out of business in current economic conditions, given the already fine balance between profit and loss. The detrimental effects of heat on the quality of meat and eggs would reduce the market price and the effects on fertility would reduce availability. The GM results given in Figs 6.18 and 6.19 may therefore not reflect the full extent of the increase in stress levels predicted by the model system.

In summary, animals already farmed near the limits of their thermal tolerance (ie. pigs & chickens) may have serious problems under climate change, and the farmers may suffer accordingly in reduced income and increased costs. One likely outcome is that prices will rise, affecting the smaller, possibly more 'organic', producers more severely than the larger farmers. Farm management policy may have to change, with more investment in the design of efficient and economically viable methods to alleviate heat stress. The next section reviews some of the methods of alleviating environmental stress, and some practical recommendations for the UK under a future climate.

7.5 ALLEVIATING THERMAL STRESS

Animals under thermal stress are less productive and suffer more than animals kept in thermoneutral conditions. If the predictions for the impact of climate change on livestock stress levels presented in this Thesis are realised, methods for reducing thermal stress will need to be introduced, especially for chickens, if a severe loss of productivity and profit is to be avoided. For animals outdoors in hot conditions, it is usually enough to provide a shade and adequate drinking water and allow the animals to alleviate stress from solar radiation themselves (MAFF, 1995). It is difficult, however, for animals indoors to modify their own thermal environment, beyond moving to different parts of the house, which may be impossible in a broiler house with 15000 birds, for example. The climate within buildings is normally controlled by the producer, and modifications to reduce thermal stress by altering the indoor climate must be made by human control. An animal indoors which would normally use behavioural responses to alleviate thermal stress (eg. pigs burrowing in straw to relieve cold) must have facilities provided by the producer. In the UK, where heat stress can already be a problem on a few days a year, especially in broiler houses, recommendations exist to avert major problems. For example, efficient insulation of

the roof reduces penetration by solar radiation, and correct installation and good maintenance of the ventilation system, including having a standby generator for use during breakdowns, is essential (MAFF, 1996). Chicken farmers usually reduce stocking densities in hot conditions, which reduces temperature and humidity within the building. In some cases, all the birds of one sex are removed, and thinning may occur beyond that (D.R.Charles, pers. comm.). Modification of the lighting regime may be used to reduce stress. There is approximately a 30% reduction in heat production in chickens during darkness (Lundy et al, 1978), and the effect is most pronounced in broiler breeders (Macleod et al, 1980). For pigs, which can have serious heat stress problems at relatively low temperatures due to their poor sweating/panting ability, a wallow, preferably a mud wallow, is essential. Pigs need behavioural freedom (eg. to wallow, group together, burrow) since their physiological ability to thermoregulate is relatively poor (Chapter 4).

Under climate change, more sophisticated alleviation techniques may be required in the UK. Scientists and Engineers in countries such as Israel, South Africa, the US and Australia, where animals are already kept much nearer their limits of tolerance, have developed several designs for reducing thermal stress in extreme climates. In cold conditions, such as central northern North America, it is recommended that pasture land provides a variety of favourable microclimates through use of topography and trees, to allow outdoor animals to choose a comfortable environment and maintain intake (Houseal & Olson, 1995). For indoor animals, devices which store energy from the sun and release it slowly through the night are used to reduce diurnal variations in temperature. One such installation uses a solar collector to heat up a box of rocks during the day; air is then passed through the box at night, giving energy savings of about 40% (Sokhansanj & Jordan, 1981). Tests were carried out in March in Minnesota, where the diurnal range is large, and it is relatively sunny. Such a scheme may not be much use in the UK. Radiant heaters certainly are used in the UK (eg. Alsam & Wathes, 1991), especially for chicks and weanling (2 - 3 week old) pigs, which need a fairly constant temperature regime (Overhults & DeShazer, 1982).

In a changed climate, however, it is likely that heat stress which will cause more problems than cold stress. In a visionary paper, Beede & Collier (1986) recognised the possibility of climate change and proposed various strategies, both nutritional and environmental, for keeping normal production during heat stress. Nutrient strategies include decreasing forage to concentrate ratio, which reduces heat generated in the stomach, increasing water availability, increased vitamin and mineral concentration in the feed to replenish losses caused by reduced feed intake, and providing more meals to encourage higher food consumption. Behaviour modifications such as grazing at night only minimises work, and lowers heat production during the day (Ansell, 1981).

Strategies to modify the thermal environment have received much attention. Barth (1982) outlined several methods for relieving heat stress. The first is to shade the building as much as possible, using foliage or overhangs. Aiding evaporative cooling by spraying the animals or the roof of the building, and cooling drinking water are also useful. Air conditioning is expensive, and is not profitable outside extreme climates such as the southern USA; additional problems with air conditioning include dust and poor ammonia removal (Ryan et al, 1992). Poultry houses in the tropics are usually aligned East-West to reduce the solar load (Smith, 1981), but such alignment is sometimes modified to allow beneficial effects of the prevailing wind. In the humid tropics, increased air movement is often the only way to cool animals effectively.

Proposals have been made to use subterranean heat exchangers to heat or cool the incoming air (eg. Spengler & Stombaugh, 1982). Tubes are buried in the soil at about 1 - 2 metres depth, where the annual range of temperature is very small; air coming into the house is passed through the tubes, giving a stable temperature inside.

A great deal of research relates to enhancing evaporative heat loss from animals. Pigs have shown significant weight gain benefits when sprinkled with water at regular intervals at very high temperatures ($> 30^{\circ}\text{C}$) (Nichols et al, 1982b; Fehr et al, 1982; Baccari et al, 1993). Wilson et al (1982) reviewed the designs and benefits of spray cooling broiler chickens. A misting system where water is atomised was found to

lower the effective temperature in the building by 3 to 4.5°C, improve bird body weight and pay for the initial outlay within three years. Atomisers operating with compressed air were more efficient in terms of reduction of effective temperature than using high pressure water sprays - without the cost of the water pump (Bottcher et al, 1989). Cattle outdoors in hot climates are currently cooled using sprays. In Saudi Arabia, for example, where the mean daily maximum temperature in the summer is 47°C, fertility is severely depressed with no environment modification. Air pre-cooled by evaporative cooling was forced over cattle and the conception rate was compared with cattle sprayed with water then air at ambient temperature. Over 80% of the air cooled cattle, and 60% of the spray cooled cattle became pregnant - a difference significant at the 5% level (Ryan et al, 1992). The danger of spraying animals, especially those in houses, at high humidities is the associated increase in humidity, which may more than counteract the cooling effects of spray; there are cases where flocks have died because of badly timed spraying (MAFF, 1996; D.J.Parsons, pers. comm.). Generally, providing well-sited well-ventilated and shaded buildings is the most economical and effective first step to minimising heat stress (Bucklin et al, 1991). More costly methods such as sprinklers and fans can then be introduced for the hottest conditions.

A few studies have looked at conductive cooling of chickens by providing cooled perches. Laying hens have heat stress partially alleviated by roosting on a water-cooled pipe, which lowers metabolic rate by about 19% (Muiruri & Harrison, 1991a).

There is an associated benefit in feed intake, egg production and hatchability (Muiruri & Harrison, 1991b). Reilly et al (1991) tested the feasibility of using water cooled perches in open-plan broiler houses.

The study found that animals used cooled pipes with no encouragement when under heat stress, and there were benefits in terms of daily weight gain and feed to weight gain ratio.

Alleviation measures for the UK under climate change

For the UK, enhanced stress alleviation methods will probably not be needed for ruminants outdoors. Some expensive schemes outlined in the previous section are pointless for use in the UK even under climate change (eg. spraying cattle). Adequate shade provision should be sufficient to reduce any additional stress, though in some cases better designed shelters may be needed than at present. For animals indoors, however, better thermal control methods will be needed to avoid major losses under climate change. The best options will be to use the simplest methods first, such as careful building alignment, shading of buildings and use of better insulation materials.

Reducing stocking densities and/or growth rates may also help reduce the heat and humidity load on the animals. For pigs, which use behavioural thermoregulation far more than physiological processes, measures as simple as providing adequate facilities to enable behavioural adaptation, such as a wallow, and the freedom to group and separate, could be sufficient. For chickens, more frequent thinning of stock density may be needed, while enhanced cooling with reversible fans to blow air over the animals and internal fans to circulate the air will be more necessary. At present in the UK misting systems are hardly used, but they may need to be introduced in the future if careful building design and siting is not sufficient to relieve increased heat stress duration.

7.6 FUTURE WORK

7.6.1 Using the current model

The models as described in this Thesis can be used without modification for a variety of future experiments on the effects of climate on thermal balance of livestock. As predictions of future climate improve, the models can be used with the new scenarios to make better predictions; the models are not restricted to the scenarios used in the

current work. However, more measurements are needed of heat loss and heat production of animals, linking feed intake, energy metabolism and the thermal environment. Much of the data used to validate the present models are more than twenty years old, and some relate to breeds which have died out. Genetic modification and vastly increased growth rates in the past twenty years may have caused changes in both metabolic rate and the thermoregulatory responses of animals.

Some calorimetric studies are still being done (eg. on cattle at the Centre for Dairy Research, Reading University (S.B.Cammell, pers. comm.) and on chickens at the Roslin Institute, Edinburgh (eg. MacLeod, 1991)) but more are needed to enable updated validation and empirical tuning of the models. Obtaining quality data of the heat losses and thermoregulatory behaviour of animals is necessarily more expensive than producing computer models, but the investment must be made as a priority if predictions of future scenarios are to be accurate as animal breeds and growth rates change.

In addition, the effects of pregnancy and lactation on feed intake and metabolic rate have not been quantified. Abdalla et al (1993) reported that lactating ewes are significantly ($P < 0.05$) more sensitive to heat than pregnant ewes. Since cattle and sheep are likely to suffer heat stress most at the times of peak lactation, measurements of the effects of environmental conditions on heat losses from pregnant and lactating animals would be extremely useful.

7.6.2 Modifying the current model

There is scope to improve and extend the models. This final section discusses some ways this can be done. The sensitivity analyses showed that wind, rain and solar radiation are important variables influencing the thermal status of an animal. However, these variables, especially rainfall, have been modelled simply. The generation of hourly rainfall data should be improved with further measurements of

and incidence of thermal stress of four species of livestock given the environmental conditions.

- The models were used with current and climate change weather scenarios to predict the potential impact of a change in climate on the duration of thermal stress experienced by livestock in the UK.
- An assessment of the potential economic consequences of climate change was made by linking the thermal balance models with models of feed intake, grass growth and building heat balance designed elsewhere.
- Climate change will have little effect on the heat balance of ruminants outdoors or on the suitability of a site for grazing livestock. Ruminant livestock enterprises should not be significantly affected by a change in climate.
- Non-ruminant animals indoors will experience significantly more heat stress under climate change, with an associated decrease in productivity. Practical measures to alleviate increased heat stress should be implemented.
- The priority for the immediate future is for more measurements of feed intake, heat production and loss from livestock under specified environmental conditions rather than more computer modelling.

REFERENCES

- Abdalla, E. B., E. A. Kotby, and H. D. Johnson. 1993. Physiological responses to heat-induced hyperthermia of pregnant and lactating ewes. *Small Ruminant Research* 11 (2):125-134.
- Achenbach, E. 1977. The effect of surface roughness on the heat transfer from a circular cylinder to the cross flow of air. *Int. J. Heat Mass Transfer* 20:359-369.
- Aguiar, R., and M. Collares-Pereira. 1992. TAG: A time-dependent, autoregressive, Gaussian model for generating synthetic hourly radiation. *Solar Energy* 49 (3):167-174.
- Ain Baziz, H., P. A. Geraert, J. C. F. Padilha, and S. Guillaumin. 1996. Chronic heat exposure enhances fat deposition and modifies muscle and fat partition in broiler carcasses. *Poult. Sci.* 75 (4):505-513.
- Akumu, G. 1994. Mitigation strategy or hidden agenda? *Tiempo* 11:1-3.
- Alexander, G. 1974. Heat loss from sheep. In *Monteith & Mount* (1974):173-203.
- Alexander, G., and D. Williams. 1962. Temperature regulation in the new-born lamb: 6. Heat exchanges in lambs in a hot environment. *Aust. J. agric. Res.* 13:122-143.
- Alsam, H., and C. M. Wathes. 1991a. Conjoint preferences of chicks for heat and light intensity. *Br. Poult. Sci.* 32:899-916.
- Alsam, H., and C. M. Wathes. 1991b. Thermal preferences of chicks brooded at different air temperatures. *Br. Poult. Sci.* 32:917-927.
- Ansell, R. H. 1981. Extreme heat stress in dairy cattle and its alleviation: a case report. In: *Clark* (1981):285-306.
- Arkin, H., E. Kimmel, A. Berman, and D. Broday. 1991. Heat transfer properties of dry and wet furs of dairy cows. *Trans. Amer. Soc. Agric. Eng.* 34 (6):2550-2558.
- Armstrong, A. C. 1996. The impact of climate change on grassland production and utilisation. *Aspects of Applied Biology* 45:79-84.
- ASAE. 1982. *Livestock Environment II. Proceedings of the second international livestock environment symposium.* April 20-23, 1982, Iowa State

University, Ames, Iowa.
American Society of Agricultural Engineers, St
Joseph, Michigan.

ASAE Standards. 1987. Dimensions of livestock and poultry. In ASAE Data: ASAE D321.2, pp 391-398. .

Aschoff, J., H. Biebach, A. Heise, and T. Schmidt. 1974. Day-night variation in heat balance. In Monteith & Mount (1974):147-172.

Atkins, P.W. 1994. Physical Chemistry. 5th ed. Oxford University Press, Oxford. 1031 pp

Azzam, S. M., J. E. Kinder, M. K. Nielsen, L. A. Werth, K. E. Gregory, L. V. Cundiff, and R. M. Koch. 1993. Environmental effects on neonatal mortality of beef-calves. Journal of Animal Science 71:282-290.

Baccari, F., A. L. B. A. Gayao, and J. R. V. Nunes. 1993. Effect of water cooling on growth rate of large white-Landrace gilts during thermal stress. In: Collins & Boon (1993):889-894.

Baker, B. B., J. D. Hanson, R. M. Bourdon, and J. B. Eckert. 1993. The potential effects of climate change on ecosystem processes and cattle production on US rangelands. Climatic Change 25 (2):97-117.

Bakken, G. S. 1976. A heat transfer analysis of animals: unifying concepts and the application of metabolism chamber data to field ecology. J. theor. Biol. 60:337-384.

Baldwin, B. A. 1974. Behavioural Thermoregulation. In Monteith & Mount (1974): 97-117.

Barrow, E., E. Hulme, and T. Jiang. 1994. SPECTRE: Spatial and Point Estimates of Climate Change due to Transient Emissions. Climatic Research Unit, Norwich, 38 pp.

Barth, C. L. 1982. State-of-the-art for summer cooling for dairy cows. In: ASAE (1982):52-61.

Beede, D. K., and R. J. Collier. 1986. Potential nutritional strategies for intensively managed cattle during thermal stress. Journal of Animal Science 62:543-554.

Bennett, J. W. 1972. The maximum metabolic response of sheep to cold: effects of rectal temperature, shearing, feed consumption, body posture and body weight. Aust. J. agric. Res. 23:1045-1058.

- Berman, A. 1968. Nychthermal and seasonal patterns of thermoregulation in cattle. *Aust. J. agric. Res.* 19:181.
- Bianca, W. 1959a. Acclimatization of calves to a hot dry environment. *J. Agric. Sci.* 52:296-304.
- Bianca, W. 1959b. Acclimatization of calves to a hot humid environment. *J. Agric. Sci.* 52:305-312.
- Bianca, W. 1965. Reviews of the progress of dairy science. Section A: Physiology. Cattle in a hot environment. *J. Dairy Res.* 32:291-345.
- Black, J. L., G. T. Davies, and J. F. Fleming. 1993. Role of computer simulation in the application of knowledge to animal industries. *Aust. J. agric. Res.* 44 (3):541-555.
- Black, J. L., and P. J. Reis, eds. 1978. Physiological and environmental limitations to wool growth - proceedings of a National Workshop, Leura, NSW, Australia, April 1978. Univ. of New England Publishing Unit, Armidale, NSW.
- Blaxter, K. L. 1967. The energy metabolism of ruminants, 2nd ed. Hutchinson, London.
- Blaxter, K. L., N. McC. Graham, F. W. Wainman, and D. G. Armstrong. 1959. Environmental temperature, energy metabolism and heat regulation in sheep. II - The partition of heat losses in closely clipped sheep. *J. Agric. Sci.* 52:25-49.
- Blaxter, K. L., and F. W. Wainman. 1964. The effect of increased air movement on the heat production and emission of steers. *J. Agric. Sci.* 62:207-214.
- Bolortsetseg, B., and G. Tuvaansuren. 1996. The potential impacts of climate change on pasture and cattle production in Mongolia. *Water Air and Soil Pollution* 92:95-105.
- Boon, C. R. 1981. The effect of departures from lower critical temperature on the group postural behaviour of pigs. *Anim. Prod.* 33:71-79
- Bottcher, R. W., G. R. Baughman, and D. J. Kesler. 1989. Evaporative cooling using a pneumatic misting system. *Trans. Amer. Soc. Agric. Eng.* 32(2): 671-676.
- Bottomley, G. A. 1978. Weather Conditions and Wool Growth. In: Black & Reis (1978):115-125.

- Bouchillon, C. W., F. N. Reece, and J. W. Deaton. 1970. Mathematical Modeling of Thermal Homeostasis in a Chicken. *Trans. Amer. Soc. Agric. Eng.* 13:648-652.
- Bowman, P. J., G. M. McKeon, and D. H. White. 1995. An evaluation of the impact of long-range climate forecasting on the physical and financial performance of wool-producing enterprises in Victoria. *Aust. J. agric. Res.* 46 (4):687-702.
- Briggs, H. M., and D. M. Briggs. 1980. *Modern Breeds of Livestock*, 4th ed. Macmillan, London.
- Brody, S. 1964. *Bioenergetics and Growth*, 2nd ed. Hafner, New York.
- Broecker, W. S. 1975. Climatic change: are we on the brink of a pronounced global warming? *Science* 189:460-463.
- Bruce, J. M. 1981. Ventilation and Temperature control criteria for pigs. In: Clark (1981):197-217.
- Bruce, J. M. 1993. Interactions between the animal and its environment. Pages 495-508 {In} J. M. Forbes and J. France, eds. *Quantitative Aspects of Ruminant Digestion*. CAB International, Cambridge.
- Bruce, J. M., and P. J. Broadbent. 1989. New techniques in modelling cattle production systems. Pages 180-205 {In} C. J. C. Phillips, ed. *New Techniques in Cattle Production*. Butterworths, London.
- Bruce, J. M., and J. J. Clark. 1979. Models of heat production and critical temperature for growing pigs. *Animal production* 28:353-369.
- Brugge, R. 1991. The record-breaking heatwave of 1-4 August 1990 over England and Wales. *Weather* 46 (1):2-10.
- Bucklin, R. A., L. W. Turner, D. K. Beede, D. R. Bray, and R. W. Hemken. 1991. Methods to relieve heat stress for dairy cows in hot, humid climates. *Appl. Engng. Agric.* 7(2):241-247.
- Campbell, G. S., A. J. McArthur, and J. L. Monteith. 1980. Windspeed dependence of heat and mass transfer through coats and clothing. *Boundary-Layer Meteorology* 18:485-493.
- Cannell, M. G. R., and C. E. R. Pitcairn, eds. 1993. *Impacts of the Mild Winters and Hot Summers in the United Kingdom in 1988-1990*. HMSO, for the UK Department of the Environment, London.

- Cena, K., and J. A. Clark. 1973. Thermal Radiation from Animal Coats: Coat Structure and Measurements of Radiative Temperature. *Phys. Med. Biol.* 18(3):432-443.
- Cena, K., and J. A. Clark. 1978. Thermal Insulation of Animal Coats and Human Clothing. *Phys. Med. Biol.* 23 (4):565-591.
- Cena, K., and J. L. Monteith. 1975a. Transfer processes in animal coats: 1. Radiative transfer. *Proc. R. Soc. Lond. B* 188:377-393.
- Cena, K., and J. L. Monteith. 1975b. Transfer processes in animal coats: 2. Conduction and convection. *Proc. R. Soc. Lond. B* 188:395-411.
- Cena, K., and J.L. Monteith. 1975c. Transfer processes in animal coats: 3. Water vapour diffusion. *Proc. R. Soc. Lond. B* 188:413-423.
- Charles, D. R. 1986. Temperature for broilers. *World's Poultry Science Association Journal* 42:249-258.
- Charles, D. R. 1991. Physiological requirements for shelter engineering. *Farm Buildings and Engineering* 8(2):13-16.
- Charles, D. R. 1994. Comparative climatic requirements. Pages 3-24 {In} C. M. Wathes and D. R. Charles, eds. *Livestock Housing*. CAB International, Wallingford.
- Chou, K. C., and R. B. Corotis. 1981. Simulations of hourly wind speed and array wind power. *Solar Energy* 26 (3):199-212.
- Christensen, K. S. 1993. Numerical Prediction of Buoyant Air Flow in Livestock Buildings. In: Collins & Boon (1993):1063-1070.
- Clapperton, J. L., J. P. Joyce, and K. L. Blaxter. 1965. Estimates of the contribution of solar radiation to the thermal exchanges of sheep at a latitude of 55N. *J. Agric. Sci.* 64:37-49.
- Clark, J. A., ed. 1981. Environmental aspects of housing for animal production. *Proceedings of 31st Easter School in Agricultural Science*, University of Nottingham. Butterworths, London.
- Clark, J. A., G. D. MacLeod, and D. R. Charles. 1982. Causes of Feather Wear in Poultry. In: *ASAE* (1982):343-347.

- Close, W. H. 1987. The influence of the thermal environment on the productivity of pigs. Pages 9-24 {In} A. T. Smith and T. L. J. Lawrence, eds. Pig Housing and the Environment - Occasional Publication No 11 of the British Society of Animal Production. British Society of Animal Production, Edinburgh.
- Close, W. H., and L. E. Mount. 1978. The effects of plane of nutrition and environmental temperature on the energy metabolism of the growing pig. 1) Heat loss and critical temperature. Br. J. Nutr. 40:413-421.
- Close, W. H., and P. K. Poornan. 1993. Outdoor pigs: their requirements, appetite and environmental responses {In} P. C. Garnsworthy and D. J. A. Cole, eds. Recent Advances in Animal Nutrition 1993. Nottingham University Press, .
- Cole, R.J. 1976. The longwave radiation environment around buildings. Buildings and Environment 11(1): 3-13
- Collins, E., and C. Boon, eds. 1993. Livestock Environment IV. Fourth International Symposium, University of Warwick, Coventry, England, 6-9 Jul 1993. American Society of Agricultural Engineers, St Joseph, Michigan, USA.
- Corotis, R. B., A. B. Sigl, and M. P. Cohen. 1977. Variance analysis of wind characteristics for energy conversion. Journal of Applied Meteorology 16 (11):1149-1157.
- Cowpertwait, P. S. P. 1994. A generalised point process model for rainfall. Proc. R. Soc. Lond. A. 447:23-37.
- Cowpertwait, P. S. P. 1995. A generalised spatial-temporal model for rainfall based on a clustered point process. Proc. R. Soc. Lond. A. 450:163-175.
- D'Alfonso, T. H., H. B. Manbeck, and W. B. Roush. 1996. A case study of temperature uniformity in three laying hen production buildings. Trans. Amer. Soc. Agric. Eng. 39 (2):669-675.
- Davidson, H. R. 1966. The Production and Marketing of Pigs, 3rd ed. Longmans, .
- Davis, R. H., O. E. M. Hassan, and A. H. Sykes. 1973. Energy utilisation in the laying hen in relation to ambient temperature. J. Agric. Sci. 81:173-177.
- Degelman, L. O. 1976. A weather simulation model for building energy analysis. Pages 435-447 {In} ASHRAE Trans. Symposium on Weather Data, Seattle, WA.,

- Deighton, T., and J. C. D. Hutchinson. 1940. Studies on the metabolism of fowls. II. The effect of activity on metabolism. *J. Agric. Sci.* 30:141-157.
- Doney, J. M. 1963. The effects of exposure in blackface sheep with particular reference to the roles of the fleece. *J. Agric. Sci.* 60:267-273.
- Dowling, D. F., and T. Nay. 1960. Cyclic changes in the follicles and hair coat in cattle. *Aust. J. agric. Res.* 11:1064-1071.
- Eckert, J. B., B. B. Baker, and J. D. Hanson. 1995. The impact of global warming on local incomes from range livestock systems. *Agricultural Systems* 48 (1):87-100.
- Ede, A. J. 1967. An introduction to heat transfer - principles and calculations. Pergamon Press, .
- Ehrlemark, A. G., and K. G. Sallvik. 1996. A model of heat and moisture dissipation from cattle based on thermal properties. *Trans. Amer. Soc. Agric. Eng.* 39 (1):187-194.
- Emmans, G. C. 1974. The effects of temperature on the performance of laying hens. Pages 199 {In} T. R. Morris and B. M. Freeman, eds. *Energy Requirements of Poultry*. British Poultry Science Ltd, .
- Fehr, R. L., K. T. Priddy, S. G. McNeill, and D. G. Overhults. 1982. Limiting swine stress with evaporative cooling. In: *ASAE* (1982):577-583.
- Finck, J. L. 1930. Mechanism of heat flow in fibrous materials. *Bur. Stand. J. Res.* 5:973-984.
- France, J., and J. H. M. Thornley. 1984. *Mathematical Models in Agriculture*, 1st ed. Butterworths, London.
- France, J., J. H. M. Thornley, and D. E. Beever. 1984. Opinion: mechanistic modelling in ruminant nutrition and production. *Research and Development in Agriculture* 1:65-71.
- Fuentes, U., V. Sept, D. Heimann, and R. Sausen. 1995. Statistical-dynamical downscaling of global climate simulations. 6th International Meeting on Statistical Climatology, University College, Galway, Ireland. 19-23 June 1995. pp 37-40. .
- Futang, W. 1993. The potential implications of climate change for Chinese vegetation and agriculture. In: Liangzhi et al, 1993:27-32.

- Gannon, M. A. 1996. The energy balance of pigs outdoors. Ph.D. Dissertation. University of Nottingham.
- Garnsworthy, P. C., T. K. Lightowler, H. L. Woolley, and D. R. Charles. 1993. Some effects of temperature and humidity on dairy cows in Britain. In: Collins & Boon (1993):1139-1145.
- Garrett, W. N., T. E. Bond, and N. Pereira. 1967. Influence of Shade Height on Physiological Responses of Cattle During Hot Weather. Trans. Amer. Soc. Agric. Eng. 10 (4):433-434,438.
- Gatenby, R. M. 1977. Conduction of heat from sheep to ground. Agric. Meteorol. 18:387-400.
- Gatenby, R. M., J. L. Monteith, and J. A. Clark. 1983a. Temperature and humidity gradients in a sheep's fleece. 1. Gradients in the steady state. Agric. Meteorol. 29:1-10.
- Gatenby, R. M., J. L. Monteith, and J. A. Clark. 1983b. Temperature and humidity gradients in a sheep's fleece. 2. The energetic significance of transients. Agric. Meteorol. 29:83-103.
- Gates, D. M. 1980. Biophysical Ecology. Springer-Verlag, New York.
- Gates, R. S., D. G. Overhults, and S. H. Zhang. 1996. Minimum ventilation for modern broiler facilities. Trans. Amer. Soc. Agric. Eng. 39 (3):1135-1144.
- Gates, R. S., and M. B. Timmons. 1988. Stochastic and deterministic analysis of evaporative cooling benefits for laying hens. Trans. Amer. Soc. Agric. Eng. 31 (3):904-909.
- Gebremedhin, K. G. 1987. Effect of animal orientation with respect to wind direction on convective heat loss. Agricultural and Forest Meteorology 40:199-206.
- Giles, L. R., and J. M. Gooden. 1993. Application of the Fick principle to the continuous measurement of energy expenditure in pigs. Aust. J. agric. Res. 44 (7):1423-1439.
- Glass, M. H., and R. H. Jacob. 1991. Losses of sheep following adverse weather after shearing. Australian Veterinary Journal 69 (6):142-143.
- Gonzalez-Jimenez, E., and K. L. Blaxter. 1962. The metabolism and thermal regulation of calves in the first month of life. Br. J. Nutr. 16:199-212.

- Gordon, C. J. 1996. Homeothermy: Does it impede the response to cellular injury? *J. therm. Biol.* 21 (1):29-36.
- Graham, N. M., F. W. Wainman, K. L. Blaxter, and D. G. Armstrong. 1959. Environmental temperature, energy metabolism and heat regulation in sheep. 1. Energy metabolism in closely clipped sheep. *J. Agric. Sci.* 52:13-24.
- Gregory, N. G. 1995. The role of shelterbelts in protecting livestock: a review. *New Zealand Journal of Agricultural Research* 38 (4):423-450.
- Gyalistras, D., and A. Fischlin. 1995. Downscaling III: Applications to ecosystem modelling. 6th International Meeting on Statistical Climatology, University College, Galway, Ireland. 19-23 June 1995. pp 189 - 192. .
- Hales, J. R. S., and G. D. Brown. 1974. Net energetic and thermoregulatory efficiency during panting in the sheep. *Comp. Biochem. Physiol. A.* 49A: 413-422.
- Hales, J. R. S., and M. E. D. Webster. 1967. Respiratory function during thermal tachypnoea in sheep. *J. Physiol.* 190:241-260.
- Harrington, R. 1996. Insect Pests in a Changing Climate. Presented at the Royal Meteorological Society Margary Lecture, Imperial College, London, 20 March 1996. .
- Harrison, P. A., R. E. Butterfield, and T. E. Downing, eds. 1995. Climate change and agriculture in Europe: assessment of impacts and adaptations. Environmental Change Unit, University of Oxford, Oxford.
- Hart, E. 1985. Sheep - a guide to management. Crowood Press, Marlborough, Wiltshire.
- Heber, A. J., C. R. Boon, and M. W. Peugh. 1996. Air patterns and turbulence in an experimental livestock building. *J. agric. Engng Res.* 64 (3):209-226.
- Hewitson, B. C. 1995. The development of climate downscaling: techniques and applications. 6th International Meeting on Statistical Climatology, University College, Galway, Ireland. 19-23 June 1995. pp 33-36. .
- Hewitt, G. F., G. L. Shires, and T. R. Bott. 1994. Process heat transfer. CRC Press, Boca Raton, Florida.
- Higgins, K. P., and V. A. Dodd. 1989. A Model of the Bioclimatic Value of Shelter to Beef Cattle. *J. agric. Engng Res.* 42 (3):149-164.

- Hill, M. O., P. D. Carey, and S. M. Wright. 1994. Species dispersal modelling. Presented at: Demonstrating climate change impacts in the UK: the DoE/NERC Core Model programme, University of Newcastle, 14-15 December 1994. .
- Hoff, S. J., K. A. Janni, and L. D. Jacobson. 1993. Modeling newborn piglet thermal interactions with a surface energy balance model. *Trans. Amer. Soc. Agric. Eng.* 36 (1):151-159.
- Hofmeyr, H. S., A. J. Guidry, and F. A. Waltz. 1969. Effects of Temperature and Wool Length on Surface and Respiratory Evaporative Losses of Sheep. *J. Appl. Physiol.* 26(5):517-523.
- Holmes, C. W. 1970. Effects of air temperature on body temperatures and sensible heat loss of Friesian and Jersey calves at 12 and 76 days of age. *Animal production* 12:493-501.
- Holmes, C. W. 1981. A note on the protection provided by the hair coat or fleece of the animal against the thermal effects of simulated rain. *Animal production* 32:225-226.
- Holmes, C. W., and N. A. McLean. 1975. Effects of air temperature and air movement on the heat produced by young Friesian and Jersey calves, with some measurements of the effects of artificial rain. *New Zealand Journal of Agricultural Research* 18:277-284.
- Holmes, C. W., and L. E. Mount. 1967. Heat loss from groups of growing pigs under various conditions of environmental temperature and air movement. *Animal production* 9:435-452.
- Horton-Smith, C., and E. C. Amoroso, eds. 1966. *Physiology of the domestic fowl*. Oliver & Boyd, Edinburgh.
- Houghton, J. T., B. A. Callander, and S. K. Varney, eds. 1992. *Climate Change 1992 - The supplementary report to the IPCC scientific assessment*. Cambridge University Press, Cambridge.
- Houghton, J. T., G. J. Jenkins, and J. J. Ephraums, eds. 1990. *Climate Change: The IPCC Scientific Assessment*. Cambridge University Press, Cambridge.
- Houghton, J. T., L. G. Meira Filho, B. A. Callander, N. Harris, A. Kattenberg, and K. Maskell, eds. 1995. *Climate Change 1995: The Science of Climate Change. Contribution of WGI to the Second Assessment Report of the Intergovernmental Panel on Climate Change*. Cambridge University Press, Cambridge.

- Houseal, G. A., and B. E. Olson. 1995. Cattle use of microclimates on a northern latitude winter range. *Canadian Journal of Animal Science* 75 (4):501-507.
- Hutchinson, J. C. D. 1954. Evaporative cooling in fowls. *J. Agric. Sci.* 45:48-59.
- Idso, S.B., and R.D. Jackson. 1969. Thermal radiation from the atmosphere. *J. Geophys. Res.* 74: 5397-5403
- Ingram, D. L. 1964a. The Effect of Environmental Temperature on Body Temperatures, Respiratory Frequency and Pulse Rate in the Young Pig. *Res. vet. Sci.* 5:348-356.
- Ingram, D. L. 1964b. The Effect of Environmental Temperature on Heat Loss and Thermal Insulation in the Young Pig. *Res. vet. Sci.* 5:357-364.
- Ingram, D.L. 1965. Evaporative Cooling in the Pig. *Nature* 297:415-416.
- Ingram, D.L. 1974. Heat loss and its control in pigs. In Monteith & Mount (1974):233-254.
- Ingram, D. L., and K. F. Legge. 1969. The effect of environmental temperature on respiratory ventilation in the pig. *Resp. Physiol* 8:1-12.
- Innes, S. 1986. How fast should a dead whale cool? *Can. J. Zool.* 64:2064-2065.
- IPCC. 1994a. Radiative Forcing of Climate Change. University College, London and CGER, Tsukuba, Japan, .
- IPCC. 1994b. Technical Guidelines for Assessing Climate Change Impacts and Adaptations. University College, London and CGER, Tsukuba, Japan, .
- Iqbal, M. 1980. Prediction of hourly diffuse solar radiation from measured hourly global solar radiation on a horizontal surface. *Solar Energy* 24 (5): 491-503
- Jessen, C., and G. Kuhnen. 1996. Seasonal variations of body temperature in goats living in an outdoor environment. *J. therm. Biol.* 21 (3):197-204.
- Jones, J. E., and K. Phelps. 1996. A review of sources of meteorological data and weather generators for practical use in agricultural and horticultural modelling. *Aspects of Applied Biology* 46:5-12.
- Jones, P. D., and D. Conway. 1995. The use of weather types for GCM downscaling.

6th International Meeting on Statistical Climatology, University College, Galway, Ireland. 19-23 June 1995. pp 193 - 196. .

Joyce, J. P., and K. L. Blaxter. 1964. The effect of air movement, air temperature and infrared radiation on the energy requirements of sheep. *Br. J. Nutr.* 18:5-27.

Joyce, J. P., K. L. Blaxter, and C. Park. 1966. The Effect of Natural Outdoor Environments on the Energy Requirements of Sheep. *Res. vet. Sci.* 7:342-359.

Kabuga, J. D. 1990. The influence of thermal conditions on the conception rate of Holstein-Friesian cattle in the humid tropics. *Agricultural and Forest Meteorology* 53:33-43.

Katz, R. W., and B. G. Brown. 1992. Extreme events in a changing climate: variability is more important than averages. *Climatic Change* 21:289-302.

Kaushish, S. K., S. A. Karim, and P. S. Rawat. 1995. Physiological responses of unshorn and shorn native and crossbred sheep under heat exposure. *Indian Journal of Animal Sciences* 65 (6):714-717.

Kerslake, D. McK. 1972. The stress of hot environments. Cambridge University Press, .

Kettlewell, P. J., and P. Moran. 1992. A study of heat production and heat loss in crated broiler chickens: A mathematical model for a single bird. *Br. Poult. Sci.* 33:239-252.

Kingsolver, J. G. 1989. Weather and the population dynamics of insects: integrating physiological and population ecology. *Physiological Zoology* 62 (2):314-334.

Klinedinst, P. L., D. A. Wilhite, G. L. Hahn, and K. G. Hubbard. 1993. The potential effects of climate change on summer season dairy cattle milk production and reproduction. *Climatic Change* 23 (1):21-36.

Knapp, B. J., and K. W. Robinson. 1954. The role of water for heat dissipation by a Jersey cow and a Corriedale ewe. *Aust. J. agric. Res.* 5:568-577.

Knight, K. M., S. A. Klein, and J. A. Duffie. 1991. A methodology for the synthesis of hourly weather data. *Solar Energy* 46 (2):109-120.

Kovarik, M. 1964. Flow of heat in an irradiated protective cover. *Nature* 201: 1085-1087.

- Kubisch, H. M., M. Makarechian, and P. F. Arthur. 1991. A note on the influence of climatic variables and age on the response of beef-calves to different housing types. *Animal production* 52:400-403.
- Lamb, H. H. 1972. British Isles Weather types and a register of the daily sequence of circulation patterns, 1861-1971, Vol. Geophysical Memoirs No.116, Second number, volume 16. HMSO, London.
- Le Maho, Y., P. Delclitte, and J. Chatonnet. 1976. Thermoregulation in fasting emperor penguins under natural conditions. *Am. J. Physiol.* 231:913-922.
- Liangzhi, G., W. Lianhai, Z. Dawei, and H. Xiangling, eds. 1993. Proceedings of international symposium on climate change, natural disasters and agricultural strategies, Beijing, 26-29 May 1993. China Meteorological Press, Beijing.
- Lundy, H., M. G. MacLeod, and T. R. Jewitt. 1978. An automated multi-calorimeter system: preliminary experiments on laying hens. *Br. Poult. Sci.* 19 (2): 173-186.
- Lyth, P. 1996. Shelterbelts for sheep. *The Sheep Farmer* Jan/Feb 96:26.
- MacLeod, M. G. 1990. energy and nitrogen intake, expenditure and retention at 20C in growing fowl given diets with a wide range of energy and protein contents. *Br. J. Nutr.* 64:625-637.
- MacLeod, M.G. 1991. Fat deposition and heat production as responses to surplus dietary energy in fowls given a wide range of metabolisable energy:protein ratios. *Br. Poult. Sci.* 32:1097-1108.
- MacLeod, M. G., S. G. Tullett, and T. R. Jewitt. 1980. Circadian variation in the metabolic rate of growing chickens and laying hens of a broiler strain. *Br. Poult. Sci.* 21 (3):155-159.
- MAFF. 1995b. Heat stress in pigs: solving the problem. MAFF Publication No. PB 1316. .
- MAFF. 1995a. Heat stress in sheep: solving the problem. MAFF Publication PB 2111.
- MAFF. 1996. Heat stress in poultry: solving the problem. MAFF Publication PB 1315. .
- Mannion, A. M. 1995. Agriculture and Environmental Change: Temporal and Spatial Dimensions. Wiley, Chichester.

- Matthews, A. M., A. C. Armstrong, J. R. Turnpenny, J. A. Clark, A. J. McArthur, D. J. Parsons, and K. Cooper. 1997. Modelling the impact of climate change on grassland and livestock systems. Climatic Change Submitted, June 1997.
- Mavi, H. S., G. Singh, S. S. Mathauda, R. Singh, G. S. Mahi, and O. P. Jhorar. 1993. Climate change and wheat yield in the Punjab (India). In: Liangzhi et al, 1993:58-65.
- McArthur, A. J. 1980. Air Movement and heat loss from sheep. 3. Components of Insulation in a controlled environment. Proc. R. Soc. Lond. B 209:219-237.
- McArthur, A. J. 1987. Thermal Interaction between animal and microclimate: a Comprehensive model. J. theor. Biol. 126:203-238.
- McArthur, A. J. 1990. Thermal Interaction between animal and microclimate: specification of a "Standard Environmental Temperature" for animals outdoors. J. theor. Biol. 148:331-343.
- McArthur, A. J. 1991a. Forestry and shelter for livestock. Forest Ecology and Management 45:93-107.
- McArthur, A. J. 1991b. Thermal radiation exchange, convection and the storage of latent heat in animal coats. Agricultural and Forest Meteorology 53 (4):325-336.
- McArthur, A. J., and J. L. Monteith. 1980a. Air movement and heat loss from sheep. 1. Boundary layer insulation of a model sheep, with and without fleece. Proc. R. Soc. Lond. B 209:187-208.
- McArthur, A. J., and J. L. Monteith. 1980b. Air movement and heat loss from sheep. 2. Thermal insulation of fleece in wind. Proc. R. Soc. Lond. B 209:209-217.
- McArthur, A. J., and J. C. Ousey. 1994. Heat loss from a wet animal: changes with time in the heat balance of a physical model representing a newborn homeotherm. J. therm. Biol. 19 (2):81-89.
- McCrabb, G. J., B. J. McDonald, and L. M. Hennoste. 1993a. Heat stress during mid-pregnancy in sheep and the consequences for placental and fetal growth. J. Agric. Sci. 120:265-271.

- McCrabb, G. J., B. J. McDonald, and L. M. Hennoste. 1993b. Lamb birth-weight in sheep differently acclimatized to a hot environment. *Aust. J. agric. Res.* 44 (5):933-943.
- McGechan, M. B., and G. Cooper. 1995. A simulation model operating with daily weather data to explore silage and haymaking opportunities in climatically different areas of Scotland. *Agricultural Systems* 48:315-343.
- McIntosh, D. H., and A. S. Thom. 1969. *Essentials of Meteorology*. Wykeham Publications, London.
- McKetta, J. J., ed. 1992. *Heat transfer design methods*. Marcel Dekker, New York.
- McLean, J. A. 1963. The partition of insensible losses of body weight and heat from cattle under various climatic conditions. *J. Physiol.* 167:427-447.
- McLean, J. A. 1974. Loss of heat by evaporation. In Monteith & Mount (1974):19-31.
- McLean, J. A., and D. T. Calvert. 1972. Influence of air humidity on the partition of heat exchanges in cattle. *J. Agric. Sci.* 78:302-307.
- Mearns, L. O., R. W. Katz, and S. H. Schneider. 1984. Extreme high-temperature events: changes in their probabilities with changes in mean temperature. *J. Clim. Appl. Meteorol.* 23 (12):1601-1613.
- Meteorological Office. 1994. *The Hadley Centre for Climate Prediction and Research. Summary of Research Programme.* .
- Mikami, M., T. Toya, and N. Yasuda. 1996. An analytical method for the determination of the roughness parameters over complex regions. *Boundary-Layer Meteorology* 79:23-33.
- Misson, B. H. 1976. The effects of temperature and relative humidity on the thermoregulatory responses of grouped and isolated neonate chicks. *J. Agric. Sci.* 86:35-43.
- Mitchell, D. 1974. Convective heat transfer from Man and other animals. In Monteith & Mount (1974):59-76.
- Mitchell, M. A. 1985. Effects of Air Velocity on convective and radiant heat transfer from domestic fowls at environmental temperatures of 20 and 30 degC. *Br. Poult. Sci.* 26:413-423.
- Mitchell, M. A., and P. J. Kettlewell. 1994. Road transportation of broiler

- chickens - induction of physiological stress. *World's Poultry Science Association Journal* 50 (1):57-59.
- Mohr, E. G., and H. Krzywanek. 1995. Endogenous Oscillator and Regulatory Mechanisms of Body Temperature in Sheep. *Physiology and Behavior* 57 (2):339-347.
- Monteith, J. L., and L. E. Mount, eds. 1974. Heat loss from animals and Man - proceedings of the twentieth Easter School in agricultural science, University of Nottingham, 1973. Butterworths, London.
- Monteith, J. L., and M. H. Unsworth. 1990. *Principles of Environmental Physics*, 2nd ed. Edward Arnold, London.
- Moore, R. B., J. W. Fuquay, and W. J. Drapala. 1992. Effects of late-gestation heat stress on postpartum milk production and reproduction in dairy cattle. *Journal of Dairy Science* 75:1877-1882.
- Morrison, S. R., T. E. Bond, and H. Heitman. 1967. Skin and Lung Moisture Loss from Swine. *Trans. Amer. Soc. Agric. Eng.* 10:691-696.
- Morrison, S. R., and H. Heitman. 1982. Performance of Swine Following Periods of Heat Stress. In: *ASAE* (1982):584-589.
- Mount, L. E. 1966. The effect of wind speed on heat production in the newborn pig. *Quarterly Journal of Experimental Physiology* 51:18-26.
- Mount, L. E. 1967. The Heat Loss from New-Born Pigs to the Floor. *Res. vet. Sci.* 8:175-186.
- Mount, L. E. 1968. *The climatic physiology of the pig*. Edward Arnold, London.
- Mount, L. E. 1974. The concept of thermal neutrality. Pages 425-439 {In} J. L. Monteith and L. E. Mount, eds. *Heat loss from Animals and Man*. Butterworths, London.
- Mount, L. E. 1979. *Adaptation to Thermal Environment - Man and his productive animals*, 1st ed. Edward Arnold, London.
- Mount, L. E., and D. Brown. 1982. The use of meteorological records in estimating the effects of weather on sensible heat loss from sheep. *Agric. Meteorol.* 27:241-255.
- Mount, L. E., and D. L. Ingram. 1965. *The effects of Ambient Temperature and Air*

- Movement on Localised Sensible Heat-Loss from the Pig. *Res. vet. Sci.* 6:84-91.
- Muiruri, H. K., and P. C. Harrison. 1991b. Effect of roost temperature on performance of chickens in hot ambient environments. *Poult. Sci.* 70: 2253-2258.
- Muiruri, H. K., and P. C. Harrison. 1991a. Effects of peripheral foot cooling on metabolic rate and thermoregulation of fed and fasted chicken hens in a hot environment. *Poult. Sci.* 70:74-79.
- Nagorcka, B. N. 1978. The effect of photoperiod on wool growth. In: Black & Reis (1978):127-137.
- Naizhuang, L., and J. Zhifeng. 1993. Possible influences of climate change on freshwater fishery in China. In: Liangzhi et al, 1993:176-181.
- Nichols, D. A., D. R. Ames, and R. H. Hines. 1982a. Effect of Temperature on Performance and Efficiency of Finishing Swine. In: ASAE (1982):376-379.
- Nichols, D. A., D. R. Ames, and R. H. Hines. 1982b. Evaporative cooling systems for swine. In: ASAE (1982):204-207.
- Nienaber, J. A., G. L. Hahn, T. P. McDonald, and R. L. Korthals. 1996. Feeding patterns and swine performance in hot environments. *Trans. Amer. Soc. Agric. Eng.* 39 (1):195-202.
- Oke, T. R. 1987. *Boundary Layer Climates*, 2nd ed. Routledge, London.
- Olson, L. L., J. A. De Shazer, and F. B. Mather. 1974. Convective, radiative and evaporative heat losses of White Leghorn layers as affected by bird density per cage. *Trans. Amer. Soc. Agric. Eng.* 17:960-967.
- O'Neill, S. J. B., and N. Jackson. 1974. The heat production of hens and cockerels maintained for an extended period of time at a constant environmental temperature of 23 C. *J. Agric. Sci.* 82:549-552.
- Orgill, J. F., and K. G. T. Hollands. 1977. Correlation equation for hourly diffuse radiation on a horizontal surface. *Solar Energy* 19:357-359.
- Osbaldiston, G. W. 1966. The response of the immature chicken to ambient temperature. In: Horton-Smith & Amoroso (1966):228-234.
- Overhults, D. G., and J. A. DeShazer. 1982. Infrared heat for reducing environmental stress on weaned pigs. In: ASAE (1982):362-369.

- Parsons, D. J., K. Cooper, A. C. Armstrong, A. M. Matthews, J. R. Turnpenny, J. A. Clark, and A. J. McArthur. 1997b. Integrated models of livestock systems for climate change studies. 1. Grazing systems. Global Change Biology Submitted, June 1997.
- Parsons, D. J., K. Cooper, A. C. Armstrong, A. M. Matthews, J. Turnpenny, J. A. Clark, A. J. McArthur, and D. Viner. 1995. Integrated models of grassland and livestock systems to assess the impact of climate change. Report for the Year July 1994-June 1995. Contract reference CSA 2523, Silsoe Research Institute, Silsoe, 1995. .
- Parsons, D. J., K. Cooper, A. C. Armstrong, A. M. Matthews, J. Turnpenny, J. A. Clark, A. J. McArthur, and D. Viner. 1996. Integrated Models of grassland and livestock systems to assess the impact of climate change. *Report for the Year July 1995-June 1996*. Contract reference: CSA 2523, Silsoe Research Institute, Silsoe, 1996. .
- Parsons, D. J., K. Cooper, A. C. Armstrong, A. M. Matthews, J. R. Turnpenny, J. A. Clark, A. J. McArthur, and D. Viner. 1997a. Integrated models of grassland and livestock systems to assess the impact of climate change. Final Report, June 1997, Contract ref CSA 2523, Silsoe Research Institute. .
- Parsons, K. C. 1993. Human thermal environments. Taylor & Francis, London.
- Payne, C. G. 1966. Environmental temperature and egg production. In: Horton-Smith & Amoroso (1966):235-241.
- Petherick, J. C. 1983. A note on allometric relationships in Large White X Landrace pigs. *Animal production* 36:497-500.
- Poczopko, P. 1981. The environmental physiology of juvenile animals. In: Clark (1981):109-130.
- Porter, V. 1991. Cattle - a handbook to the breeds of the world. Christopher Helm, London.
- Poultry World. 1996. Take the heat out. *Poultry World* 2 Aug - 5 Sep 1996:6.
- Precht, H., J. Christopherson, H. Hensel, and W. Larcher. 1973. Temperature and Life. Springer-Verlag, Berlin.
- Prescott, M. L., K. M. Havstad, K. M. Olsonrutz, E. L. Ayers, and M. K. Petersen. 1994. Grazing behavior of free ranging beef cows to initial and prolonged exposure to fluctuating thermal environments. *Applied Animal Behaviour Science* 39 (2):103-113.

- Quinn, A. D. 1996. The ventilation of a chick transport vehicle. Ph.D. Thesis. University of Nottingham.
- Rahmstorf, S. 1997. Ice cold in Paris. *New Scientist* 8 Feb 1997:26-30.
- Randall, J. M., and C. R. Boon. 1994. Ventilation control and systems. Pages 149-182 {In} C. M. Wathes and D. R. Charles, eds. *Livestock Housing*. CAB International, Wallingford.
- Redbo, I., I. Mossberg, A. Ehrlemark, and M. Stahlhogberg. 1996. Keeping growing cattle outside during winter - behavior, production and climatic demand. *Animal Science* 62 (1):35-41.
- Reilly, W. M., K. W. Koelkebeck, and P. C. Harrison. 1991. Performance evaluation of heat-stressed commercial broilers provided water-cooled floor perches. *Poult. Sci.* 70:1699-1703.
- Reynard, N., and N. Arnell. 1994. Modelling changes in regional hydrological characteristics. Presented at: Demonstrating climate change impacts in the UK: the DoE/NERC Core Model programme, University of Newcastle, 14-15 December 1994. .
- Richards, S. A. 1971. The significance of changes in the temperature of the skin and body core in the regulation of heat loss. *J. Physiol.* 216:1-10.
- Richards, S. A. 1974. Aspects of physical thermoregulation in the fowl. In Monteith & Mount (1974):255-275.
- Richards, S. A. 1976. Evaporative water loss in domestic fowls and its partition in relation to ambient temperature. *J. Agric. Sci.* 87:527-532.
- Richards, S. A. 1977. The influence of loss of plumage on temperature regulation in laying hens. *J. Agric. Sci.* 89:393-398.
- Richardson, C. W. 1981. Stochastic simulation of daily precipitation, temperature and solar radiation. *Water Resour. Res.* 17:182-190.
- Richardson, C. W., and A. D. Nicks. 1990. Weather generator description. In: EPIC - Erosion/Productivity Impact Calculator: 1. Model Documentation, edited by A.N.Sharpley & J.R.Williams. US Department of Agriculture Technical Bulletin No. 1768, 235 pp. .
- Romijn, C., and W. Lokhorst. 1966. Heat regulation and energy metabolism in the domestic fowl. In: Horton-Smith & Amoroso (1966):211-227.

- Ryan, D. P., M. P. Boland, E. Kopel, D. Armstrong, L. Munyakazi, R. A. Godke, and R. H. Ingraham. 1992. Evaluating 2 different evaporative cooling management systems for dairy cows in a hot dry climate. *Journal of Dairy Science* 75:1052-1059.
- Ryder, M. L. 1973. *Hair*, Vol. The Institute of Biology's Studies in Biology, no.41. Edward Arnold, London.
- Ryder, M. L. 1975. The production and properties of wool and other animal fibres, Vol. *Textile Progress* 7 (no.3), 63., .
- Sallvik, K., and B. Wejfeldt. 1993. Lower Critical Temperature for Fattening Pigs on Deep Straw Bedding. In: Collins & Boon (1993):909-914.
- Samara, M. H., K. R. Robbins, and M. O. Smith. 1996. Interaction of feeding time and temperature and their relationship to performance of the broiler breeder hen. *Poult. Sci.* 75 (1):34-41.
- Schoeller, D. A. 1988. Measurement of energy expenditure in free-living humans by using doubly-labeled water. *Journal of Nutrition* 118 (7):1278-1289.
- Schoeller, D. A., and J. M. Hnilicka. 1996. Reliability of the doubly-labeled water method for the measurement of total daily energy expenditure in free-living subjects. *Journal of Nutrition* 126 (1):348S-354S.
- Schofield, C. P., and J. A. Marchant. 1996. Measuring the size and shape of pigs using image analysis. Paper 96G-035, AgEng 96 Conference, Madrid, 1996.
- Schofield, C. P., R. P. White, M. R. Holden, and B. P. Gill. 1997. Commercial development of a video imaging system for the continuous monitoring of pigs. Confidential Report to the Meat and Livestock Commission, CR/747/96/1522. .
- Seino, H. 1993. Implications of climatic warming for Japanese crop production. In: Liangzhi et al, 1993:44-53.
- Semenov, M. A., and J. R. Porter. 1995. Climatic variability and the modelling of crop yields. *Agricultural and Forest Meteorology* 73:265-283.
- Senft, R. L., and L. R. Rittenhouse. 1985. A model of thermal acclimation in cattle. *Journal of Animal Science* 61:297-306.
- Shao, J., and P. J. Lister. 1994. The prediction of road surface state and simulation of the shading effect. *Boundary-Layer Meteorology* 73:411-

- Shuhua, L. 1993. Climatic warming impacts on agricultural pests. In: Liangzhi et al, 1993:182-186.
- Silanikove, N. 1987. Impact of shelter in hot Mediterranean climate on feed intake, feed utilization and body fluid distribution in sheep. *Appetite* 9 (3):207-215.
- Silanikove, N. 1992. Effects of water scarcity and hot environment on appetite and digestion in ruminants - a review. *Livestock Production Science* 30 (3): 175-194.
- Silanikove, N., and M. Gutman. 1992. Interrelationships between lack of shading shelter and poultry litter supplementation - food-intake, live weight, water metabolism and embryo loss in beef-cows grazing dry Mediterranean pasture. *Animal production* 55 (3):371-376.
- Slee, J., and H. B. Carter. 1961. A comparative study of fleece growth in Tasmanian fine Merino and Wiltshire Horn ewes. *J. Agric. Sci.* 57:11-19.
- Smith, A. T. 1994. Pig housing. Pages 273-304 {In} C. M. Wathes and D. R. Charles, eds. *Livestock Housing*. CAB International, Wallingford.
- Smith, W. K. 1981. Poultry housing problems in the tropics and subtropics. In: Clark (1981):235-259.
- Sokhansanj, S., and K. A. Jordan. 1981. Experimanetal and simulation studies of a rock solar heat storage in a livestock building. *Trans. Amer. Soc. Agric. Eng.* 24(3):721-724.
- Spencer, J.W. 1982. A comparison of methods for estimating hourly diffuse solar radiation from global solar radiation. *Solar Energy* 29 (1): 19-32
- Spengler, R. W., and D. P. Stombaugh. 1982. Design and optimisation of a subterranean heat exchanger for swine ventilation. In: ASAE (1982):184-192.
- Stafford Smith, D. M., I. R. Noble, and G. K. Jones. 1985. A heat balance model for sheep and its use to predict shade-seeking behaviour in hot conditions. *J. Appl. Ecol.* 22:753-774.
- Stansbury, W. F., J. J. McGlone, and L. F. Tribble. 1987. Effects of season, floor type, air temperature and snout coolers on sow and litter performance. *Journal of Animal Science* 65:1507-1513.

- Suarez, M. E. 1988. Radiation budget of animals outdoors. M.Phil. Thesis. University of Nottingham.
- Szelenyi, Z., A. Palko, and M. Szekely. 1996. Heat-induced acute hyperthermia results in a reversible depression of cold defence in the rat (*Rattus Norvegicus*). *J. therm. Biol.* 21 (3):163-170.
- The Times. January 6 1996. Hotter-than-ever world adds to fear of climate change. .
- The Times. July 10 1995. The clouds part on a mystery. .
- The Times. July 13 1995. Tree rings hold clue to the hottest news this century. .
- The Times. March 23 1995. Blooms 'herald global warming'. .
- The Times. October 25 1996. Scientists may have overplayed threat of global warming. .
- Thompson, B. K., and R. M. G. Hamilton. 1993. The relationship between meteorological changes and daily feed intake or shell strength of eggs of Leghorn hens. *Canadian Journal of Animal Science* 73 (2):465-469.
- Thompson, G. E. 1973. Review of the progress of Dairy Science - Climatic physiology of cattle. *J. Dairy Res.* 40:441-473.
- Timmons, M. B., and P. E. Hillman. 1993. Partitional heat losses in heat stressed poultry as affected by wind speed. In: Collins & Boon (1993): 265-272.
- Tregear, R. T. 1966. Physical functions of skin. Academic Press, London.
- Troen, I., and E. L. Petersen. 1989. European Wind Atlas. for the Commission of the European Communities by Riso National Laboratory, Denmark, Roskilde, Denmark.
- Turnpenny, J. R., J. A. Clark, A. J. McArthur, D. J. Parsons, K. Cooper, A. M. Matthews, and A. C. Armstrong. 1997. Integrated models of livestock systems for climate change studies. 2. Intensive Systems. *Global Change Biology* Submitted, June 1997.
- Tzschentke, B., M. Nichelmann, and T. Postel. 1996. Effects of ambient temperature, age and wind speed on the thermal balance of layer-strain fowls. *Br. Poult. Sci.* 37:501-520.
- Unsworth, M.H., and J.L. Monteith. 1975. Longwave radiation at the ground. 1. Angular distribution of incoming radiation. *Q. J. Roy. Met. Soc.* 101: 13-25

- Upton, M. 1976. Agricultural production economics and resource-use. Oxford University Press, Oxford.
- Vandenheede, M., B. Nicks, R. Shehi, B. Canart, I. Dufrasne, R. Biston, and P. Lecomte. 1995. Use of a shelter by grazing fattening bulls - effects of climatic factors. *Animal Science* 60 (1):81-85.
- Van Kampen, M. 1974. Physical Factors in energy expenditure. Pages 199 {In} T. R. Morris and B. M. Freeman, eds. *Energy Requirements of poultry*. British Poultry Science Ltd, .
- Van Wijk, W. R., and D. A. De Vries. 1963. Periodic temperature variations {In} W. R. Van Wijk, ed. *Physics of Plant Environment*. North-Holland Publishing Company, Amsterdam.
- Verstegen, M. W. A., W. H. Close, I. B. Start, and L. E. Mount. 1973. The effects of environmental temperature and plane of nutrition on heat loss, energy retention and deposition of protein and fat in groups of growing pigs. *Br. J. Nutr.* 30:21-35.
- Viner, D., and M. Hulme. 1994. The Climate Impacts LINK Project: Providing climate change scenarios for impacts assessment in the UK. Report for the UK Department of the Environment, for contract PECD 7/12/96. .
- VIS. 1988. Mild Weather benefits cattle. *Veterinary Record* 123 (2):60-61.
- VIS. 1991. Damp weather causes respiratory problems in cattle. *Veterinary Record* 128 (4):72-73.
- Waggoner, P. E. 1989. Anticipating the frequency distribution of precipitation if climate change alters its mean. *Agricultural and Forest Meteorology* 47:321-337.
- Walsberg, G. E., and J. R. King. 1978. The relationship of external surface area of birds to skin surface area and body mass. *Journal of Experimental Biology* 76:185-189.
- Wang, H., and E. S. Takle. 1995. A numerical simulation of boundary-layer flows near shelterbelts. *Boundary-Layer Meteorology* 75:141-173.
- Wang, H., and E. S. Takle. 1996. On three-dimensionality of shelterbelt structure and its influences on shelter effects. *Boundary-Layer Meteorology* 79:83-105.
- Ward, R.C., and M. Robinson. 1990. *Principles of Hydrology*. 3rd ed, McGraw-Hill, London. 365 pp

- Wathes, C. M., and J. A. Clark. 1981a. Sensible heat transfer from the fowl: Boundary layer resistance of a model fowl. *Br. Poult. Sci.* 22:161-173.
- Wathes, C. M., and J. A. Clark. 1981c. Sensible heat transfer from the fowl: Radiative and convective heat losses from a flock of broiler chickens. *Br. Poult. Sci.* 22:185-196.
- Wathes, C. M., and J. A. Clark. 1981b. Sensible heat transfer from the fowl: Thermal resistance of the pelt. *Br. Poult. Sci.* 22:175-183.
- Watson, R. T., M. C. Zinyowera, and R. H. Moss, eds. 1995. *Climate Change 1995: Impacts, Adaptations and Mitigation of Climate Change: Scientific-Technical Analyses*. Cambridge University Press, Cambridge.
- Webster, A. J. F. 1974. Heat loss from Cattle with particular emphasis on the effects of cold. In Monteith & Mount (1974):205-231.
- Webster, A. J. F., A. Tuddenham, C. A. Saville, and G. B. Scott. 1993. Thermal stress on chickens in transit. *Br. Poult. Sci.* 34 (2):267-277.
- Whitmore, W. T., and B. A. Young. 1986. The effects of thermal environment on resting and summit metabolic rates in mature sheep. *Canadian Journal of Animal Science* 66 (1):338.
- Whittow, G. C. 1962. The significance of the extremities of the ox (*Bos taurus*) in thermoregulation. *J. Agric. Sci.* 58:109-120.
- Whittow, G. C. 1971. Cardio-acceleration in the ox (*Bos taurus*) during hyperthermia. *Res. vet. Sci.* 12:495-496.
- Whittow, G.C., and J.D. Findlay. 1968. Oxygen cost of thermal panting. *Am. J. Physiol.* 214:94
- Wiernusz, C. J., and R. G. Teeter. 1996. Acclimation effects on fed and fasted broiler thermobalance during thermoneutral and high ambient temperature exposure. *Br. Poult. Sci.* 37:677-687.
- Wiersma, F., and G. L. Nelson. 1967. Nonevaporative heat transfer from the surface of a bovine. *Trans. Amer. Soc. Agric. Eng.* 10(6):733-737.
- Wigley, T. M. L. 1985. Impact of extreme events. *Nature* 316:106-107.
- Wigley, T. M. L. 1988. The effect of changing climate on the frequency of absolute extreme

- events. *Climate Monitor* 17 (2):44-55.
- Wilby, R. L. 1994. Stochastic weather type simulation for regional climate change impact assessment. *Water Resources Research* 30 (12):3395-3403.
- Wilks, D. S. 1992. Adapting stochastic weather generation algorithms for climate change studies. *Climatic Change* 22 (1):67-84.
- Williams, L. A., G. J. Rowlands, and A. M. Russell. 1986. Effect of wet weather on lameness in dairy cattle. *Veterinary Record* 118 (10):259-261.
- Wilson, J. L., H. A. Hughes, and W. D. Weaver. 1982. Evaporative cooling in broiler houses. In: *ASAE* (1982):193-203.
- Yinsuo, Z., L. Shoudong, F. Jinzhao, and Z. Chuandao. 1993. The impact of climate change on animal husbandry in pastoral area of China. In: *Liangzhi et al*, 1993:169-175.
- Yorkshire Post. March 24 1995. Antarctic ice crack 'may herald catastrophic melt-down'.
- Zhou, W., J. Wang, and S. Yamamoto. 1996. Effects of heat production attributable to forced walking on thermoregulatory physiological responses of chickens in a warm environment. *Br. Poult. Sci.* 37(4):829-840.

APPENDIX A: SUMMARY OF DEFAULT INPUTS TO THE THERMAL BALANCE MODELS

The descriptions of the variables are given in the main text; this Appendix is for reference only.

EWE/UNICORN:

Variable	Value	Notes
l_h	5 mm	Coat depth on head
l_L	3 mm	Coat depth on legs
r_{st}	100 s m^{-1}	Non-shivering
r_{sh}	400 s m^{-1}	
r_{sLmax}	800 s m^{-1}	Vasoconstriction
r_{sLmin}	125 s m^{-1}	Vasodilation
c'	$9.1 \times 10^{-6} \text{ m}$	
F_r	38 min^{-1}	
$e_s(T_{resp})$	6100 Pa	Saturated vapour pressure at temperature of respiratory tissue
T_b	39°C	
p	500 m^{-1}	
E_c	10 W m^{-2}	Below LCT. Cutaneous only [$E_r = E_r(e_a)$]
ρ_c	0.26	

CATTLE:

Variable	Value	Notes
l_h, l_L	12 mm	
r_{stmax}	$20.7 m_b^{0.41} s m^{-1}$	
r_{stmin}	$30 s m^{-1}$ $50 s m^{-1}$	dairy beef
r_{sL}, r_{sh}	$400 s m^{-1}$	
c'	$2.4 \times 10^{-5} m$	
T_b	$38^{\circ}C$	
p	$1800 s m^{-1}$	
E	$17 W m^{-2}$	Total (respiratory + cutaneous) below LCT
ρ_c	0.3 0.1	dairy beef

PIG:

Variable	Value	Notes
r_{sL}	$400 s m^{-1}$	
r_{stmax}	$40.0 m_b^{0.33}$	
r_{stmin}	$24.2 m_b^{0.33}$	
T_b	$39^{\circ}C$	
E	$10 W m^{-2}$	below LCT

BROILER CHICKEN:

Variable	Value	Notes
r_{st}	120 - 400 s m ⁻¹	
r_{sLmax}	800 s m ⁻¹	
r_{sLmin}	80 s m ⁻¹	
T_b	41°C	
E	10 W m ⁻²	below LCT

APPENDIX B: CLIMATE CHANGE SCENARIO

The monthly predictions made by the UKHI model were extracted using the Spatial and Point Estimates of Climate Change due to Transient Emissions (SPECTRE) package produced by the Climatic Research Unit at the University of East Anglia (Barrow et al, 1994). The following table B-1 gives annual temperature and precipitation summaries of the baseline (1961-90) climatology and the predictions for 2050 using emissions scenarios IPCC92a, 92c and 92f (see Chapter 1 for more details).

[Table B-1. Annual mean temperature and rainfall for baseline and climate change scenarios]

SCENARIO	BOXWORTH		PWLLPEIRON	
	T _a (°C)	Rain (mm)	T _a (°C)	Rain (mm)
Baseline	9.6	564	8.1	1777
IPCC 92a	10.8	610	9.2	1940
IPCC 92c	10.6	604	9.1	1916
IPCC 92f	11.0	616	9.4	1959

Table B-1 shows that both temperature and precipitation are predicted to increase under climate change at both sites. However, these annual means mask the variability of the changes through the year. The seasonal effects of the predicted changes are shown in Table B-2 for one site (Boxworth). The figures in Table B-2 were used as input to the generation of daily weather data for the climate of 2050 (Matthews et al, 1997).

[Table B-2. Monthly mean temperature and precipitation for Boxworth: current and 2050 with Scenario IPCC 92a]

	T _a (°C): baseline	T _a (°C): 2050	T _a change: baseline to 2050 (°C)	Rainfall (mm): baseline	Rainfall (mm): 2050	% rainfall change: baseline to 2050
January	3.4	5.0	+ 1.6	45.6	53.9	+ 18.2
February	3.2	5.0	+ 1.8	31.6	35.3	+ 11.7
March	6.2	7.7	+ 1.5	46.6	53.5	+ 14.8
April	7.7	8.8	+ 1.1	45.4	49.6	+ 9.3
May	10.9	12.2	+ 1.3	49.4	53.0	+ 7.3
June	14.1	15.1	+ 1.0	54.7	58.7	+ 7.3
July	16.6	17.6	+ 1.0	45.1	45.3	+ 0.4
August	16.5	17.6	+ 1.1	51.3	53.3	+ 3.9
September	14.2	15.4	+ 1.2	46.5	47.4	+ 1.9
October	10.7	11.7	+ 1.0	54.7	59.4	+ 8.6
November	6.7	7.6	+ 0.9	44.9	46.8	+ 4.2
December	4.9	6.1	+ 1.2	48.2	53.9	+ 11.8

The greatest changes in temperature are predicted to occur in the winter and early spring, with a rise of 1.8°C predicted for February. The implication from the data in Table B-2 is that summers will become warmer, and winters will become shorter, with March temperatures in 2050 predicted to be similar to current April temperatures. The greatest increase in rainfall is predicted for the winter, while July to September will experience similar precipitation to the present. The overall picture is for much milder, wetter winters and slightly warmer summer weather.